

This file is part of the following work:

Hossain, Md Elius (2017) *Lanthanoid formamidates and halogenoaluminate complexes of the rare earths and alkaline earths: synthesis and reactivity*. PhD Thesis, James Cook University.

Access to this file is available from:

<https://doi.org/10.25903/5ccbcc1fc1876>

Copyright © 2017 Md Elius Hossain

The author has certified to JCU that they have made a reasonable effort to gain permission and acknowledge the owners of any third party copyright material included in this document. If you believe that this is not the case, please email

researchonline@jcu.edu.au

Lanthanoid formamidinates and halogenoaluminate complexes of the rare earths and alkaline earths; synthesis and reactivity

A thesis submitted for the degree of

Doctor of Philosophy

by

Md Elius Hossain

M.Phil. (KUET), M.S. & B.Sc.(Hons) (DU)

Bangladesh

Discipline of Chemistry

College of Science and Engineering

James Cook University

Townsville, Australia

October 2017



Dedication

This little effort is dedicated:

To my beautiful mother, a strong and hardworking woman with a great vision.

To the soul of my adoring younger brother Imdad (late), my true best friend.

To my lovely wife, my best friend, my soulmate.

“ইমদাদ, তোর কথা মনে করে আমি প্রতিনিয়ত চোখের পানি গোপন করার বৃথা চেষ্টা করি কিন্তু আমার হৃদয়ের যন্ত্রণা কিছুতেই প্রশমিত হয় না। যদিও সময়ের প্রয়োজনে আমাকে পথ চলতে হয়, হাসতে হয়, তবুও আমি তোর অনুপস্থিতি সবসময় অনুভব করি ভাই। আমার বিশ্বাস, আল্লাহ্ তোকে খুব শান্তিতে রেখেছেন, দোয়া করি যেখানেই থাক ভাল থাক।”

Table of Contents

Title.....	i
Dedication.....	ii
Table of Contents.....	iii
Abstract.....	vi
Abbreviations.....	ix
Declaration.....	x
Acknowledgements.....	xi

CHAPTER 1

GENERAL INTRODUCTION

1.1 The rare earth elements.....	2
<i>1.1.1 Occurrence and isolation.....</i>	<i>2</i>
<i>1.1.2 Electronic configurations and oxidation states.....</i>	<i>7</i>
<i>1.1.3 The lanthanoid contraction.....</i>	<i>9</i>
<i>1.1.4 Coordination chemistry of lanthanoids.....</i>	<i>11</i>
<i>1.1.5 Organometallic chemistry of lanthanoids.....</i>	<i>12</i>
1.2 The alkaline earth elements.....	12
<i>1.2.1 Occurrence and isolation.....</i>	<i>13</i>
<i>1.2.2 Electronic configurations, oxidation states and properties.....</i>	<i>16</i>
<i>1.2.3 Uses of alkaline earth elements.....</i>	<i>17</i>
<i>1.2.4 Organometallic chemistry of alkaline earth elements.....</i>	<i>18</i>
1.3 The ligands.....	18
<i>1.3.1 Bulky ligands in rare earths organometallic chemistry.....</i>	<i>19</i>
<i>1.3.2 Chemistry of the formamidinate ligands.....</i>	<i>20</i>
<i>1.3.3 Synthetic pathways.....</i>	<i>21</i>
1.4 The current study.....	24
1.5 References.....	26

CHAPTER 2
CHEMISTRY OF HALOGENOALUMINATE LANTHANOID-ARENE
COMPLEXES

2.1 Introduction.....	33
2.2 Research Plan.....	43
2.3 Results and Discussion.....	44
2.3.1 <i>Synthesis and Characterisation</i>	44
2.3.2 <i>X-ray Crystal Structures</i>	45
2.3.2.1 <i>Iodoaluminate lanthanoid(III) complexes in toluene</i>	45
2.3.2.2 <i>Iodoaluminate lanthanoid(II) complexes in toluene</i>	55
2.3.2.3 <i>Iodoaluminate lanthanoid(III) complexes in mesitylene</i>	65
2.3.2.4 <i>Bromoaluminate lanthanoid(III) complexes in toluene</i>	71
2.3.2.5 <i>Bromoaluminate lanthanoid(II) complexes in toluene</i>	76
2.3.3 <i>Catalysis for the Polymerisation of Isoprene</i>	79
2.3.4 <i>Discussion</i>	81
2.4 Conclusions.....	83
2.5 Experimental.....	84
2.6 X-ray crystal data.....	89
2.7 References.....	94

CHAPTER 3
CHEMISTRY OF HALOGENOALUMINATE ALKALINE EARTH-ARENE
COMPLEXES

3.1 Introduction.....	101
3.2 Research Plan.....	115
3.3 Results and Discussion.....	116
3.3.1 <i>Synthesis and Characterisation</i>	116
3.3.2 <i>X-ray Crystal Structures</i>	118
3.3.2.1 <i>Iodoaluminate Ae(II) complexes in toluene</i>	118
3.3.2.2 <i>Iodoaluminate Ae(II) complexes in mesitylene</i>	127

3.3.3 <i>Discussion</i>	134
3.4 Conclusions.....	134
3.5 Experimental.....	135
3.6 X-ray crystal data.....	137
3.7 References.....	139

CHAPTER 4

FORMAMIDINATE CHEMISTRY OF DIVALENT AND TRIVALENT LANTHANOIDS

4.1 Introduction.....	149
4.2 Research Plan.....	173
4.3 Results and Discussion.....	174
4.3.1 <i>Synthesis and Characterisation</i>	174
4.3.2 <i>X-ray Crystal Structures</i>	178
4.3.3 <i>Discussion</i>	191
4.4 Conclusions.....	192
4.5 Experimental.....	193
4.6 X-ray crystal data.....	199
4.7 References.....	203

CHAPTER 5

CONCLUDING REMARKS

Concluding Remarks.....	207
References.....	211

APPENDICES

1 Related Chemistry with Relevance to This Thesis.....	212
2 Experimental Procedures.....	222
3 Publications.....	227

Abstract

This thesis focuses on the synthesis and characterisation of halogenoaluminate π -arene complexes of rare earths and alkaline earths and compares the similarities between the two groups of metals. This thesis also discusses the reactivity of divalent rare earth N,N'-bis(aryl)formamidinate (ArForm) complexes.

Study of the synthesis of halogenoaluminate π -arene complexes of rare earths has yielded several new complexes containing η^6 -arene, $[\text{Ln}(\text{arene})(\text{AlX}_4)_n]$ (Ln = La, Ce, Pr, Nd, Gd, Sm, Eu, Yb; arene = toluene, mesitylene; X = Br, I; n = 2, 3). Divalent compounds of Sm, Eu and Yb have lattice solvated toluene molecules; however, the trivalent complexes are unsolvated. $[\text{Eu}(\eta^6\text{-MeC}_6\text{H}_5)(\text{AlI}_4)_2]_n \cdot \text{PhMe}$, $[\text{Yb}(\eta^6\text{-MeC}_6\text{H}_5)(\text{AlI}_4)_2]_n \cdot 1/2\text{PhMe}$ and $[\text{Eu}(\eta^6\text{-MeC}_6\text{H}_5)(\text{AlBr}_4)_2]_n \cdot \text{PhMe}$ are the first examples of polymeric structures among these complexes. All of the complexes have nine coordinated metal centres; however, the ytterbium complex $[\text{Yb}(\eta^6\text{-MeC}_6\text{H}_5)(\text{AlI}_4)_2]_n \cdot 1/2\text{PhMe}$ has an eight coordinate Yb^{2+} centre, due to the lanthanoid contraction effect.

The iodoaluminate and bromoaluminate complexes of lanthanoids were found to be isostructural and comparable with the chloroaluminate complexes in the literature. The Ln-X (X = Br, I), Ln-centroid and the average Ln-C bond distances in the divalent complexes are longer than that of the trivalent complexes. This was expected, as the divalent ions are larger than trivalent ions. Furthermore, the Ln-I distances in the iodoaluminate complexes are longer than the Ln-Br distances in the bromoaluminate complexes. These differences are associated with the larger ionic radii of Ln^{2+} and I⁻ ions than the Ln^{3+} and Br⁻ ions, respectively.

The geometry of the complexes could be best described as distorted pentagonal bipyramidal, with the arene molecule at an axial position (the centroid-Ln-I/Br angles are close to the straight angle, 180°). The lanthanoid contraction was also evidenced by the gradual decrease of the Ln-X (X = Br, I), Ln-centroid and the average Ln-C bond distances in the trivalent complexes of lanthanoids (from lanthanum to gadolinium). This trend was also accessible among the divalent complexes from samarium to ytterbium, and there was an intense change in ytterbium as it is the smallest metal among the metals used for the synthesis here. The

catalytic activity of $[\text{Nd}(\eta^6\text{-C}_6\text{H}_5\text{Me})(\text{AlI}_4)_3]$ for isoprene polymerisation was performed at ambient temperature, and was less effective than the literature results of analogous chloroaluminate complexes.

Investigation of the iodoaluminate π -arene complexes of alkaline earths (Ae) has given several new complexes involving η^6 -arene, $[\text{Ae}(\text{arene})_m(\text{AlI}_4)_2]$ (Ae = Ca, Sr, Ba; arene = toluene, mesitylene; $m = 1, 2$). The Ca-centroid and the average Ca-C distances in the mesitylene complex were somewhat reduced than that of the toluene complex. This fact evidenced a stronger Ca-arene interaction in mesitylene complexes than in the toluene analogue, probably due to more electron donating effect of three methyl groups in mesitylene molecule than by one methyl group in toluene. Both complexes have a zigzag polymer structure. The strontium complex is isostructural with the samarium and europium complexes reported in chapter 2 due to their similar atomic radii.

The barium complex $[(\text{Ba}(\eta^4\text{-C}_6\text{H}_5\text{Me})_2(\text{AlI}_4)_2)]$ has the barium centre sandwiched between two toluene molecules both in an η^4 -fashion giving the barium centre an eight coordination. Nevertheless, the other complexes have only one arene molecule bonded to the metal centre. The Ba-I, Ba-C contacts are comparable with other analogous complexes considering the ionic radii of metals and iodide.

Reactivity of divalent the formamidinate complexes $[\text{Yb}(\text{Form})_2(\text{thf})_2]$ (Form = $[\text{RNCHNR}]$; R = 2,6-Me₂ (XylForm); 2,4,6-Me₃ (MesForm); 2,6-Et₂ (EtForm); 2,6-ⁱPr₂ (DippForm)) has been studied by using different oxidants such as Cl₃CCCl₃, BrCH₂CH₂Br and ICH₂CH₂I. Benzophenone has also been used to study the reactivity of the less sterically demanding ytterbium formamidinate complexes. Reactions of $[\text{Yb}(\text{DippForm})_2(\text{thf})_2] \cdot 2\text{THF}$ with BrCH₂CH₂Br and ICH₂CH₂I yielded the halide complexes $[\text{Yb}(\text{DippForm})_2\text{X}(\text{thf})]$ (X = Br, I). However, all other divalent formamidinate complexes gave the homoleptic tris-formamidinate complexes $[\text{Yb}(\text{Form})_3]$ (Form = XylForm, MesForm and EtForm). Reactions with benzophenone also resulted in the tris-formamidinate complexes. This is probably due to the redistribution of the less bulky formamidinates. The nmr spectrum of these complexes could not be integrated due to the paramagnetic nature of trivalent ytterbium.

With the intention of the isolation of cationic complexes $[L_2Ln]^+[AlX_4/BPh_4/SbCl_6]^-$, a range of halide abstraction reactions has been performed using different halide abstracting reagents such as AlX_3 ($X = Cl, Br, I$), $SbCl_5$ and $AgBPh_4$. Unexpectedly, all attempts to prepare cationic complexes from the halide abstraction reactions consistently gave ligand; however, on one occasion we isolated the reported complex $[YbI_2(thf)_5]^+[YbI_4(thf)_2]^-$. The reaction between $[Yb(DippForm)_2(thf)_2]$ and cobalt carbonyl gave the cobalt complex $[Co(DippFormCO)(CO)_3].THF$ in place of the expected cationic complex $[Yb(DippForm)_2]^+[Co(CO)_4]^-$.

A deliberate RTP reaction using two formamidines of dissimilar steric bulk such as DippForH and XylFormH afforded the heteroleptic tris-formamidinate complex $[Yb(DippForm)(XylForm)_2].PhMe$ for the first time. In addition, $[Eu(XylForm)_2(\mu-OH)(thf)]_2$ and $[Eu(EtForm)_2(thf)_2]$ have been synthesised by the RTP reactions involving XylFormH and EtFormH, respectively. $[Yb(MesForm)_2(\mu-OH)]_2$ was also isolated by the similar procedure using ytterbium. The formation of $[Yb(MesForm)_2(\mu-OH)]_2$ and $[Eu(XylForm)_2(\mu-OH)(thf)]_2$ probably involves a trace amount of water and the presence of the hydroxyl group in the complexes was further confirmed from IR spectra.

Abbreviations

RE = rare earth

REE = rare earth elements

Ln = lanthanoid metal

ArFormH = N,N'-bis(aryl) formamidine

DippFormH = N,N'-bis(2,6-diisopropylphenyl)formamidine

EtFormH = N,N'-bis(2,6-diethylphenyl)formamidine

MesFormH = N,N'-bis(2,4,6-trimethylphenyl)formamidine

XylFormH = N,N'-bis(2,6-dimethylphenyl)formamidine

RTP = redox transmetalation/protolysis

thf = tetrahydrofuran (solvent), THF = tetrahydrofuran (coordinated)

PhMe = toluene

Ae = alkaline earth metal

Å = Ångström unit, 10^{-10}m

CN = coordination number

Eqn. = Equation, Fig. = Figure

IR = Infrared

NMR = Nuclear magnetic resonance

Me = Methyl group

ppm = parts per million

Cp = cyclopentadienyl

Et₂O = diethyl ether

BP = Benzophenone

EDTA = ethylenediaminetetraacetic acid

h = hour, d = day, r.t. = room temperature

Ph = phenyl

η = hapticity

pm = picometer, 10^{-12}m

DME = 1,2-dimethoxyethane

MeCN = acetonitrile

Declaration

To the best of my knowledge, this thesis contains no material which has been accepted for the award of any other degree or diploma at any university or other institution, and contains no material previously published or written by any other person except where due reference is made in the text.

Md Elius Hossain

Discipline of Chemistry

James Cook University

Townsville, Australia

October 2017

Acknowledgements

Firstly, I would like to thank the MASTER of rare earths Prof. Peter Junk for your tremendous support, encouragement and guidance over the years. It was an absolute privilege to join your group, and working in a field I never thought of! Thank you for supporting me to overcome all the frustrations and hard time I embraced for the last three and half years. It has been a pleasure to work with you, and definitely, you are not only a great supervisor but also a great MATE, thank you.

I would like to thank Prof. Glen Deacon for his valuable advice, continuous support and help he has given me throughout my study. Many thanks to my secondary supervisor Dr Murray Davies for providing me with necessary chemicals whenever I asked for, and helping me out with the administrivia (it was unequivocally throbbing!). I would also like to thank Prof. Reiner Anwander of Tübingen University, Germany for performing the catalysis experiments in his lab.

I would like to give a big thanks to all the Junkies (Safaa, Mehdi, Nazli, Areej, Aymeric, Sophie) and office buddies (Ioana, Hannah, Simon, Amanda) for all the fun times, supports and encouragements. I would like to thank Dr Jun Wang for not only train me in the art of air-sensitive chemistry but also offer valuable advice over the years. X-ray crystallography was an entirely new technique as well as the most hated subject to me in my undergraduate level. However, it was great fun to play with the structures, certainly, with the support of you, Jun, many thanks for that. I would also like to acknowledge the supports I received from Dr Bill, particularly regarding the ChemDraw structures. Many thanks to A/Prof. Bruce Bowden and Dr Mark Robertson for assisting me with the NMR problems.

Many thanks to the technical staff in the Discipline of Chemistry at JCU, in particular, Dr Winnie Lee (PhD Sister) and Shiyoh Nobile for their support during the demonstration sessions. A special thanks to Dr Mark Barnes for his support during the lab sessions and for always being there for me. Furthermore, a special mention to Dr Dana Roberts for her cooperation with the IR spectroscopy. I would also like to thank the store people (Stratis and David) for their help to get necessary chemicals and consumables during my study. A special thanks to Stratis for receiving parcels for me and emailing the good news to me.

I would like to appreciate and acknowledge the support I received from the Bangladeshi community in Townsville. A special thanks to Shariar bhai, Afrin bhabi, Ilias bhai, Jakaria bhai and Tania bhabi for supporting me in settling down in Townsville back in 2014. I would also like to thank the Bangladeshi mates, Alim, Suchandan, Dilip bhai for their tremendous support and all the fun times over the years. Furthermore, a sincere thanks to Beg bhai, Rafi bhai, Shahead bhai, Swapan bhai, Rana bhai, Zahid bhai and their families for all the fun times and yummy foods, you guys are awesome, thank you.

I would like to thank James Cook University and Australian Government for supporting me with the International Postgraduate Research Scholarship (IPRS) award. I would also like to thank the Australian Research Council (ARC) for funding our research project.

I would like to express my sincere gratitude from the bottom of my heart to my family; especially, my MOTHER (MAA), a woman with a great vision who would have seen the future in me, and always worked hard to give me the opportunities to grow up. Because of you, I am here today writing my PhD thesis here in Australia, nobody else around us had thought it would be possible by me. Thank you for your support and trust in me, I will always appreciate the care and love you have given me throughout my life. I would like to remember my adoring younger brother Imdad (a legend in our family), I am sorry you will never be with us, be happy and keep smiling wherever you are. I would also like to thank my elder sisters, younger brother and their kids for their love and support over the last decades.

I would like to thank my new family (in-laws), especially, Abbu and Ammu for accepting me as your son and for all your encouragement and support over the years. I would also like to thank Suddhi and Buddhi for your love and well wishes. Last but not least, to my lovely wife Zukti, I am truly blessed to have you in my life. Thank you for your support and love over the past four years. Thank you for putting up with my stress and frustration during my PhD journey. I wish you were here in Townsville since the beginning of my journey! Nevertheless, thanks for joining with me after a long wait, and latter is always better than never!

To all my friends and well-wishers, thank you.

CHAPTER 1

GENERAL INTRODUCTION

1.1 The rare earth elements

The rare earth elements (REE) comprise the largest chemically coherent group in the periodic table being made up of the group three elements, scandium, yttrium and lanthanum, and the 14 elements from cerium (Ce) to lutetium (Lu).¹ The term lanthanoids refers to lanthanum and the elements cerium through to lutetium. Scandium and yttrium are included in the rare earths due to their close resemblance to lanthanoids. Generally, the symbol Ln is used to refer to the lanthanoid elements.² The Finnish chemist Johan Gadolin was the pioneer of lanthanoid discovery, who got a black mineral oxide (earth) known as gadolinite in 1794 and named the oxide 'yttria'. Immediately after Gadolin, a new earth, ceria was obtained by M.H. Klaproth, J.J. Berzelius and W. Hisinger from cerite. However, the separation of these earths into components was successfully performed by Swede C.G. Mosander in 1839–1843. He separated oxides of cerium and lanthanum along with a mixed oxide 'didymia' from ceria. It was found that many of the lanthanoids occur together in the same minerals and because of their similar properties, separation of different lanthanoids was extremely challenging.³ Therefore, it was difficult to distinguish one element from another or from its mineral precursor and often led to confusion. This problem was resolved after the invention of the spectroscope. At the beginning of the 20th century (1907), the series was completed after the discovery of lutetium by Georges Urban and Carl Auer von Welsbach.⁴ The element promethium was separated from the fission products of uranium in 1945.⁵

1.1.1 Occurrence and isolation

All the lanthanoids occur in the earth's crust except promethium. ¹⁴⁷Pm is the most stable isotope of promethium, formed by the fission reaction of heavy nuclei in nuclear reactors.⁴ ⁶ There is a generally held perception that all rare earth metals are found from relatively rare minerals.⁴ In reality, some lanthanoids, for example, cerium and neodymium are more abundant than common metals such as cobalt and lead in the earth's crust while, the least abundant thulium occurs in similar quantities to mercury and silver.^{6, 7} Promethium can be produced synthetically by the fission reaction of uranium.⁴⁻⁶ Table 1.1 shows the natural abundance of the lanthanoids in the earth's crust. It is clear from the table that the lighter

Chapter 1

lanthanoids are more abundant than the heavier ones. In addition, the elements with even atomic number are more abundant than those with odd atomic number.³

Table 1.1: The natural abundance of lanthanoids in earth's crust.

Metal	La	Ce	Pr	Nd	Pm	Sm	Eu	Gd	Tb	Dy	Ho	Er	Tm	Yb	Lu	Y
Abundance (ppm)	35	66	9.1	40	0.0	7	2.1	6.1	1.2	4.5	1.3	3.5	0.5	3.1	0.8	31

The major natural sources of lanthanoids are Bastnasite LnFCO_3 , Monazite $(\text{Ln}, \text{Th})\text{PO}_4$ and Xenotime $(\text{Y}, \text{Ln})\text{PO}_4$ ores. Among the three ores, Monazite is richer in earlier lanthanoids whereas Xenotime is richer in later lanthanoids. In addition, Chinese rare earth reserves, mainly in the form of ionic ores from southern provinces cover more than 70% of the world's total reserve of lanthanoids.³ These Chinese ion-absorption ores, weathered granites with lanthanides adsorbed onto the surface of aluminium silicates, are in some cases low in cerium and rich in the heavier lanthanides (Longnan) whilst the Xunwu deposits are rich in the lighter metals; the small particle size makes them easy to mine. The Chinese ores have made them a leading player in lanthanide chemistry. Besides China, some other countries such as Australia, USA, Brazil and India have deposits of rare earths.⁵⁻⁸ Table 1.2 demonstrates the natural abundance of the lanthanoids in common ores.

Table 1.2: The natural abundance of the lanthanoids in ores.³ #

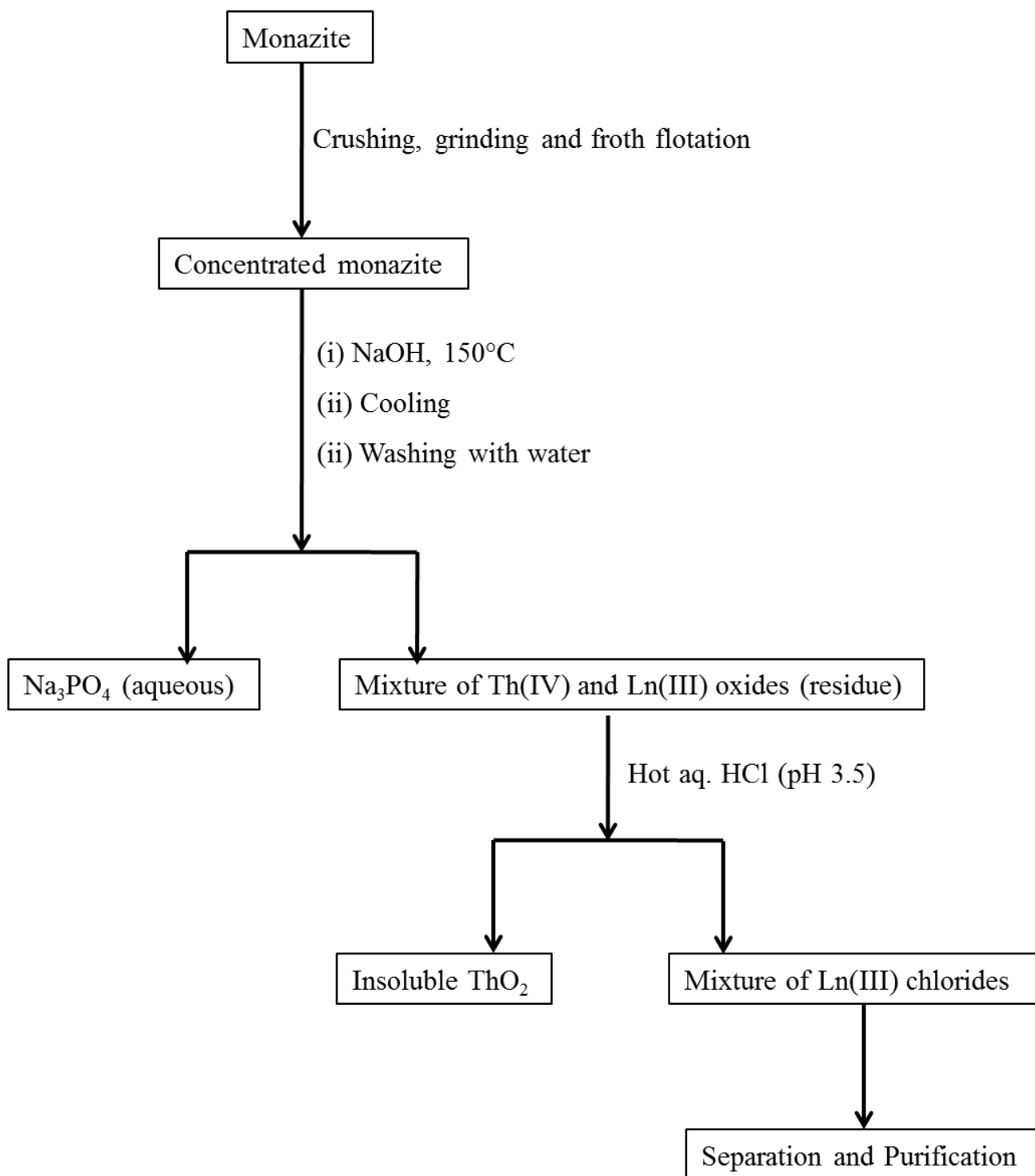
%	La	Ce	Pr	Nd	Pm	Sm	Eu	Gd	Tb	Dy	Ho	Er	Tm	Yb	Lu	Y
Monazite	20	43	4.5	16	0	3	0.1	1.5	0.05	0.6	0.05	0.2	0.02	0.1	0.02	2.5
Bastnasite	33.2	49.1	4.3	12	0	0.8	0.12	0.17	160	310	50	35	8	6	1	0.1
Xenotime	0.5	5	0.7	2.2	0	1.9	0.2	4	1	8.6	2	5.4	0.9	6.2	0.4	60.0

#Italic bold values are in ppm.

Chapter 1

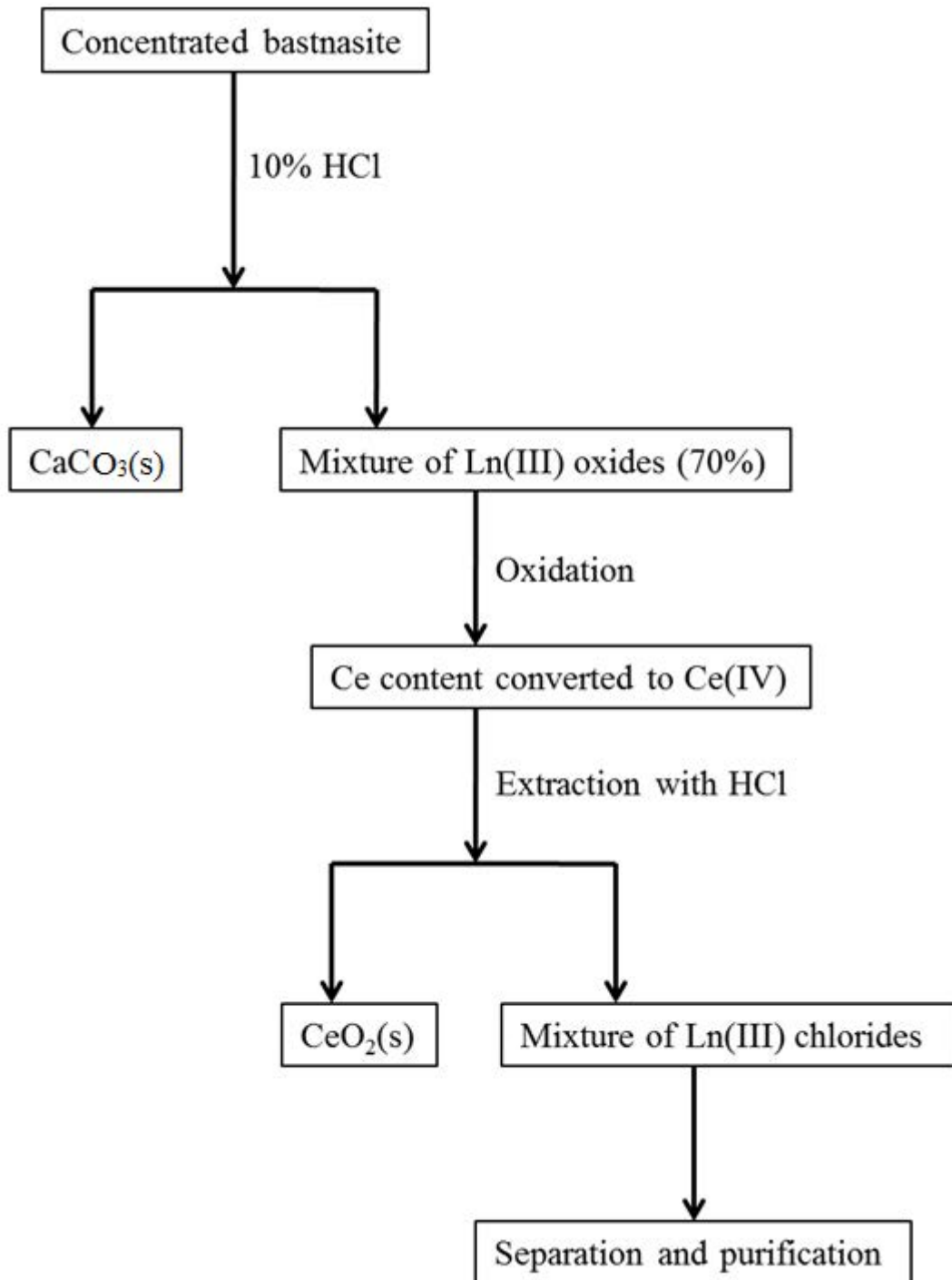
All the lanthanoids but Pm can be isolated from monazite whereas only the lighter lanthanoids can be obtained from bastnasite. The ores are first crushed, grinded and then the froth flotation technique is employed to concentrate them. After initial concentration, phosphate and thorium from monazite are removed by heating with caustic soda at 150°C. The phosphate present in the ore is converted to Na_3PO_4 . After cooling, washing with water dissolves the phosphate leaving a mixture of hydrated Th(IV) and Ln(III) oxides. Treating the residue with hot HCl (pH 3.5) gives a mixture of LnCl_3 solution and insoluble ThO_2 . The mixture of LnCl_3 solution is then purified and separated.^{2, 3} For the isolation of lanthanoids from bastnasite, previously concentrated ore is treated with 10% HCl to remove calcium carbonate. After the successful removal of calcium carbonate, the ore contains about 70% lanthanoid oxides. The cerium content of the resultant mixture is then converted to Ce(IV) by roasting in air. Additional treatment of the mixture with HCl results in an aqueous solution of LnCl_3 with insoluble CeO_2 .^{2, 3} The separation of individual lanthanoids from the mixture is difficult due to the similarities of their ion size and other properties. Solvent extraction and ion-exchange methods are employed for the separation of lanthanoids.² The simplified processes of the isolation of REE from two minerals are illustrated in Scheme 1.1 and 1.2.

Chapter 1



Scheme 1.1: Illustration of the isolation of REE from monazite.

Chapter 1



Scheme 1.2: Illustration of the isolation of REE from bastnasite.

Chapter 1

1.1.2 Electronic configurations and oxidation states

The general electronic configuration of lanthanoids is $[\text{Xe}]4f^n5d^06s^2$ except in cerium, gadolinium and lutetium. The ground state electronic configuration of lanthanum is $[\text{Xe}]5d^16s^2$ but after lanthanum, the energy of the 4f level falls below that of 5d as the 4f orbitals penetrate the xenon core more and hence the subsequent electrons are added to the shielded 4f orbitals. Ce has the arrangement $[\text{Xe}]4f^15d^16s^2$ whereas Pr avails $[\text{Xe}]4f^35d^06s^2$ configuration and this pattern continues to Eu which has half-filled ($4f^7$) f-orbital. Due to the high stability of the half-filled f subshell, the next electron in gadolinium is added to the 5d orbital giving $[\text{Xe}]4f^75d^16s^2$ configuration.

However, in terbium, the previous pattern is resumed ($[\text{Xe}]4f^95d^06s^2$) and continues to ytterbium, $[\text{Xe}]4f^{14}5d^06s^2$. After getting the more stable full-filled ($4f^{14}$) f-orbital, the next electron in lutetium goes to the 5d orbital resulting in the $[\text{Xe}]4f^{14}5d^16s^2$ configuration.^{3, 6, 9}

The electronic configuration of scandium and yttrium are $[\text{Ar}]3d^14s^2$ and $[\text{Kr}]4d^15s^2$ respectively. These two metals have no 4f electrons and are not considered as true lanthanoids. However, yttrium has some resemblance to the chemical properties of the lanthanoids because of its similar size and identical ionic charge particularly to the heavier elements. On the other hand, the chemical properties of scandium deviate slightly from the lanthanoids since it is smaller than any other lanthanoid.^{4, 10} Lanthanoids have similar chemical properties because of the small energy differences on the addition of f-electrons. Moreover, the 4f orbitals penetrate the xenon core significantly, therefore, the 4f electrons are shielded enough to prevent them from participating in bonding. Because of these shielded 4f orbitals, the lanthanoid chemistry is quite different from the d-block transition elements where the d electrons participate in chemical reactions.^{3, 6} Table 1.3 displays the different properties of lanthanoids, transition metals and group I metals.

Chapter 1

Table 1.3: Comparison of some important properties of lanthanoids, transition metals and group I metals.³

	Lanthanoids	Transition metals	Group I
Electron configurations of ions	Variable	Variable	Noble gas
Stable oxidation states	Usually 3+	Variable	1+
Coordination numbers in complexes	Commonly 8-10	Usually 6	Often 4-6
Coordination polyhedra in complexes	Minimise repulsion	Directional	Minimise repulsion
Trends in coordination numbers	Often constant in block but contraction plays a role	Often constant in Ln block	Increase down group
Donor atoms in complexes	'Hard' preferred	'Hard' and 'soft'	'Hard' preferred
Hydration energy	High	Usually moderate	Low
Ligand exchange reactions	Usually fast	Fast and slow	Fast
Magnetic properties of ions	Independent of environment	Depends on environment and ligand field	None
Electronic spectra of ions	Sharp lines	Broad lines	None
Crystal field effects in complexes	Weak	Strong	None
Organometallic compounds	Usually ionic, some with covalent character	Covalently bonded	Ionically bonded
Organometallics in low oxidation states	Few	Common	None
Multiply bonded atoms in complexes	None	Common	None

The most stable oxidation state of all lanthanoids is +3, however, complexes of +4, +2 and 0 oxidation states are also found but less frequently. The oxidation states with empty, half-filled and full-filled 4f shells are stable except Sm(II) which has 4f⁶ configuration. The divalent compounds for all lanthanoids plus yttrium have recently been published, whereas Ce, Pr and Tb can give +4 oxidation states.^{4-7, 10, 11} The electronic configuration of lanthanoids and different ions are listed in Table 1.4.

Chapter 1

1.1.3 The lanthanoid contraction

As we go across the series from La to Lu, both the atomic and ionic radii of the Ln^{3+} ions exhibit a gradual decrease. However, europium and ytterbium show a sudden increase in their atomic radii from the previous atom samarium and thulium respectively. These atoms have a tendency to adopt the +2 oxidation state with greater radii, similar to barium. On the contrary, the ionic radii of Ln^{3+} ions have a steady decrease across the series; this phenomenon is commonly known as the lanthanoid contraction.^{3,4,7}

Table 1.4: Electronic configurations of lanthanoids and different ions.²

Name of element	Symbol	Atomic number	Ground state electronic configuration			
			Ln	Ln^{2+}	Ln^{3+}	Ln^{4+}
Scandium	Sc	21	$[\text{Ar}]3d^14s^2$		$[\text{Ar}]$	
Yttrium	Y	39	$[\text{Kr}]4d^15s^2$		$[\text{Kr}]$	
Lanthanum	La	57	$[\text{Xe}]5d^16s^2$	$[\text{Xe}]5d^1$	$[\text{Xe}]4f^0$	
Cerium	Ce	58	$[\text{Xe}]4f^15d^16s^2$	$[\text{Xe}]4f^2$	$[\text{Xe}]4f^1$	$[\text{Xe}]4f^0$
Praseodymium	Pr	59	$[\text{Xe}]4f^36s^2$	$[\text{Xe}]4f^3$	$[\text{Xe}]4f^2$	$[\text{Xe}]4f^1$
Neodymium	Nd	60	$[\text{Xe}]4f^46s^2$	$[\text{Xe}]4f^4$	$[\text{Xe}]4f^3$	
Promethium	Pm	61	$[\text{Xe}]4f^56s^2$	$[\text{Xe}]4f^5$	$[\text{Xe}]4f^4$	
Samarium	Sm	62	$[\text{Xe}]4f^66s^2$	$[\text{Xe}]4f^6$	$[\text{Xe}]4f^5$	
Europium	Eu	63	$[\text{Xe}]4f^76s^2$	$[\text{Xe}]4f^7$	$[\text{Xe}]4f^6$	
Gadolinium	Gd	64	$[\text{Xe}]4f^75d^16s^2$	$[\text{Xe}]4f^75d^1$	$[\text{Xe}]4f^7$	
Terbium	Tb	65	$[\text{Xe}]4f^96s^2$	$[\text{Xe}]4f^9$	$[\text{Xe}]4f^8$	$[\text{Xe}]4f^7$
Dysprosium	Dy	66	$[\text{Xe}]4f^{10}6s^2$	$[\text{Xe}]4f^{10}$	$[\text{Xe}]4f^9$	$[\text{Xe}]4f^8$
Holmium	Ho	67	$[\text{Xe}]4f^{11}6s^2$	$[\text{Xe}]4f^{11}$	$[\text{Xe}]4f^{10}$	
Erbium	Er	68	$[\text{Xe}]4f^{12}6s^2$	$[\text{Xe}]4f^{12}$	$[\text{Xe}]4f^{11}$	
Thulium	Tm	69	$[\text{Xe}]4f^{13}6s^2$	$[\text{Xe}]4f^{13}$	$[\text{Xe}]4f^{12}$	
Ytterbium	Yb	70	$[\text{Xe}]4f^{14}6s^2$	$[\text{Xe}]4f^{14}$	$[\text{Xe}]4f^{13}$	
Lutetium	Lu	71	$[\text{Xe}]4f^{14}5d^16s^2$	$[\text{Xe}]4f^{14}5d^1$	$[\text{Xe}]4f^{14}$	

Chapter 1

Due to the shielded nature of 4f orbitals, they cannot compensate for the effect of increased nuclear charge after the addition of electrons, consequently, the size decreases.⁴ The trends in atomic and ionic radii are listed in Table 1.5 as well as shown in Fig. 1.1.

Table 1.5: Atomic and ionic radii of the lanthanoids (pm).³

La	Ce	Pr	Nd	Pm	Sm	Eu	Gd	Tb	Dy	Ho	Er	Tm	Yb	Lu
187.7	182.5	182.8	182.1	181.0	180.2	204.2	180.2	178.2	177.3	176.6	175.7	174.6	194.0	173.4
La ³⁺	Ce ³⁺	Pr ³⁺	Nd ³⁺	Pm ³⁺	Sm ³⁺	Eu ³⁺	Gd ³⁺	Tb ³⁺	Dy ³⁺	Ho ³⁺	Er ³⁺	Tm ³⁺	Yb ³⁺	Lu ³⁺
103.2	101.0	99.0	98.3	97.0	95.8	94.7	93.8	92.3	91.2	90.1	89.0	88.0	86.8	86.1

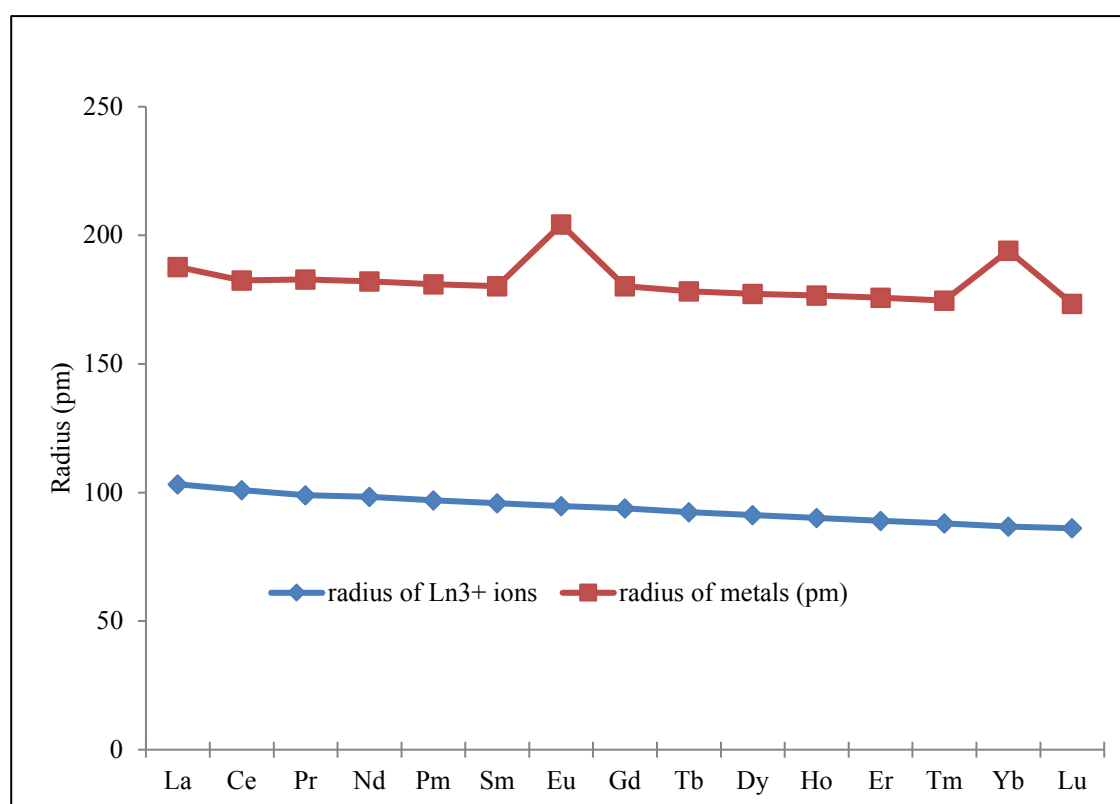


Fig. 1.1: Metallic and ionic radii of lanthanoids.

Chapter 1

1.1.4 Coordination chemistry of lanthanoids

The lanthanoids have diverse coordination chemistry compared to that of transition metals.^{3, 9} Lanthanoids adopt variable coordination numbers ranging from three to 12 whereas many transition metals have definite coordination numbers.^{3, 6} Because of the variable coordination number, X-ray crystallography is the ultimate way to determine the actual coordination number of lanthanoids.³ Though both low and high coordination numbers are possible, lanthanoids favour the high coordination numbers due to their large ionic radii and high charge. Low coordination numbers are favoured by bulky ligands and high coordination numbers (10 or more) necessitates chelating ligands having small bites such as sulphate or nitrate groups. Moreover, the high coordination numbers are more common in larger, lighter lanthanoids than in heavier, smaller cations.⁹ The geometry of compounds is dependent on the coordination numbers. The coordination number and the corresponding geometry are furnished in Table 1.6.

Table 1.6: Coordination numbers and corresponding geometry of Ln³⁺ ions.¹²

Coordination number (CN)	Common geometry
3	Planar/Pyramidal
4	Tetrahedral
5	Square pyramidal/Trigonal bipyramidal
6	Octahedral
7	Monocapped trigonal prism
8	Square antiprism/dodecahedral
9	Tricapped trigonal prism/Trigonal prism/Monocapped square antiprism
10	Bicapped dodecahedron/Pentagonal antiprism
11	Monocapped pentagonal antiprism
12	Icosahedron

Chapter 1

1.1.5 Organometallic chemistry of lanthanoids

Organometallic chemistry is a particularly interesting sub-branch of inorganic chemistry because of the practical applications of organometallic compounds. Generally, organometallic compounds contain at least one metal-carbon bond. However, some zero-valent metal complexes, hydrides, and dinitrogen complexes having no metal-carbon bonds are regarded as organometallic compounds because of their similar chemical properties and reactivities with organometallic compounds.¹³ In contrast, metal cyanides possessing an M–C bond are excluded from organometallic compounds as they behave mostly like inorganic coordination compounds. The shielded f-orbitals in lanthanoids have limited interaction with ligands and the outer 5d, 6s and 6p orbitals are responsible for the bonding with ligands. Due to the presence of vacant d, s and p orbitals, lanthanoid ions are hard Lewis acids and facilitate bonding with hard bases having O, N, and light halide donor atoms.^{5, 7, 13} Organolanthanoid complexes are highly air and moisture sensitive because of having high affinity to oxygen and are handled with care under inert atmosphere.^{3, 13, 14}

The organometallic chemistry of lanthanoids has started flourishing after 1980, however, the organolanthanoid complexes of cyclopentadienyl were reported more than 60 years ago.¹⁵ The modern analytical techniques, especially, single crystal X-ray diffraction has enabled us to understand the structures of these air and moisture sensitive compounds.¹⁶ The progress of organolanthanoid chemistry depends on the exploration of new ligand systems and therefore, the challenge is now to find ligands other than bulky cyclopentadienyl to take forward this novel field.

1.2 The alkaline earth elements

The group II elements in the periodic table consisting of beryllium (Be), magnesium (Mg), calcium (Ca), strontium (Sr), barium (Ba), and radium (Ra) are known as alkaline earth metals. They are called alkaline earth metals because they form alkaline solutions (hydroxides) after reacting with water, and are found in the earth's crusts.¹⁷ They are highly reactive (less reactive than group I), typically divalent, and commonly form

Chapter 1

colourless ionic compounds. Radium is extremely scarce as well as radioactive and is formed in the ^{238}U decay series as ^{226}Ra (half-life 1622 year). It was discovered by Pierre and Marie Curie from the uranium ore pitchblende.^{2, 10, 18} Beryllium is not readily available metal in the earth's crust; however, it is found in the pegmatite rocks as surface deposits of beryl, $\text{Be}_3\text{Al}_2[\text{Si}_6\text{O}_{18}]$.¹⁹ Magnesium is the eighth most abundant element in the earth's crust and third most abundant in the sea.² Calcium is the fifth most abundant element while strontium and barium are less bountiful but not rare.²⁰ The elements magnesium, calcium, strontium and barium are widely distributed in minerals and as dissolved salts in the ocean.² Barium, calcium and strontium are silvery metals, while beryllium and magnesium are greyish white in colour.¹⁰

1.2.1 Occurrence and isolation

The alkaline earth elements are mostly found in the earth's crust as different minerals as well as some in the ocean as dissolved salts. Beryllium is the least abundant among the alkaline earths because it is difficult to extract. It exists in the silicate minerals beryl, $\text{Be}_3\text{Al}_2[\text{Si}_6\text{O}_{18}]$ and phenacite, Be_2SiO_4 in small quantities. Moreover, it is found in the precious minerals emerald and aquamarine.² In 1798, beryllium was first discovered by the French chemist Louise Nicholas Vauquelin and named the element glaucinium (Greek glykys = sweet) because its compounds tasted sweet.¹⁹ The name beryllium derives from the gemstone beryl, which incorporates this element. Magnesium is the eighth most abundant element in the earth's crust and considerable amount of magnesium salts are available in the ocean (about 0.13%). In 1755, magnesium oxide was separated from lime by Joseph Black and magnesium metal was isolated through electrolysis by Humphry Davy in 1808.²⁰ Dolomite ($\text{MgCO}_3 \cdot \text{CaCO}_3$) and magnetite (MgCO_3) are the carbonate minerals of magnesium, and are found in China, North Korea, Austria, Turkey and Greece.¹⁸ There are also deposits of sulphates, for example, epsomite ($\text{MgSO}_4 \cdot 7\text{H}_2\text{O}$) and kieserite ($\text{MgSO}_4 \cdot \text{H}_2\text{O}$). Carnalite ($\text{KCl} \cdot \text{MgCl}_2 \cdot 6\text{H}_2\text{O}$) is a mineral of magnesium; however, it is used to extract potassium. A wide range of silicate minerals including olivine ($(\text{Mg}, \text{Fe})_2\text{SiO}_4$), talc ($\text{Mg}_3(\text{OH})_2\text{Si}_4\text{O}_{10}$), chrysotile ($\text{Mg}_3(\text{OH})_4\text{Si}_2\text{O}_5$) and micas such as $\text{K}^+[\text{Mg}_3(\text{OH})_2(\text{AlSi}_3\text{O}_{10})^-]$ are the sources of magnesium.¹⁸

Chapter 1

Calcium is the fifth most abundant element in the earth's crust and exists in many common minerals all over the world. The common minerals of calcium are the limestone (CaCO_3), gypsum ($\text{CaSO}_4 \cdot 2\text{H}_2\text{O}$), fluorite (CaF_2) and apatite ($\text{Ca}_5(\text{PO}_4)_3(\text{F}, \text{Cl}, \text{OH})$). Limestone can be found in two crystalline forms such as calcite and aragonite. Calcite is the most common and forms rhombohedral colourless crystals. Aragonite is commonly red-brown or yellow in colour (colours derive from impurities) and is responsible for the colour of the landscape of the red sea area, the Bahamas and the Florida Keys; the crystals are orthorhombic. Limestone is a source of CaO and has enormous commercial importance. The natural abundance of strontium and barium are far less than those of magnesium and calcium. However, they are well known due to their occurrence as concentrated ores which makes their extraction easier. The minerals of strontium are celestite (SrSO_4) and strontianite (SrCO_3) whereas the one and only available mineral of barium is baryte (BaSO_4). Radium is radioactive and extremely scarce. The Nobel Prize for Chemistry was awarded to Marie Curie for isolating radium from uranium ore pitchblende. The natural abundances of beryllium, magnesium, calcium, strontium and barium (in ppm) are shown in Fig. 1.2 (Logarithm of the abundances are taken).²

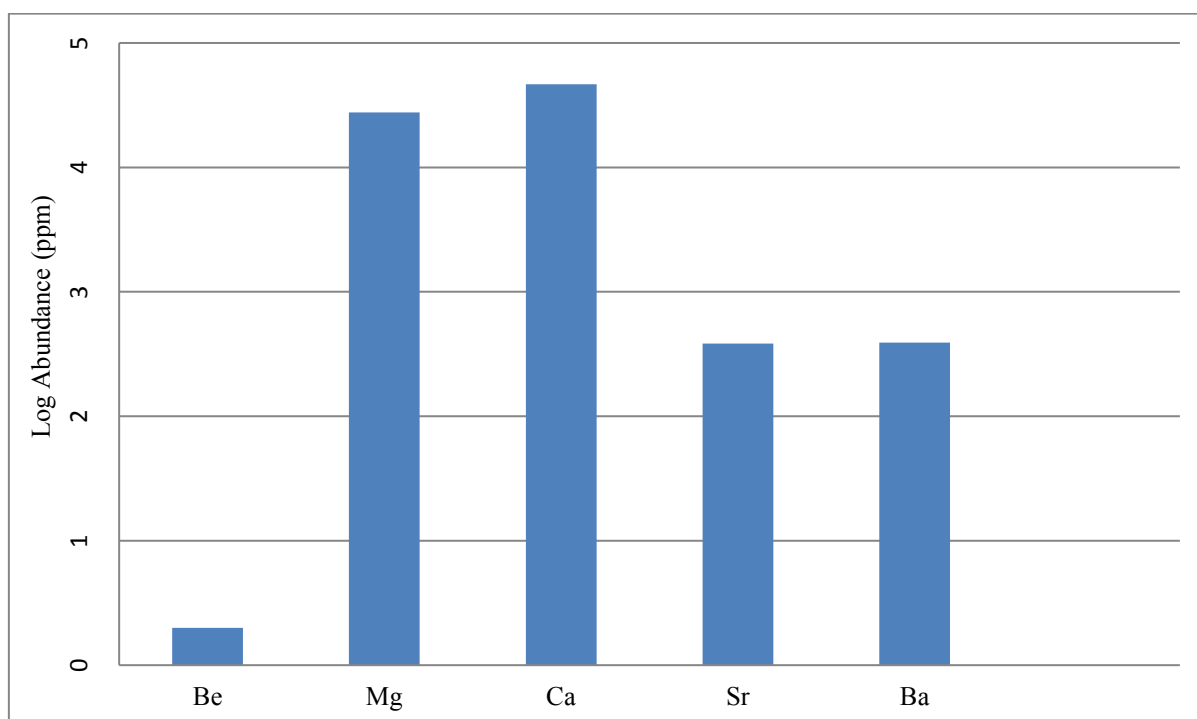


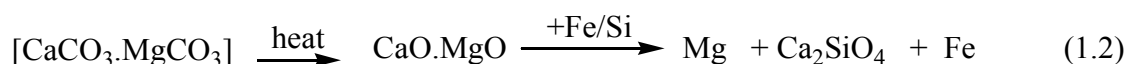
Fig. 1.2: Abundance of the alkaline earth elements in the earth's crust in ppm (excluding Ra).

Chapter 1

Extraction of the group two metals by chemical reduction is not easy as they are strong reducing agents and they react with carbon to form carbides. They are very reactive, react promptly with water and strongly electropositive, therefore, they cannot be displaced with another metal in aqueous solutions. Electrolysis of the fused chloride of the metals (NaCl added to lower the melting point) can be used to extract the metals; however, strontium and barium have a tendency to form a colloidal suspension.^{2, 18} To extract beryllium, beryll is heated with Na_2SiF_6 to get water soluble BeF_2 and $\text{Be}(\text{OH})_2$ precipitate. Then beryllium is obtained either by reduction of BeF_2 with Mg (Eqn. 1.1), or by the electrolysis of BeCl_2 fused with sodium chloride.^{2, 18}



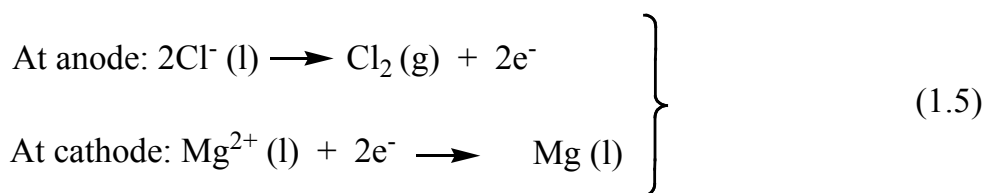
Magnesium is the only alkaline earth metal produced on a large scale. It is either produced by thermal decomposition of dolomite or by the electrolysis of fused MgCl_2 . Dolomite is thermally decomposed to MgO and CaO at about $1177\text{ }^\circ\text{C}$, MgO is then reduced to Mg by ferrosilicon in Ni vessels (Eqn. 1.2). Finally, Mg is separated by vacuum distillation.^{2, 18}



Electrolysis of fused MgCl_2 is also important and involves the production of MgCl_2 from sea water followed by the electrolysis of it. At first step, slaked lime, $\text{Ca}(\text{OH})_2$ is added to the sea water, and calcium ions dissolved and $\text{Mg}(\text{OH})_2$ is precipitated (Eqn. 1.3). $\text{Mg}(\text{OH})_2$ is then filtered off, neutralised with HCl followed by evaporation and heating at $717\text{ }^\circ\text{C}$ to produce anhydrous MgCl_2 (Eqn. 1.4). Finally, magnesium is obtained by the electrolysis of the molten MgCl_2 and solidification of it (Eqn. 1.5).^{2, 18}



Chapter 1



Calcium metal is produced by the electrolysis of fused CaCl_2 and CaF_2 . The CaCl_2 is obtained either as a waste product from the Solvay process, or from CaCO_3 and HCl . The strontium and barium metals are extracted on a smaller scale by the reduction of the corresponding oxides by aluminium or by electrolysis of their fused chlorides.^{2, 18}

1.2.2 Electronic configurations, oxidation states and properties

The electronic configurations and some other physical parameters of the alkaline earth metals are shown in Table 1.7. The valence shell of these elements has two s electrons; the loss of the two valent s electrons results in a stable noble gas electronic configuration.^{17, 19} Considering the size of the elements, the alkaline earth elements can simply be classified into two groups; beryllium and magnesium as light alkaline earths while the heavy alkaline earths comprise of calcium, strontium, barium and radium.¹⁹ The omnipresent +2 oxidation state of the alkaline earth elements are due to their tendency to lose the two s electrons in the ultimate shell to get a noble gas configuration.¹⁹ The alkaline earth elements are highly electropositive like rare earth elements, demonstrated by their chemical reactivity and standard electrode potential.¹⁰

Table 1.7: Pertinent properties of the alkaline earth elements.^{2, 10}

Element	Electronic configuration	Melting point (°C)	Ionic radii (Å)	E° (V) vs SHE [$\text{M}^{2+}(\text{aq}) + 2\text{e} \rightarrow \text{M}(\text{s})$]
Be	[He] $2s^2$	1278	0.34	-1.85
Mg	[Ne] $3s^2$	651	0.78	-2.37
Ca	[Ar] $4s^2$	843	1.06	-2.87
Sr	[Kr] $5s^2$	769	1.27	-2.89
Ba	[Xe] $6s^2$	725	1.43	-2.90
Ra	[Rn] $7s^2$	400	1.57	-2.92

Chapter 1

Beryllium has a high charge/size ratio, and consequently most beryllium compounds are covalent rather than ionic, although forms a cationic complex $[\text{Be}(\text{H}_2\text{O})_4]^{2+}$ with neutral ligand water. The chemistry of magnesium is intermediate between that of beryllium and the heavier elements, heavier elements form ionic complexes.^{2, 10} Calcium, strontium, barium, and radium form a series with closely connected physical and chemical properties of the elements and their compounds vary systematically with increasing size. Radium is the most electropositive among the alkaline earths and shows the highest ionic nature.¹⁰ Calcium and strontium ions have the similar ionic radii and chemical properties as the lanthanoid ions Yb^{2+} and Eu^{2+} respectively.^{10, 19} Beryllium and magnesium do not give any colour to a flame test while the flame test can be used to distinguish between compounds of calcium (orange-red, but pale green when viewed through blue glass), strontium (crimson, but violet through blue glass) and barium (apple-green).²

1.2.3 Uses of alkaline earth elements

Beryllium is used in the manufacture of the body parts in high speed aircraft, missiles and in communication satellites as it is one of the lightest metals known. Moreover, it has a high thermal conductivity, a very high melting point, inertness towards aerial oxidation and non-magnetic in nature. The high melting point and low cross-section for neutron capture enables beryllium to be useful in the nuclear energy industry. Due to its low electron density, Be is a poor absorber of electromagnetic radiation, and is used in X-ray tube windows.² Magnesium and aluminium alloys have greater mechanical strength and resistance to corrosion as a result of the presence of magnesium, and fabrication properties show a significant improvement. Therefore, Mg/Al alloys are used in aircraft and automobile body parts and lightweight tools. Other uses include flares, fireworks and photographic flashlights. Mg also has some medical applications including the indigestion powders, milk of magnesia, $\text{Mg}(\text{OH})_2$ and a purgative (epsom salts, $\text{MgSO}_4 \cdot 7\text{H}_2\text{O}$). Mg^{2+} is an essential component of chlorophyll in green plants and both Mg^{2+} and Ca^{2+} ions are used as catalysts for diphosphate-triphosphate transformations in biological systems.²

Calcium compounds have a wide variety of uses, for example, calcium oxide is used in building mortar, and calcium carbonate is used in the manufacture of steel, glass, cement and concrete. Recently, calcium carbonate and calcium hydroxide are used for the

Chapter 1

desulphurisation processes. A huge quantity of calcium hydroxide is also used for the production of bleaching powder and in water treatment. Strontium minerals are used in the manufacture of faceplate glass in colour television cathode-ray tubes in order to stop X-ray emissions. Moreover, SrO enhances the television picture quality. Barium sulphate is used as a weighting material in oil- and gas-well drilling fields. The ability of barium sulphate to stop the passage of X-rays leads to its use as a 'barium meal' in radiology for imaging the alimentary tract. Radium was extensively used in radiotherapy, however has been superseded by radioisotopes synthesised in nuclear reactors.²

1.2.4 Organometallic chemistry of alkaline earth elements

In the last 25 years, the organometallic chemistry of alkaline earth metals has undergone a renaissance; especially the heavy organoalkaline-earth metal compounds have been recognised to have significant potential.²¹ However, the organomagnesium compounds (Grignard reagents) have been widely used in organic and inorganic syntheses since their discovery in 1900.¹⁰ These compounds have potential applications in different areas including polymerization initiation, organic synthetic chemistry, catalysis, and materials chemistry.²¹ Organoberyllium compounds are highly toxic, extremely reactive, and are not explored extensively.²² Organometallic chemistry of the heavier elements has focused on the cyclopentadienyls and other π -systems such as fluorenyl and indenyl.²³⁻³² This is due to the unique capability of this system to stabilise the alkaline earth metal centres sterically and electronically.³³ Organometallic compounds of alkaline earth metals need to be handled under air and moisture free conditions similar to the organometallic rare earth complexes.

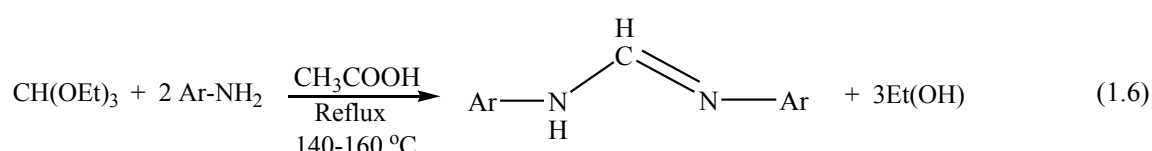
1.3 The ligands

Ligands are ions or neutral molecules that bond to a central metal atom or ion to form a complex. Electronic as well as the steric ligand effects play a major role in the synthesis of organometallic complexes.³⁴ To find a new ligand system other than the ubiquitous cyclopentadienyl-based ligands is the most challenging job in organometallic chemistry.

Chapter 1

We intend to use two different categories of ligands for this work. Firstly, we chose arenes (toluene and mesitylene) as ligands to synthesise rare earth species as well as some heavy alkaline earth complexes. There are several reasons for the interest in arenes as a ligand in organometallic chemistry. For example, (i) arenes are readily available to use; (ii) in terms of catalysis, arenes are easier to substitute by incoming substrates compared to the negatively charged cyclopentadienyl ligands; (iii) by varying the nature of the ancillary ligands, a variation in the hapticity of the arene ligands could be generated; (iv) arene complexes are highly reactive and are potential precursors for catalysts such as in hydrogenation and polymerisation reactions and (v) synthesis of potential derivatives of the arene complexes.

Secondly, the highly versatile and readily available N,N'-bis(aryl)formamidinate ligands have been chosen for this research, though several alternatives of cyclopentadienyl-based ligands are on hand. Formamidinates are the most prominent and are easily tuneable both electronically as well as sterically. These ligands can easily be synthesized in high yields by heating one equivalent of triethyl orthoformate and two equivalents of the appropriate substituted aniline (Eqn. 1.6) to reflux usually in the presence of acetic acid catalyst.^{35, 36} By changing the substituents on the aryl groups, the ligands can be sterically and electronically modulated.



1.3.1 Bulky ligands in rare earths organometallic chemistry

Bulky ligands not only stabilise low coordination numbers but also focus reactivity to a small defined portion of the metal surface thereby enhancing control and selectivity. A much wider range of ligand types, other than cyclopentadienyl ligand, greatly increases possible steric and electronic variation, hence increasing the possibility of stabilising terminal alkyls, hydrides and fluorides. Bulky ligands can be used to induce C-X (e.g. X = F, Cl, Br, H) activation either by steric engineering or through C-X-Ln complexation and to promote reductive behaviour in the normally non-reducing Ln(III) state.^{37, 38}

Chapter 1

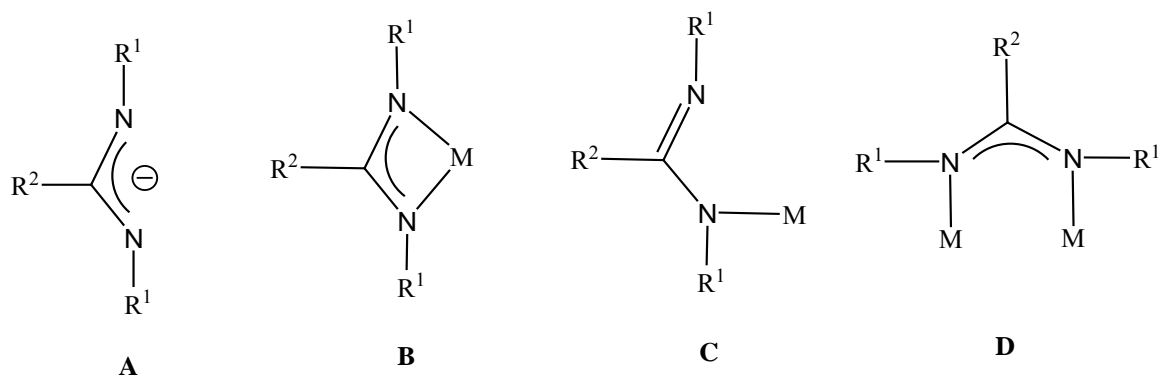
1.3.2 Chemistry of the formamidinate ligands

Anionic N-centred donor ligands have been extensively used in the field of organometallic chemistry as well as in coordination chemistry. Though several alternatives of cyclopentadienyl-based ligands are on hand, the highly versatile amidinate anion is most prominent and readily available.^{39, 40} The amidinate chemistry has started its journey with the discovery of N,N,N'-tris(trimethylsilyl) benzamidinate, $\text{PhC(=NSiMe}_3\text{)[N(SiMe}_3\text{)}_2]$ in 1973.⁴¹ Amidinate anions having the general formula, $[\{\text{R}^1\text{NC(R}^2\text{)=NR}^1\}]^-$ (where, $\text{R}^1 = \text{H, alkyl, cycloalkyl, aryl, trimethylsilyl}$ and $\text{R}^2 = \text{H, alkyl, aryl}$), are readily tuneable electronically as well as sterically and form different compounds with transition, main group and rare earth metals.^{39, 40} The amidinate ligands can be tuned by inserting different substituents both at the backbone carbon and nitrogen atoms. Moreover, they can easily be prepared with commercially available starting materials and considered as steric cyclopentadienyl equivalents.^{42, 43}

When the substituent at backbone carbon of amidinates is a proton, the amidinates are known as formamidinates. The steric and electronic effects of a proton at the backbone carbon of formamidinate, $[\text{RNC(H)=NR}]^-$, is lower compared to other amidinates.^{37, 38, 44, 45} Moreover, the backbone carbon can be used as a key tool to follow the reaction pathways or the formation of new formamidinate complexes by changes in the NMR spectrum since the resonances are often distinct from the other protons in the molecule.⁴⁶ The substituents on the aryl rings can be changed and this affects their solubilities as well as altering the steric and electronic effects.^{35, 37, 47, 48}

The coordination chemistry of amidinates exhibit both chelating and bridging modes. The general structures of amidinate anions as well as their various coordination modes are shown in scheme 1.3.^{39, 40, 42} The most common coordination mode involves the chelating mode (B) whereas the monodentate metal coordination (C) is rare. The monodentate coordination can be found in amidinates with extremely bulky substituents. In addition, the bridging coordination mode (D) is common in transition metal chemistry.^{39, 40, 42}

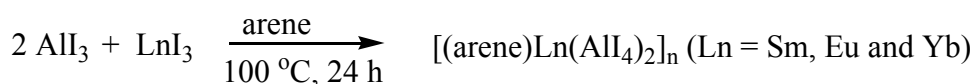
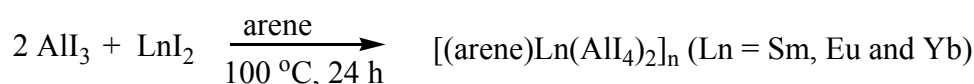
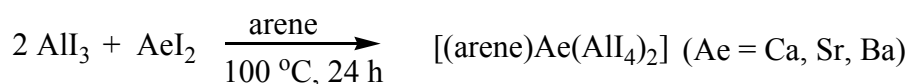
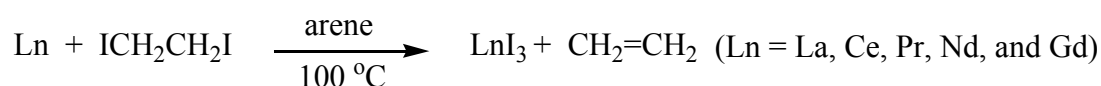
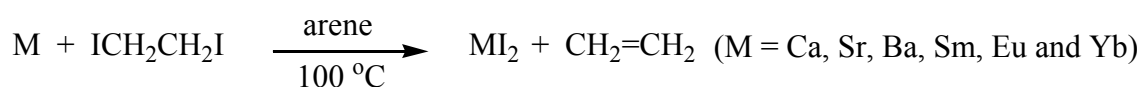
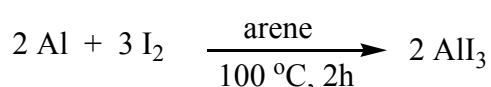
Chapter 1



Scheme 1.3: General structure of amidinate anions (A) and various coordination modes of amidinates (B-D).

1.3.3 Synthetic pathways

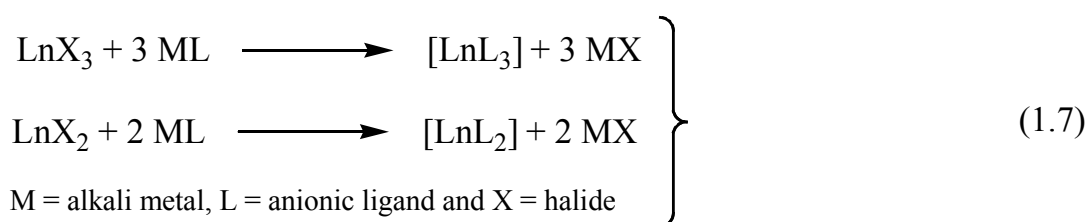
A viable synthetic approach for the arene complexes involves the one pot reaction between aluminium halides and lanthanoid halides or alkaline earth halides in the corresponding arene solvent. The aluminium iodide is prepared in a Schlenk flask by heating aluminium powder and iodine in arene solvents. Then stoichiometric amount of metal (lanthanoids or alkaline earths) and diiodoethane have been added to the aluminium iodide solution. After heating the mixture for approx. 24 hours, the corresponding arene complexes have been crystallised at room temperature (Scheme 1.4).



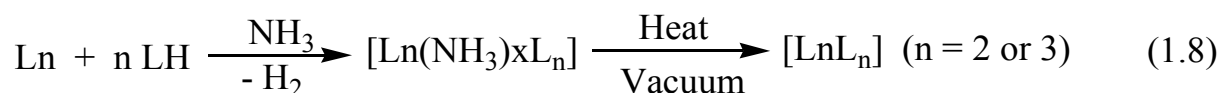
Scheme 1.4: Synthetic routes for the arene complexes of rare earths and alkaline earths.

Chapter 1

Synthetic approaches for the lanthanoid formamidinate complexes involve metathesis or salt elimination, direct metalation, protolysis, and redox transmetalation/protolysis (RTP) reactions. The treatment of the rare earth halides with alkali metal substituted ligands are known as the metathesis or salt elimination reactions (Eqn. 1.7).⁴⁹⁻⁵² Metathesis reactions occasionally result in low yields or form unwanted side products where the alkali metal can be retained forming an 'ate' species or the alkali metal halide binds to the lanthanoid complex.⁵³

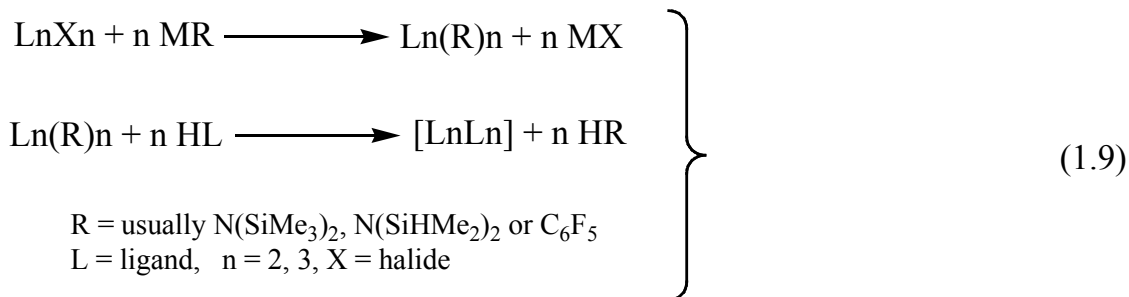


Direct metalation involves the direct reaction between the ligand and the metal in a suitable solvent (Eqn. 1.8). Since the rare earths are highly electropositive, the presence of an oxide layer on their surface impedes the metal-based reactions. Therefore, activation of the metal surface is required. Usually, the metals are activated by the condensation of ammonia into the reaction mixture, or the addition of mercury salts or mercury metal.⁵⁰

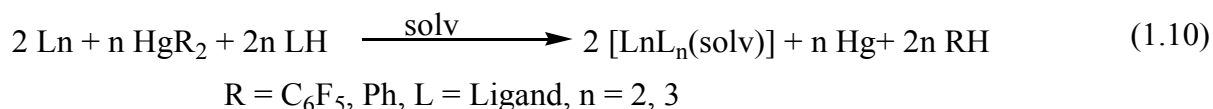


In protolysis reactions, a lanthanoid precursor, LnR_n is treated with a protic ligand, LH (Eqn. 1.9).^{49, 50, 54-58} As the reactants are highly soluble in common solvents, this reaction can be performed in the absence of coordinating/donor solvents.⁵⁰ As a result this reaction is a highly versatile approach for the synthesis of homoleptic complexes; heteroleptic complexes can be synthesized by using coordinating/donor solvents.^{51, 55, 57, 59, 60} Two steps requirements are the main disadvantage of the protolysis reactions, each step involves air and moisture sensitive compounds.

Chapter 1



To overcome these issues, the redox transmetalation/protolysis (RTP) reaction using organomercurals is an alternative route to get various organolanthanoid complexes. RTP involves the treatment of a rare earth metal with a diarylmercurial such as diphenylmercury (weaker oxidant) or bis(pentafluorophenyl)mercury (stronger oxidant) and a protic ligand (Eqn. 1.10).^{37, 54, 61-69} As this route is a one-pot procedure and the only air-sensitive material is the lanthanoid metal, it is more straightforward compared to the metathesis or protolysis routes. Donor solvents such as tetrahydrofuran (THF) or 1,2-dimethoxyethane (DME) are normally used in RTP reactions. However, reaction in a non-donor solvent, for example in toluene requires more forcing conditions (heating).⁷⁰ The key disadvantage of this type of reactions is the involvement of mercury reagents as it raises environmental concerns and requires care in handling.⁷¹



1.4 The current study

This thesis focuses on the synthesis and characterisation of lanthanoid formamidates and halogenoaluminate complexes of rare earths and alkaline earths. Four different formamidates (Fig. 1.3) of varying steric bulk have been used for the study of lanthanoid formamidinate chemistry. For the halogenoaluminate complexes, we have chosen two aromatic ligand such as toluene and mesitylene.

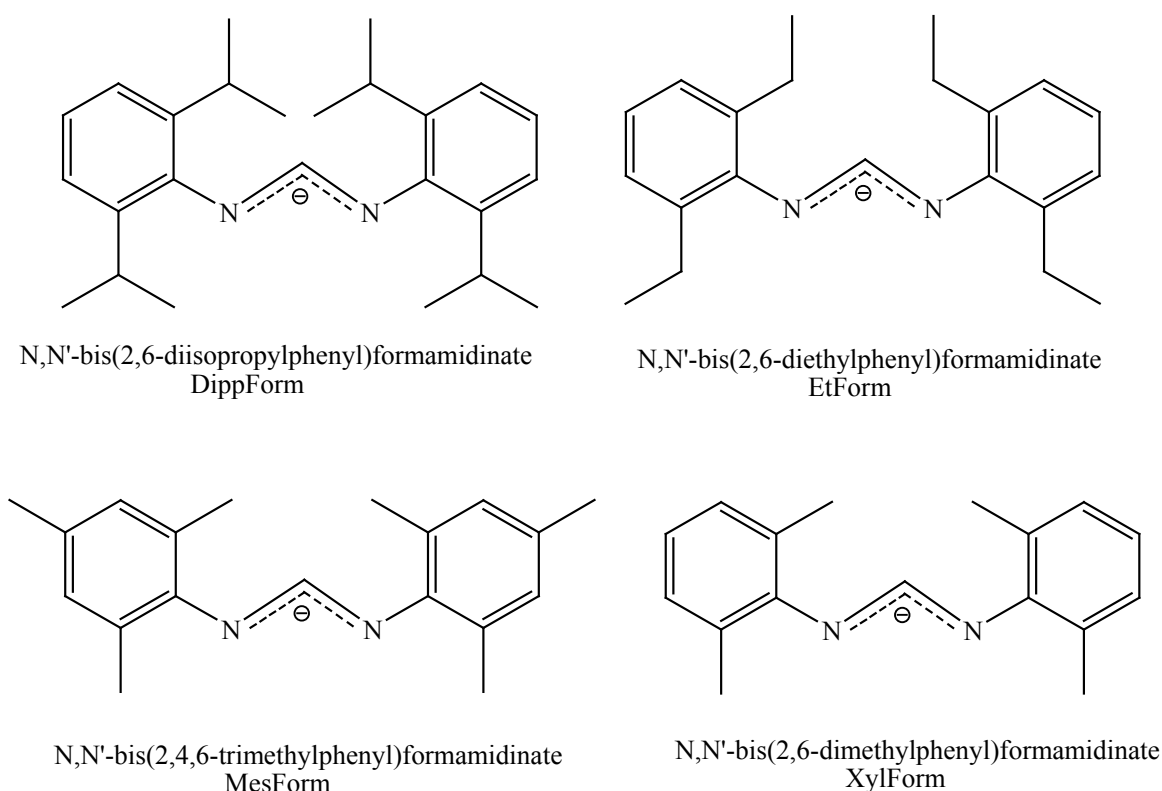


Fig. 1.3: Formamidinate ligands used in chapter 4.

Chapter 2 investigates the chemistry of lanthanoid halogenoaluminate π -arene complexes. A series of iodoaluminate π -arene complexes have been synthesised using two different arenes such as toluene and mesitylene. In addition, some bromoaluminate complexes have been isolated. Catalytic activity of the neodymium complex $[\text{Nd}(\eta^6\text{-C}_6\text{H}_5\text{Me})(\text{AlI}_4)_3]$ has been studied for isoprene polymerisation, and found comparable with the literature.⁷²

Chapter 1

Chapter 3 discusses the isolation and characterisation of iodoaluminate π -arene complexes of alkaline earths. These are the first ever reported bimetallic complexes of alkaline earths featuring metal- π arene interactions and are synthesised using two different arenes such as toluene and mesitylene.

Chapter 4 ventures away from the halogenoaluminate π -arene complexes and discusses the chemistry of lanthanoid formamidinates. The reactivity of divalent formamidinate lanthanoids has been examined, and halide abstraction reactions have been performed to obtain cationic complexes. However, the reactions to obtain cationic complexes from the halide abstraction route have been unsuccessful at this stage. An unusual cobalt complex, $[\text{Co}(\text{DippFormCO})(\text{CO})_3]\cdot\text{THF}$ was isolated from one of the attempted syntheses of a cationic complex. Moreover, for the first time a mixed formamidinate complex of ytterbium $[\text{Yb}(\text{DippForm})(\text{XylForm})_2]\cdot\text{PhMe}$ was deliberately synthesised (using RTP with different ligands) and characterised.

1.5 References

1. T. Saito, *Inorganic Chemistry*, Kanagawa University, Yokohama, 2004.
2. C. E. Housecroft and A. G. Sharpe, *Inorganic Chemistry*, Pearson Education Ltd., London, 2005.
3. S. Cotton, *Lanthanide and actinide chemistry*, John Wiley & Sons, Chichester, 2006.
4. T. Moeller, *The Chemistry of the Lanthanides*, Reinhold Publishing Corporation, New York, 1963.
5. B. T. Kiboum, *A Lanthanide Lanthology, Part II, M-Z*, Molycorp Inc., New York, 1994.
6. T. Imamoto, in *Lanthanides in Organic Synthesis*, eds. A. R. Katritzky, O. Meth-Cohn and C. W. Rees, Academic Press, London, 1994.
7. B. T. Kiboum, *A Lanthanide Lanthology, Part I, A-L*, Molycorp Inc., New York, 1993.
8. P. L. Watson, presented in part at the Rare Earth Horizons 1987, NSW, April, 1987.
9. C. M. Sturza, R. Boscencu and V. Nacea, *Farmacia*, 2008, **3**, 326-338.
10. F. A. Cotton, G. Wilkinson, C. A. Murillo and M. Bochman, *Advanced Inorganic Chemistry*, John Wiley & Sons, New York, 1999.
11. M. R. MacDonald, J. E. Bates, J. W. Ziller, F. Furche and W. J. Evans, *J. Am. Chem. Soc.*, 2013, **135**, 9857-9868.
12. D. J. Evans, PhD thesis, Monash University, 2005.
13. S. Komiya, K. Tatsumi, K. Mashima, T. Ito, M. Hurano, A. Fukuoka, F. Ozawa, K. Maruoka, Miyaura and T. Takeda, in *Synthesis of organometallic compounds: A*

Chapter 1

- practical guide*, ed. S. Komiya, John Wiley & Sons, Chichester, 1st edn., 1997, pp. 1-74.
14. F. T. Edelman, in *Comprehensive Organometallic Chemistry II*, eds. E. W. Abel, F. G. A. Stone and G. Wilkinson, Pergamon Press, Oxford, 1995, vol. 4, ch. 2.
 15. G. Wilkinson and J. Birmingham, *J. Am. Chem. Soc.*, 1954, **76**, 6210.
 16. C.-H. Huang, *Rare earth coordination chemistry: fundamentals and applications*, John Wiley & Sons, Singapore, 2011.
 17. R. D. Madan, *Modern Inorganic Chemistry*, S. Chand Publishing, New Delhi, 1987.
 18. J. D. Lee, *Concise Inorganic Chemistry*, Chapman & Hall, London, 1991.
 19. N. N. Greenwood and A. Earnshaw, *Chemistry of the Elements*, Butterworth-Heinemann, Oxford, 1997.
 20. R. E. Krebs, *The History and Use of Our Earth's Chemical Elements: A Reference Guide*, Greenwood Press, Connecticut, 1998.
 21. A. G. Goos, P. J. R. Flores, Y. Takahashi and K. Ruhlandt-Senge, in *Encyclopedia of Inorganic and Bioinorganic Chemistry*, John Wiley & Sons, 2011.
 22. D. Naglav, M. R. Buchner, G. Bendt, F. Kraus and S. Schulz, *Angew. Chem. Int. Ed.*, 2016, **55**, 10562-10576.
 23. R. A. Williams, T. P. Hanusa and J. C. Huffman, *J. Am. Chem. Soc.*, 1990, **112**, 2454-2455.
 24. F. Weber, H. Sitzmann, M. Schultz, C. D. Sofield and R. A. Andersen, *Organometallics*, 2002, **21**, 3139-3146.
 25. R. A. Williams, T. P. Hanusa and J. C. Huffman, *Organometallics*, 1990, **9**, 1128-1134.
 26. C. J. Burns and R. A. Andersen, *J. Organomet. Chem.*, 1987, **325**, 31-37.

Chapter 1

27. M. Schultz, C. J. Burns, D. J. Schwartz and R. A. Andersen, *Organometallics*, 2000, **19**, 781-789.
28. T. P. Hanusa, *Organometallics*, 2002, **21**, 2559-2571.
29. J. S. Overby and T. P. Hanusa, *Organometallics*, 1996, **15**, 2205-2212.
30. G. Moesges, F. Hampel and P. v. R. Schleyer, *Organometallics*, 1992, **11**, 1769-1770.
31. K. A. Allan, B. G. Gowenlock and W. E. Lindsell, *J. Organomet. Chem.*, 1974, **65**, 1-7.
32. S. R. Drake and D. J. Otway, *Polyhedron*, 1992, **11**, 745-758.
33. J. S. Alexander and K. Ruhlandt-Senge, *Eur. J. Inorg. Chem.*, 2002, **2002**, 2761-2774.
34. H. Clavier and S. P. Nolan, *Chem. Commun.*, 2010, **46**, 841-861.
35. R. M. Roberts, *J. Org. Chem.*, 1949, **14**, 277-284.
36. R. M. Roberts, *J. Am. Chem. Soc.*, 1949, **71**, 3848-3849.
37. M. L. Cole, G. B. Deacon, C. M. Forsyth, P. C. Junk, K. Konstas and J. Wang, *Chem. Eur. J.*, 2007, **13**, 8092-8110.
38. M. L. Cole, G. B. Deacon, P. C. Junk and K. Konstas, *Chem. Commun.*, 2005, 1581-1583.
39. F. T. Edelman, in *Adv. Organomet. Chem.*, eds. F. A. Hill and M. J. Fink, Academic Press, Oxford, 2008, vol. 57, ch. 3, pp. 183-352.
40. F. T. Edelman, in *Adv. Organomet. Chem.*, eds. F. A. Hill and M. J. Fink, Academic Press, 2013, vol. 61, ch. 2, pp. 55-289.
41. A. Sanger, *Inorg. Nucl. Chem. Lett.*, 1973, **9**, 351-354.
42. F. T. Edelman, *Chem. Soc. Rev.*, 2009, **38**, 2253-2268.

Chapter 1

43. F. T. Edelman, *Chem. Soc. Rev.*, 2012, **41**, 7657-7672.
44. M. L. Cole and P. C. Junk, *Chem. Commun.*, 2005, 2695-2697.
45. M. L. Cole, G. B. Deacon, C. M. Forsyth, P. C. Junk, D. Polo-Cerón and J. Wang, *Dalton Trans.*, 2010, **39**, 6732-6738.
46. M. L. Cole, G. B. Deacon, P. C. Junk and J. Wang, *Organometallics*, 2012, **32**, 1370-1378.
47. K. M. Kuhn and R. H. Grubbs, *Org. Lett.*, 2008, **10**, 2075-2077.
48. P. C. Junk and M. L. Cole, *Chem. Commun.*, 2007, 1579-1590.
49. S. Cotton, in *Comprehensive Coordination Chemistry II*, eds. J. A. McCleverty and T. J. Meyer, Pergamon, Oxford, 2003, vol. 3, ch. 2, pp. 93-188.
50. T. J. Boyle and L. A. M. Ottley, *Chem. Rev.*, 2008, **108**, 1896-1917.
51. D. Bradley, R. Mehrotra, I. Rothwell and A. Singh, *Alkoxo and Aryloxo Derivatives of Metals*, Academic press, London, 2001.
52. M. Bochkarev, L. N. Zakharov and G. S. Kalinina, *Organoderivatives of Rare Earth Elements*, Kluwer, Dordrecht, 1995.
53. K. Izod, S. T. Liddle and W. Clegg, *Inorg. Chem.*, 2004, **43**, 214-218.
54. G. B. Deacon, C. M. Forsyth and S. Nickel, *J. Organomet. Chem.*, 2002, **647**, 50-60.
55. D. M. Barnhart, D. L. Clark, J. C. Gordon, J. C. Huffman, R. L. Vincent, J. G. Watkin and B. D. Zwick, *Inorg. Chem.*, 1994, **33**, 3487-3497.
56. M. Lappert, A. Protchenko, P. Power and A. Seeber, *Metal Amide Chemistry*, John Wiley & Sons, Chichester, 2008.
57. F. T. Edelman, D. M. M. Freckmann and H. Schumann, *Chem. Rev.*, 2002, **102**, 1851-1896.

Chapter 1

58. G. B. Deacon, J. E. Cosgriff, E. T. Lawrenz, C. M. Forsyth and D. L. Wilkinson, in *Synthetic Methods of Organometallic and Inorganic Chemistry*, eds. W. A. Herrmann and F. T. Edelman, Georg Thieme Verlag, Stuttgart, 1997, vol. 6, p. 226.
59. M. N. Bochkarev, *Chem. Rev.*, 2002, **102**, 2089-2118.
60. R. C. Mehrotra, A. Singh and U. M. Tripathi, *Chem. Rev.*, 1991, **91**, 1287-1303.
61. G. B. Deacon and C. M. Forsyth, in *Inorganic Chemistry Highlights*, eds. G. Meyer, D. Naumann and L. Wesemann, Wiley-VCH, Weinheim, 2002, ch. 7, pp. 139-151.
62. G. B. Deacon, T. C. Feng, S. Nickel, M. I. Ogden and A. H. White, *Aust. J. Chem.*, 1992, **45**, 671-683.
63. G. B. Deacon, T. C. Feng, P. MacKinnon, R. H. Newnham, S. Nickel, B. W. Skelton and A. H. White, *Aust. J. Chem.*, 1993, **46**, 387-399.
64. G. B. Deacon, C. M. Forsyth and R. H. Newham, *Polyhedron*, 1987, **6**, 1143-1145.
65. L. Clark, G. B. Deacon, C. M. Forsyth, P. C. Junk, P. Mountford and J. P. Townley, *Dalton Trans.*, 2010, **39**, 6693-6704.
66. G. B. Deacon, P. B. Hitchcock, S. A. Holmes, M. F. Lappert, P. MacKinnon and R. H. Newnham, *Chem. Commun.*, 1989, 935-937.
67. G. B. Deacon, P. C. Junk and G. J. Moxey, *Chem. Asian J.*, 2009, **4**, 1717-1728.
68. G. B. Deacon, G. D. Fallon, C. M. Forsyth, S. C. Harris, P. C. Junk, B. W. Skelton and A. H. White, *Dalton Trans.*, 2006, 802-812.
69. G. B. Deacon, M. G. Gardiner, P. C. Junk, J. P. Townley and J. Wang, *Organometallics*, 2012, **31**, 3857-3864.
70. G. B. Deacon, T. Feng, C. M. Forsyth, A. Gitlits, D. C. Hockless, Q. Shen, B. W. Skelton and A. H. White, *Dalton Trans.*, 2000, 961-966.

Chapter 1

71. W. F. Fitzgerald and R. P. Mason, in *Met. Ions Biol. Syst.*, eds. A. Sigel and H. Sigel, Marcel Dekker Inc., New York, 1997, vol. 34, ch. 3, pp. 53-101.
72. P. Biagini, G. Lugli and R. Millini, *New J. Chem.*, 1995, **19**, 713-722.

CHAPTER 2

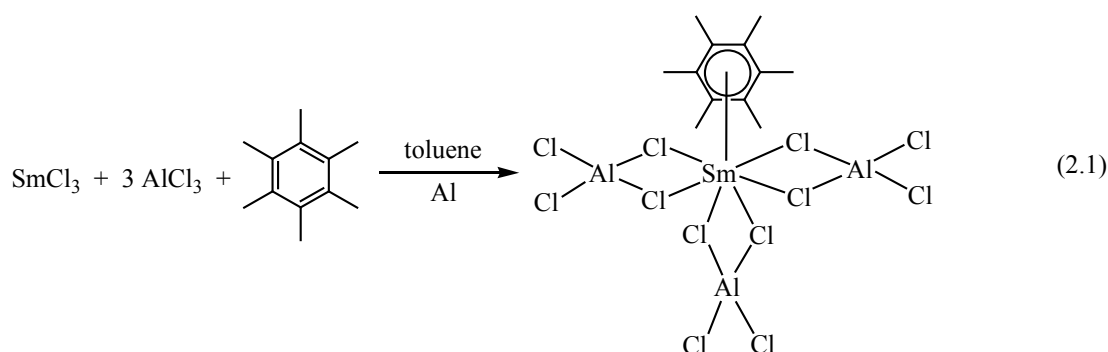
CHEMISTRY OF HALOGENOALUMINATE LANTHANOID-ARENE COMPLEXES

2.1 Introduction

The organometallic complexes of rare earths involving π -ligands have mainly focused on the ubiquitous aromatic anionic ligand systems such as cyclopentadienide $C_5H_5^-$, pentamethylcyclopentadienide $C_5Me_5^-$, cyclooctatetraenide ($C_8H_8^{2-}$), and mixed species with charged π -donors.¹⁻¹⁹ However, several organolanthanoid compounds containing neutral arenes have been reported. These compounds have considerable interest not only for the versatile coordination modes of arenes with lanthanoid metals but also for the potential applications in catalysis. Though different types of lanthanoid-arene complexes have been reported, the bimetallic complexes, for example, the halogenoaluminate lanthanoid-arene complexes are among the most exciting and challenging organometallic compounds. Due to the high reactivity of these complexes, they are considered to be a potential catalysts for some polymerisation reactions.²⁰⁻²⁴

This direction of lanthanoid-arene chemistry had started its journey more than thirty years ago; however, most of the reported compounds involve chloroaluminates $[AlCl_4]^-$, whereas bromo- and iodoaluminate ($[AlBr_4]^-$ and $[AlI_4]^-$) complexes are not so common.^{1, 25-30} High catalytic activity of some of these complexes for polymerisation of alkenes and dienes have also been reported.³¹⁻³³ The first chloroaluminate arene complex of samarium, $[Sm(\eta^6-C_6Me_6)(AlCl_4)_3]$ was reported in 1986 by Cotton and Schwotzer, synthesised by refluxing the mixture of samarium trichloride and aluminium trichloride.^{34, 35} Yellow plates of $[Sm(\eta^6-C_6Me_6)(AlCl_4)_3]$ was crystallised from a blood red solution (indicative of a Sm(II) species also being present) in 14% total yield (Eqn. 2.1). The complex forms a distorted pentagonal bipyramidal coordination polyhedron with the η^6 -arene in an axial position. The mean Sm-Cl and Sm-C distances are 2.85 and 2.89 Å, respectively. The Cl-Sm-Cl bond angle for adjacent chlorine atoms were within the range of 69.4-71.1°. Subsequently, a homologous series of trivalent lanthanoid η^6 -arene complexes has been prepared by a similar method using less substituted arenes such as tetramethylbenzene, mesitylene, *m*-xylene, toluene or even benzene as follows.

Chapter 2



$[\text{Sm}(\eta^6\text{-MeC}_6\text{H}_5)(\text{AlCl}_4)_3]$ was synthesised by the reaction of SmCl_3 , AlCl_3 and aluminium powder in toluene.³⁶ It has similar structure with a coordination geometry analogous to that of $[\text{Sm}(\eta^6\text{-C}_6\text{Me}_6)(\text{AlCl}_4)_3]$. The central metal atom $\text{Sm}(\text{III})$ bonds to six carbon atoms in the toluene ring and six chlorides. The average Sm-C and Sm-Cl distances are 2.91 Å and 2.84 Å respectively. A similar reaction between activated AlCl_3 , excess aluminium powder and SmCl_3 in *m*-xylene gave yellow crystals of $[\text{Sm}(\eta^6\text{-Me}_2\text{C}_6\text{H}_4)(\text{AlCl}_4)_3]$ in 16% yield.^{37, 38} Two independent $[\text{Sm}(\eta^6\text{-Me}_2\text{C}_6\text{H}_4)(\text{AlCl}_4)_3]$ moieties were observed in the asymmetric unit, both having the distorted pentagonal bipyramid coordination polyhedra with an axial *m*-xylene. The average Sm-C and Sm-Cl distances are 2.90 Å and 2.83 Å, for one moiety, and 2.88 Å, 2.84 Å for the other, respectively. The mean Sm-Cl distances (2.83 Å and 2.84 Å in two different moieties) are slightly shorter than the 2.85 Å found in $[\text{Sm}(\eta^6\text{-C}_6\text{Me}_6)(\text{AlCl}_4)_3]$.³⁴ Most probably, this is due to the increased steric effect of the C_6Me_6 ligand. However, there were no clear differences between the average Sm-C distances.

AlCl_3 , activated by heating with aluminum powder reacts with SmCl_3 in benzene to give the neutral arene complex, $[\text{Sm}(\eta^6\text{-C}_6\text{H}_6)(\text{AlCl}_4)_3 \cdot \text{C}_6\text{H}_6]$.³⁹ The average Sm-C and Sm-Cl distances are 2.92 Å and 2.83 Å, respectively and the geometry is analogous to the previously reported samarium complexes. $[\text{Ln}(\eta^6\text{-C}_6\text{H}_6)(\text{AlCl}_4)_3 \cdot \text{C}_6\text{H}_6]$ ($\text{Ln} = \text{La}, \text{Nd}$) compounds were synthesised by the same method and characterised by elemental analysis and IR spectroscopy.⁴⁰ The compounds were found to be isomorphous and isostructural with $[\text{Sm}(\eta^6\text{-C}_6\text{H}_6)(\text{AlCl}_4)_3 \cdot \text{C}_6\text{H}_6]$. Moreover, the Nd-C (2.93 Å) and Nd-Cl (2.85 Å) bond lengths are comparable to the Sm-C (2.92 Å) and Sm-Cl (2.83 Å) bond lengths considering the estimated standard deviations. A neutral arene complex of ytterbium, $[\text{Yb}(\eta^6\text{-C}_6\text{Me}_6)(\text{AlCl}_4)_3 \cdot \text{MeC}_6\text{H}_5]$ was also synthesised by heating the mixture of aluminium

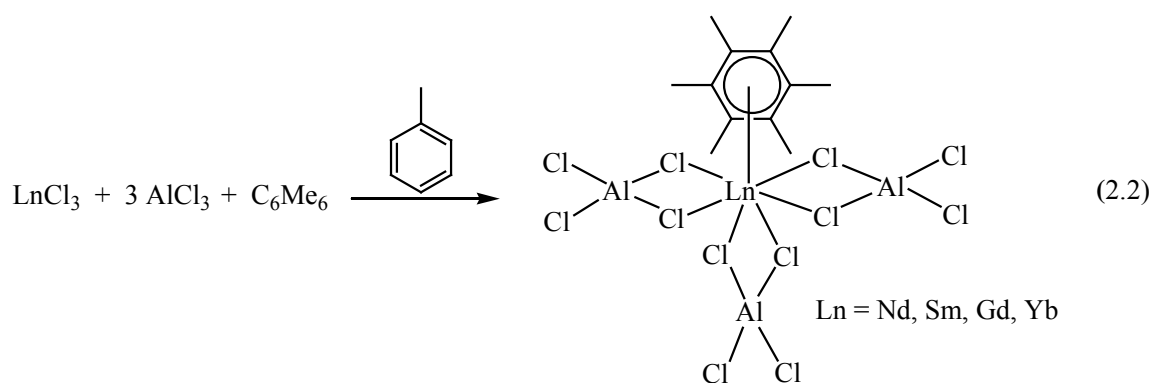
Chapter 2

powder, YbCl₃, AlCl₃ and hexamethylbenzene in toluene.⁴¹ The complex was isostructural with [Sm(η^6 -C₆H₆)(AlCl₄)₃.C₆H₆] and other properties were analogous.

The η^6 -benzene complexes of lanthanoids [Ln(η^6 -C₆H₆)(AlCl₄)₃.C₆H₆] (Ln = La, Nd, Sm) have been synthesised by the reaction of LnCl₃ (Ln = La, Nd, Sm) with activated AlCl₃ in benzene (the yields were 56%, 62% and 38%, respectively).⁴² All three complexes have the similar IR spectra, and the absorption bands are due to the benzene ring in their structures. For Nd, the Cl-M-Cl bond angles for the adjacent chlorine atoms in the plane range from 68.8° to 73.2° and that for Sm range from 68.9° to 73.4°. The mean bond distance of Sm-C is (2.91 Å) shorter than the Nd-C (2.93 Å) because of the lanthanoid contraction.

Liang *et al* have introduced direct syntheses without the requirement for the reducing agent (aluminium powder) in 1994 (Eqn. 2.2). A series of neutral η^6 -C₆Me₆ complexes of lanthanoids, [Ln(η^6 -C₆Me₆)(AlCl₄)₃.MeC₆H₅] (Ln = Nd, Sm, Gd, Yb) was prepared by the direct reaction of LnCl₃, AlCl₃, and C₆Me₆ in toluene in good yields (Nd 47%, Sm 63%, Gd 59% and Yb 62%), and characterised by elemental analysis as well as IR and mass spectrometry.⁴³ The phenyl ring C=C skeletal vibrations appear in the ranges of 1558-1570 and 1440-1488cm⁻¹, and out-of-plane ring bendings at 710-675 cm⁻¹. No parent molecular ions were observed in the mass spectrum; however, AlCl₃, LnCl₃, C₆Me₆ ions and some fragments that are ascribed to the moieties containing AlCl₃ and C₆Me₆ groups connected to the central metal could be observed clearly. Neutral arene complexes are fairly unstable under the measurement conditions (vacuum up to 10⁻⁶ mbar) as the higher molecular weight fragments were very low (< 1%). These compounds decompose in electron donor solvents such as diethyl ether and THF, and are hardly soluble in aromatic solvents. The mean Ln-C distances in [Yb(η^6 -C₆Me₆)(AlCl₄)₃.MeC₆H₅] and [Sm(η^6 -C₆Me₆)(AlCl₄)₃.MeC₆H₅] are 2.86 and 2.89 Å, respectively. The bond lengths are comparable considering the estimated standard deviations. The Cl-Ln-Cl bond angles for the adjacent chlorine atoms in the plane range from 69.6 to 70.8 and 69.4 to 71.1° in [Yb(η^6 -C₆Me₆)(AlCl₄)₃.MeC₆H₅] and [Sm(η^6 -C₆Me₆)(AlCl₄)₃.MeC₆H₅], respectively.

Chapter 2



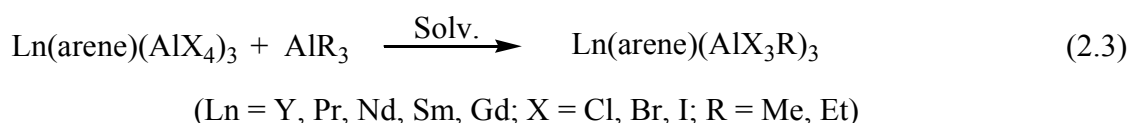
$[\text{Nd}(\eta^6\text{-MeC}_6\text{H}_5)(\text{AlCl}_4)_3]$ was isolated unexpectedly from the attempted synthesis of $[\text{Nd}(\eta^6\text{-1,3,5-}^t\text{BuC}_6\text{H}_3)(\text{AlCl}_4)_3]$ by the reaction of NdCl_3 , 1,3,5-tri-*tert*-butylbenzene and AlCl_3 (molar ratio 1:1:3) in toluene at 80°C for half an hour.⁴⁴ This complex is isomorphous and isostructural with $[\text{Sm}(\eta^6\text{-MeC}_6\text{H}_5)(\text{AlCl}_4)_3]$ ³⁶, and the average Nd-C and Nd-Cl distances are 2.926 Å and 2.857 Å, respectively. The same compound was also prepared by the reaction of $\text{NdCl}_3(\text{THF})_2$ and an excess of AlCl_3 in toluene and characterised by IR spectra and X-ray diffraction.⁴⁵ This research group also reported analogous compounds of Y and Yb, prepared by heating an excess of AlCl_3 and the respective lanthanoid salts in toluene.

The reaction of NdCl_3 , AlCl_3 and mesitylene in the molar ratio of 1:3:1 in benzene at 70°C gave purple-red crystals of $[\{\text{Nd}(\eta^6\text{-1,3,5-Me}_3\text{C}_6\text{H}_3)(\text{AlCl}_4)_3\} \cdot \text{C}_6\text{H}_6]$ in 47% yield. The compound was then characterised by elemental analysis, IR and MS spectra as well as X-ray diffraction.⁴⁶ The IR and mass spectra were found to be similar to the complex $[\text{Nd}(\eta^6\text{-C}_6\text{Me}_6)(\text{AlCl}_4)_3 \cdot \text{MeC}_6\text{H}_5]$ ⁴³; however, the average Nd-C bond length was 2.916 Å which is shorter than 2.926 Å in $[\text{Nd}(\eta^6\text{-MeC}_6\text{H}_5)(\text{AlCl}_4)_3]$ and 2.93 Å in $[\text{Nd}(\eta^6\text{-C}_6\text{H}_6)(\text{AlCl}_4)_3]$. The differences in Nd-C bond distances in these analogous complexes might reflect the variation of the interaction between different arenes and Nd metal. The more electron donating groups on the ring, the stronger the Nd-C bond (shorter distance). The Nd-Cl bond distance is 2.865 Å which is similar to 2.857 Å in $[\text{Nd}(\eta^6\text{-MeC}_6\text{H}_5)(\text{AlCl}_4)_3]$ and 2.852 Å $[\text{Nd}(\eta^6\text{-C}_6\text{H}_6)(\text{AlCl}_4)_3]$. Moreover, the Cl-Nd-Cl bond angles for adjacent chlorine atoms in the plane are also comparable with the analogous complexes, which range from 68.9 to 72.7° , 68.8 to 73.2° and 69.4 to 81.2° in $[\{\text{Nd}(\eta^6\text{-1,3,5-Me}_3\text{C}_6\text{H}_3)(\text{AlCl}_4)_3\} \cdot \text{C}_6\text{H}_6]$, $[\text{Nd}(\eta^6\text{-MeC}_6\text{H}_5)(\text{AlCl}_4)_3]$ and $[\text{Nd}(\eta^6\text{-C}_6\text{H}_6)(\text{AlCl}_4)_3]$,

Chapter 2

respectively. The first praseodymium chloroaluminate arene complex $[\text{Pr}(\eta^6\text{-Me}_2\text{C}_6\text{H}_4)(\text{AlCl}_4)_3]$ was synthesised by the reaction of PrCl_3 and AlCl_3 in *m*-xylene and found to be isostructural with other lanthanoid analogues.⁴⁷

Several compounds containing alkylated aluminium fragments AlX_3R ($\text{R} = \text{Me}, \text{Et}$) have been prepared in high yield by the metal exchange reactions between $[\text{Ln}(\eta^6\text{-arene})(\text{AlX}_4)_3]$ and the appropriate AlR_3 (Eqn. 2.3).²¹ The NMR spectra of some neodymium complexes at different temperature exhibited a fluxional behavior of the $[\text{AlX}_3\text{R}]^-$ ligands and an exchange of the $\eta^6\text{-arene}$ ligand with the aromatic solvent was evident. The catalytic activity of the $[\text{Ln}(\eta^6\text{-arene})(\text{AlX}_3\text{R})_3]$ complexes in the polymerisation of butadiene and ethylene has been tested and found stereospecific. In addition to that, the catalytic activity of the $[(\eta^6\text{-arene})\text{Nd}(\text{AlCl}_4)_3]\text{-AlR}_3$ ($\text{R} = \text{Et}, \text{}^i\text{Bu}$ and C_8H_7) systems for the polymerisation of butadiene has been studied and no activity was observed when the arene is hexamethylbenzene.²² Organoaluminium compounds used with the arene complex remarkably controls the catalytic activity; the activity of $\text{Al}(\text{}^i\text{Bu})_3$ being higher than that of $\text{Al}(\text{}^i\text{Bu})_2\text{H}$. No activity was displayed with AlEt_3 , AlEt_2Cl , and $\text{Al}(\text{C}_8\text{H}_{17})_3$. With the increased amount of $\text{Al}(\text{}^i\text{Bu})_3$, the catalytic activity increased, the molecular weight of the polybutadiene decreased, and the *cis*-1,4 isomer was dominant ($\sim 96\%$). The optimised temperature was 50°C and the effect of solvents on the polymerisation activity decreased in the order: petrol > benzene > toluene.



$[\text{Nd}(\eta^6\text{-C}_6\text{H}_6)(\text{AlCl}_4)_3]$ in the presence of trialkylaluminium compounds in hexane or toluene catalyses the polymerisation of isoprene²³ as well as the copolymerisation of isoprene and butadiene²⁴ to form *cis*-1,4 polymers. Similar to the prior report, the activity of the arene complex depends solely on the nature of the AlR_3 reagent. The effect of various alkylaluminiums on polymerisation of isoprene in hexane is shown in Table 2.1. Moreover, the $[\text{Nd}(\eta^6\text{-C}_6\text{H}_6)(\text{AlCl}_4)_3]$ complex and a La analogue have been tested for the catalysis of the alkylation of benzene with 1-hexene. Two isomers, 1-phenylhexane and

Chapter 2

2-phenylhexane in the ratio of 28:72 have been observed; however, lanthanoid trichlorides have been found to be inactive under the same conditions.²⁵

Table 2.1: The effect of various alkylaluminiums on polymerisation of isoprene in hexane.²³

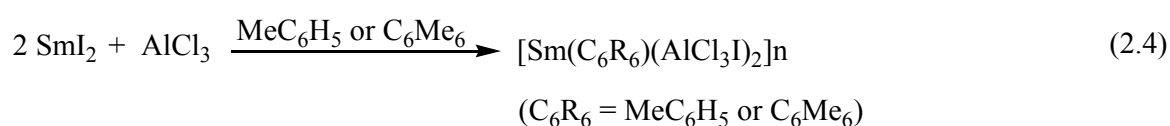
AlR ₃	Amount of catalyst used (mol Nd) (g isoprene) ⁻¹	Conversion (%)	Microstructure	
			<i>cis</i> -1,4	3,4
Al(ⁱ Bu) ₃	1.85 x 10 ⁻⁵	52.5	-	-
	3.70 x 10 ⁻⁵	71.5	93.8	6.2
	5.60 x 10 ⁻⁵	84.6	92.6	7.4
Al(ⁱ Bu) ₂ H	5.60 x 10 ⁻⁵	46.5	93.1	6.9
	7.20 x 10 ⁻⁵	48.5	-	-
	9.00 x 10 ⁻⁵	63.1	92.7	7.3
AlEt ₃	5.60 x 10 ⁻⁵	0		
	1.20 x 10 ⁻⁴	0		

A cyclotetrameric complex of Eu(II), [Eu(η^6 -Me₆C₆)(AlCl₄)₂]₄ was synthesised by heating the mixture of EuCl₃, freshly sublimed AlCl₃ and hexamethylbenzene at 60°C for 3 days in toluene (17% yield).^{48, 49} The average Eu(II)-C distance is 2.999 Å and is comparable with the Sm(III)-C 2.89 Å in Sm(η^6 -C₆Me₆)(AlCl₄)₃, if the difference of the ionic radii of Eu(II) (1.09 Å) and Sm(III) (0.964 Å) is considered.

Mixed-halogeno aluminate arene complexes of samarium and thulium were reported by Fagin *et al.*⁵⁰ Divalent samarium complexes [Sm(η^6 -C₆R₆)(AlCl₃I)₂]_n (C₆R₆ = MeC₆H₅ or C₆Me₆) were obtained by the reaction of unsolvated SmI₂ with AlCl₃ in toluene and hexamethylbenzene (Eqn. 2.4). However, under the same conditions, the more strongly reducing lanthanoid diiodide TmI₂ resulted in no analogous products; the trivalent arene complex Tm(η^6 -MeC₆H₅)(AlCl_{4-x}I_x)₃ was formed by the reaction of TmI₂ and AlCl₃ in the presence of naphthalene in toluene. Crystal structures confirmed that at least three of the halide positions in both samarium compounds were composed of a mixture of iodine and chlorine atoms, whereas in the thulium compound, at least one of the halide positions was composed of a mixture of iodine and chlorine atoms. Although [Sm(η^6 -C₆Me₆)(AlCl₃I)₂]_n

Chapter 2

is similar to $[\text{Sm}(\eta^6\text{-MeC}_6\text{H}_5)(\text{AlCl}_3\text{I})_2]_2$ by composition, in the solid state the former is dimeric rather than polymeric. The average Sm-C distance in $[\text{Sm}(\eta^6\text{-C}_6\text{Me}_6)(\text{AlCl}_3\text{I})_2]_n$ was 3.0 Å which is higher than the other analogous trivalent samarium complexes. Considering the differences in the ionic radii of divalent (1.22 Å) and trivalent (1.132 Å) ions, the differences in Sm-C distances are consistent.⁵¹ The structure of $\text{Tm}(\eta^6\text{-MeC}_6\text{H}_5)(\text{AlCl}_{4-x}\text{I}_x)_3$ is comparable to the trivalent ytterbium analogue $\text{Yb}(\eta^6\text{-MeC}_6\text{H}_5)(\text{AlCl}_4)_3$.⁴⁵ The average Tm-C distance was 2.83 Å whereas in $\text{Yb}(\eta^6\text{-MeC}_6\text{H}_5)(\text{AlCl}_4)_3$, the Yb-C distance was 2.84 Å.



Recently, lanthanum(III) chloroaluminate complexes $\text{La}(\eta^6\text{-C}_6\text{H}_5\text{Me})(\text{AlCl}_4)_3$ and $[\text{La}(\eta^6\text{-C}_6\text{Me}_6)(\text{AlCl}_4)_3] \cdot 0.5\text{C}_6\text{H}_6$ have been synthesised by Cotton's method.³⁴ Furthermore, the parallel-slipped π - π stacking intermolecular interactions between the coordinated hexamethylbenzene ligand and a sandwiched benzene molecule (Fig. 2.1) was observed for the first time in $[\text{La}(\eta^6\text{-C}_6\text{Me}_6)(\text{AlCl}_4)_3] \cdot 0.5\text{C}_6\text{H}_6$ complex.^{52, 53} The La-C bond distances range from 2.927 to 3.035 Å and 2.956 to 3.006 Å for $\text{La}(\eta^6\text{-C}_6\text{H}_5\text{Me})(\text{AlCl}_4)_3$ and $[\text{La}(\eta^6\text{-C}_6\text{Me}_6)(\text{AlCl}_4)_3] \cdot 0.5\text{C}_6\text{H}_6$, respectively. DFT calculations have confirmed that the lanthanoid-arene interaction is mainly electrostatic, and the lanthanoid-arene bonding energy in the hexamethylbenzene complex (33.15 kcal/mol) is higher than in the toluene complex (26.28 kcal/mol). Strong polarization of the coordinated hexamethylbenzene has been confirmed by both DFT and ¹H NMR spectra.

A half-sandwich dysprosium(III) chloroaluminate complex $\text{Dy}(\eta^6\text{-C}_6\text{Me}_6)(\text{AlCl}_4)_3$ was synthesised by a similar method and characterised magnetically as well as by X-ray diffraction.⁵⁴ The X-ray confirmed a comparable geometry and bonding properties with other reported lanthanoid-arene complexes. For the first time, this lanthanoid chloroaluminate complex was tested for magnetic behaviour and found to be a single-ion magnet with an energy barrier of 101 K and a hysteresis loop observed at 3 K.

Chapter 2

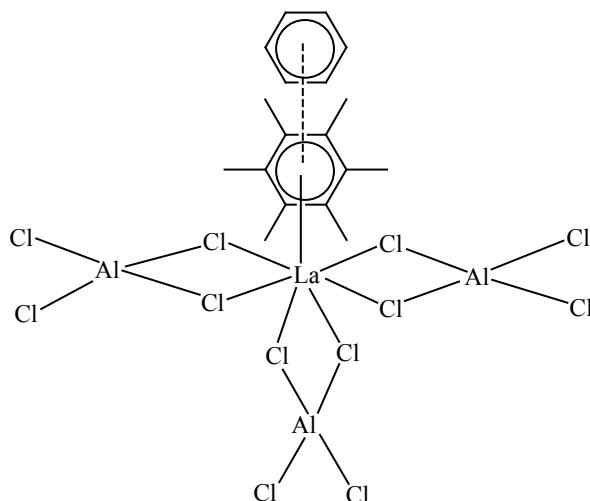


Fig. 2.1: Structure of $[\text{La}(\eta^6\text{-C}_6\text{Me}_6)(\text{AlCl}_4)_3] \cdot 0.5\text{C}_6\text{H}_6$.

Bromoaluminate arene complexes of lanthanoids $\text{Ln}(\eta^6\text{-MeC}_6\text{H}_5)(\text{AlBr}_4)_3$ ($\text{Ln} = \text{Y}, \text{Pr},$ and Gd) and $\text{Nd}(\eta^6\text{-Me}_4\text{C}_6\text{H}_2)(\text{AlBr}_4)_3$ were isolated by a similar method to the chloroaluminates by using AlBr_3 in place of AlCl_3 .^{21, 45}

Despite being prepared by differing synthetic approaches, all the reported complexes are isostructural having the distorted pentagonal bipyramidal coordination polyhedra with the arene molecule in an axial position. The bond lengths and bond angles are comparable for all the lanthanoid complexes considering the ionic radii. The published halogenoaluminate lanthanoid-arene complexes till now and some of their properties/structural parameters are listed in Table 2.2.

Chapter 2

Table 2.2: Properties/structural parameters of reported halogenoaluminate lanthanoid-arene complexes.

Complex	Colour / m.p.	Ln-C / Ln- C _{avg} (Å)	Ln- Cl _{avg} (Å)	Ref.
Y(η^6 -MeC ₆ H ₅)(AlCl ₄) ₃	Pale yellow	-	-	45
Y(η^6 -MeC ₆ H ₅)(AlBr ₄) ₃	Colourless	-	-	45
Y(η^6 -MeC ₆ H ₅)(AlCl ₃ Me) ₃	Colourless crystals	-	-	21
[La(η^6 -C ₆ H ₆)(AlCl ₄) ₃].C ₆ H ₆	-	-	-	40,42
La(η^6 -C ₆ H ₅ Me)(AlCl ₄) ₃	Yellow crystals	2.927- 3.035	-	52
[La(η^6 -C ₆ Me ₆)(AlCl ₄) ₃].0.5C ₆ H ₆	Yellow crystals	2.956- 3.006	-	52,53
Pr(η^6 -Me ₂ C ₆ H ₄)(AlCl ₄) ₃	-	2.949	2.873	47
Pr(η^6 -MeC ₆ H ₅)(AlCl ₃ Et) ₃	Pale green crystals	-	-	21
Pr(η^6 -MeC ₆ H ₅)(AlBr ₄) ₃	Pale green	-	-	45
Nd(η^6 -MeC ₆ H ₅)(AlCl ₄) ₃	-	2.926	2.857	44
[Nd(η^6 -1,3,5-Me ₃ C ₆ H ₃)(AlCl ₄) ₃].C ₆ H ₆	Purple-red crystals	2.916	2.865	46
[Nd(η^6 -C ₆ H ₆)(AlCl ₄) ₃].C ₆ H ₆	Dark tar	2.93	2.85	22,42
Nd(η^6 -C ₆ Me ₆)(AlCl ₄) ₃	-	-	-	22
Nd(η^6 -MeC ₆ H ₅)(AlCl ₃ Me) ₃	Light blue crystalline solids	-	-	21
Nd(η^6 -MeC ₆ H ₅)(AlCl ₃ Et) ₃	Light blue crystals	-	-	21
Nd(η^6 -Me ₄ C ₆ H ₂)(AlCl ₃ Me) ₃	Light blue crystals	-	-	21
Nd(η^6 -Me ₄ C ₆ H ₂)(AlCl ₃ Et) ₃	-	-	-	21
[Nd(η^6 -C ₆ Me ₆)(AlCl ₄) ₃].MeC ₆ H ₅	Blue crystals, 103°C (dec)	-	-	43
Nd(η^6 -Me ₄ C ₆ H ₂)(AlBr ₄) ₃	Light blue	-	-	45
Nd(η^6 -MeC ₆ H ₅)(AlBr ₃ Et) ₃	Light blue crystals	-	-	21
Nd(η^6 -MeC ₆ H ₅)(AlI ₃ Et) ₃	Light blue crystals	-	-	21
[Sm(η^6 -MeC ₆ H ₅)(AlCl ₃ I) ₂] _n	Red brown crystals, 85°C (dec)	-	-	50

Chapter 2

Table 2.2 (continued)

$[\text{Sm}(\eta^6\text{-C}_6\text{Me}_6)(\text{AlCl}_3\text{I})_2]_n$	Red crystals, 210°C (dec)	3.00	-	50
$[\text{Sm}(\eta^6\text{-C}_6\text{H}_6)(\text{AlCl}_4)_3] \cdot \text{C}_6\text{H}_6$	Yellow	2.92	2.83	39,42
$\text{Sm}(\eta^6\text{-MeC}_6\text{H}_5)(\text{AlCl}_4)_3$	Yellow	2.91	2.84	36
$\text{Sm}(\eta^6\text{-MeC}_6\text{H}_5)(\text{AlCl}_3\text{Me})_3$	Yellow crystals	-	-	21
$\text{Sm}(\eta^6\text{-1,3-Me}_2\text{C}_6\text{H}_4)(\text{AlCl}_4)_3$	Yellow, >110°C (dec)	2.89	2.836	37
$[\text{Sm}(\eta^6\text{-C}_6\text{Me}_6)(\text{AlCl}_4)_3] \cdot (\text{MeC}_6\text{H}_5)_{1.5}$	Yellow plates	2.89	2.85	34,35
$[\text{Sm}(\eta^6\text{-C}_6\text{Me}_6)(\text{AlCl}_4)_3] \cdot \text{MeC}_6\text{H}_5$	Yellow crystals, 104°C (dec)	2.89	2.85	43
$[\text{Eu}(\eta^6\text{-C}_6\text{Me}_6)(\text{AlCl}_4)_2]_4 \cdot (\text{C}_6\text{H}_2\text{Me}_4)$	Green crystals, >140°C(dec)	2.999	3.04	48,49
$\text{Gd}(\eta^6\text{-MeC}_6\text{H}_5)(\text{AlCl}_4)_3$	Colourless	-	-	45
$[\text{Gd}(\eta^6\text{-C}_6\text{Me}_6)(\text{AlCl}_4)_3] \cdot \text{MeC}_6\text{H}_5$	Yellow crystals, 103°C (dec)	-	-	43
$\text{Gd}(\eta^6\text{-MeC}_6\text{H}_5)(\text{AlBr}_4)_3$	Colourless	-	-	45
$\text{Gd}(\eta^6\text{-MeC}_6\text{H}_5)(\text{AlBr}_3\text{Me})_3$	Colourless crystals	-	-	21
$[\text{Yb}(\eta^6\text{-C}_6\text{Me}_6)(\text{AlCl}_4)_3] \cdot \text{MeC}_6\text{H}_5$	Deep blue crystals, 104°C (dec)	2.86	2.785	41,43

2.2 Research Plan

This chapter intends to expand the series of halogenoaluminate lanthanoid-arene complexes, especially the iodoaluminate complexes, as this section has not been explored extensively yet. Most of the published complexes involve chloroaluminates and limited to some selected lanthanoids such as neodymium, samarium, praseodymium, europium and gadolinium. It was our intention to attempt to extend this series for all lanthanoids as well as to modify the synthetic method. Reactivity and catalytic activity of some of the complexes have also been studied.

The IR spectra of the complexes were recorded in nujol mulls (mineral oil) between sodium chloride plates. The IR spectra of all the complexes show similar absorption patterns including the presence of C–H aromatic stretches of the coordinated solvent molecule at about 3000 cm^{-1} and sp^3 C-H stretching at around 2900 cm^{-1} comparable to the reported literature.^{42, 52, 55} Microanalysis was performed to determine purity and to confirm the composition of bulk material was similar to the X-ray crystal structure composition and EDTA complexometric titration was performed to determine the metal composition. The complexes were insoluble in most non-polar solvents and decomposed in polar organic solvents like thf. Therefore, no NMR experiments were performed.

2.3.2 X-ray Crystal Structures

2.3.2.1 Iodoaluminate lanthanoid(III) complexes in toluene

The X-ray crystal structures of the monomeric complexes of lanthanoids $\text{Ln}(\eta^6\text{-C}_6\text{H}_5\text{Me})(\text{AlI}_4)_3$; Ln = La (**1**), Ce (**2**), Nd (**3**) and Gd (**4**) have been determined. The structure of $\text{La}(\eta^6\text{-C}_6\text{H}_5\text{Me})(\text{AlI}_4)_3$ (**1**) (Fig. 2.2) shows a nine coordinate species where the lanthanum(III) centre is connected to six iodides and an η^6 -bound arene. Two independent molecules of **1** were observed in the asymmetric unit having the coordination polyhedron as a distorted pentagonal bipyramid with the η^6 -arene located at an axial position. The other axial position opposite to the arene centroid consist of an iodide (I10) (the centroid-La-I angle is 178.07°), which has the shortest La-I bond length among all the La-I bonds. Therefore, I10 is more strongly bound to the La^{3+} centre than the other iodides. This compound is isostructural to the reported lanthanum complex $\text{La}(\eta^6\text{-C}_6\text{H}_5\text{Me})(\text{AlCl}_4)_3$.⁵² The La-C bond lengths range from 2.971(9) to 3.057(9) Å with a La-centroid distance being 2.663(4) Å. These distances are comparable with those of $\text{La}(\eta^6\text{-C}_6\text{H}_5\text{Me})(\text{AlCl}_4)_3$ where the La-C bond lengths fall in the range from 2.927(7) to 3.035(7) Å with a La-centroid distance being 2.633(7) Å.⁵²

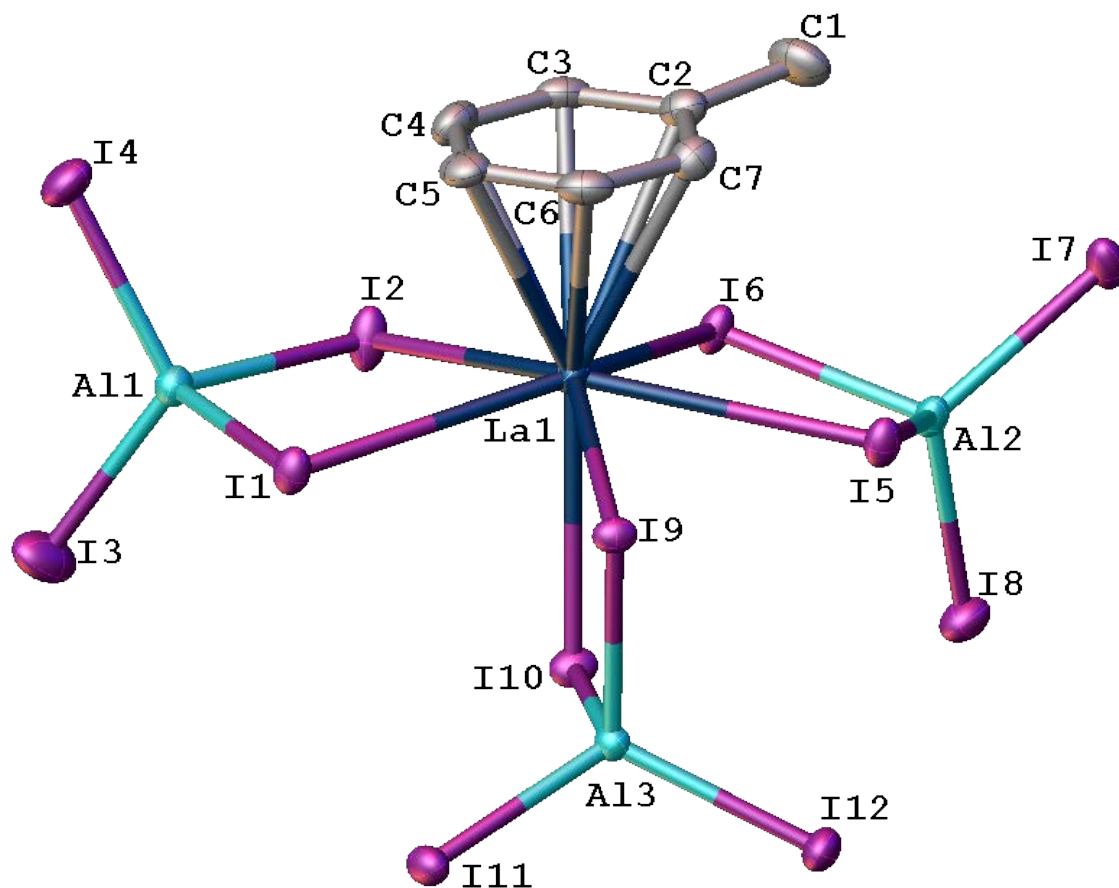


Fig. 2.2: Molecular structure of $\text{La}(\eta^6\text{-C}_6\text{H}_5\text{Me})(\text{AlI}_4)_3$ (**1**), representative of the isostructural complexes **2**, **3** and **4**. Hydrogen atoms have been omitted for clarity.

The La-centroid distances in the corresponding cyclopentadienyl complexes are 2.53 Å in $[\text{La}(\text{AlMe}_4)_2\{1,2,4\text{-(Me}_3\text{C)}_3\text{C}_5\text{H}_2\}]^{56}$, 2.522 and 2.516 Å in $[\text{Cp}^*\text{-}_2\text{La}(\text{AlMe}_4)]^{57}$, which demonstrates a relatively weaker La-arene bond in the arene-haloaluminates than in the cyclopentadienyl compounds. The La-C bond lengths fall in the range from 2.764(1)–2.806(1) Å in $[\{\eta^5\text{-C}_5\text{Me}_4\text{C}_2\text{H}_4\text{NMe}_2(\text{AlMe}_3)\}\text{La}(\text{AlMe}_4)_2]^{58}$, 2.756(2)–2.843(2) Å in $[(\text{C}_5\text{Me}_4\text{C}_2\text{H}_4\text{NMe}_2)\text{La}(\text{AlMe}_4)_2]^{58}$, 2.732(1)–2.846(1) Å in $[(\text{C}_5\text{Me}_4\text{C}_6\text{H}_4\text{NMe}_2)\text{La}(\text{AlMe}_4)_2]^{58}$, 2.753(2)–2.801(3) Å in $(\text{C}_5\text{Me}_5)\text{La}(\text{AlMe}_4)_2^{59}$, 2.547–2.561 Å in $[\{(\text{C}_5\text{Me}_5)_2\text{La}(\text{AlEt}_4)\}_2]^{60}$ and 2.7502(11) – 2.8228(10) Å in $[(\text{C}_5\text{Me}_4\text{H})\text{La}(\text{AlMe}_4)_2]^{61}$. Therefore, the significantly longer La-C bond lengths (2.927(7)– 3.035(7) Å) in **1** reveals a substantially weaker La-arene interaction in it compared to the cyclopentadienyl complexes. This fact is further confirmed by their dissociation to the starting materials in THF solution.⁴⁵

Chapter 2

The La-C(arene) distances in $[\text{K}([\text{18}]\text{-crown-6})][\text{La}\{\eta^5\text{-C}_5\text{H}_3(\text{SiMe}_3)_{2-1,3}\}_2\text{-}(\text{C}_6\text{H}_6)]$ fall in the range from 2.75(1) to 2.79(1) Å with an average of 2.635(6) Å and a La-centroid length of 2.427(6) Å.^{62, 63} The average U-C bond lengths in the analogous uranium chloroaluminate complexes are 2.91 Å in $\text{U}(\eta^6\text{-C}_6\text{H}_6)(\text{AlCl}_4)_3$ ⁶⁴, 2.92 Å in $\{\text{U}(\eta^6\text{-C}_6\text{Me}_6)\text{Cl}_2\}_2(\mu\text{-Cl})_3\text{AlCl}_4$ ⁶⁵, and 2.92 Å in $[\text{U}(\eta^6\text{-C}_6\text{Me}_6)\text{Cl}_2(\mu\text{-Cl})_3\text{UCl}_2(\eta^6\text{-C}_6\text{Me}_6)][\text{AlCl}_4]$ ⁶⁶, whereas the average La-C bond length in **1** is 3.0065 Å. From these data, it can be concluded that the toluene is more weakly bound to the metal centre in **1** compared to the cyclopentadienyl, crown ether and uranium chloroaluminate complexes. A comparison of M-C(arene)/M-C(Cp) and M-(ring centroid) distances (Å) are shown in Table 2.3.

The La-I bond distances range from 3.2801(10) Å to 3.3668(9) Å in **1**, whereas the La-Cl bond distances in $[\text{La}(\eta^6\text{-C}_6\text{Me}_6)(\text{AlCl}_4)_3].0.5\text{C}_6\text{H}_6$ range from 2.9083(10) Å to 2.9298(9) Å.⁵³ These bond lengths are comparable if we consider the ionic radii of chlorides (1.81 Å) and iodides (2.20 Å) in the bonds.^{51, 67} After subtracting the ionic radii from the bond distances, the effective La-I bond distances range from 1.0502(10) Å to 1.1668(9) Å in **1** and those of La-Cl bond distances in $[\text{La}(\eta^6\text{-C}_6\text{Me}_6)(\text{AlCl}_4)_3].0.5\text{C}_6\text{H}_6$ range from 1.0983(10) Å to 1.1198(9) Å. The I-La-I bond angles for adjacent chlorine atoms in the plane range from 70.670(15)° to 140.007(18)° and that of I-Al-I bond angles fall in the range 98.97(8)-116.34(9)° however, most of the I-Al-I angles are close to the idealised tetrahedral angle (~ 109.5°).

Chapter 2

Table 2.3: A comparison of M-C(arene)/M-C(Cp) and M-(ring centroid) distances (Å).

Compound	M-C(arene)/M-C(Cp)	M-C Average	M-(Cent.)	Ref.
La(η^6 -C ₆ H ₅ Me)(AlI ₄) ₃	2.971(9)-3.057(9)	3.0065	2.663(4)	This work
La(η^6 -C ₆ H ₅ Me)(AlCl ₄) ₃	2.927(7)-3.035(7)	2.9765	2.633(7)	52
[La(η^6 -C ₆ Me ₆)(AlCl ₄) ₃].0.5C ₆ H ₆	2.956(4)-3.006(4)	2.9805	2.628(4)	52, 53
U(η^6 -C ₆ H ₆)(AlCl ₄) ₃		2.91		64
{U(η^6 -C ₆ Me ₆)Cl ₂] ₂ (μ -Cl) ₃ AlCl ₄ }		2.92		65
[U(η^6 -C ₆ Me ₆)Cl ₂ (μ -Cl) ₃ UCl ₂ (η^6 -C ₆ Me ₆)] [AlCl ₄]		2.92		66
[La(AlMe ₄) ₂ {1,2,4-(Me ₃ C) ₃ C ₅ H ₂ }]			2.53	56
[Cp* ₂ La(AlMe ₄) ₂]			2.522, 2.516	57
[{ η^5 -C ₅ Me ₄ C ₂ H ₄ NMe ₂ (AlMe ₃)}La(AlMe ₄) ₂]	2.764(1)-2.806(1)			58
[(C ₅ Me ₄ C ₂ H ₄ NMe ₂)La(AlMe ₄) ₂]	2.756(2)-2.843(2)			58
[(C ₅ Me ₄ C ₆ H ₄ NMe ₂)La(AlMe ₄) ₂]	2.732(1)-2.846(1)			58
(C ₅ Me ₅)La(AlMe ₄) ₂	2.753(2)-2.801(3)			59
[{(C ₅ Me ₅) ₂ La(AlEt ₄)} ₂]	2.547-2.561			60
[(C ₅ Me ₄ H)La(AlMe ₄) ₂] ₂	2.7502(11)-2.8228(10)			61
[K([18]-crown-6)] [La{ η^5 -C ₅ H ₃ (SiMe ₃) ₂ -1,3} ₂ (C ₆ H ₆)]	2.75(1)-2.79(1)	2.635(6)	2.427(6)	62, 63

Compound **2** is the first compound of this kind with cerium; however, it is isostructural with **1** and has two molecules in the asymmetric unit. The Ce-C bond lengths fall in the range from 2.947(12) to 3.035(12) Å with a Ce-centroid distance of 2.634(6) Å and are comparable with **1**. The mean U-C distances in the analogous uranium-arene complexes span the range from 2.91-2.92 Å⁶⁴⁻⁶⁶ and the mean Ce-C bond distances in the corresponding cyclopentadienyl complexes fall in the range 2.72(5)-2.83(3) Å.^{62, 63, 68-73} Moreover, the Ce-centroid distances in the corresponding cyclopentadienyl complexes are 2.328-2.55 Å.^{62, 63, 68, 70, 71, 73} Therefore, the Ce-C bond lengths as well as the Ce-centroid distance in **2** are significantly elongated than the corresponding uranium complexes and the cyclopentadienyl complexes. A comparison of M-C(arene)/M-C(Cp) and M-(ring centroid) distances (Å) are given in Table 2.4.

Chapter 2

The Ce-I bond distances range from 3.2260(12) Å to 3.3181(12) Å, similar to **1**. The I-Ce-I bond angles for adjacent chlorine atoms in the plane range from 70.65(2)° to 141.108(3)° and most of the I-Al-I bond angles are closer to the idealised tetrahedral angle.

Table 2.4: A comparison of M-C(arene)/M-C(Cp) and M-(ring centroid) distances (Å).

Compound	M-C(arene)/M-C(Cp)	M-C Average	M-(Cent.)	Ref.
Ce(η^6 -C ₆ H ₅ Me)(AlI ₄) ₃	2.947(12)-3.035(12)	2.9813	2.634(6)	This work
U(η^6 -C ₆ H ₆)(AlCl ₄) ₃		2.91		64
{U(η^6 -C ₆ Me ₆)Cl ₂] ₂ (μ -Cl) ₃ AlCl ₄ }		2.92		65
[U(η^6 -C ₆ Me ₆)Cl ₂ (μ -Cl) ₃ UCl ₂ (η^6 -C ₆ Me ₆)] [AlCl ₄]		2.92		66
Cp' ₂ CeH [Cp'=1,3,4-(Me ₃ C) ₃ (C ₅ H ₂)]		2.81(2)	2.53	71
(C ₅ Me ₅)CeI ₂ (thf) ₃	2.749(13)-2.844(14)	2.7968	2.523(13)	68
[(C ₅ Me ₅) ₂ CeCl ₂ K(THF)] _n	2.77	2.79 (2)		69
[Ce(C ₅ Me ₅) ₂ I(bipy)]		2.83(3)		72
[Cp' ₂ Ce(2,3,4,6-C ₆ HF ₄)]		2.82	2.55	73
[Cp' ₂ Ce(2,3,4,5-C ₆ HF ₄)]		2.82	2.54	73
[{Ce(C ₅ H ₄ Bu ^t) ₂ (μ -I)} ₂]		2.77(3)		74
[(η^5 -C ₅ H ₃ Bu ^t ₂ Ce(μ_2 -Cl)] ₂	2.75(1)-2.85(2)	2.79(5)	2.52	70
[K([18]-crown-6)][Ce{ η^5 -C ₅ H ₃ (SiMe ₃) ₂ -1,3} ₂ -(C ₆ H ₆)]	2.588(5)- 2.787(5)	2.72(5)	2.328	62,63

Nd(η^6 -C₆H₅Me)(AlI₄)₃ **3** to consist of one molecule in the asymmetric unit but is isostructural with **1** and **2**. The Nd-C bond lengths span the range from 2.885(8) Å to 3.011(7) Å with an Nd-centroid distance of 2.579(3) Å. On the other hand, the Nd-C bond lengths in the corresponding chloroaluminate complexes Nd(η^6 -MeC₆H₅)(AlCl₄)₃, [Nd(η^6 -1,3,5-Me₃C₆H₃)(AlCl₄)₃].C₆H₆ and [Nd(η^6 -C₆H₆)(AlCl₄)₃].C₆H₆ range from 2.871(5)-2.999(6), 2.898(9)-2.933(9) and 2.93(2)-2.94(2) Å, respectively.^{22, 42, 44, 46} The average Nd-C bond lengths of the complexes are 2.926, 2.916 and 2.933 Å, respectively.^{22, 42, 44, 46} The Nd-C bond distances in **3** are slightly elongated than the corresponding chloroaluminate complexes exhibit a weaker Nd-C bond in it; however, the bond lengths are comparable with **1** and **2**. Moreover, the Nd-C bond lengths in **3** are significantly

Chapter 2

longer than the M-C bonds in the corresponding uranium-arene complexes and neodymium cyclopentadienyl complexes (Table 2.5).

Table 2.5: A comparison of M-C(arene)/M-C(Cp) and M-(ring centroid) distances (Å).

Compound	M-C(arene)/M-C(Cp)	M-C Average	M-(Cent.)	Ref.
Nd(η^6 -C ₆ H ₅ Me)(AlI ₄) ₃	2.885(8) Å to 3.011(7)	2.9333	2.579(3)	This work
Nd(η^6 -MeC ₆ H ₅)(AlCl ₄) ₃	2.871(5) Å to 2.999(6)	2.926		44
[Nd(η^6 -1,3,5-Me ₃ C ₆ H ₃)(AlCl ₄) ₃].C ₆ H ₆	2.898(9)-2.933(9)	2.916		46
[Nd(η^6 -C ₆ H ₆)(AlCl ₄) ₃].C ₆ H ₆	2.93(2)-2.94(2)	2.933		22,42
U(η^6 -C ₆ H ₆)(AlCl ₄) ₃		2.91		64
{U(η^6 -C ₆ Me ₆)Cl ₂] ₂ (μ -Cl) ₃ AlCl ₄ }		2.92		65
[U(η^6 -C ₆ Me ₆)Cl ₂ (μ -Cl) ₃ UCl ₂ (η^6 -C ₆ Me ₆)] [AlCl ₄]		2.92		66
[Nd(C ₅ H ₄ Bu ^t) ₂ I(py) ₂]		2.76(5)		74
[Nd(AlMe ₄) ₂ {1,2,4-(Me ₃ C) ₃ C ₅ H ₂ }]	2.694(2)-2.768(2)		2.45	56
[{ η^5 -C ₅ Me ₄ C ₂ H ₄ NMe ₂ (AlMe ₃)}Nd(AlMe ₄) ₂]	2.706(1)-2.748(1)			58
[(C ₅ Me ₄ C ₆ H ₄ NMe ₂)Nd(AlMe ₄) ₂]	2.667(2)-2.788(1)			58
[K([18]-crown-6)][Nd{ η^5 -C ₅ H ₃ (SiMe ₃) ₂ -1,3} ₂ (C ₆ H ₆)]	2.555(5)-2.763(5)	2.6865	2.292	63

The equatorial Nd-I bond lengths in **3** range from 3.2296(11) to 3.3296(9), are rather longer than the Nd-I(10) length of 3.1376(7) Å. The Nd-Cl bond lengths in Nd(η^6 -MeC₆H₅)(AlCl₄)₃ fall in the range from 2.799(1) to 2.902(1) Å.⁴⁴ Nd-halide distances are comparable if we consider the ionic radii of the halides. The I-Nd-I bond angles for adjacent iodine atoms in the plane range from 68.513(14)^o to 140.369(17)^o, similar to **1** and **2**. The majority of the I-Al-I bond angles are closer to the idealised tetrahedral angle.

The X-ray crystal structure of complex **4** reveals an analogous structure of **1**, **2** and **3**. Moreover, it is isostructural with the reported complex Gd(η^6 -MeC₆H₅)(AlCl₄)₃.⁴⁵ The asymmetric unit contains two individual molecules in it, and the Gd-C bond lengths span the range from 2.868(9) to 2.978(9) Å with a Gd-centroid distance of 2.5495(5) Å. The Gd-C distances in the formally zerovalent bis(benzene) sandwich complex Gd(1,3,5-t-

Chapter 2

$\text{Bu}_3\text{C}_6\text{H}_3)_2$ are 2.585-2.660 Å (average 2.630Å) and Gd-centroid distance is 2.219 Å.⁷⁴ The Gd-centroid distance in the corresponding cyclopentadienyl complex $[\text{Gd}(\eta^5\text{-C}_5\text{Me}_4\text{SiMe}_3)\{(\mu\text{-Me})_2(\text{AlMe}_2)\}_2]$ is 2.393(2).⁷⁵ So, the Gd-arene bonds in **4** are significantly weaker than the Gd-arene bonds in the corresponding uranium-arene (Table 2.6), cyclopentadienyl and the zerovalent benzene complexes.

The equatorial Gd-I bond lengths in **4** range from 3.1991(10) to 3.3089(9)Å with an axial iodide (I10) being the shortest distance (3.1513(10) Å) to gadolinium. The I-Gd-I bond angles for adjacent chlorine atoms in the plane range from 68.11(2)° to 140.81(2)°. Most of the I-Al-I angles are closer to the idealised tetrahedral angle. The selected bond lengths (Å) and bond angles (°) for **1**, **2**, **3** and **4** are shown in Table 2.7 and 2.8, respectively.

The average Ln-C distances as well as the Ln-C(centroid) distances in the trivalent iodoaluminate lanthanoid complexes display a gradual decrease (Fig. 2.3) from lanthanum to gadolinium due to the lanthanoid contraction.

Chapter 2

Table 2.6: A comparison of M-C(arene)/M-C(Cp) and M-(ring centroid) distances (Å).

Compound	M-C(arene)/M-C(Cp)	M-C Average	M-(Cent.)	Ref.
Gd(η^6 -C ₆ H ₅ Me)(AlI ₄) ₃	2.868(9)-2.978(9)	2.9035	2.5495(5)	This work
U(η^6 -C ₆ H ₆)(AlCl ₄) ₃		2.91		64
{U(η^6 -C ₆ Me ₆)Cl ₂] ₂ (μ -Cl) ₃ AlCl ₄ }		2.92		65
[U(η^6 -C ₆ Me ₆)Cl ₂ (μ -Cl) ₃ UCl ₂ (η^6 -C ₆ Me ₆)] [AlCl ₄]		2.92		66
Gd(1,3,5-t-Bu ₃ C ₆ H ₃) ₂	2.585-2.660	2.630	2.219	74
[Gd(η^5 -C ₅ Me ₄ SiMe ₃){(μ -Me) ₂ (AlMe ₂) ₂ }]			2.393(2)	75

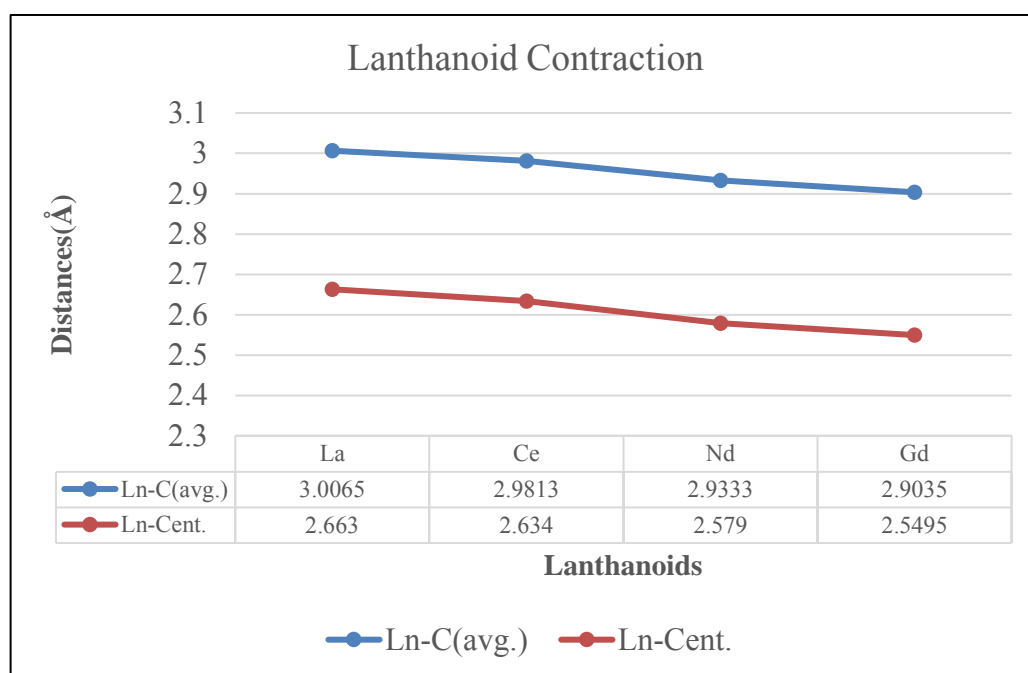


Fig. 2.3: Lanthanoid contraction in iodoaluminate lanthanoid(III) complexes in toluene.

Chapter 2

Table 2.7: The selected bond lengths (Å) for Ln(η^6 -C₆H₅Me)(AlI₄)₃; Ln = La (1), Ce (2), Nd (3) and Gd (4).

Ln =	La (1)	Ce (2)	Nd (3)	Gd (4)
Ln(1)-I(1)	3.3330(9)	3.3181(12)	3.3294(9)	3.3089(9)
Ln(1)-I(2)	3.2801(10)	3.2615(11)	3.2296(11)	3.2414(8)
Ln(1)-I(5)	3.3668(9)	3.3537(11)	3.2653(8)	3.2720(9)
Ln(1)-I(6)	3.3155(8)	3.2989(11)	3.2760(9)	3.1991(10)
Ln(1)-I(9)	3.2813(9)	3.2622(12)	3.3296(9)	3.2069(10)
Ln(1)-I(10)	3.2502(10)	3.2260(12)	3.1376(7)	3.1513(10)
Ln(1)-C(2)	3.057(9)	3.037(12)	3.011(7)	2.978(9)
Ln(1)-C(3)	3.007(8)	2.991(11)	2.953(7)	2.931(10)
Ln(1)-C(4)	2.971(9)	2.974(10)	2.928(8)	2.892(9)
Ln(1)-C(5)	2.988(9)	2.964(11)	2.897(7)	2.868(9)
Ln(1)-C(6)	2.995(9)	2.948(12)	2.885(8)	2.883(9)
Ln(1)-C(7)	3.021(9)	2.974(12)	2.926(8)	2.896(9)
Ln(1)-C(avg.)	3.0065	2.9813	2.9333	2.9035
Ln(1)-C(cent.)	2.663(4)	2.634(6)	2.579(3)	2.5495(5)
Al(1)-I(1)	2.590(3)	2.565(3)	2.577(3)	2.563(3)
Al(1)-I(2)	2.575(3)	2.581(3)	2.589(2)	2.582(3)
Al(1)-I(3)	2.482(3)	2.499(4)	2.481(2)	2.498(3)
Al(1)-I(4)	2.471(3)	2.487(4)	2.500(2)	2.484(3)
Al(2)-I(5)	2.568(3)	2.585(4)	2.576(3)	2.585(3)
Al(2)-I(6)	2.582(2)	2.578(4)	2.581(3)	2.575(3)
Al(2)-I(7)	2.484(3)	2.480(4)	2.490(3)	2.469(3)
Al(2)-I(8)	2.496(3)	2.478(3)	2.486(3)	2.479(3)
Al(3)-I(9)	2.603(3)	2.608(3)	2.582(2)	2.604(3)
Al(3)-I(10)	2.597(2)	2.594(3)	2.580(2)	2.592(3)
Al(3)-I(11)	2.483(2)	2.486(4)	2.492(2)	2.486(3)
Al(3)-I(12)	2.487(2)	2.487(4)	2.495(2)	2.486(3)

Chapter 2

Table 2.8: The selected bond angles (°) for Ln(η^6 -C₆H₅Me)(AlI₄)₃; Ln = La (1), Ce (2), Nd (3) and Gd (4).

Ln =	La (1)	Ce (2)	Nd (3)	Gd (4)
Centroid-Ln-I(axial)	178.07(8)	178.55(12)	179.51(8)	179.34(10)
I(2)-Ln(1)-I(1)	72.419(16)	72.56(3)	72.915(14)	72.10(2)
I(2)-Ln(1)-I(5)	138.528(19)	138.54(3)	137.255(17)	138.25(2)
I(5)-Ln(1)-I(1)	140.007(18)	139.83(3)	137.069(16)	138.99(2)
I(6)-Ln(1)-I(1)	138.36(2)	138.30(3)	140.318(17)	138.51(2)
I(6)-Ln(1)-I(2)	68.394(15)	68.29(3)	68.513(14)	68.11(2)
I(6)-Ln(1)-I(5)	71.735(15)	71.82(3)	73.144(15)	72.87(2)
I(6)-Ln(1)-I(9)	139.459(18)	139.43(3)	140.369(17)	140.81(2)
I(9)-Ln(1)-I(1)	71.213(15)	71.05(3)	69.188(13)	70.393(19)
I(9)-Ln(1)-I(2)	141.11(2)	141.108(3)	137.444(16)	139.32(2)
I(9)-Ln(1)-I(5)	70.670(15)	70.65(2)	69.664(13)	70.56(2)
I(10)-Ln(1)-I(1)	80.015(17)	80.13(3)	80.973(15)	80.64(2)
I(10)-Ln(1)-I(2)	82.813(19)	82.50(3)	77.190(14)	79.99(3)
I(10)-Ln(1)-I(5)	80.623(17)	80.68(3)	79.397(14)	80.14(3)
I(10)-Ln(1)-I(6)	81.674(17)	81.13(3)	81.819(16)	81.43(3)
I(10)-Ln(1)-I(9)	77.819(16)	78.18(4)	78.437(13)	78.96(3)
I(1)-Al(1)-I(2)	98.28(9)	97.89(12)	97.99(8)	97.05(9)
I(3)-Al(1)-I(1)	110.08(9)	110.69(15)	112.05(9)	114.77(11)
I(3)-Al(1)-I(2)	110.33(10)	110.34(14)	109.67(10)	106.62(11)
I(4)-Al(1)-I(1)	111.58(10)	111.58(13)	110.13(9)	112.62(12)
I(4)-Al(1)-I(2)	107.81(9)	107.58(15)	106.56(9)	112.19(10)
I(4)-Al(1)-I(3)	117.10(10)	117.01(15)	118.35(9)	112.45(11)
I(6)-Al(2)-I(5)	98.97(8)	98.60(12)	98.18(8)	96.29(9)
I(7)-Al(2)-I(5)	111.67(11)	111.85(13)	110.88(10)	111.88(11)
I(7)-Al(2)-I(6)	112.20(9)	112.28(14)	108.27(11)	107.92(11)
I(7)-Al(2)-I(8)	112.12(9)	112.11(14)	115.77(10)	117.33(11)
I(8)-Al(2)-I(5)	114.77(9)	114.80(15)	110.68(11)	111.07(11)
I(8)-Al(2)-I(6)	106.28(10)	106.33(13)	111.66(10)	110.26(11)
I(10)-Al(3)-I(9)	104.18(8)	103.72(13)	104.89(7)	102.17(9)
I(11)-Al(3)-I(9)	105.46(9)	105.50(13)	109.50(8)	110.29(10)
I(11)-Al(3)-I(10)	110.73(9)	110.88(12)	109.06(8)	110.32(10)
I(12)-Al(3)-I(9)	110.05(9)	110.04(12)	111.31(8)	106.11(10)
I(12)-Al(3)-I(10)	109.34(9)	109.66(13)	108.26(8)	111.08(11)
I(12)-Al(3)-I(11)	116.34(9)	116.23(15)	113.44(8)	115.90(10)

Chapter 2

2.3.2.2 Iodoaluminate lanthanoid(II) complexes in toluene

The divalent samarium complex $[\text{Sm}(\eta^6\text{-MeC}_6\text{H}_5)(\text{AlI}_4)_2]_n \cdot \text{PhMe}$ (**5**) (Fig. 2.4 and 2.5) has been synthesised by the procedure described in scheme 2.1, and the compound crystallises on the orthorhombic space group $P2_12_12_1$ (No. 19), with a polymeric structure. The Sm^{2+} ion is coordinated to two AlI_4^- ligands with an η^6 toluene molecule at an axial position. The geometry surrounding the Sm^{2+} ion can be described as a distorted pentagonal bipyramid. The Sm-C bond lengths extend the range from 2.955(18) to 3.083(11) Å with a Sm-centroid distance of 2.6884(4) Å, and are comparable with the reported samarium complex $[\text{Sm}(\eta^6\text{-C}_6\text{Me}_6)(\text{AlCl}_3\text{I})_2]_n$, in which the Sm-C bond lengths and the Sm-centroid distances are 2.970(6)-3.063(6) Å and 2.655 Å, respectively.⁵⁰

The Sm-Cp(centroid) lengths in the cyclopentadienyl complex $(\text{C}_5\text{Me}_5)_2\text{Sm}(\text{THF})(\eta^2\text{-Et})\text{AlEt}_3$ fall in the range 2.434-2.446 Å⁷⁶. In the fluorenyl complex $\eta^5\text{-bis}(\text{Me}_3\text{Si-fluorenyl})\text{Sm}(\text{THF})_2$, the Sm-Cp(centroid) distances fall in the range 2.67-2.70 Å⁷⁷ and that of 2.629-2.633 Å in $(\text{C}_{13}\text{H}_9)_2\text{Sm}(\text{THF})_2$.⁷⁸ On the other hand, the Sm-Ph(centroid) distance in $\eta^6\text{-bis}(\text{Me}_3\text{Si-fluorene-AlMe}_3)\text{Sm}$ is 2.74 Å and that of 2.76 Å in $\eta^6\text{-bis}(\text{Me}_3\text{Si-fluorene-AlEt}_3)\text{Sm}$.⁷⁷ In $[\text{Sm}(\text{AlMe}_4)_2\{1,2,4\text{-(Me}_3\text{C)}_3\text{C}_5\text{H}_2\}]$, the Sm-Cp distances are 2.668(1)-2.748(1) Å and that of Sm-Cp(centroid) is 2.42 Å.⁵⁶ The Sm-Cp(centroid) contacts in $[(\text{C}_5\text{Me}_5)\text{Sm}(\mu\text{-I})(\text{thf})_2]_2$ is 2.534 Å.⁷⁹

From the literature data, it is obvious that the samarium-arene bonds are significantly weaker than the corresponding cyclopentadienyl complexes (as Cps are charged but arenes are neutral) except the fluorenyl-Cp complexes, where the bond strengths are almost analogous. However, the samarium-arene bonds in **5** are significantly stronger than the Sm-Ph(centroid) bonds in the fluorene complexes. The mean Sm-C bond length in **5** (3.0221 Å) is considerably longer than that of the mean Sm-C bond lengths in the corresponding samarium chloroaluminate arene complexes (Table 2.2) and the mean U-C bond lengths in the analogous uranium-arene complexes (Table 2.6), also support the weaker bond strength of samarium with the toluene molecule.

In **5**, the equatorial Sm-I bond lengths range from 3.3585(13) to 3.6029(14) Å (average 3.4455 Å) with an axial Sm-I(6) of 3.3968(12) Å. The average Sm-Cl bond distances in

Chapter 2

the corresponding chloroaluminate samarium complexes $[\text{Sm}(\eta^6\text{-C}_6\text{H}_6)(\text{AlCl}_4)_3]\cdot\text{C}_6\text{H}_6$, $\text{Sm}(\eta^6\text{-MeC}_6\text{H}_5)(\text{AlCl}_4)_3$, $\text{Sm}(\eta^6\text{-1,3-Me}_2\text{C}_6\text{H}_4)(\text{AlCl}_4)_3$, $[\text{Sm}(\eta^6\text{-C}_6\text{Me}_6)(\text{AlCl}_4)_3]\cdot(\text{MeC}_6\text{H}_5)_{1.5}$ and $[\text{Sm}(\eta^6\text{-C}_6\text{Me}_6)(\text{AlCl}_4)_3]\cdot\text{MeC}_6\text{H}_5$ are 2.83, 2.84, 2.836, 2.85 and 2.85 Å, respectively (Table 2.2). These bond lengths are comparable if we consider the ionic radii of chlorides and iodides. The I-Sm-I bond angles range from 68.30(3) to 143.20(3)° and most of the I-Al-I angles are closer to the idealised tetrahedral angle.

Compound $[\text{Eu}(\eta^6\text{-MeC}_6\text{H}_5)(\text{AlCl}_4)_2]_n\cdot\text{PhMe}$ (**6**) is isostructural with **5**. The Eu-C bond lengths fall in the range 2.97(2)-3.099(16) Å with an average Eu-C length of 3.018 Å. The Eu-C distances in $[\text{Eu}(\eta^6\text{-C}_6\text{Me}_6)(\text{AlCl}_4)_2]_4\cdot(\text{C}_6\text{H}_2\text{Me}_4)$ range from 2.917(15) to 3.066(12) Å with an average Eu-C distance of 2.999(23) Å.^{48,49} $[\text{Eu}(\eta^6\text{-C}_6\text{Me}_6)(\text{AlCl}_4)_2]_4\cdot(\text{C}_6\text{H}_2\text{Me}_4)$ is the only reported chloroaluminate complex of europium so far having a distorted pentagonal bipyramid geometry and **6** is comparable with it. However, the reported complex forms a cyclotetramer composed of four $\text{Eu}(\text{C}_6\text{Me}_6)(\text{AlCl}_4)_2$ units, whereas complex **6** forms a polymer.

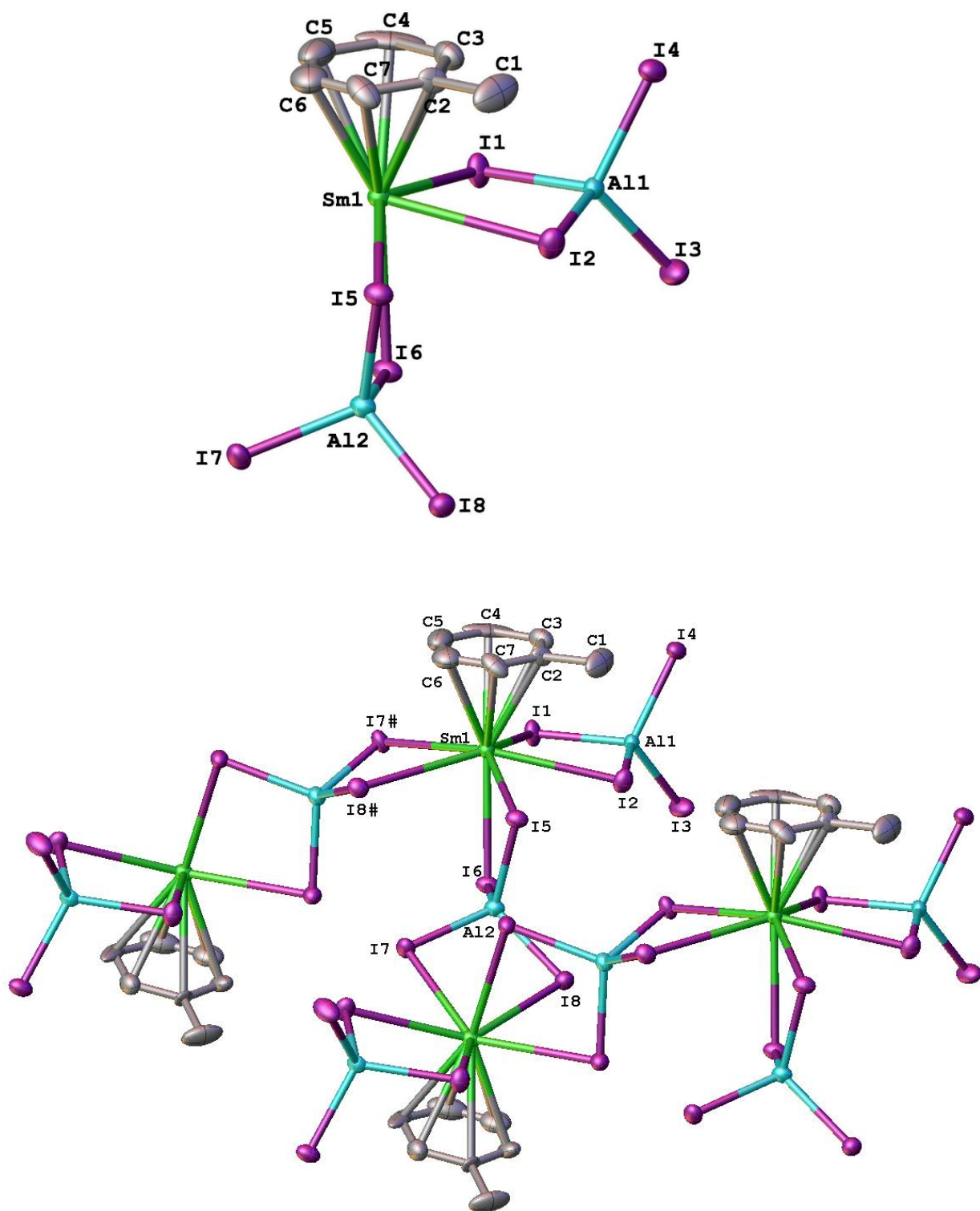


Fig. 2.4: A monomeric repeat unit (top) and the one dimensional extended framework for $[\text{Sm}(\eta^6\text{-MeC}_6\text{H}_5)(\text{AlI}_4)_2]_n \cdot \text{PhMe}$ (**5**) (bottom), representative of the isostructural complex **6**. Hydrogen atoms and the solvent of crystallisation (toluene) have been omitted for clarity.

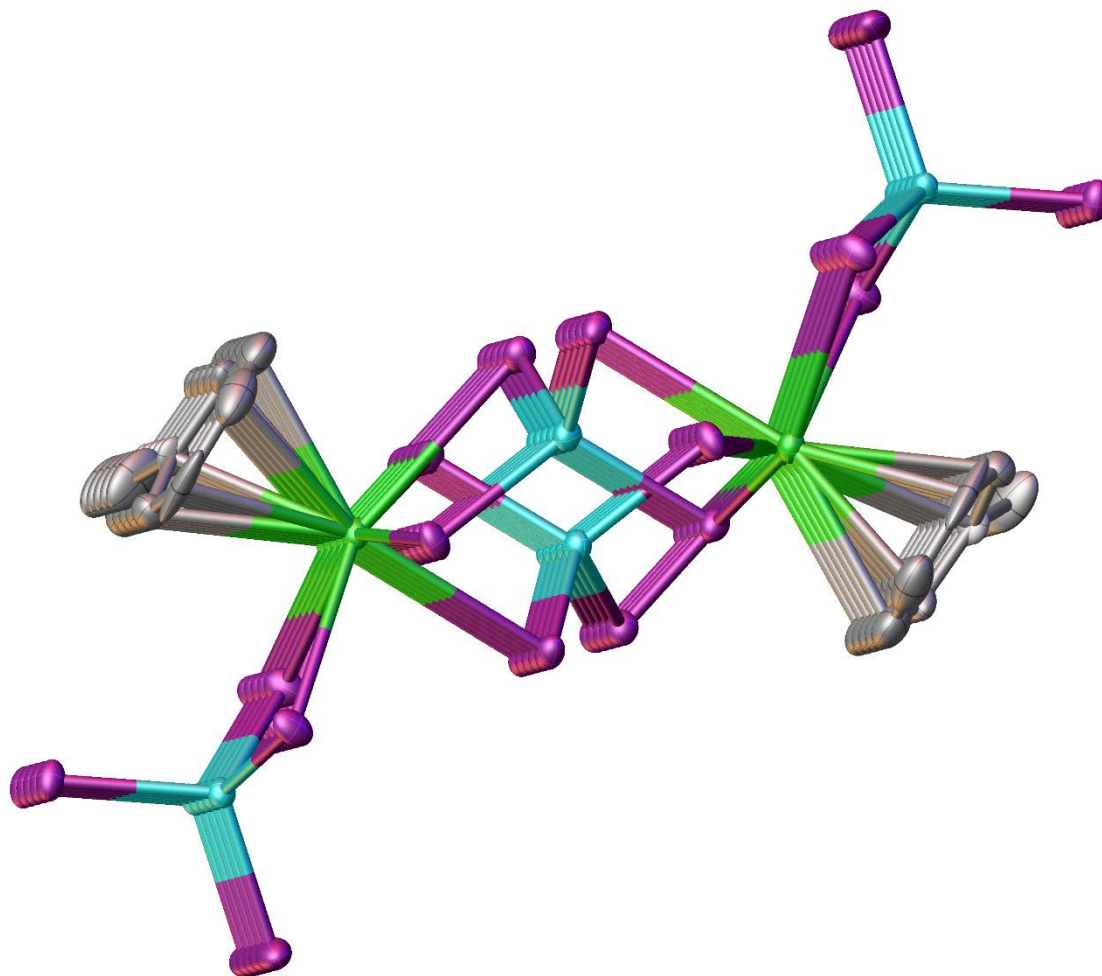


Fig. 2.5: The Sm-arene double stranded polymer with two bridging AlI_4^- units and two terminal AlI_4^- units for $[\text{Sm}(\eta^6\text{-MeC}_6\text{H}_5)(\text{AlI}_4)_2]_n\text{PhMe}$ (**5**), representative of the isostructural complex **6**. Hydrogen atoms and the solvent of crystallisation (toluene) have been omitted for clarity.

The Eu-centroid distance in **6** is 2.691(6) Å, and that in the corresponding cyclopentadienyl complexes are 2.4423(13) and 2.4619(5) Å in $(\text{C}_5\text{Me}_5)_2\text{Eu}(\text{DADC}_6\text{F}_5)$ ($\text{DADC}_6\text{F}_5 = \text{C}_6\text{F}_5\text{NC}(\text{Me})\text{C}(\text{Me})\text{NC}_6\text{F}_5$)⁸⁰, 255.0(2) in $[(\eta^5\text{-C}_5\text{H}_5)\text{V}(\mu^2\text{-}\eta^6\text{:}\eta^6\text{-C}_{10}\text{H}_8)_2\text{Eu}(\text{thf})(\text{dme})]^{81}$. In the binuclear complex of Eu(II) $[\mu^2\text{-}\eta^4\text{:}\eta^4\text{-C}_{10}\text{H}_8][\text{EuI}(\text{DME})_2]$, the Eu-centroid distance is 2.583(3)⁸² and the average Eu-C distance in the indene complex $(\eta^5\text{:}\eta^1\text{-C}_9\text{H}_5\text{-1-Me-3-CH}_2\text{SiMe}_2\text{NC}_4\text{H}_8)_2\text{Eu}$ is 2.911(18)⁸³. From the average Eu-C distances as well as the Eu-centroid distances of the reported complexes, it is seen that the Eu-arene bonds in **6** is significantly weaker than the corresponding cyclopentadienyl, indene and naphthalene complexes.

Chapter 2

The equatorial Eu-I bond lengths range from 3.3683(14) to 3.6062(14) Å (average 3.4529 Å) with an axial Eu-I(6) of 3.3849(13) Å, similar to **5** and are comparable with [Eu(η^6 -C₆Me₆)(AlCl₄)₂]₄.(C₆H₂Me₄) if we consider the ionic radii of chlorides and iodides. The I-Eu-I bond angles range from 68.56(3) to 142.61(3)° and most of the I-Al-I angles are closer to the idealised tetrahedral angle. The selected bond lengths (Å) and bond angles (°) for **5** and **6** are listed in Table 2.9 and 2.10, respectively.

Table 2.9: The selected bond lengths (Å) for [Ln(η^6 -MeC₆H₅)(AlI₄)₂]_n.PhMe; Ln = Sm (5**) and Eu (**6**).**

Ln =	Sm (5)	Eu (6)
Ln(1)-I(1)	3.3585(13)	3.3683(14)
Ln(1)-I(2)	3.4307(13)	3.4083(14)
Ln(1)-I(5)	3.4159(13)	3.4230(14)
Ln(1)-I(6)	3.3968(12)	3.3849(13)
Ln(1) ¹ -I(7)	3.4681(13)	3.4587(15)
Ln(1) ¹ -I(8)	3.6029(14)	3.6062(14)
Ln(1)-C(2)	3.0831(4)	3.099(16)
Ln(1)-C(3)	3.037(17)	3.029(15)
Ln(1)-C(4)	2.955(18)	3.01(2)
Ln(1)-C(5)	2.98(2)	2.97(2)
Ln(1)-C(6)	3.01(2)	2.97(2)
Ln(1)-C(7)	3.068(16)	3.030(19)
Ln(1)-C(avg.)	3.0221	3.018
Ln(1)-C(cent.)	2.6884(4)	2.690(5)
Al(1)-I(1)	2.540(4)	2.546(5)
Al(1)-I(2)	2.558(5)	2.550(5)
Al(1)-I(3)	2.500(4)	2.507(5)
Al(1)-I(4)	2.506(4)	2.505(5)
Al(2)-I(5)	2.542(5)	2.546(5)
Al(2)-I(6)	2.559(4)	2.554(5)
Al(2)-I(7)	2.525(5)	2.528(4)
Al(2)-I(8)	2.529(4)	2.531(5)

(**5**) ¹1/2+x,3/2-y,1-z; (**6**) ¹-1/2+x,1/2-y,1-z

Chapter 2

Table 2.10: The selected bond angles (°) for [Ln(η^6 -MeC₆H₅)(AlI₄)₂]_n.PhMe; Ln = Sm (5) and Eu (6).

Ln =	Sm (5)	Eu (6)
Centroid-Ln-	171.2(2)	173.7(2)
I(axial)		
I(1)-Ln(1)-I(2)	71.79(3)	72.15(3)
I(1)-Ln(1)-I(5)	140.74(3)	140.85(4)
I(1)-Ln(1)-I(6)	84.12(3)	84.12(4)
I(1)-Ln(1)-I(7) ²	68.30(3)	68.69(3)
I(1)-Ln(1)-I(8) ²	135.36(3)	135.75(4)
I(2)-Ln(1)-I(7) ²	137.46(3)	138.38(4)
I(2)-Ln(1)-I(8) ²	143.20(3)	142.61(3)
I(5)-Ln(1)-I(2)	71.95(3)	77.60(3)
I(5)-Ln(1)-I(7) ²	138.36(4)	137.99(3)
I(5)-Ln(1)-I(8) ²	73.43(3)	72.73(3)
I(6)-Ln(1)-I(2)	76.94(3)	77.60(3)
I(6)-Ln(1)-I(5)	73.52(3)	73.61(3)
I(6)-Ln(1)-I(7) ²	84.90(3)	84.89(3)
I(6)-Ln(1)-I(8) ²	81.70(3)	81.30(3)
I(7) ² -Ln(1)-I(8) ²	68.43(3)	68.56(3)
I(1)-Al(1)-I(2)	102.68(16)	103.10(17)
I(3)-Al(1)-I(1)	110.73(17)	110.70(19)
I(3)-Al(1)-I(2)	110.75(16)	110.65(19)
I(3)-Al(1)-I(4)	112.09(17)	112.42(18)
I(4)-Al(1)-I(1)	110.36(16)	109.84(19)
I(4)-Al(1)-I(2)	109.84(16)	109.73(19)
I(5)-Al(2)-I(6)	106.13(16)	106.20(16)
I(7)-Al(2)-I(5)	111.53(17)	111.18(18)
I(7)-Al(2)-I(6)	110.29(17)	110.50(18)
I(7)-Al(2)-I(8)	103.84(16)	103.81(16)
I(8)-Al(2)-I(5)	110.81(17)	111.16(18)
I(8)-Al(2)-I(6)	114.36(18)	114.09(19)

(5) ²-1/2+x,3/2-y,1-z; (6) ²-1/2+x,1/2-y,1-z

Chapter 2

Complex $\text{Yb}(\eta^6\text{-MeC}_6\text{H}_5)(\text{AlI}_4)_2]_{n.1/2}\text{PhMe}$ (**7**) (Fig. 2.6 and 2.7), while divalent, like Sm and Eu is rather different due to the much smaller size of Yb^{2+} compared with the other two, and therefore, we get a different structure due to diminished coordination number. Complex **7** is the first polymeric structure of ytterbium among the halogenoaluminate complexes.

The Yb-C contacts fall in the range 2.896(10)-2.961(10) Å with an average of 2.920 Å, which are slightly smaller than the Ln-C contacts in **5** and **6** (Table 2.9). This is due to the differences in the ionic radii of the metals. The Yb-C contacts in the corresponding trivalent chloroaluminate complex of ytterbium $[\text{Yb}(\eta^6\text{-C}_6\text{Me}_6)(\text{AlCl}_4)_3]\cdot\text{MeC}_6\text{H}_5$ range from 2.739(35) to 3.010(48) Å with an average of 2.865 Å, and are fairly comparable with **7**. In the corresponding cyclopentadienyl complex of ytterbium $\text{Yb}(\text{C}_5\text{Me}_5)_2\text{AlCl}_4$, the Yb-C distances fall in the range 2.559(3)-2.609(3) Å⁸⁴, which is considerably smaller than that of in **7**. The distinct difference in the Yb-C bond lengths reveals the weaker bond strength in the arene complex compared to the cyclopentadienyl counterparts due to neutral vs charged ligands.

The equatorial Yb-I contacts range from 3.1442(10) to 3.2917(10) Å and the axial Yb-I contact is 3.2917(10) Å which is reasonably smaller than the Ln-I contacts in **5** and **6**. The Yb-Cl contacts in $[\text{Yb}(\eta^6\text{-C}_6\text{Me}_6)(\text{AlCl}_4)_3]\cdot\text{MeC}_6\text{H}_5$ are comparable considering the ionic radii of chlorides and bromides. The I-Yb-I bond angles range from 77.19(4) to 155.60(2)° and most of the I-Al-I angles are closer to the idealised tetrahedral angle. The selected bond lengths (Å) and bond angles (°) for **5** and **6** are itemised in Table 2.9 and 2.10, respectively. The contribution of the lanthanoid contraction in divalent complexes is shown in Fig. 2.8. The Ln-C(avg.) and Ln-Centroid distances in **5** and **6** are similar; however, there is a sudden decrease in **7** that also reduced the coordination number of Yb.

Chapter 2

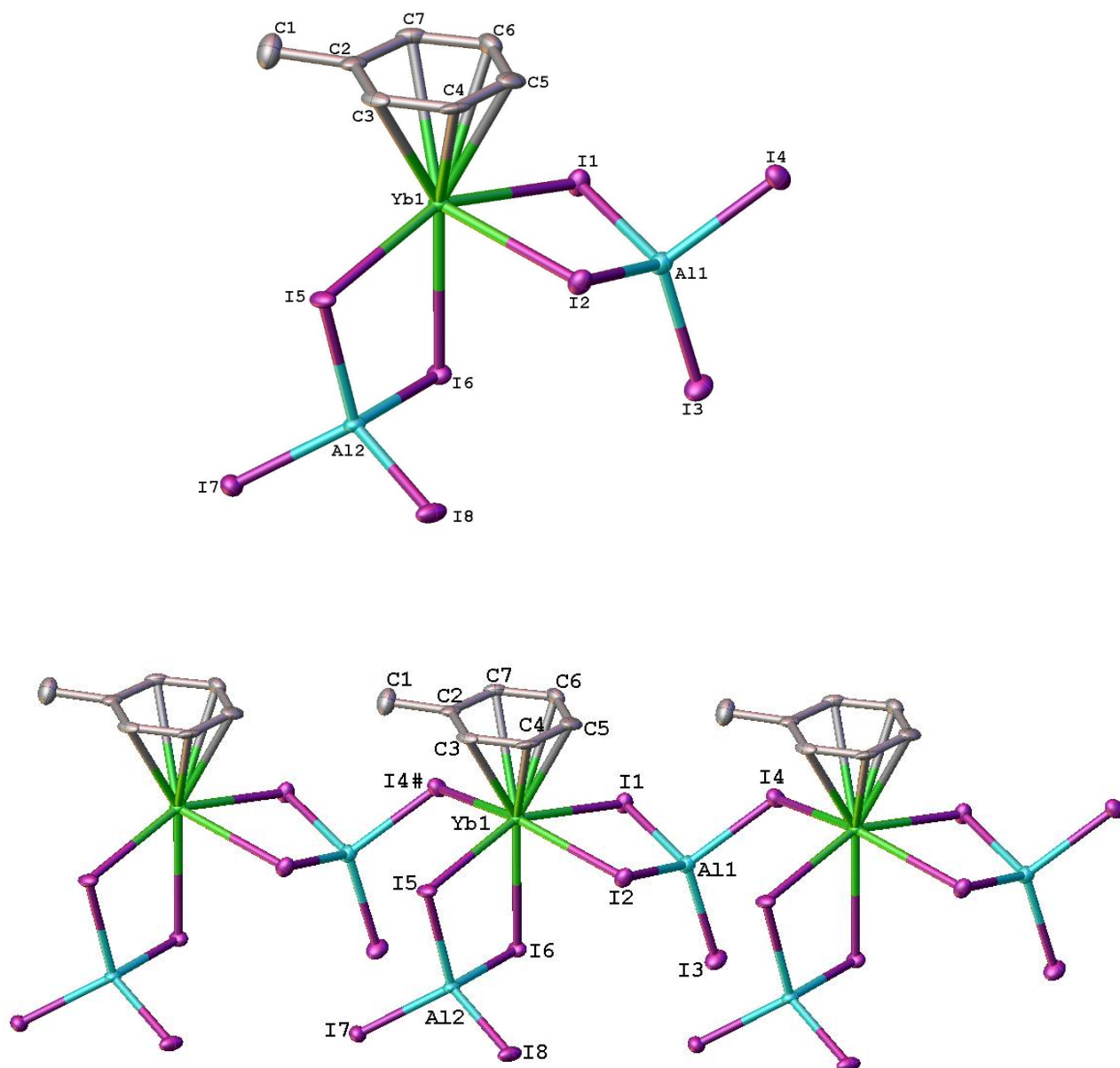


Fig. 2.6: A monomeric repeat unit (top) and the one dimensional extended framework for $[\text{Yb}(\eta^6\text{-MeC}_6\text{H}_5)(\text{AlI}_4)_2]_n \cdot 1/2\text{PhMe}$ (**7**) (bottom). Hydrogen atoms and the solvent of crystallisation (toluene) have been omitted for clarity.

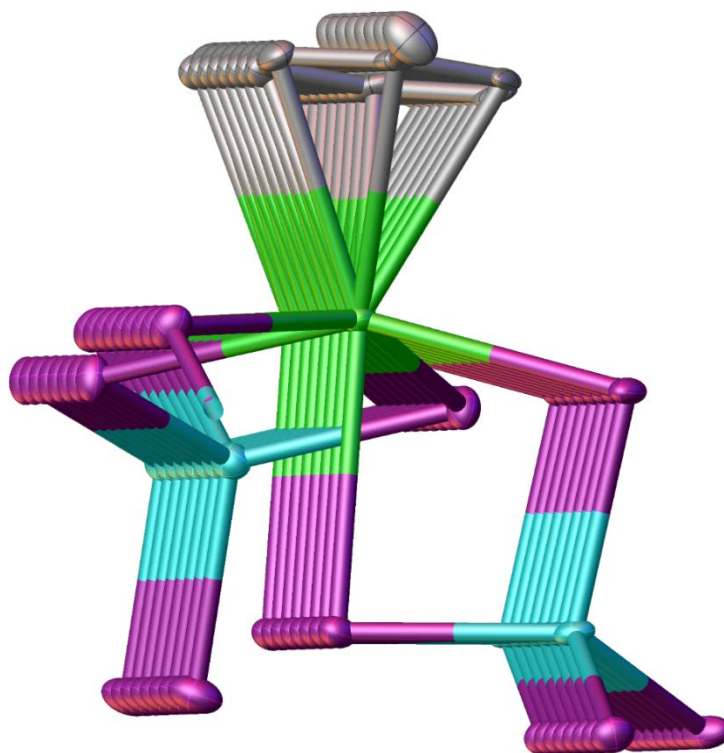


Fig. 2.7: The Yb-arene single stranded polymer with two AlI_4^- units for $[\text{Yb}(\eta^6\text{-MeC}_6\text{H}_5)(\text{AlI}_4)_2]_n \cdot 1/2\text{PhMe}$ (7). Solvent of crystallisation (toluene) have been omitted for clarity.

Table 2.11: The selected bond lengths (\AA) for $[\text{Yb}(\eta^6\text{-MeC}_6\text{H}_5)(\text{AlI}_4)_2]_n \cdot 1/2\text{PhMe}$ (7)

	Yb (7)		Yb (7)
Yb(1)-I(1)	3.2321(13)	Yb(1)-C(avg.)	2.920
Yb(1)-I(2)	3.2228(10)	Yb(1)-C(cent.)	2.565(4)
Yb(1) ¹ -I(4)	3.2829(10)	Al(1)-I(1)	2.569(3)
Yb(1)-I(5)	3.1442(10)	Al(1)-I(2)	2.549(3)
Yb(1)-I(6)	3.2917(10)	Al(1)-I(3)	2.477(3)
Yb(1)-C(2)	2.961(10)	Al(1)-I(4)	2.563(3)
Yb(1)-C(3)	2.945(10)	Al(2)-I(5)	2.577(3)
Yb(1)-C(4)	2.903(11)	Al(2)-I(6)	2.567(3)
Yb(1)-C(5)	2.899(11)	Al(2)-I(7)	2.495(3)
Yb(1)-C(6)	2.896(10)	Al(2)-I(8)	2.496(3)
Yb(1)-C(7)	2.920(10)		

¹+x,1+y,+z

Chapter 2

Table 2.12: The selected bond angles ($^{\circ}$) for $[\text{Yb}(\eta^6\text{-MeC}_6\text{H}_5)(\text{AlI}_4)_2]_n \cdot 1/2\text{PhMe}$ (7).

	Yb (7)		Yb (7)
Centroid-Ln-I(axial)	177.24(10)	I(2)-Al(1)-I(4)	109.31(12)
I(1)-Yb(1)-I(4) ²	81.90(3)	I(3)-Al(1)-I(1)	110.10(12)
I(1)-Yb(1)-I(6)	78.74(3)	I(3)-Al(1)-I(2)	112.74(12)
I(2)-Yb(1)-I(1)	78.95(2)	I(3)-Al(1)-I(4)	112.71(12)
I(2)-Yb(1)-I(4) ²	155.60(2)	I(4)-Al(1)-I(1)	104.92(11)
I(2)-Yb(1)-I(6)	81.06(2)	I(6)-Al(2)-I(5)	102.67(10)
I(4) ² -Yb(1)-I(6)	80.49(3)	I(7)-Al(2)-I(5)	109.47(12)
I(5)-Yb(1)-I(1)	154.40(2)	I(7)-Al(2)-I(6)	113.14(12)
I(5)-Yb(1)-I(2)	88.82(2)	I(7)-Al(2)-I(8)	112.16(11)
I(5)-Yb(1)-I(4) ²	102.46(3)	I(8)-Al(2)-I(5)	108.98(12)
I(5)-Yb(1)-I(6)	77.19(4)	I(8)-Al(2)-I(6)	109.95(12)
I(2)-Al(1)-I(1)	106.60(12)		

²+x,-1+y,+z

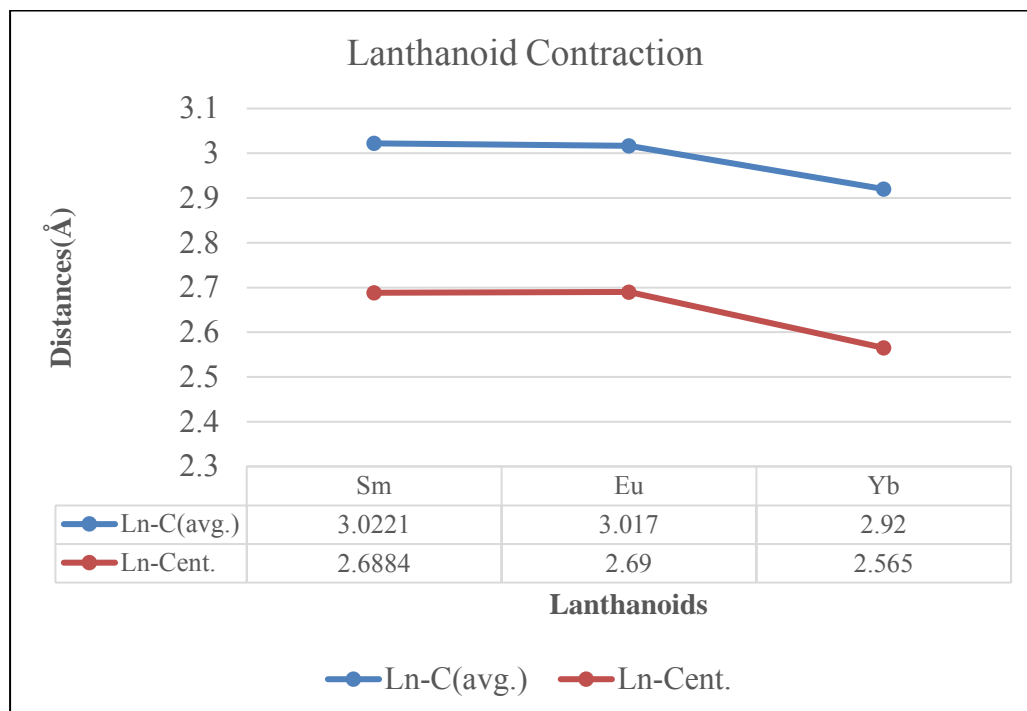


Fig. 2.8: Lanthanoid contraction in iodoaluminate lanthanoid(II) complexes in toluene.

Chapter 2

$\text{Ce}(\eta^6\text{-C}_6\text{H}_3\text{Me}_3)(\text{AlI}_4)_3$ (**9**) crystallises with one molecule in the asymmetric unit and is isostructural with **2**. The Ce-C bond contacts as well as the Ce-centroid distance in **9** are significantly elongated than in the corresponding uranium chloroaluminate and cyclopentadienyl complexes (Table 2.4 and 2.13) suggest a weaker metal-arene interaction in the iodoaluminate arene complexes.

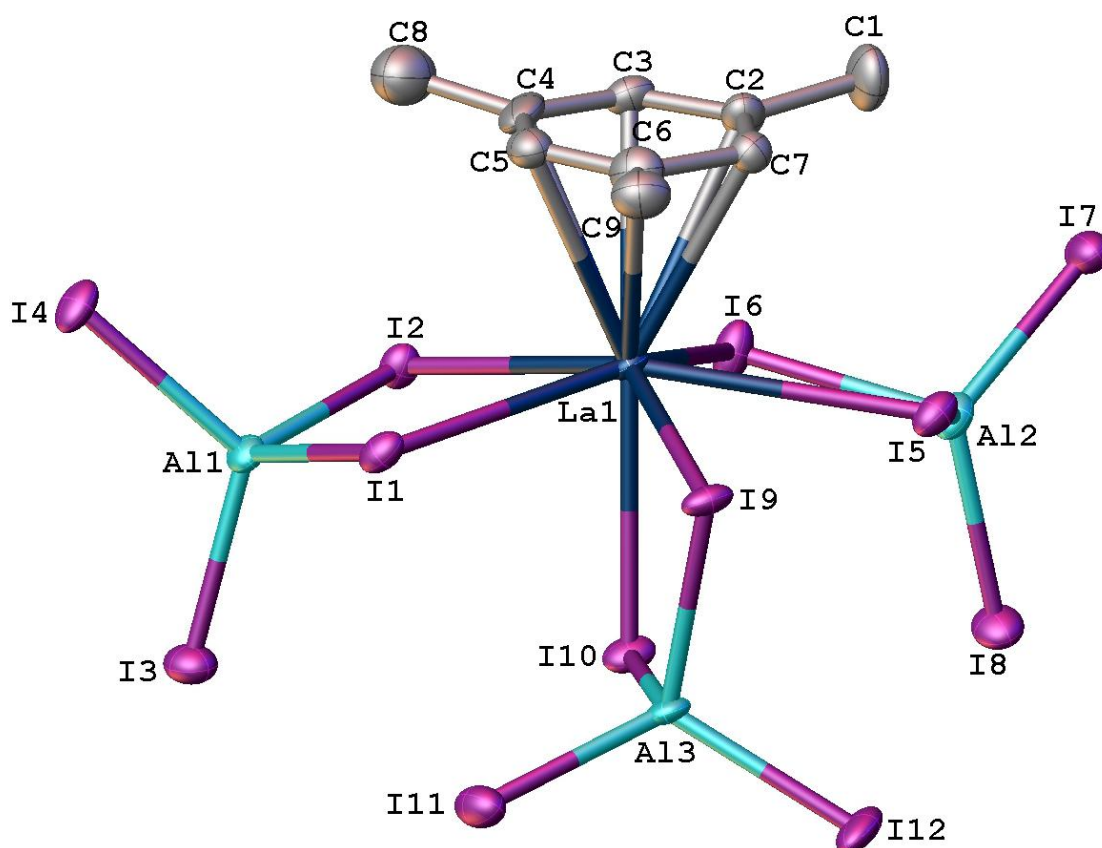


Fig. 2.9: Molecular structure of $\text{La}(\eta^6\text{-C}_6\text{H}_3\text{Me}_3)(\text{AlI}_4)_3$ (**8**), representative of the isostructural complexes **9**, **10**, **11**, **12** and **13**. Hydrogen atoms have been omitted for clarity.

X-ray crystallography shows $\text{Pr}(\eta^6\text{-C}_6\text{H}_3\text{Me}_3)(\text{AlI}_4)_3$ (**10**) to consist of one molecule in the asymmetric unit and isostructural with **1-4**, **8** and **9**. The Pr-C contacts range from 2.927(9) - 2.995(11) Å with a Pr-centroid contact being 2.615(4) Å. The average Pr-C length in **10** (2.9648 Å) is comparable with the corresponding chloroaluminate Pr(III) complex $\text{Pr}(\eta^6\text{-Me}_2\text{C}_6\text{H}_4)(\text{AlCl}_4)_3$, where the mean Pr-C length is 2.949 Å (Table 2.2). The mean Pr-C contacts fall in the range from 2.76 to 2.808 Å for the cyclopentadienyl

Chapter 2

complexes $[(\text{Pr}\{\eta\text{-}[\text{C}_5\text{H}_3\text{-}(\text{SiMe}_3)_2]\}_2\text{Cl})_2]^{85}$, $[(\text{C}_5\text{Me}_5)_2\text{Pr}(\mu\text{-Cl})_2\text{Na}(\text{dme})_2]^{86}$, 87 , $[(\text{Bu}^t\text{Cp})_2\text{PrCl}]_2^{88}$, $[(t\text{-BuCp})_2\text{PrCl}\cdot 2\text{THF}]^{89}$ and $[\{\text{Li}(\text{C}_4\text{H}_8\text{O})_3\}\text{Br}\{\text{Pr}(\text{C}_9\text{H}_{13})_3\}]^{90}$. The Pr-centroid distances of the complexes range from 2.489(9) to 2.589(7) Å. In the diindenyl complex $[(\text{C}_9\text{H}_7)_2\text{PrCl}(\text{thf})_2]$, the mean Pr-C distance is 2.810 Å and that of the Pr-centroid being 2.534(2).⁹¹ Both the average Pr-C distance (2.9648 Å) and the Pr-centroid distance in **10** are larger than in the cyclopentadienyl and indenyl complexes suggest a more weakly bound arene system in the iodoaluminate arene complexes.

The Pr-I distances in **10** range from 3.2292(10) to 3.2897(15) Å with an average of 3.2845 Å and the average Pr-Cl bond length in $\text{Pr}(\eta^6\text{-Me}_2\text{C}_6\text{H}_4)(\text{AlCl}_4)_3$ is 2.873 Å (Table 2.2). If we consider the ionic radii of halides, the Pr-halide distances are similar in both compounds. The I-Pr-I and I-Al-I angles are comparable with the other iodoaluminate complexes.

The X-ray crystal structure of $\text{Nd}(\eta^6\text{-C}_6\text{H}_3\text{Me}_3)(\text{AlI}_4)_3$ **11** is isostructural with **3** with similar bond lengths and bond angles for all atoms, and is comparable with the corresponding chloroaluminate complexes (Table 2.5). The La-C bond contacts are weaker than that of in the cyclopentadienyls complexes as well as in the uranium chloroaluminate complexes (Table 2.5 and 2.13).

The Sm-C bond lengths in **12** extend the range from 2.89(2) to 2.946(12) Å with an average Sm-C distance of 2.9267 Å, and are comparable with the reported samarium complexes $[\text{Sm}(\eta^6\text{-C}_6\text{H}_6)(\text{AlCl}_4)_3]\cdot\text{C}_6\text{H}_6$,^{39, 42} $\text{Sm}(\eta^6\text{-MeC}_6\text{H}_5)(\text{AlCl}_4)_3$,³⁶ $\text{Sm}(\eta^6\text{-1,3-Me}_2\text{C}_6\text{H}_4)(\text{AlCl}_4)_3$ ³⁷ and $[\text{Sm}(\eta^6\text{-C}_6\text{Me}_6)(\text{AlCl}_4)_3]\cdot\text{MeC}_6\text{H}_5$ ⁴³ featuring the mean Sm-C bond length of 2.92, 2.91, 2.89 and 2.89 Å, respectively. The Sm-C bond contacts in the literature compounds slightly vary due to the number of alkyl substituents on the arenes. Arenes with more methyl substituents have stronger Sm-C interactions because of the electron donating effect of the substituents. The average Sm-I contact in **12** is 3.2614 Å and that of the Sm-Cl contacts in the literature compounds ($[\text{Sm}(\eta^6\text{-C}_6\text{H}_6)(\text{AlCl}_4)_3]\cdot\text{C}_6\text{H}_6$,^{39,42} $\text{Sm}(\eta^6\text{-MeC}_6\text{H}_5)(\text{AlCl}_4)_3$,³⁶ $\text{Sm}(\eta^6\text{-1,3-Me}_2\text{C}_6\text{H}_4)(\text{AlCl}_4)_3$ ³⁷ and $[\text{Sm}(\eta^6\text{-C}_6\text{Me}_6)(\text{AlCl}_4)_3]\cdot\text{MeC}_6\text{H}_5$ ⁴³) vary from 2.83-2.85 Å. These distances are comparable considering the ionic radii of chlorides (1.81 Å) and iodides (2.20 Å).⁵¹

Chapter 2

The Gd-C contacts in **13** span the range from 2.881(6)-2.943(7) Å with a Gd-centroid distance of 2.548(3) Å are comparable with **4** where the Gd-C bond lengths span the range from 2.868(9)-2.978(9) Å with a Gd-centroid distance of 2.5495(5) Å. The Gd-C distances in the formally zerovalent bis(benzene) sandwich complex $\text{Gd}(\text{1,3,5-t-Bu}_3\text{C}_6\text{H}_3)_2$ are 2.585-2.660 Å (average 2.630 Å) and Gd-centroid distance is 2.219 Å.⁷⁴ The Gd-centroid distance in the corresponding cyclopentadienyl complex $[\text{Gd}(\eta^5\text{-C}_5\text{Me}_4\text{SiMe}_3)\{\mu\text{-Me}\}_2(\text{AlMe}_2)\}_2]$ is 2.393(2).⁷⁵ The Gd-arene bonds in **13** are significantly weaker than the Gd-arene bonds in the corresponding uranium-arene (Table 2.6), cyclopentadienyl and the zerovalent benzene complexes.

The selected bond lengths (Å) and bond angles (°) for **8**, **9**, **10**, **11**, **12** and **13** are shown in Table 2.13 and 2.14, respectively. Because of the lanthanoid contraction, both the Ln-C(avg.) and Ln-Centroid distances in the trivalent mesitylene complexes show a gradual decrease (Fig. 2.10) from lanthanum to gadolinium.

Chapter 2

Table 2.13: The selected bond lengths (Å) for Ln(η^6 -C₆H₃Me₃)(AlI₄)₃; Ln = La (8), Ce (9), Pr (10), Nd (11), Sm (12) and Gd (13).

Ln =	La (8)	Ce (9)	Pr (10)	Nd (11)	Sm (12)	Gd (13)
Ln(1)-I(1)	3.318(2)	3.3003(16)	3.3796(15)	3.2764(15)	3.3638(19)	3.3557(13)
Ln(1)-I(2)	3.320(2)	3.3021(11)	3.2776(11)	3.2772(11)	3.2756(16)	3.2359(8)
Ln(1)-I(5)	3.402(2)	3.3879(17)	3.2897(15)	3.3687(16)	3.2467(18)	3.2485(13)
Ln(1)-I(6)	3.3066(19)	3.2893(12)	3.2896(10)	3.2630(12)	3.2511(19)	3.2498(8)
Ln(1)-I(9)	3.2693(19)	3.2503(11)	3.2413(10)	3.2246(11)	3.2757(17)	3.1943(8)
Ln(1)-I(10)	3.2784(19)	3.2527(12)	3.2292(10)	3.2220(11)	3.1556(18)	3.1785(8)
Ln(1)-C(2)	3.01(2)	3.007(14)	2.995(11)	2.946(12)	2.97(2)	2.943(7)
Ln(1)-C(3)	3.00(2)	2.961(13)	2.953(10)	2.925(12)	2.93(2)	2.889(7)
Ln(1)-C(4)	3.01(2)	2.999(14)	2.981(10)	2.972(12)	2.91(2)	2.907(7)
Ln(1)-C(5)	3.02(2)	2.988(14)	2.927(9)	2.942(12)	2.89(2)	2.881(6)
Ln(1)-C(6)	2.97(3)	2.995(14)	2.980(10)	2.968(11)	2.95(2)	2.918(7)
Ln(1)-C(7)	3.02(2)	2.945(12)	2.953(11)	2.927(12)	2.91(2)	2.904(7)
Ln(1)-C(avg.)	3.0033	2.9825	2.9648	2.9466	2.9267	2.9070
Ln(1)-C(cent.)	2.660(9)	2.634(6)	2.615(4)	2.597(5)	2.575(9)	2.548(3)
Al(1)-I(1)	2.578(7)	2.576(4)	2.555(3)	2.575(4)	2.566(6)	2.560(2)
Al(1)-I(2)	2.594(6)	2.592(4)	2.588(3)	2.595(4)	2.573(7)	2.588(2)
Al(1)-I(3)	2.487(7)	2.483(4)	2.487(3)	2.476(4)	2.494(7)	2.487(2)
Al(1)-I(4)	2.491(6)	2.497(4)	2.507(3)	2.497(4)	2.491(7)	2.503(2)
Al(2)-I(5)	2.554(7)	2.560(4)	2.577(3)	2.560(4)	2.584(6)	2.576(2)
Al(2)-I(6)	2.601(7)	2.589(4)	2.589(3)	2.585(4)	2.586(6)	2.590(2)
Al(2)-I(7)	2.513(7)	2.506(5)	2.500(3)	2.506(4)	2.480(6)	2.494(2)
Al(2)-I(8)	2.470(7)	2.487(4)	2.483(3)	2.480(4)	2.497(7)	2.488(2)
Al(3)-I(9)	2.603(7)	2.597(4)	2.593(3)	2.591(4)	2.619(7)	2.596(2)
Al(3)-I(10)	2.593(7)	2.601(4)	2.603(3)	2.598(4)	2.588(6)	2.598(2)
Al(3)-I(11)	2.488(6)	2.492(4)	2.473(3)	2.487(4)	2.492(7)	2.473(2)
Al(3)-I(12)	2.478(6)	2.470(4)	2.487(3)	2.471(4)	2.478(6)	2.490(2)

Chapter 2

Table 2.14: The selected bond angles (°) for Ln(η^6 -C₆H₃Me₃)(AlI₄)₃; Ln = La (8), Ce (9), Pr (10), Nd (11), Sm (12) and Gd (13).

Ln =	La (8)	Ce (9)	Pr (10)	Nd (11)	Sm (12)	Gd (13)
Centroid-Ln-I(axial)	177.1(2)	177.24(12)	177.54(10)	177.81(14)	177.2(5)	178.53(7)
I(2)-Ln(1)-I(1)	72.81 (5)	72.92(2)	72.09(3)	73.02(2)	71.33(5)	72.08(3)
I(2)-Ln(1)-I(5)	139.76(5)	139.59(3)	139.82(3)	139.37(3)	136.42(5)	139.48(19)
I(5)-Ln(1)-I(1)	138.43(5)	138.27(3)	137.98(3)	138.04(3)	138.08(5)	137.73(3)
I(6)-Ln(1)-I(1)	138.36(2)	139.55(3)	139.63(3)	139.51(3)	139.09(4)	139.16(18)
I(6)-Ln(1)-I(2)	68.394(15)	69.27(2)	69.42(4)	69.17(2)	68.47(4)	69.07(3)
I(6)-Ln(1)-I(5)	71.735(15)	72.08(2)	73.00(3)	72.06(2)	73.37(4)	73.12(3)
I(6)-Ln(1)-I(9)	136.70(5)	136.74(3)	138.74(3)	136.63(3)	141.97(5)	138.87(2)
I(9)-Ln(1)-I(1)	70.10(5)	70.09(2)	69.03(3)	70.11(2)	70.53(5)	68.83(2)
I(9)-Ln(1)-I(2)	138.78(5)	138.86(3)	136.67(3)	138.92(3)	137.66(5)	136.47(2)
I(9)-Ln(1)-I(5)	69.30(5)	69.20(2)	69.97(3)	69.03(2)	70.14(4)	70.06(2)
I(10)-Ln(1)-I(1)	81.09(6)	81.12(3)	81.41(2)	81.08(2)	80.20(5)	81.15(13)
I(10)-Ln(1)-I(2)	80.29(5)	79.89(2)	78.52(2)	79.46(2)	77.35(4)	77.73(14)
I(10)-Ln(1)-I(5)	81.50(6)	81.47(3)	81.26(2)	81.34(2)	78.51(4)	81.26(14)
I(10)-Ln(1)-I(6)	78.98(6)	78.67(3)	79.54(2)	78.37(3)	83.99(5)	78.85(14)
I(10)-Ln(1)-I(9)	76.88(5)	77.27(2)	77.50(2)	77.59(2)	78.73(4)	78.09(14)
I(1)-Al(1)-I(2)	99.2(2)	98.78(14)	99.24(11)	97.91(12)	97.8(2)	97.80(7)
I(3)-Al(1)-I(1)	112.4(3)	112.70(15)	107.61(12)	113.06(14)	109.6(2)	107.73(8)
I(3)-Al(1)-I(2)	108.1(2)	108.34(15)	111.75(11)	108.50(13)	112.0(3)	112.06(8)
I(4)-Al(1)-I(1)	107.0(2)	107.12(14)	116.03(12)	107.26(13)	114.2(3)	116.53(8)
I(4)-Al(1)-I(2)	110.6(3)	110.52(15)	105.46(12)	110.51(14)	108.4(2)	105.89(8)
I(4)-Al(1)-I(3)	117.8(2)	117.74(16)	115.56(12)	117.80(15)	113.8(2)	115.46(8)
I(6)-Al(2)-I(5)	99.8(2)	99.49(15)	98.51(10)	98.64(12)	97.3(2)	97.06(7)
I(7)-Al(2)-I(5)	115.2(3)	115.61(15)	106.84(11)	115.84(15)	111.3(2)	107.65(8)
I(7)-Al(2)-I(6)	104.8(3)	105.66(15)	110.77(12)	105.66(15)	111.6(2)	111.08(8)
I(7)-Al(2)-I(8)	116.0(2)	115.71(17)	117.71(12)	115.70(14)	115.8(3)	117.52(8)
I(8)-Al(2)-I(5)	108.3(3)	107.64(16)	112.78(12)	107.78(15)	110.4(2)	112.88(8)
I(8)-Al(2)-I(6)	111.5(3)	111.55(15)	108.56(12)	111.93(15)	108.8(2)	108.77(7)
I(10)-Al(3)-I(9)	103.2(2)	102.71(13)	102.42(11)	102.21(13)	103.2(2)	101.25(7)
I(11)-Al(3)-I(9)	110.5(2)	110.53(15)	107.88(11)	110.73(13)	107.4(2)	108.20(7)
I(11)-Al(3)-I(10)	108.8(3)	108.36(13)	109.17(12)	108.42(15)	109.6(2)	109.43(7)
I(12)-Al(3)-I(9)	107.3(3)	107.69(14)	111.01(12)	107.93(14)	110.1(2)	110.92(7)
I(12)-Al(3)-I(10)	109.3(2)	109.37(15)	108.39(11)	109.26(13)	109.3(2)	108.70(8)
I(12)-Al(3)-I(11)	116.9(3)	117.21(16)	116.99(12)	117.24(15)	116.5(3)	117.16(8)

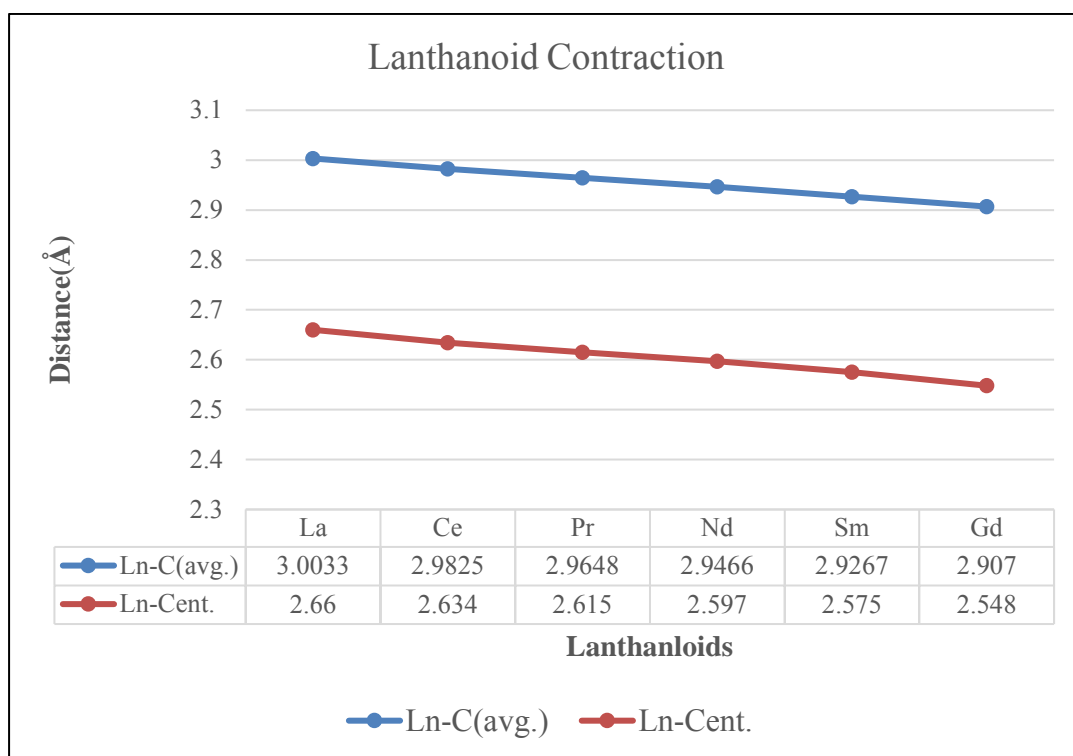
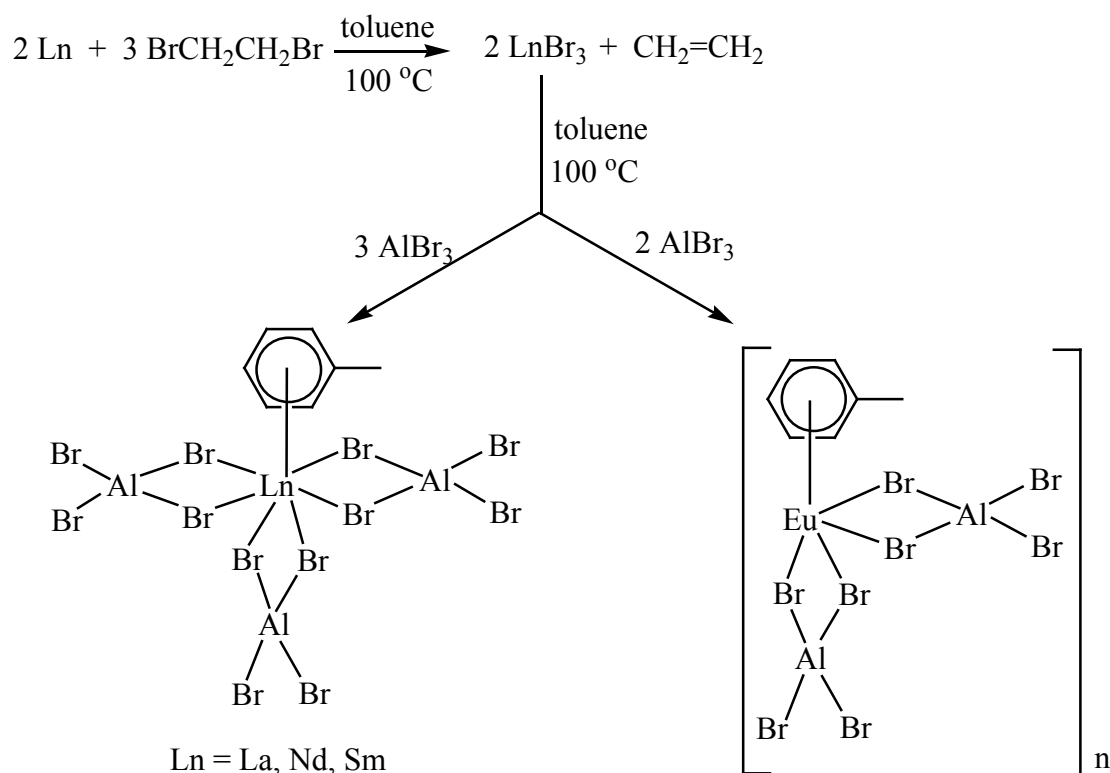


Fig. 2.10: Lanthanoid contraction in iodoaluminate lanthanoid(III) complexes in mesitylene.

2.3.2.4 Bromoaluminate lanthanoid(III) complexes in toluene

Trivalent monomeric bromoaluminate complexes of lanthanoids $\text{Ln}(\eta^6\text{-C}_6\text{H}_5\text{Me})(\text{AlBr}_4)_3$ (Ln = La (**14**), Nd (**15**) and Sm (**16**)) (Fig. 2.11) have been synthesised by the reaction of aluminium bromide, dibromoethane and lanthanoid metals in toluene (Scheme 2.3). A divalent compound of Eu (**17**) was also obtained by the similar method. (Scheme 2.3). Trivalent bromoaluminate complexes are isostructural with the corresponding iodoaluminate trivalent complexes of lanthanoids in toluene. However, $\text{Sm}(\eta^6\text{-C}_6\text{H}_5\text{Me})(\text{AlBr}_4)_3$ (**16**) comes with a trivalent Sm^{3+} metal centre, whereas iodoaluminate samarium complex **5** has divalent samarium centre with a polymeric structure. On the other hand, the europium complex $[\text{Eu}(\eta^6\text{-C}_6\text{H}_5\text{Me})(\text{AlBr}_4)_2]_n \cdot \text{PhMe}$ (**17**) features a divalent Eu^{2+} centre with a polymeric structure and is analogous to **6**. This result confirms the divalent state of Eu is much more stable than that of Sm.



Scheme 2.3: Synthesis of bromoaluminate π -arene complexes of lanthanoids in toluene.

The La-C contacts in **14** range from 2.948(8) to 3.061(8) Å with a La-centroid distance of 2.646(3) Å. These values are similar to the analogous lanthanoid complexes **1**, **8** and $\text{La}(\eta^6\text{-C}_6\text{H}_5\text{Me})(\text{AlCl}_4)_3$ (Table 2.2, 2.7 and 2.13). The La-centroid bond distance and the average La-C bond distance (2.9931 Å) are significantly longer than the corresponding uranium chloroaluminate complexes and cyclopentadienyl complexes of lanthanum (Table 2.3), which tells a weaker bond of lanthanum with the π -ligand.

The La-Br bond contacts are comparable with the corresponding iodoaluminate and chloroaluminate complexes if we consider the differences of the ionic radii of halides. The Br-Al-I angles are closer to the idealised tetrahedral angle. The complexes **15** and **16** are isostructural with the iodoaluminate complexes and are comparable with the corresponding chloroaluminate complexes. The Ln-C bond contacts are weaker than that of in the cyclopentadienyls complexes as well as in the uranium chloroaluminate complexes (Table 2.5). The selected bond lengths (Å) and bond angles ($^\circ$) for **14**, **15** and **16** are shown in Table 2.15 and 2.16, respectively.

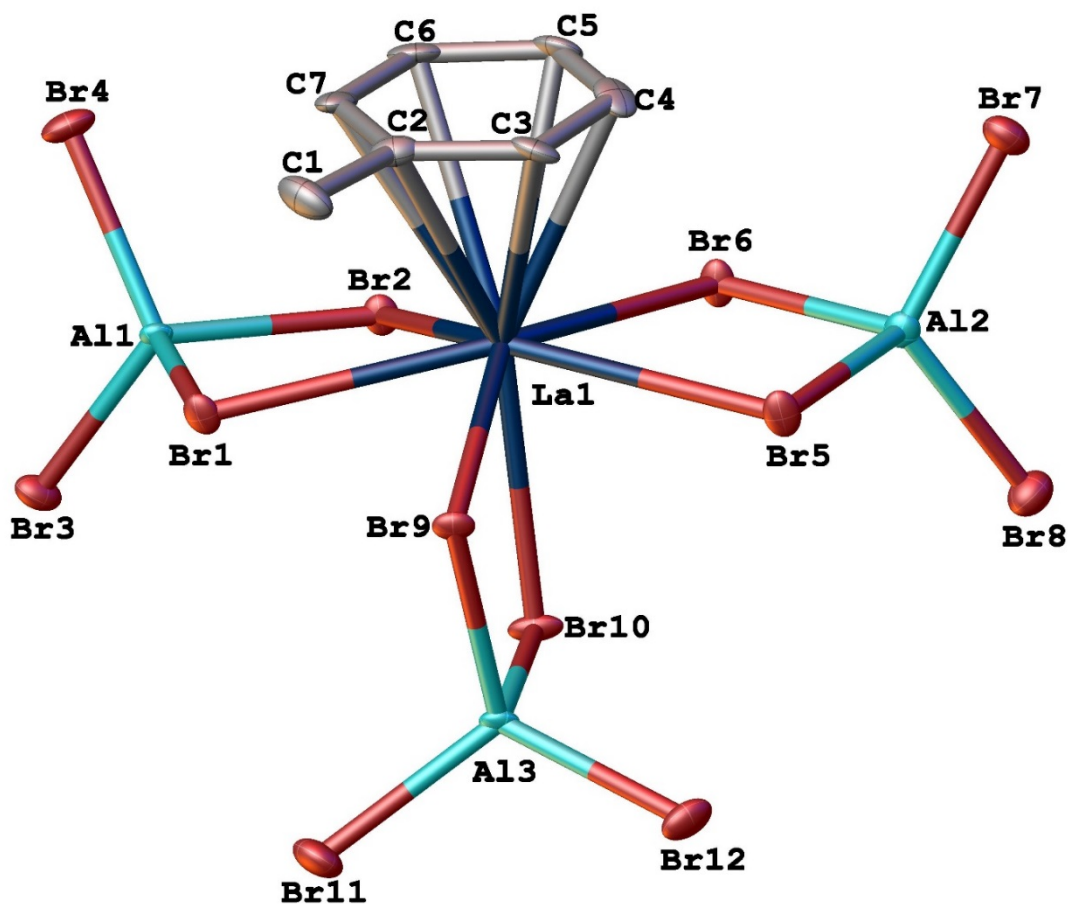


Fig. 2.11: Molecular structure of $\text{La}(\eta^6\text{-C}_6\text{H}_5\text{Me})(\text{AlBr}_4)_3$ (**14**), representative of the isostructural complexes **15** and **16**. Hydrogen atoms have been omitted for clarity.

The Ln-C(avg.) and Ln-Centroid distances in the trivalent bromoaluminate complexes display a gradual decrease (Fig. 2.12) which also support the lanthanoid contraction.

Chapter 2

Table 2.15: The selected bond lengths (Å) for $\text{La}(\eta^6\text{-C}_6\text{H}_5\text{Me})(\text{AlBr}_4)_3$; Ln = La (14), Nd (15) and Sm (16).

Ln =	La (14)	Nd (15)	Sm (16)
Ln(1)-Br(1)	3.0575(10)	3.0434(8)	2.9897(10)
Ln(1)-Br(2)	3.0722(12)	3.0041(8)	3.0105(12)
Ln(1)-Br(5)	3.0887(10)	3.0109(9)	3.0256(10)
Ln(1)-Br(6)	3.0478(10)	3.0287(10)	2.9866(10)
Ln(1)-Br(9)	3.0744(10)	3.0315(8)	3.0151(10)
Ln(1)-Br(10)	3.0060(10)	2.9507(8)	2.9213(10)
Ln(1)-C(2)	3.061(8)	3.002(6)	2.981(8)
Ln(1)-C(3)	2.978(8)	2.984(6)	2.879(7)
Ln(1)-C(4)	2.940(8)	2.936(6)	2.849(8)
Ln(1)-C(5)	2.948(8)	2.896(6)	2.874(8)
Ln(1)-C(6)	2.988(8)	2.870(6)	2.916(8)
Ln(1)-C(7)	3.044(8)	2.907(6)	2.959(8)
Ln(1)-C(ave.)	2.9931	2.9325	2.9096
Ln(1)-C(cent.)	2.646(3)	2.577(3)	2.550(3)
Al(1)-Br(1)	2.342(2)	2.3521(19)	2.340(3)
Al(1)-Br(2)	2.356(2)	2.3565(19)	2.347(2)
Al(1)-Br(3)	2.239(3)	2.245(2)	2.242(2)
Al(1)-Br(4)	2.250(2)	2.257(2)	2.251(3)
Al(2)-Br(5)	2.354(2)	2.3391(19)	2.351(3)
Al(2)-Br(6)	2.362(3)	2.3514(19)	2.356(2)
Al(2)-Br(7)	2.257(3)	2.2486(19)	2.256(3)
Al(2)-Br(8)	2.241(3)	2.242(2)	2.243(3)
Al(3)-Br(9)	2.369(2)	2.3635(19)	2.364(2)
Al(3)-Br(10)	2.359(2)	2.3610(19)	2.359(3)
Al(3)-Br(11)	2.253(3)	2.2578(19)	2.251(2)
Al(3)-Br(12)	2.255(3)	2.2504(19)	2.259(2)

Chapter 2

Table 2.16: The selected bond angles (°) for La(η^6 -C₆H₅Me)(AlBr₄)₃; Ln = La (14), Nd (15) and Sm (16).

Ln =	La (14)	Nd (15)	Sm (16)
Centroid-Ln-Br(axial)	174.76(8)	175.54(6)	176.01(9)
Br(2)-Ln(1)-Br(1)	71.13(3)	71.85(2)	71.85(3)
Br(2)-Ln(1)-Br(5)	136.13(3)	138.79(3)	136.52(3)
Br(5)-Ln(1)-Br(1)	143.55(3)	142.15(2)	141.63(3)
Br(6)-Ln(1)-Br(1)	138.75(3)	136.40(2)	138.80(3)
Br(6)-Ln(1)-Br(2)	68.03(3)	67.79(2)	67.70(3)
Br(6)-Ln(1)-Br(5)	71.36(3)	71.64(2)	72.02(3)
Br(6)-Ln(1)-Br(9)	140.37(3)	136.407(19)	140.26(3)
Br(9)-Ln(1)-Br(1)	71.34(2)	72.17(2)	70.60(2)
Br(9)-Ln(1)-Br(2)	135.87(2)	140.27(2)	136.62(2)
Br(9)-Ln(1)-Br(5)	72.86(3)	70.83(2)	71.97(3)
Br(10)-Ln(1)-Br(1)	84.50(3)	79.25(3)	83.58(3)
Br(10)-Ln(1)-Br(2)	80.02(3)	82.19(2)	79.48(3)
Br(10)-Ln(1)-Br(5)	79.36(3)	83.85(3)	79.30(3)
Br(10)-Ln(1)-Br(6)	83.09(3)	79.64(3)	81.81(3)
Br(10)-Ln(1)-Br(9)	74.08(3)	75.08(2)	75.54(3)
Br(1)-Al(1)-Br(2)	98.75(9)	97.80(7)	97.37(9)
Br(3)-Al(1)-Br(1)	108.77(10)	110.26(8)	108.95(11)
Br(3)-Al(1)-Br(2)	113.16(10)	110.23(8)	113.98(10)
Br(4)-Al(1)-Br(1)	111.24(10)	109.11(8)	111.80(10)
Br(4)-Al(1)-Br(2)	107.14(10)	110.67(8)	107.43(11)
Br(4)-Al(1)-Br(3)	116.40(10)	117.07(8)	115.83(10)
Br(6)-Al(2)-Br(5)	98.73(9)	97.80(7)	97.34(9)
Br(7)-Al(2)-Br(5)	108.95(11)	111.76(8)	109.14(10)
Br(7)-Al(2)-Br(6)	110.15(10)	107.36(8)	110.72(11)
Br(7)-Al(2)-Br(8)	117.42(11)	116.01(8)	117.03(10)
Br(8)-Al(2)-Br(5)	110.07(10)	108.86(8)	110.49(11)
Br(8)-Al(2)-Br(6)	109.90(11)	113.62(8)	110.33(10)
Br(10)-Al(3)-Br(9)	101.56(9)	101.01(7)	100.71(10)
Br(11)-Al(3)-Br(9)	111.58(10)	107.79(8)	112.24(10)
Br(11)-Al(3)-Br(10)	107.80(10)	112.65(8)	107.83(10)
Br(12)-Al(3)-Br(9)	107.77(10)	112.14(8)	107.79(10)
Br(12)-Al(3)-Br(10)	112.52(10)	107.78(8)	112.87(10)
Br(12)-Al(3)-Br(11)	114.83(10)	114.68(8)	114.59(11)

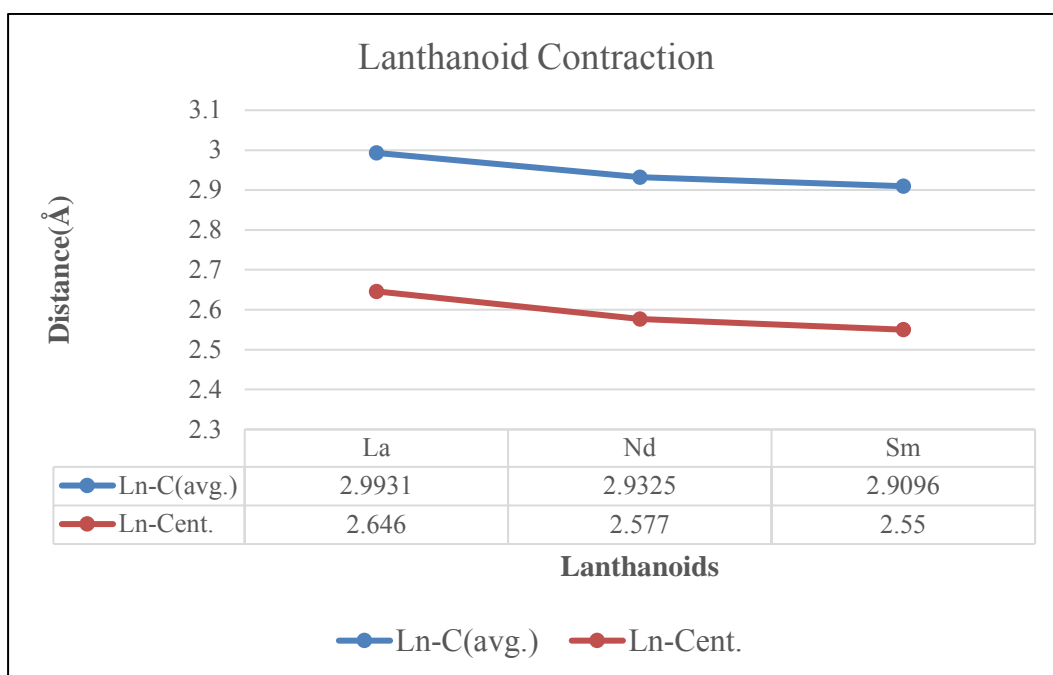


Fig. 2.12: Lanthanoid contraction in bromoaluminate lanthanoid(III) complexes in toluene.

2.3.2.5 Bromoaluminate lanthanoid(II) complexes in toluene

Complex $[\text{Eu}(\eta^6\text{-MeC}_6\text{H}_5)(\text{AlBr}_4)_2]_n \cdot \text{PhMe}$ (**17**) (Fig. 2.13 and 2.14) is isostructural with **5** and **6**. The Eu-C bond lengths fall in the range 3.010(5)-3.094(5) Å with an average Eu-C length of 3.0398 Å and are comparable with **6** and $[\text{Eu}(\eta^6\text{-C}_6\text{Me}_6)(\text{AlCl}_4)_2]_4 \cdot (\text{C}_6\text{H}_2\text{Me}_4)$.^{48, 49}

The Eu-centroid distance in **17** (2.6981(5) Å) is significantly elongated than that in the corresponding cyclopentadienyl complexes⁸⁰⁻⁸². Therefore, the Eu-arene bonds in **17** is weaker than the cyclopentadienyl complexes. The equatorial Eu-Br bond lengths range are comparable to **6** and $[\text{Eu}(\eta^6\text{-C}_6\text{Me}_6)(\text{AlCl}_4)_2]_4 \cdot (\text{C}_6\text{H}_2\text{Me}_4)$ after considering the ionic radii of halides. The Br-Al-Br angles are close to the idealised tetrahedral angle. The selected bond lengths (Å) and bond angles (°) for **17** are listed in Table 2.17 and 2.18, respectively.

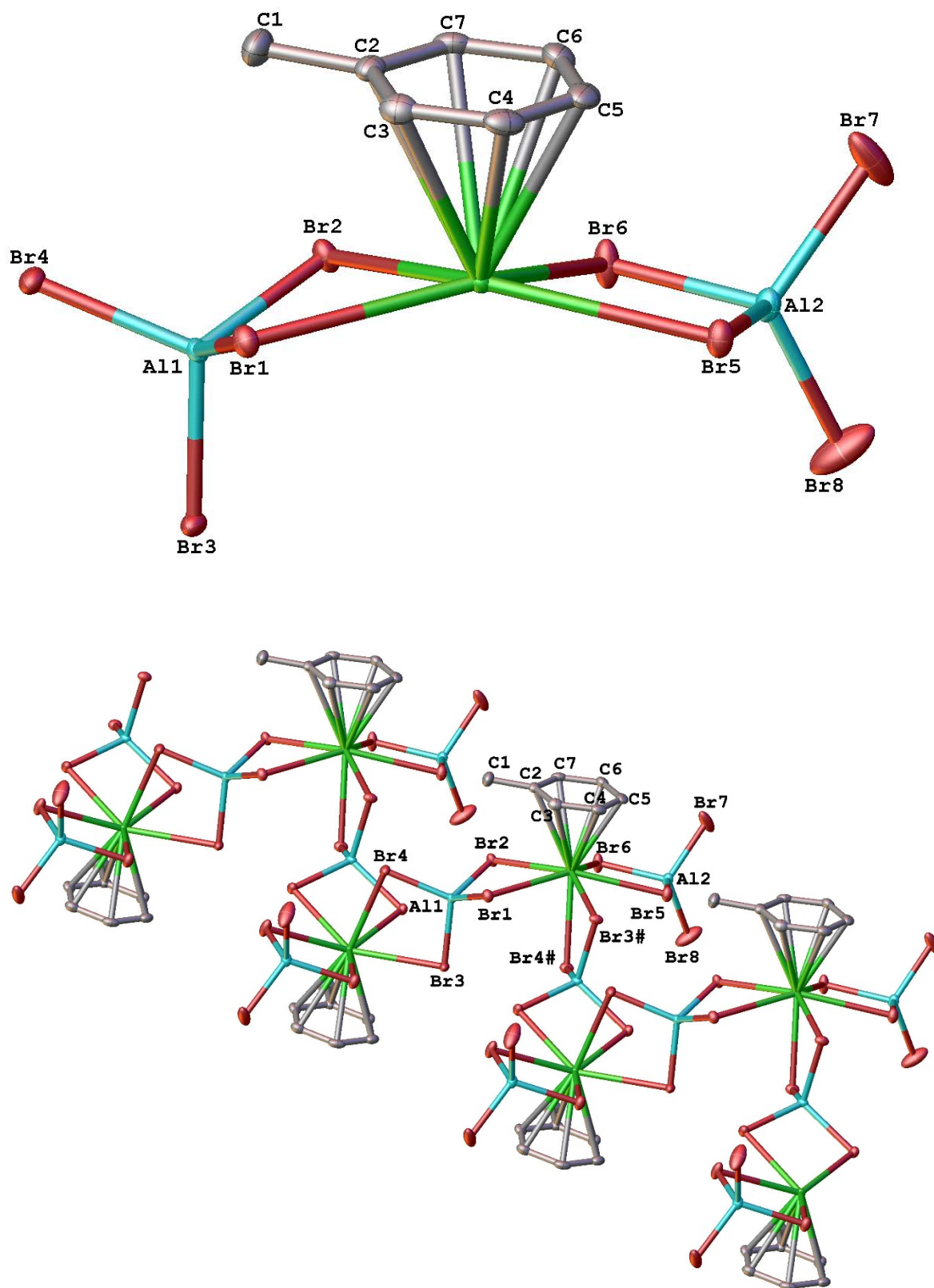


Fig. 2.13: A monomeric repeat unit (top) and the one dimensional extended framework for $[\text{Eu}(\eta^6\text{-MeC}_6\text{H}_5)(\text{AlBr}_4)_2]_n \cdot \text{PhMe}$ (**17**) (bottom). Hydrogen atoms and the solvent of crystallisation (toluene) have been omitted for clarity.

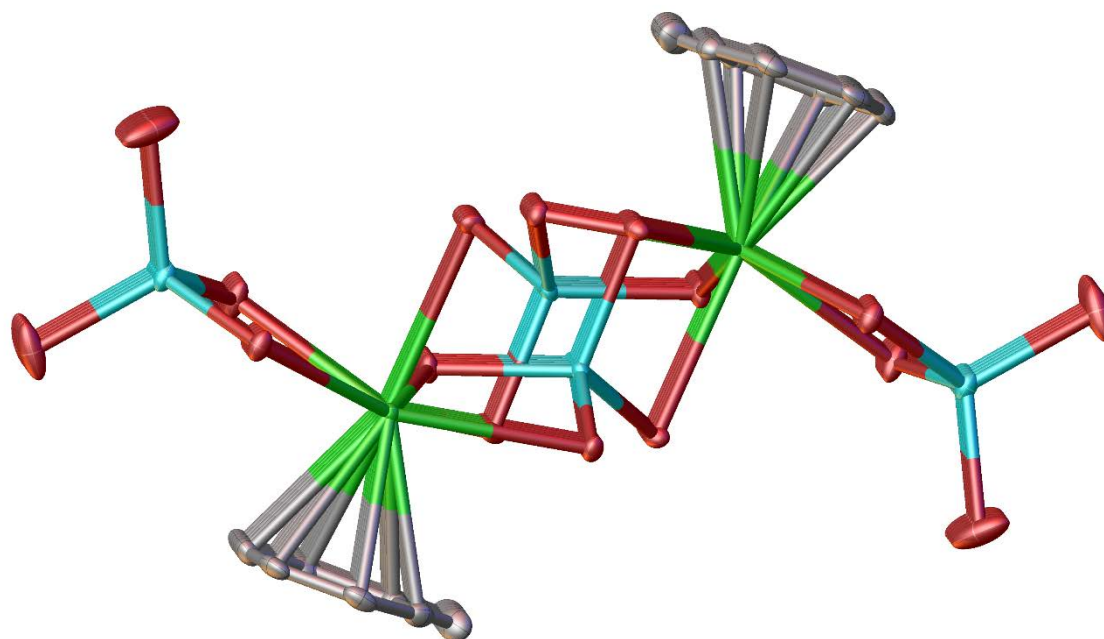


Fig. 2.14: The Eu-arene double stranded polymer with two bridging AlBr_4^- units and two terminal AlBr_4^- units for $[\text{Eu}(\eta^6\text{-MeC}_6\text{H}_5)(\text{AlBr}_4)_2]_n\cdot\text{PhMe}$ (**17**). Hydrogen atoms and the solvent of crystallisation (toluene) have been omitted for clarity.

Table 2.17: The selected bond lengths (Å) for $[\text{Eu}(\eta^6\text{-MeC}_6\text{H}_5)(\text{AlBr}_4)_2]_n\cdot\text{PhMe}$ (**17**).

	Eu (17)		Eu (17)	
Eu(1)-Br(1)	3.1661(13)	Eu(1)-C(7)	3.039(5)	
Eu(1)-Br(2)	3.1925(8)	Eu(1)-C(avg.)	3.0398	
Eu(1) ¹ -Br(3)	3.1391(8)	Eu(1)-C(cent.)	2.6981(5)	
Eu(1) ¹ -Br(4)	3.1475(8)	Al(1)-Br(1)	2.2911(16)	
Eu(1)-Br(5)	3.1698(8)	Al(1)-Br(2)	2.3048(17)	
Eu(1)-Br(6)	3.1438(9)	Al(1)-Br(3)	2.3034(15)	
Eu(1)-C(2)	3.094(5)	Al(1)-Br(4)	2.3026(15)	
Eu(1)-C(3)	3.053(5)	Al(2)-Br(5)	2.3225(16)	
Eu(1)-C(4)	3.033(5)	Al(2)-Br(6)	2.3329(16)	
Eu(1)-C(5)	3.010(5)	Al(2)-Br(7)	2.2705(18)	
Eu(1)-C(6)	3.010(5)	Al(2)-Br(8)	2.2517(17)	

¹1/2-x,-1/2+y,1/2-z

Chapter 2

Table 2.18: The selected bond angles (°) for [Eu(η^6 -MeC₆H₅)(AlBr₄)₂]_n.PhMe (17).

	Eu (17)		Eu (17)
Centroid-Ln-Br(axial)	169.28(5)	Br(6)-Eu(1)-Br(4) ²	84.73(3)
Br(1)-Eu(1)-Br(2)	69.477(14)	Br(6)-Eu(1)-Br(5)	70.39(2)
Br(1)-Eu(1)-Br(5)	143.488(16)	Br(1)-Al(1)-Br(2)	104.07(6)
Br(3) ² -Eu(1)-Br(1)	72.05(2)	Br(1)-Al(1)-Br(3)	109.60(6)
Br(3) ² -Eu(1)-Br(2)	139.22(2)	Br(1)-Al(1)-Br(4)	112.66(6)
Br(3) ² -Eu(1)-Br(4) ²	72.388(18)	Br(3)-Al(1)-Br(2)	111.73(6)
Br(3) ² -Eu(1)-Br(5)	73.79(3)	Br(4)-Al(1)-Br(2)	111.41(6)
Br(3) ² -Eu(1)-Br(6)	140.590(17)	Br(4)-Al(1)-Br(3)	107.42(6)
Br(4) ² -Eu(1)-Br(1)	79.30(3)	Br(5)-Al(2)-Br(6)	102.82(6)
Br(4) ² -Eu(1)-Br(2)	87.567(16)	Br(7)-Al(2)-Br(5)	110.42(7)
Br(4) ² -Eu(1)-Br(5)	78.45(3)	Br(7)-Al(2)-Br(6)	107.47(7)
Br(5)-Eu(1)-Br(2)	137.442(16)	Br(8)-Al(2)-Br(5)	110.12(7)
Br(6)-Eu(1)-Br(1)	135.35(2)	Br(8)-Al(2)-Br(6)	111.99(7)
Br(6)-Eu(1)-Br(2)	68.422(19)	Br(8)-Al(2)-Br(7)	113.48(7)

²1/2-x, 1/2+y, 1/2-z

2.3.3 Catalysis for the Polymerisation of Isoprene

The catalytic activity experiments were performed at Prof. Reiner Anwander Lab in the University of Tübingen, Germany. Thanks to Prof. Anwander and his group for this contribution.

The catalytic activity of **3** for the polymerisation of isoprene was performed (Table 2.19 and Eqn. 2.5) at ambient temperature. TIBA or TMA (0.15 mmol, 1.5 equiv.) was added to a suspension of Nd(η^6 -C₆H₅Me)(AlI₄)₃ (0.01 mmol, 1equiv) in 0.5 ml toluene. The mixture was aged at ambient temperature for 10 and 90 minutes, respectively. This mixture was added to a solution of DIBAH (0.50 mmol, 50 equiv.) and isoprene (10 mmol, 1000 equiv.) in 3 ml *n*-hexane. The polymerisation was carried out at ambient temperature for 5 h. The reaction was terminated by pouring the polymerisation mixture into 200 mL of

Chapter 2

methanol containing 0.1% (w/w) 2,6-di-tert-butyl-4-methylphenol as a stabilizer. The polymer was dried under vacuum at ambient temperature to constant weight.

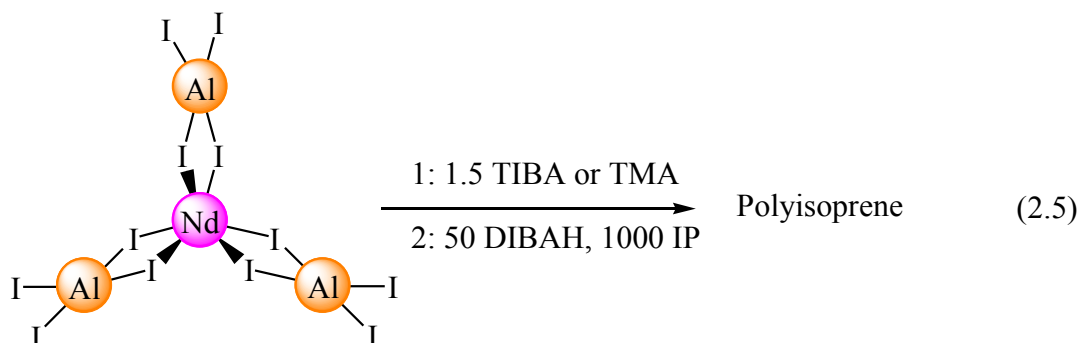


Table 2.19: Catalytic activity of 3 in the polymerisation of isoprene.

Pre-catalyst	Co-catalyst ^[a] (equiv.)	Prereact. Time [min]	Time [h]	Yield (%)	<i>cis</i> - 1,4 ^[b]	<i>trans</i> - 1,4 ^[b]	3,4 ^[b]	$M_n^{[c]}$ (x 10 ⁴)	$M_w/M_n^{[c]}$	$T_G^{[d]}$
Nd(AlI ₄) ₃	TIBA/DIBAH (1.5/50)	10	5	16	83.3	5.3	11.4	2.9	6.74	59.2
Nd(AlI ₄) ₃	TMA/DIBAH (1.5/50)	90	5	25	86.4	0.0	13.6	2.7	7.67	60.0

^[a] TIBA = Triisobutylaluminium; DIBAH = Diisobutylaluminium hydride ^[b] Determined by ¹H, ¹³C NMR spectroscopy in CDCl₃ against polystyrene standards. ^[c] Determined by GPC against polystyrene standards. ^[d] Determined by DSC at 10 K/min.

The polymer itself was only partly soluble in chloroform or tetrahydrofuran (very high molecular weight; difficult to handle which also makes GPC analysis difficult; this was also pointed out by Biagini et al. who examined similar complexes).²¹ Therefore, the microstructure (*cis*-, *trans*-, 3,4-content) as well as the M_n and PDI represents only the soluble part of the polymer. It could be shown by GPC analysis that only 36% and 42% of the polymer were analysed, respectively.

2.3.4 Discussion

The iodoaluminate and bromoaluminate complexes of lanthanoids were found to be isostructural and comparable with the reported chloroaluminate complexes. Some important structural parameters of the iodo- and bromoaluminate lanthanoid-arene complexes (**1-17**) are summarised in Table 2.20. The Ln-centroid and the average Ln-C bond distances in the trivalent compounds prepared in both toluene and mesitylene are similar, which suggest that the metal ligand interaction is independent of the substituents in the ligands. The Ln-X, Ln-centroid and the average Ln-C bond distances in the divalent complexes are longer than that of the trivalent complexes as divalent ions are larger than trivalent ions. Moreover, the Ln-I distances in the iodoaluminate complexes are longer than the Ln-Br distances in the bromoaluminate complexes. These differences are associated with the larger ionic radii of Ln²⁺ and I⁻ ions than the Ln³⁺ and Br⁻ ions, respectively.⁵¹

The geometry of all the complexes could be best described as distorted pentagonal bipyramid, with the arene molecule at an axial position (the centroid-Ln-I/Br angles are close to the straight angle). The gradual decrease of the Ln-X, Ln-centroid and the average Ln-C bond distances in the trivalent complexes of lanthanoids (lanthanum to gadolinium) support the lanthanoid contraction effect. This trend is also accessible among the divalent complexes from samarium to ytterbium, and there is a dramatic change in ytterbium as it is the smallest metal among the complexes reported in this chapter. The catalytic activity of Nd(η^6 -C₆H₅Me)(AlI₄)₃ in isoprene polymerisation was performed at ambient temperature, and were found less effective than the literature results of analogous complexes.

Chapter 2

Table 2.20: Summary of structural parameters of the iodo- and bromoaluminate lanthanoid-arene complexes (1-17).

	Ln- C(avg.)	Ln- C(cent.)	Ln-X (avg.)	Crystal system	Space group
La(η^6 -C ₆ H ₅ Me)(AlI ₄) ₃ (1)	3.0065	2.663(4)	3.3044	Monoclinic	<i>P2₁/n</i>
Ce(η^6 -C ₆ H ₅ Me)(AlI ₄) ₃ (2)	2.9813	2.634(6)	3.2869	Monoclinic	<i>P2₁/n</i>
Nd(η^6 -C ₆ H ₅ Me)(AlI ₄) ₃ (3)	2.9333	2.579(3)	3.2613	Monoclinic	<i>P2₁/c</i>
Gd(η^6 -C ₆ H ₅ Me)(AlI ₄) ₃ (4)	2.9035	2.5495(5)	3.2299	Monoclinic	<i>P2₁/n</i>
[Sm(η^6 -MeC ₆ H ₅)(AlI ₄) ₂] _n .PhMe (5)	3.0221	2.6884(4)	3.4455	Orthorhombic	<i>P2₁2₁2₁</i>
[Eu(η^6 -MeC ₆ H ₅)(AlI ₄) ₂] _n .PhMe (6)	3.0180	2.691(6)	3.4416	Orthorhombic	<i>P2₁2₁2₁</i>
[Yb(η^6 -MeC ₆ H ₅)(AlI ₄) ₂] _n .1/2PhMe (7)	2.9200	2.565(4)	3.2347	Monoclinic	<i>C2/c</i>
La(η^6 -C ₆ H ₃ Me ₃)(AlI ₄) ₃ (8)	3.0033	2.660(9)	3.3157	Triclinic	<i>P-1</i>
Ce(η^6 -C ₆ H ₃ Me ₃)(AlI ₄) ₃ (9)	2.9825	2.634(6)	3.2971	Monoclinic	<i>P2₁/c</i>
Pr(η^6 -C ₆ H ₃ Me ₃)(AlI ₄) ₃ (10)	2.9648	2.615(4)	3.2845	Monoclinic	<i>P2₁/c</i>
Nd(η^6 -C ₆ H ₃ Me ₃)(AlI ₄) ₃ (11)	2.9466	2.597(5)	3.2720	Monoclinic	<i>P2₁/c</i>
Sm(η^6 -C ₆ H ₃ Me ₃)(AlI ₄) ₃ (12)	2.9267	2.575(9)	3.2614	Monoclinic	<i>C2/c</i>
Gd(η^6 -C ₆ H ₃ Me ₃)(AlI ₄) ₃ (13)	2.9070	2.548(3)	3.2438	Monoclinic	<i>P2₁/c</i>
La(η^6 -C ₆ H ₅ Me)(AlBr ₄) ₃ (14)	2.9931	2.646(3)	3.0578	Monoclinic	<i>P2₁/n</i>
Nd(η^6 -C ₆ H ₅ Me)(AlBr ₄) ₃ (15)	2.9325	2.577(3)	3.0116	Monoclinic	<i>P2₁/n</i>
Sm(η^6 -C ₆ H ₅ Me)(AlBr ₄) ₃ (16)	2.9096	2.550(3)	2.9915	Monoclinic	<i>P2₁/n</i>
[Eu(η^6 -MeC ₆ H ₅)(AlBr ₄) ₂] _n .PhMe (17)	3.0398	2.6981(5)	3.1598	Monoclinic	<i>C2/c</i>

2.4 Conclusions

Compounds **1-17** extend the structural diversity attainable within the halogenoaluminate lanthanoid arene series. $[\text{Eu}(\eta^6\text{-MeC}_6\text{H}_5)(\text{AlI}_4)_2]_n \cdot \text{PhMe}$, $[\text{Yb}(\eta^6\text{-MeC}_6\text{H}_5)(\text{AlI}_4)_2]_n \cdot 1/2\text{PhMe}$ and $[\text{Eu}(\eta^6\text{-MeC}_6\text{H}_5)(\text{AlBr}_4)_2]_n \cdot \text{PhMe}$ are the first examples of polymeric structures among these complexes. Moreover, $[\text{Yb}(\eta^6\text{-MeC}_6\text{H}_5)(\text{AlI}_4)_2]_n \cdot 1/2\text{PhMe}$ is the first example of eight coordination in this series, evidence of the lanthanoid contraction. All the iodoaluminate complexes were synthesised by the treatment of aluminium iodide (prepared from aluminium powder and iodine), lanthanoid metals and diiodoethane in a one-pot reaction, leading to the isolation of various complexes by a convenient reaction scheme. Bromoaluminate complexes were synthesised by the reaction of the mixture of lanthanoid metals, aluminium bromide and dibromoethane in toluene. The catalytic activity of $\text{Nd}(\eta^6\text{-C}_6\text{H}_5\text{Me})(\text{AlI}_4)_3$ for the isoprene polymerisation was performed at ambient temperature. However, it was found less effective than the literature results of analogous complexes.

2.5 Experimental

For general procedures, see Appendix 2. Combustion analyses consistently gave variable results, and are therefore presented only in Appendix 2. Metal analyses were generally more accurate and are presented here.

Synthesis of iodoaluminate complexes in toluene

A mixture of excess Al (0.162 g, 6 mmol) and I₂ (1.90 g, 7.5 mmol) was taken in a Schlenk flask charged with 40 mL toluene. The mixture was heated with stirring in oil bath for a couple of hours at 100°C. The solution turned to colourless from red indicating the consumption of all iodine. After cooling the solution to room temperature, stoichiometric amounts Ln filings and ICH₂CH₂I were added to the solution under nitrogen atmosphere in the glove box. The mixture was heated at 100°C for 24 h, filtered and crystallised at room temperature.

La(η^6 -C₆H₅Me)(AlI₄)₃ (**1**)

La filings (0.232 g, 1.67 mmol) and ICH₂CH₂I (0.704g, 2.5 mmol) were added to the aluminium iodide solution. Colourless solution was obtained after heating and colourless crystals were grown in two days (0.82g, 27%). Metal analysis (C₇H₈Al₃I₁₂La); cal. (%) La 7.57; found La 7.54. IR (Nujol, ν/cm^{-1}): 2925 (s), 1582 (m), 1490 (m), 1463 (s), 1378 (m), 1210(m), 1178 (w), 1077 (w), 1033 (w), 786 (m), 728 (w), 682 (w).

Ce(η^6 -C₆H₅Me)(AlI₄)₃ (**2**)

1.67 mmol of Ce filings (0.234 g) and 2.5 mmol of ICH₂CH₂I (0.704g,) were added to the aluminium iodide solution. A light yellow solution was formed after heating and red crystals were obtained in two days (0.94g, 31%). Metal analysis (C₇H₈Al₃I₁₂Ce): cal. (%) Ce 7.63; found Ce 7.59. IR (Nujol, ν/cm^{-1}):2923 (s), 1463 (s), 1377 (m), 787 (m), 723 (w)

Chapter 2

Nd(η^6 -C₆H₅Me)(AlI₄)₃ (**3**)

Nd filings (0.241 g, 1.67 mmol) and ICH₂CH₂I (0.704g, 2.5 mmol) were added to the aluminium iodide solution and the mixture was heated. A light blue solution was obtained and light blue crystals were formed in 24 hours (1.27g, 41%). Metal analysis (C₇H₈Al₃I₁₂Nd): cal. (%) Nd 7.84; found Nd 7.90. IR (Nujol, ν/cm^{-1}): 3070 (m), 3045 (m), 2855 (s), 2730 (s), 1463 (s), 1377 (s), 1177(w), 789 (m), 726 (w), 680 (w).

Gd(η^6 -C₆H₅Me)(AlI₄)₃ (**4**)

1.67 mmol of Gd filings (0.263 g) and 2.5 mmol of ICH₂CH₂I (0.704g) were added to the aluminium iodide solution. After heating the mixture, a light yellow solution was formed. Yellow-orange crystals were obtained in 2 days (1.12g, 36%). Metal analysis (C₇H₈Al₃I₁₂Gd): cal. (%) Gd 8.49; found Gd 8.46. IR (Nujol, ν/cm^{-1}): 3140 (w), 2726 (m), 2560 (m), 2341 (w), 1614 (w), 1377 (s), 1157(m), 792 (w), 726 (w), 722 (m), 668 (w).

[Sm(η^6 -MeC₆H₅)(AlI₄)₂]_n.PhMe (**5**)

Sm filings (0.375 g, 2.5 mmol) and ICH₂CH₂I (0.704g, 2.5 mmol) were added to the aluminium iodide solution. After heating the mixture gave a light yellow solution. Dark crystals were obtained in 2 days (0.85g, 24%). Metal analysis (C₁₄H₁₆Al₂I₈Sm): cal. (%) Sm 10.71; found Sm 10.34.

[Eu(η^6 -MeC₆H₅)(AlI₄)₂]_n.PhMe (**6**)

2.5 mmol of Eu filings (0.379 g) and 2.5 mmol of ICH₂CH₂I (0.704g) were added to the aluminium iodide solution. Heating the mixture gave a light yellow solution and light yellow crystals were obtained in 2 days (0.59g, 17%). Metal analysis (C₁₄H₁₆Al₂EuI₈): cal. (%) Eu 10.81; found Eu 10.43. IR (Nujol, ν/cm^{-1}): 2924 (s), 2690 (w), 2250 (w), 1602 (w), 1462 (m), 1377 (s), 1154(w), 769 (w), 727 (w), 693 (w).

Chapter 2

[Yb(η^6 -MeC₆H₅)(AlI₄)₂]_n.1/2PhMe (**7**)

Yb filings (0.432 g, 2.5 mmol) and ICH₂CH₂I (0.704g, 2.5 mmol) were added to the solution followed by heating gave a red solution. Red crystals were obtained in 2 days (0.77g, 22%). Metal analysis (C_{10.5}H₁₂Al₂I₈Yb): cal. (%) Yb 12.54; found Yb 12.08. IR (Nujol, ν/cm^{-1}): 3205 (w), 2921 (s), 2726 (m), 2410 (w), 1692 (m), 1587 (m), 1462(s), 1377 (s), 1169 (w), 722 (w).

Synthesis of iodoaluminate complexes in mesitylene

A mixture of excess Al (0.162 g, 6 mmol) and I₂ (1.90 g, 7.5 mmol) was taken in a Schlenk flask charged with 40 mL mesitylene. The mixture was heated with stirring in oil bath for a couple of hours at 100°C. The solution turned to colourless from red indicating the consumption of all iodine. After cooling the solution to room temperature, stoichiometric amounts of Ln filings and ICH₂CH₂I (0.704g, 2.5 mmol) were added to the solution under nitrogen atmosphere in the glove box. The mixture was heated overnight at 100°C giving a colourless solution, which was filtered and crystallised at room temperature.

La(η^6 -C₆H₃Me₃)(AlI₄)₃ (**8**)

La filings (0.232 g, 1.67 mmol) and ICH₂CH₂I (0.704g, 2.5 mmol) were added to the aluminium iodide solution and heated. Colourless solution was formed and colourless crystals were grown in two days (0.65g, 21%). Metal analysis (C₉H₁₂Al₃I₁₂La); cal. (%) La 7.46; found La 7.37. IR (Nujol, ν/cm^{-1}): 2918 (s), 2700 (w), 2615 (w), 1460(s), 1377 (s), 1262 (w), 1029 (w), 722 (w).

Ce(η^6 -C₆H₃Me₃)(AlI₄)₃ (**9**)

Ce filings (0.234 g, 1.67 mmol) and ICH₂CH₂I (0.704g, 2.5 mmol) were added to the solution of aluminium iodide. Heating the mixture gave a red solution and red crystals were grown in two days (0.95g, 31%). Metal analysis (C₉H₁₂Al₃I₁₂Ce); cal. (%) Ce 7.52; found Ce 7.31.

Chapter 2

Pr(η^6 -C₆H₃Me₃)(AlI₄)₃ (**10**)

1.67 mmol of Pr filings (0.235 g) and 2.5 mmol ICH₂CH₂I (0.704g) were added to the aluminium iodide solution. The mixture was heated giving a red solution. Red crystals were grown in two days (0.82g, 26%). Metal analysis (C₉H₁₂Al₃I₁₂Pr); cal. (%) Pr 7.56; found Pr 7.48.

Nd(η^6 -C₆H₃Me₃)(AlI₄)₃ (**11**)

Nd filings (0.241 g, 1.67 mmol) and ICH₂CH₂I (0.704g, 2.5 mmol) were added to the AlI₃ solution. The mixture was heated giving a red solution and red crystals were grown in a week at room temperature (0.10 g, 32%). Metal analysis (C₉H₁₂Al₃I₁₂Nd); cal. (%) Nd 7.72; found Nd 7.58. IR (Nujol, ν /cm⁻¹): 2923 (s), 2854 (s), 2700 (w), 1607 (w), 1462 (m), 1377 (m), 1261(w), 1027 (w), 869 (w), 722 (w), 676 (w).

Sm(η^6 -C₆H₃Me₃)(AlI₄)₃ (**12**)

Sm filings (0.375 g, 2.5 mmol) and ICH₂CH₂I (0.704g, 2.5 mmol) were added to the aluminium iodide solution. After heating the mixture gave a light yellow solution. Dark crystals were obtained in 2 days (0.88 g, 25%). Metal analysis (C₉H₁₂Al₃I₁₂Sm): cal. (%) Sm 8.02; found Sm 7.94. IR (Nujol, ν /cm⁻¹): 3190 (w), 2726 (m), 1560 (w), 1300 (m), 1154 (w), 1026 (w), 869 (w), 722 (w).

Gd(η^6 -C₆H₃Me₃)(AlI₄)₃ (**13**)

1.67 mmol of Gd filings (0.263 g) and 2.5 mmol of ICH₂CH₂I (0.704g) were added to the aluminium iodide solution. After heating the mixture, a light yellow solution was formed. Yellow-orange crystals were obtained in 2 days (1.06 g, 35%). Metal analysis (C₉H₁₂Al₃I₁₂Gd): cal. (%) Gd 8.36; found Gd 8.45. IR (Nujol, ν /cm⁻¹): 3126 (w), 2726 (m), 2615 (m), 1377 (s), 1301 (m), 1154 (m), 1026 (w), 967 (w), 871 (w), 722 (w).

Chapter 2

Synthesis of bromoaluminate complexes in toluene

A mixture of AlBr_3 (1.6 g, 6.0 mmol), Ln filings (0.278 g, 2.0 mmol) and $\text{BrCH}_2\text{CH}_2\text{Br}$ (0.6 g, 6 mmol) was taken in a Schlenk flask charged with 40 mL toluene. The mixture was heated overnight at 100°C giving a dark muddy solution, which was filtered to remove the unreacted solid. The solution was kept at room temperature for crystallisation and dark crystals covered with muddy solution were obtained next day. No pure compound could have been isolated, so no elemental analysis was performed.



2.0 mmol of La filings (0.278 g) was used.



Nd filings (0.288 g, 2.0 mmol) was used.



Sm filings (0.30 g, 2.0 mmol) was used giving a yellow solution.



Eu filings (0.304 g, 2.0 mmol) was used giving a dark cloudy solution.

2.6 X-ray crystal data

For general procedures, see Appendix 2.

La(η^6 -C₆H₅Me)(AlI₄)₃ (1)

C₇H₈Al₃I₁₂La, $M_r = 1834.85$, monoclinic, space group $P2_1/n$ (No. 14), $a = 18.009(4)$ Å, $b = 18.952(4)$ Å, $c = 20.297(4)$ Å, $\beta = 101.79(3)^\circ$, $\alpha = \gamma = 90^\circ$, $V = 6781(2)$ Å³, $T = 173(2)$ K, $Z = 8$, $Z' = 2$, $\mu(\text{Mo } K\alpha) = 12.261$ mm⁻¹, $D_{\text{calc}} = 3.5942$ gcm⁻³, 108921 reflections measured, 15407 unique ($R_{\text{int}} = 0.0895$) which were used in all calculations. The final wR_2 was 0.0966 (all data) and R_I was 0.0425 ($I \geq 2\sigma(I)$).

Ce(η^6 -C₆H₅Me)(AlI₄)₃ (2)

C₇H₈Al₃CeI₁₂, $M_r = 1835.99$, monoclinic, space group $P2_1/n$ (No. 14), $a = 18.033(4)$ Å, $b = 18.943(4)$ Å, $c = 20.272(4)$ Å, $\beta = 102.07(3)^\circ$, $\alpha = \gamma = 90^\circ$, $V = 6772(2)$ Å³, $T = 173(2)$ K, $Z = 8$, $Z' = 2$, $\mu(\text{Mo } K\alpha) = 12.361$ mm⁻¹, $D_{\text{calc}} = 3.602$ gcm⁻³, 51299 reflections measured, 10320 unique ($R_{\text{int}} = 0.0637$) which were used in all calculations. The final wR_2 was 0.1204 (all data) and R_I was 0.0454 ($I > 2\sigma(I)$).

Nd(η^6 -C₆H₅Me)(AlI₄)₃ (3)

C₇H₈Al₃I₁₂Nd, $M_r = 1840.18$, monoclinic, space group $P2_1/c$ (No. 14), $a = 15.795(3)$ Å, $b = 14.005(3)$ Å, $c = 15.901(3)$ Å, $\beta = 105.19(3)^\circ$, $\alpha = \gamma = 90^\circ$, $V = 3394.5(13)$ Å³, $T = 173(2)$ K, $Z = 4$, $Z' = 1$, $\mu(\text{Mo } K\alpha) = 12.517$ mm⁻¹, $D_{\text{calc}} = 3.6005$ gcm⁻³, 23903 reflections measured, 6861 unique ($R_{\text{int}} = 0.0866$) which were used in all calculations. The final wR_2 was 0.1250 (all data) and R_I was 0.0498 ($I \geq 2\sigma(I)$).

Gd(η^6 -C₆H₅Me)(AlI₄)₃ (4)

C₇H₈Al₃GdI₁₂, $M_r = 1853.12$, monoclinic, space group $P2_1/n$ (No. 14), $a = 18.055(4)$ Å, $b = 18.872(4)$ Å, $c = 20.105(4)$ Å, $\beta = 102.81(3)^\circ$, $\alpha = \gamma = 90^\circ$, $V = 6680(2)$ Å³, $T = 173(2)$ K, $Z = 8$, $Z' = 2$, $\mu(\text{Mo } K\alpha) = 13.154$ mm⁻¹, $D_{\text{calc}} = 3.685$ gcm⁻³, 59439 reflections

Chapter 2

measured, 11588 unique ($R_{int} = 0.0619$) which were used in all calculations. The final wR_2 was 0.0948 (all data) and R_I was 0.0407 ($I > 2\sigma(I)$).

[Sm(η^6 -MeC₆H₅)(AlI₄)₂]_n.PhMe (5)

C₁₄H₁₆Al₂I₈Sm, $M_r = 1403.78$, orthorhombic, space group $P2_12_12_1$ (No. 19), $a = 10.992(2)$ Å, $b = 14.409(3)$ Å, $c = 19.079(4)$ Å, $\alpha = \beta = \gamma = 90^\circ$, $V = 3021.8(10)$ Å³, $T = 173(2)$ K, $Z = 4$, $Z' = 1$, $\mu(\text{MoK}\alpha) = 10.175$ mm⁻¹, $D_{calc} = 3.086$ gcm⁻³, 17103 reflections measured, 4903 unique ($R_{int} = 0.0896$) which were used in all calculations. The final wR_2 was 0.1023 (all data) and R_I was 0.0400 ($I > 2\sigma(I)$).

[Eu(η^6 -MeC₆H₅)(AlI₄)₂]_n.PhMe (6)

C₁₄H₁₆Al₂EuI₈, $M_r = 1405.39$, orthorhombic, space group $P2_12_12_1$ (No. 19), $a = 10.977(2)$ Å, $b = 14.388(3)$ Å, $c = 19.269(4)$ Å, $\alpha = \beta = \gamma = 90^\circ$, $V = 3043.3(11)$ Å³, $T = 173(2)$ K, $Z = 4$, $Z' = 1$, $\mu(\text{MoK}\alpha) = 10.235$ mm⁻¹, $D_{calc} = 3.067$ gcm⁻³, 37126 reflections measured, 6989 unique ($R_{int} = 0.0779$) which were used in all calculations. The final wR_2 was 0.1010 (all data) and R_I was 0.0439 ($I > 2\sigma(I)$).

[Yb(η^6 -MeC₆H₅)(AlI₄)₂]_n.1/2PhMe (7)

C_{10.5}H₁₂Al₂I₈Yb, $M_r = 1380.40$, monoclinic, space group $C2/c$ (No. 15), $a = 38.143(8)$ Å, $b = 8.1290(16)$ Å, $c = 19.776(4)$ Å, $\beta = 118.62(3)^\circ$, $\alpha = \gamma = 90^\circ$, $V = 5383(2)$ Å³, $T = 173(2)$ K, $Z = 8$, $Z' = 1$, $\mu(\text{MoK}\alpha) = 12.711$ mm⁻¹, $D_{calc} = 3.407$ gcm⁻³, 15661 reflections measured, 4493 unique ($R_{int} = 0.0914$) which were used in all calculations. The final wR_2 was 0.1118 (all data) and R_I was 0.0474 ($I > 2\sigma(I)$).

La(η^6 -C₆H₃Me₃)(AlI₄)₃ (8)

C₉H₁₂Al₃I₁₂La, $M_r = 1862.84$, triclinic, space group $P-1$ (No. 2), $a = 10.159(2)$ Å, $b = 18.705(4)$ Å, $c = 20.463(4)$ Å, $\alpha = 66.49(3)^\circ$, $\beta = 89.99(3)^\circ$, $\gamma = 89.98(3)^\circ$, $V = 3565.6(14)$ Å³, $T = 293(2)$ K, $Z = 4$, $Z' = 2$, $\mu(\text{MoK}\alpha) = 11.662$ mm⁻¹, $D_{calc} = 3.470$ gcm⁻³

Chapter 2

³, 28232 reflections measured, 11122 unique ($R_{int} = 0.0250$) which were used in all calculations. The final wR_2 was 0.4014 (all data) and R_I was 0.1074 ($I > 2\sigma(I)$).

Ce(η^6 -C₆H₃Me₃)(AlI₄)₃ (**9**)

C₉H₁₂Al₃CeI₁₂, $M_r = 1864.11$, monoclinic, space group $P2_1/c$ (No. 14), $a = 18.687(4)$ Å, $b = 10.137(2)$ Å, $c = 20.435(4)$ Å, $\beta = 113.50(3)^\circ$, $\alpha = \gamma = 90^\circ$, $V = 3549.9(15)$ Å³, $T = 293(2)$ K, $Z = 4$, $Z' = 1$, $\mu(\text{Mo K}\alpha) = 11.792$ mm⁻¹, $D_{calc} = 3.4876$ gcm⁻³, 28006 reflections measured, 5708 unique ($R_{int} = 0.0543$) which were used in all calculations. The final wR_2 was 0.1509 (all data) and R_I was 0.0480 ($I \geq 2\sigma(I)$).

Pr(η^6 -C₆H₃Me₃)(AlI₄)₃ (**10**)

C₉H₁₂Al₃I₁₂Pr, $M_r = 1864.84$, monoclinic, space group $P2_1/c$ (No. 14), $a = 18.607(4)$ Å, $b = 10.144(2)$ Å, $c = 20.383(4)$ Å, $\beta = 113.27(3)^\circ$, $\alpha = \gamma = 90^\circ$, $V = 3534.2(14)$ Å³, $T = 293(2)$ K, $Z = 4$, $Z' = 1$, $\mu(\text{Mo K}\alpha) = 11.936$ mm⁻¹, $D_{calc} = 3.505$ gcm⁻³, 28281 reflections measured, 6720 unique ($R_{int} = 0.0502$) which were used in all calculations. The final wR_2 was 0.1624 (all data) and R_I was 0.0577 ($I > 2\sigma(I)$).

Nd(η^6 -C₆H₃Me₃)(AlI₄)₃ (**11**)

C₉H₁₂Al₃I₁₂Nd, $M_r = 1868.23$, monoclinic, space group $P2_1/c$ (No. 14), $a = 18.645(4)$ Å, $b = 10.117(2)$ Å, $c = 20.399(4)$ Å, $\beta = 113.35(3)^\circ$, $\alpha = \gamma = 90^\circ$, $V = 3532.9(15)$ Å³, $T = 173(2)$ K, $Z = 4$, $Z' = 1$, $\mu(\text{Mo K}\alpha) = 12.030$ mm⁻¹, $D_{calc} = 3.5122$ gcm⁻³, 38490 reflections measured, 8807 unique ($R_{int} = 0.1042$) which were used in all calculations. The final wR_2 was 0.2362 (all data) and R_I was 0.0847 ($I \geq 2\sigma(I)$).

Sm(η^6 -C₆H₃Me₃)(AlI₄)₃ (**12**)

C₉H₁₂Al₃I₁₂Sm, $M_r = 1874.28$, monoclinic, space group $C2/c$ (No. 15), $a = 18.099(4)$ Å, $b = 11.555(2)$ Å, $c = 34.261(7)$ Å, $\beta = 98.51(3)^\circ$, $\alpha = \gamma = 90^\circ$, $V = 7086(3)$ Å³, $T = 293(2)$ K, $Z = 8$, $Z' = 1$, $\mu(\text{Mo K}\alpha) = 12.188$ mm⁻¹, $D_{calc} = 3.514$ gcm⁻³, 42395 reflections measured, 9689 unique ($R_{int} = 0.0809$) which were used in all calculations. The final wR_2 was 0.2255 (all data) and R_I was 0.0801 ($I > 2\sigma(I)$).

Chapter 2

Gd(η^6 -C₆H₃Me₃)(AlI₄)₃ (**13**)

C₉H₁₂Al₃GdI₁₂, $M_r = 1881.18$, monoclinic, space group $P2_1/c$ (No. 14), $a = 18.608(4)$ Å, $b = 10.105(2)$ Å, $c = 20.352(4)$ Å, $\beta = 113.19(3)^\circ$, $\alpha = \gamma = 90^\circ$, $V = 3517.7(14)$ Å³, $T = 173(2)$ K, $Z = 4$, $Z' = 1$, $\mu(\text{MoK}\alpha) = 12.492$ mm⁻¹, $D_{\text{calc}} = 3.552$ gcm⁻³, 63445 reflections measured, 10105 unique ($R_{\text{int}} = 0.0613$) which were used in all calculations. The final wR_2 was 0.1024 (all data) and R_I was 0.0390 ($I > 2\sigma(I)$).

La(η^6 -C₆H₅Me)(AlBr₄)₃ (**14**)

C₇H₈Al₃Br₁₂La, $M_r = 1270.90$, monoclinic, space group $P2_1/n$ (No. 14), $a = 10.088(2)$ Å, $b = 20.776(4)$ Å, $c = 13.468(3)$ Å, $\beta = 105.11(3)^\circ$, $\alpha = \gamma = 90^\circ$, $V = 2725.1(10)$ Å³, $T = 100(2)$ K, $Z = 4$, $Z' = 1$, $\mu(\text{MoK}\alpha) = 19.254$ mm⁻¹, $D_{\text{calc}} = 3.0973$ gcm⁻³, 4665 reflections measured, 4665 unique ($R_{\text{int}} = .$) which were used in all calculations. The final wR_2 was 0.1217 (all data) and R_I was 0.0483 ($I > 2\sigma(I)$).

Nd(η^6 -C₆H₅Me)(AlBr₄)₃ (**15**)

C₇H₈Al₃Br₁₂Nd, $M_r = 1276.23$, monoclinic, space group $P2_1/n$ (No. 14), $a = 10.039(2)$ Å, $b = 20.639(4)$ Å, $c = 13.425(3)$ Å, $\beta = 105.30(3)^\circ$, $\alpha = \gamma = 90^\circ$, $V = 2683.0(10)$ Å³, $T = 100(2)$ K, $Z = 4$, $Z' = 1$, $\mu(\text{MoK}\alpha) = 19.899$ mm⁻¹, $D_{\text{calc}} = 3.160$ gcm⁻³, 29866 reflections measured, 4495 unique ($R_{\text{int}} = 0.0639$) which were used in all calculations. The final wR_2 was 0.0909 (all data) and R_I was 0.0378 ($I > 2\sigma(I)$).

Sm(η^6 -C₆H₅Me)(AlBr₄)₃ (**16**)

C₇H₈Al₃Br₁₂Sm, $M_r = 1282.34$, monoclinic, $P2_1/n$ (No. 14), $a = 10.017(2)$ Å, $b = 20.587(4)$ Å, $c = 13.408(3)$ Å, $\beta = 105.35(3)^\circ$, $\alpha = \gamma = 90^\circ$, $V = 2666.4(10)$ Å³, $T = 100(2)$ K, $Z = 4$, $Z' = 1$, $\mu(\text{MoK}\alpha) = 20.278$ mm⁻¹, $D_{\text{calc}} = 3.194$ gcm⁻³, 27847 reflections measured, 4042 unique ($R_{\text{int}} = 0.0747$) which were used in all calculations. The final wR_2 was 0.1233 (all data) and R_I was 0.0487 ($I > 2\sigma(I)$).

Chapter 2

[Eu(η^6 -MeC₆H₅)(AlBr₄)₂]_n.PhMe (17)

C_{10.5}H₁₂Al₂Br₈Eu, $M_r = 983.40$, monoclinic, space group *C2/c* (No. 15), $a = 26.260(5)$ Å, $b = 10.176(2)$ Å, $c = 19.586(4)$ Å, $\beta = 115.03(3)^\circ$, $\alpha = \gamma = 90^\circ$, $V = 4742.0(19)$ Å³, $T = 100(2)$ K, $Z = 8$, $Z' = 1$, $\mu(\text{MoK}\alpha) = 16.193$ mm⁻¹, $D_{\text{calc}} = 2.755$ gcm⁻³, 35068 reflections measured, 5294 unique ($R_{\text{int}} = 0.0499$) which were used in all calculations. The final wR_2 was 0.0830 (all data) and R_1 was 0.0339 ($I > 2\sigma(I)$).

2.7 References

1. H. Schumann, J. A. Meese-Marktscheffel and L. Esser, *Chem. Rev.*, 1995, **95**, 865-986.
2. H. Schumann and W. Genthe, in *Handbook on the Physics and Chemistry of Rare Earths*, eds. K. A. Gscheidner and L. Eyring, Elsevier, Amsterdam, 1984, vol. 7, ch. 23, pp. 445-571.
3. H. Schumann, *Angew. Chem. Int. Ed.*, 1984, **23**, 474-493.
4. W. J. Evans, *Adv. Organomet. Chem.*, 1985, **24**, 131-177.
5. W. J. Evans, *Polyhedron*, 1987, **6**, 803-835.
6. C. J. Schaverien, in *Adv. Organomet. Chem.*, eds. F. G. A. Stone and W. Robert, Academic Press, Cambridge, 1994, vol. 36, pp. 283-362.
7. J. H. Forsberg and T. Moeller, in *Gmelin Handbook of Inorganic Chemistry, Part D6, Sc, Y, La-Lu*, eds. T. Moeller, U. Kruerke and E. Schleitzer-Rust, Springer, Berlin, 8th edn., 1983, p. 137.
8. T. J. Marks and R. D. Ernst, in *Comprehensive Organometallic Chemistry*, eds. F. G. A. Stone and E. W. Abel, Pergamon, Oxford, 1982, vol. 3, pp. 173-270.
9. I. A. Borovkov, G. K. Fukin and A. A. Trifonov, *Russ. Chem. Bull., Int. Ed.*, 2008, **57**, 541-545.
10. F. T. Edelmann, *Coord. Chem. Rev.*, 2009, **253**, 2515-2587.
11. F. T. Edelmann, *Coord. Chem. Rev.*, 2015, **284**, 124-205.
12. M. N. Bochkarev, *Coord. Chem. Rev.*, 2004, **248**, 835-851.
13. A. N. Selikhov, T. V. Mahrova, A. V. Cherkasov, G. K. Fukin, J. Larionova, J. Long and A. A. Trifonov, *Organometallics*, 2015, **34**, 1991-1999.
14. J. M. Birmingham and G. Wilkinson, *J. Am. Chem. Soc.*, 1956, **78**, 42-44.

Chapter 2

15. F. T. Edelmann, *Coord. Chem. Rev.*, 2016, **306**, 346-419.
16. M. Visseaux, F. Nief and L. Ricard, *J. Organomet. Chem.*, 2002, **647**, 139-144.
17. J.-F. L. Maréchal, E. Bulot, D. Baudry, M. Ephritikhine, D. Hauchard and R. Godard, *J. Organomet. Chem.*, 1988, **354**, C17-C18.
18. A. K. Dash, A. Razavi, A. Mortreux, C. W. Lehmann and J.-F. Carpentier, *Organometallics*, 2002, **21**, 3238-3249.
19. F. T. Edelmann, *Coord. Chem. Rev.*, 2016, **318**, 29-130.
20. F. Barbotin, R. Spitz and C. Boisson, *Macromol. Rapid Commun.*, 2001, **22**, 1411-1414.
21. P. Biagini, G. Lugli and R. Millini, *New J. Chem.*, 1995, **19**, 713-722.
22. S. Jin, J. Guan, H. Liang and Q. Shen, *J. Catal.*, 1993, **14**, 159-162.
23. J. Hu, H. Tian, Q. Shen and L. Liang, *Chin. Sci. Bull.*, 1992, **37**, 566.
24. J. Hu, L. Liang and Q. Shen, *J. Rare Earths*, 1993, **11**, 302.
25. G. B. Deacon and Q. Shen, *J. Organomet. Chem.*, 1996, **511**, 1-17.
26. M. N. Bochkarev, *Chem. Rev.*, 2002, **102**, 2089-2118.
27. F. G. N. Cloke, *Chem. Soc. Rev.*, 1993, **22**, 17-24.
28. M. N. Bochkarev, *Russ. Chem. Rev.*, 2000, **69**, 783-794.
29. F. A. Cotton, *Inorg. Chem.*, 2002, **41**, 643-658.
30. F. T. Edelmann, D. M. M. Freckmann and H. Schumann, *Chem. Rev.*, 2002, **102**, 1851-1896.
31. F. Barbotin, R. Spitz and C. Boisson, *Macromol. Rapid Commun.*, 2001, **22**, 1411-1414.
32. T. Hayakawa, Y. Nakayama and H. Yasuda, *Polym. Int.*, 2001, **50**, 1260-1264.

Chapter 2

33. A. Fischbach and R. Anwander, in *Neodymium Based Ziegler Catalysts—Fundamental Chemistry*, Springer, 2006, vol. 2004, pp. 155-281.
34. F. A. Cotton and W. Schwotzer, *J. Am. Chem. Soc.*, 1986, **108**, 4657-4658.
35. F. A. Cotton and W. Schwotzer, *Organometallics*, 1987, **6**, 1275-1280.
36. B. Fan, Q. Shen and Y. Lin, *Chin. J. Org. Chem.*, 1989, **9**, 414-414.
37. B. Fan, Q. Shen and Y. Lin, *J. Organomet. Chem.*, 1989, **376**, 61-66.
38. B. Fan, S. Jin, Q. Shen and Y. Lin, *Chin. Sci. Bull.*, 1991, **36**, 84-85.
39. B. Fan, Q. Shen and Y. Lin, *Chin. J. Inorg. Chem.*, 1991, **7**, 143.
40. B. Fan, Y. Lin and Q. Shen, *Chin. J. Appl. Chem.*, 1990, **7**, 23.
41. H.-Z. Liang, J.-W. Guan, Y.-H. Lin and Q. Shen, *Chin. J. Org. Chem.*, 1994, **14**, 380-382.
42. B. Fan, Q. Shen and Y. Lin, *J. Organomet. Chem.*, 1989, **377**, 51-58.
43. H. Liang, Q. Shen, J. Guan and Y. Lin, *J. Organomet. Chem.*, 1994, **474**, 113-116.
44. Q. Liu, Y.-H. Lin and Q. Shen, *Acta Cryst.*, 1997, **C53**, 1579-1580.
45. P. Biagini, G. Lugli and R. Millini, *Gazz. Chim. Ital.*, 1994, **124**, 217-225.
46. Y.-M. Yao, Y. Zhang, Q. Shen, Q.-C. Liu, Q.-J. Meng and Y.-H. Lin, *Chin. J. Chem.*, 2001, **19**, 588-592.
47. Q. Liu, Q. Shen, Y. Lin and Y. Zhang, *Chin. J. Inorg. Chem.*, 1998, **14**, 194-198.
48. H. Liang, Q. Shen, S. Jin and Y. Lin, *J. Chin. Rare Earth Soc.*, 1994, **12**, 193-196.
49. H. Liang, Q. Shen, S. Jin and Y. Lin, *Chem. Commun.*, 1992, 480-481.
50. A. A. Fagin, M. N. Bochkarev, S. A. Kozimor, J. W. Ziller and W. J. Evans, *Z. Anorg. Allg. Chem.*, 2005, **631**, 2848-2853.
51. R. Shannon, *Acta Cryst.*, 1976, **A32**, 751-767.

Chapter 2

52. A. S. Filatov, A. Y. Rogachev and M. A. Petrukhina, *J. Mol. Struct.*, 2008, **890**, 116-122.
53. A. S. Filatov, S. N. Gifford, D. K. Kumar and M. A. Petrukhina, *Acta Cryst.*, 2009, **E65**, m286-m287.
54. S.-S. Liu, J. W. Ziller, Y.-Q. Zhang, B.-W. Wang, W. J. Evans and S. Gao, *Chem. Commun.*, 2014, **50**, 11418-11420.
55. R. Knaanie, J. Šebek, M. Tsuge, N. Myllys, L. Khriachtchev, M. Räsänen, B. Albee, E. O. Potma and R. B. Gerber, *J. Phys. Chem. A*, 2016, **120**, 3380-3389.
56. M. Zimmermann, K. W. Törnroos, H. Sitzmann and R. Anwander, *Chem. Eur. J.*, 2008, **14**, 7266-7277.
57. H. M. Dietrich, K. W. Törnroos, E. Herdtweck and R. Anwander, *Organometallics*, 2009, **28**, 6739-6749.
58. L. N. Jende, C. Maichle-Mössmer and R. Anwander, *Chem. Eur. J.*, 2013, **19**, 16321-16333.
59. H. M. Dietrich, C. Zapilko, E. Herdtweck and R. Anwander, *Organometallics*, 2005, **24**, 5767-5771.
60. H. M. Dietrich, K. W. Törnroos and R. Anwander, *Angew. Chem. Int. Ed.*, 2011, **50**, 12089-12093.
61. M. Zimmermann, J. Volbeda, K. W. Törnroos and R. Anwander, *C. R. Chimie*, 2010, **13**, 651-660.
62. M. C. Cassani, D. J. Duncalf and M. F. Lappert, *J. Am. Chem. Soc.*, 1998, **120**, 12958-12959.
63. M. C. Cassani, Y. K. Gun'ko, P. B. Hitchcock, M. F. Lappert and F. Laschi, *Organometallics*, 1999, **18**, 5539-5547.
64. M. Cesari, U. Pedretti, Z. Zazzetta, g. Lugli and W. Marconi, *Inorg. Chim. Acta*, 1971, **5**, 439-444.

Chapter 2

65. F. A. Cotton and W. Schwotzer, *Organometallics*, 1985, **4**, 942-943.
66. F. A. Cotton, W. Schwotzer and C. Q. Simpson, *Angew. Chem. Int. Ed.*, 1986, **25**, 637-639.
67. C. E. Housecroft and A. G. Sharpe, *Inorganic Chemistry*, Pearson Education Ltd., London, 2005.
68. P. N. Hazin, J. C. Huffman and J. W. Bruno, *Organometallics*, 1987, **6**, 23-27.
69. W. J. Evans, J. M. Olofson, H. Zhang and J. L. Atwood, *Organometallics*, 1988, **7**, 629-633.
70. E. B. Lobkovsky, Y. K. Gun'ko, B. M. Bulychev, V. K. Belsky, G. L. Soloveichik and M. Y. Antipin, *J. Organomet. Chem.*, 1991, **406**, 343-352.
71. L. Maron, E. L. Werkema, L. Perrin, O. Eisenstein and R. A. Andersen, *J. Am. Chem. Soc.*, 2005, **127**, 279-292.
72. T. Mehdoui, J.-C. Berthet, P. Thuéry, L. Salmon, E. Rivière and M. Ephritikhine, *Chem. Eur. J.*, 2005, **11**, 6994-7006.
73. E. L. Werkema and R. A. Andersen, *J. Am. Chem. Soc.*, 2008, **130**, 7153-7165.
74. J. G. Brennan, F. G. N. Cloke, A. A. Sameh and A. Zalkin, *Chem. Commun.*, 1987, 1668-1669.
75. D. Robert, T. P. Spaniol and J. Okuda, *Eur. J. Inorg. Chem.*, 2008, 2801-2809.
76. W. J. Evans, T. M. Champagne, D. G. Giarikos and J. W. Ziller, *Organometallics*, 2005, **24**, 570-579.
77. H. Nakamura, Y. Nakayama, H. Yasuda, T. Maruo, N. Kanehisa and Y. Kai, *Organometallics*, 2000, **19**, 5392-5399.
78. W. J. Evans, T. S. Gummersheimer, T. J. Boyle and J. W. Ziller, *Organometallics*, 1994, **13**, 1281-1284.

Chapter 2

79. W. J. Evans, J. W. Grate, H. W. Choi, I. Bloom, W. E. Hunter and J. L. Atwood, *J. Am. Chem. Soc.*, 1985, **107**, 941-946.
80. J. A. Moore, A. H. Cowley and J. C. Gordon, *Organometallics*, 2006, **25**, 5207-5209.
81. I. L. Fedushkin, V. K. Nevodchikov, V. K. Cherkasov, M. N. Bochkarev, H. Schumann, F. Girgsdies, F. H. Görlitz, G. Kociok-Köhn and J. Pickardt, *J. Organomet. Chem.*, 1996, **511**, 157-162.
82. I. L. Fedushkin, M. N. Bochkarev, H. Schumann and L. Esser, *J. Organomet. Chem.*, 1995, **489**, 145-151.
83. S. Wang, S. Zhou, E. Sheng, M. Xie, K. Zhang, L. Cheng, Y. Feng, L. Mao and Z. Huang, *Organometallics*, 2003, **22**, 3546-3552.
84. P. L. Watson, J. F. Whitney and R. L. Harlow, *Inorg. Chem.*, 1981, **20**, 3271-3278.
85. M. F. Lappert, A. Singh, J. L. Atwood and W. E. Hunter, *Chem. Commun.*, 1981, 1190-1191.
86. I. Albrecht, E. Hahn, J. Pickardt and H. Schumann, *Inorg. Chim. Acta*, 1985, **110**, 145-147.
87. H. Schumann, I. Albrecht, J. Loebel, E. Hahn, M. B. Hossain and D. Van der Helm, *Organometallics*, 1986, **5**, 1296-1304.
88. S. Song, Q. Shen, S. Jin, J. Guan and Y. Lin, *Polyhedron*, 1992, **11**, 2857-2861.
89. Q. Shen, M. Qi, J. Guan and Y. Lin, *J. Organomet. Chem.*, 1991, **406**, 353-361.
90. Y. Luo, Y. Yao, Q. Shen, J. Sun and F. Xue, *Acta Cryst.*, 1998, **C54**, 711-712.
91. Q. Shen, M. Qi, S. Song, L. Zhang and Y. Lin, *J. Organomet. Chem.*, 1997, **549**, 95-100.

CHAPTER 3

CHEMISTRY OF

HALOGENOALUMINATE ALKALINE

EARTH-ARENE COMPLEXES

3.1 Introduction

The chemistry of six-membered π -arene complexes has attracted the interest of inorganic chemists since the characterisation of the compound $[\text{Cr}(\eta^6\text{-benzene})_2]$, synthesised by the reduction of anhydrous CrCl_3 with Al/AlCl_3 in aromatic hydrocarbon as solvent.¹ After the discovery of the first transition metal π -arene complex, this direction of chemistry has been explored comprehensively.²⁻¹¹ Moreover, six-membered π -arene complexes of U(III) and U(IV) have been reported, achieved by the AlX_3 -mediated synthesis.¹²⁻¹⁶ The lanthanoid-arene complexes, have been synthesised by using AlX_3 and LnX_3 in aromatic solvent, and their catalytic activity have also been explored extensively.¹⁷⁻⁵⁰ In chapter 2, we described a series of iodoaluminate lanthanoid π -arene complexes, synthesised by heating a mixture of in situ prepared AlI_3 (from Al metal and I_2) and $\text{LnI}_2/\text{LnI}_3$ (from Ln metal and $\text{ICH}_2\text{CH}_2\text{I}$). Even though there are distinct comparisons between divalent lanthanoids (Sm, Eu and Yb) with the heavier group 2 metals (Ba, Sr and Ca respectively), the six-membered π -arene complexes of alkaline earths are rare species (a Cambridge Crystallographic Database search found 38 hits),⁵¹⁻⁷⁰ however, their cyclopentadienyl and allyl complexes are known.⁷¹⁻⁹⁸

Alkaline earth (Ae) complexes with a π -interaction to alkene and alkyne have been known for more than forty years. The first magnesium-diene complex $\text{Mg}(\text{thf})_3(\text{s-cis-PhCH=CH-CH=CHPh})$ with trigonal bipyramidal coordination was prepared from the 1,3-diene and activated magnesium in thf⁹⁹, and $[(\text{MeC}\equiv\text{C})_2\text{BeNMe}_3]_2$ was reported involving an π -alkyne interaction.¹⁰⁰ A quite large number of other complexes having π -alkene and -alkyne interactions have also been reported.^{72, 73, 101-117} The first Ae complex $[\text{Ba}(\eta^6\text{-C}_6\text{H}_5\text{Me})(\text{Sn}_3(\text{PSi}^t\text{Bu}_3)_4)]$ (Fig.3.1) featuring Ba- η^6 (arene) interactions was obtained by the reaction of $\text{Ba}(\text{PHSi}^t\text{Bu}_3)_2$ and bis[bis(trimethylsilyl)amino]stannylene in toluene.⁵² The Ba-C bond distances range 3.36-3.48 Å.

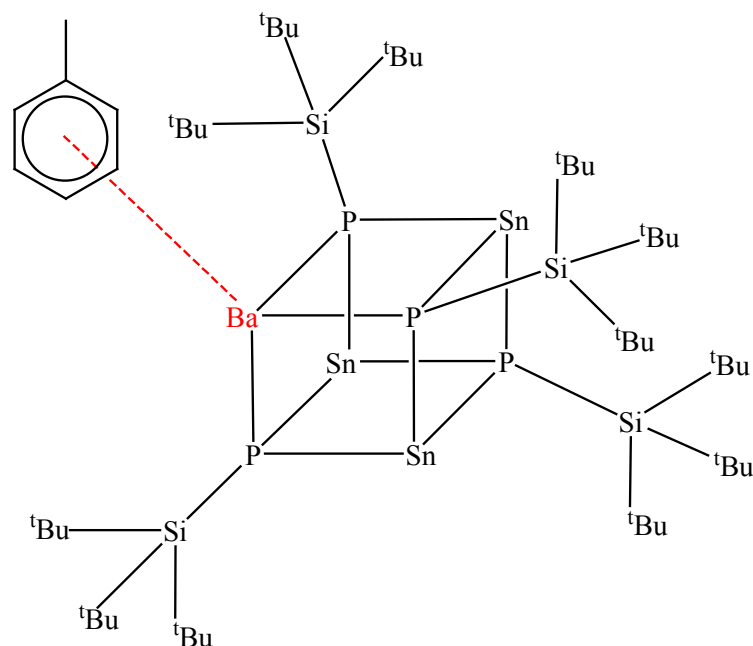


Fig. 3.1: Molecular structure of $[\text{Ba}(\eta^6\text{-C}_6\text{H}_5\text{Me})(\text{Sn}_3(\text{PSi}^t\text{Bu}_3)_4)]$.

Barium complexes $[\text{Bu}_8\text{N}_4\text{Ba}_2(\eta^6\text{-arene})_2]$ (arene = durene, naphthalene, toluene and benzene) have been synthesised by refluxing *meso*-octaalkylporphyrinogen compound $[\text{Bu}_8\text{N}_4\text{Ba}_2(\text{thf})_4]$ and the respective aromatic hydrocarbons for 24 hours.⁵³ The two arene rings in durene and naphthalene complexes bonded to the barium centre with an average distance of 3.068(7) and 3.077(7) Å, respectively. However, in benzene and toluene complexes, one barium bonded to the arene in an η^6 -fashion, and the other barium is weakly bonded with an η^2 (in benzene) or η^3 (toluene) modes. The average Ba-C(η^6) distances are 3.068(3), 3.086(5) Å in the toluene and benzene complexes, respectively.

The calix[4]arene complex of calcium $[\text{p-}^t\text{Bu-calix[4]}-(\text{OC}_5\text{H}_9)_2(\text{O})_2\text{Ca}_2\text{I}_2(\text{MeCN})_2]$ (Fig. 3.2) has a Ca- η^6 (arene) interaction and was synthesised by refluxing a mixture of $[\text{CaI}_2(\text{thf})_4]$ and $[\text{p-}^t\text{Bu-calix[4]}-(\text{OC}_5\text{H}_9)_2-(\text{O})_2\text{Ca}]\cdot\text{DME}$ overnight in acetonitrile.⁵⁴ One of the Ca^{2+} ions in the molecule bonded to two oxygen atoms, and has η^6 interactions with the two opposite aromatic rings. The Ca-C(arene) distances in the two rings range from 3.072(3)-3.515(3) and 3.014(4)-3.403(4) Å, respectively. The coordination sphere of the Ca^{2+} ion is completed by two acetonitrile solvent molecules with two acetonitrile molecules.

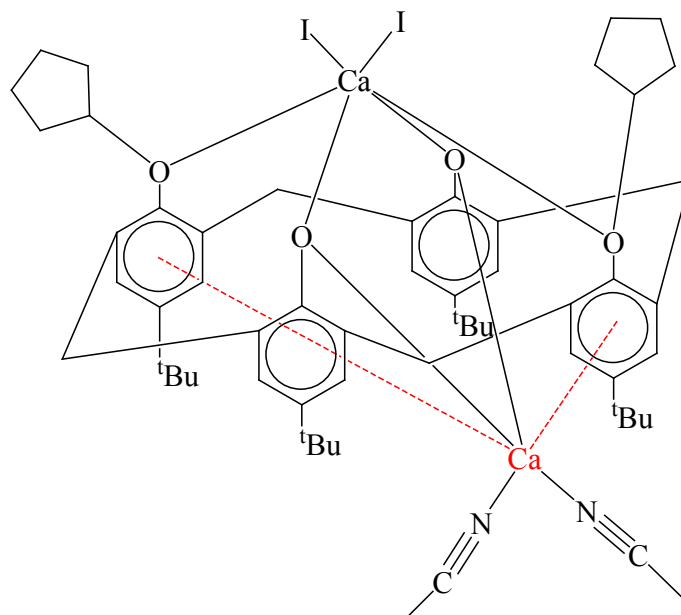


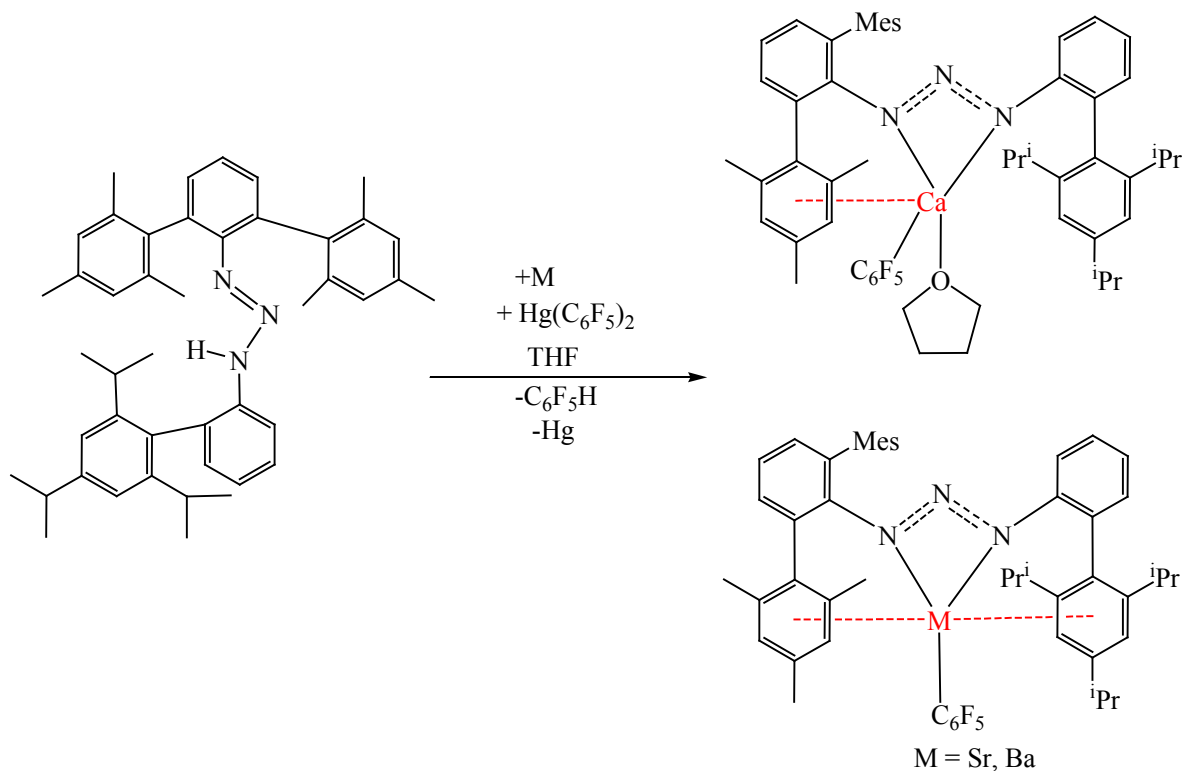
Fig. 3.2: Molecular structure of $[p\text{-}^t\text{Bu-calix[4]-(OC}_5\text{H}_9)_2(\text{O})_2\text{Ca}_2\text{I}_2(\text{MeCN})_2]$.

Aryl complexes of the heavier Ae metals Ca, Sr, and Ba have been synthesised by the one pot transmetalation/deprotonation reaction of the triazene, bis(pentafluorophenyl)mercury, and the corresponding Ae metal (Scheme 3.1). These complexes feature additional π -arene interactions with the pendent aryl substituents of the ligands.⁵⁵ In the calcium complex, the Ca^{2+} ion binds to the mesityl ring in an η^5 fashion and the Ca-C distances span the range from 3.015(7)–3.132(7) Å. In contrast, the metal ions in the Sr and Ba complexes bind not only to a mesityl group but also to the triisopropylphenyl ring of the triazene ligand in η^6 or η^5 modes. The M-C(mesityl) distances in Sr and Ba complexes range from 3.165–3.306 and 3.327–3.430 Å, respectively and that of the M-C(triisopropylphenyl) distances range 3.078–3.283 and 3.286–3.406 Å, respectively.

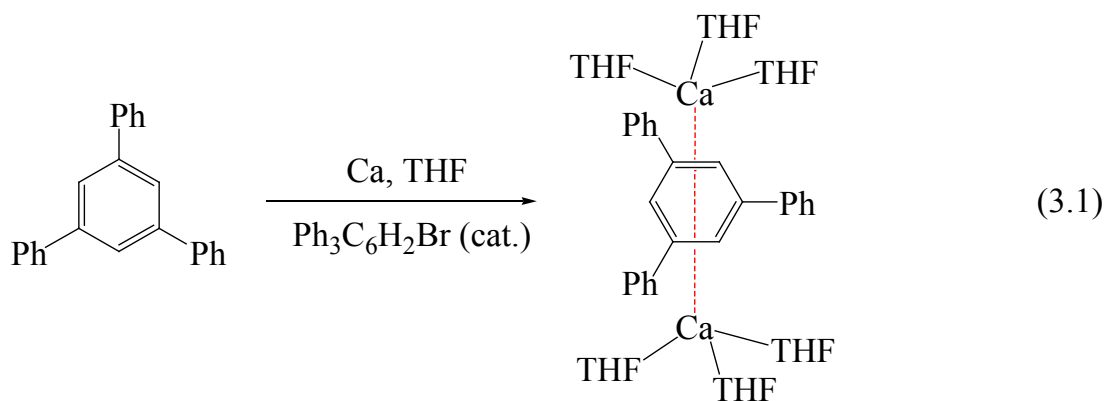
An “inverse” sandwich complex $[(\text{thf})_3\text{Ca}\{\mu\text{-C}_6\text{H}_3\text{-1,3,5-Ph}_3\}\text{Ca}(\text{thf})_3]$ (Eqn. 3.1) was synthesised by the reaction of bromo-2,4,6-triphenylbenzene and activated calcium in THF. The arene locates in between the two metal cations with a Ca-Ca and Ca-C distances of 4.279(3) and 2.592(3) Å, respectively.⁵⁶ A series of heterometallic alkaline earth-rare earth aryloxo complexes has been prepared by the treatment of a rare earth metal and a potential alkaline earth metal with 2,6-diphenylphenol (HODpp) at elevated temperatures (200–250 °C). Moreover, some charge-separated complexes $[\text{Ae}_2(\text{Odpp})_3][\text{Ln}(\text{Odpp})_4]$ were obtained for a range of metals (Ae = Ca, Sr and Ba; Ln = Nd, Sm, Ho and Yb) (Fig. 3.3).⁵⁷ The

Chapter 3

structure of the complexes feature an extensive intramolecular Ae- π bonding with the pendant phenyl groups.



Scheme 3.1: Synthesis of triazene complexes of Ca, Sr and Ba.



The addition of $[\text{Mes}(\text{I})\text{Ca}(\text{Et}_2\text{O})_4]$ solution in diethyl ether to a solution of mesityl copper in toluene at $\sim 40^\circ\text{C}$ afforded a tetrameric solvent-free iodocalcium dimesityl cuprate(I) complex $[\text{ICa}(\mu\text{-}\eta^1, \eta^6\text{-Mes}_2\text{Cu})_4]$ (Fig. 3.4).⁵⁸ The calcium atom binds to the mesityl group in the nonplanar dimesityl cuprate anion in an η^6 fashion having a Ca-C distances in the range of 2.792(5)-2.866(6) Å (average Ca-C length is 282.9 Å). It also attached to the aryl

Chapter 3

ipso-carbon atom in the planar dimesityl cuprate ion in a η^1 mode. Two calcium atoms have a separation of 4.1743(17) Å, and are bridged by two iodine atoms to each other forming a four-membered Ca_2I_2 ring with the Ca-I distances in the range from 3.0398(12)–3.0950(11) and 307.67(12)–313.28(13) Å (average Ca-I length of 3.086 Å).

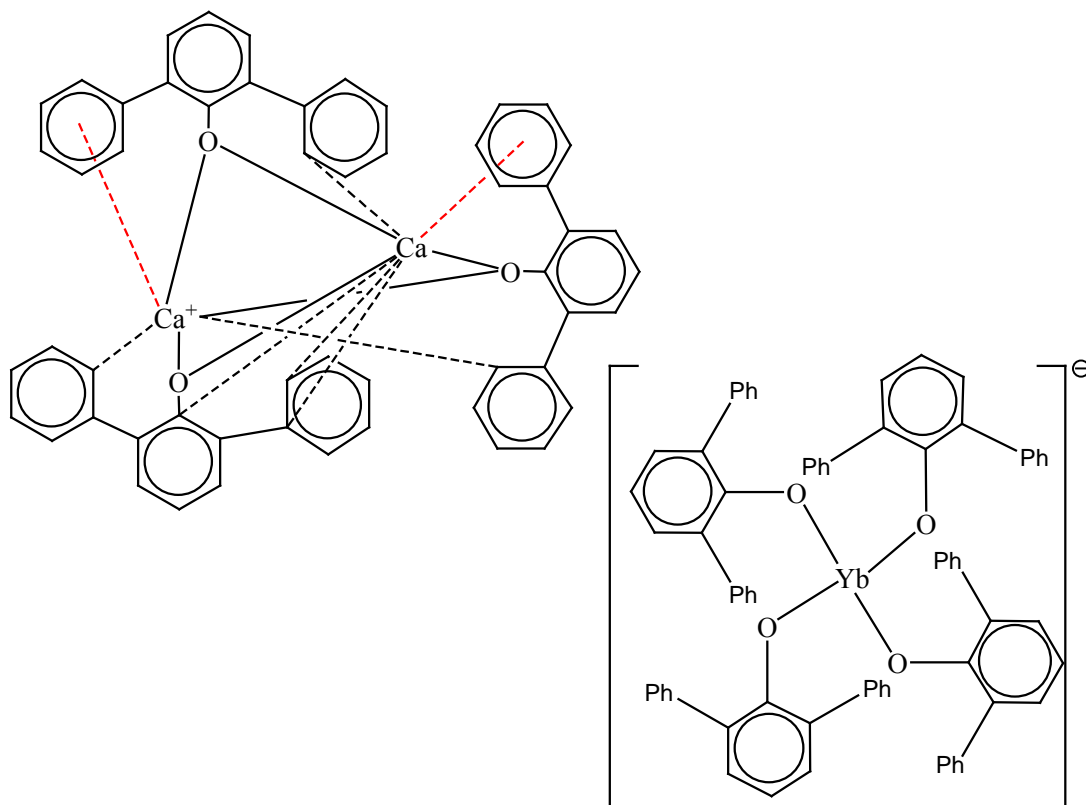


Fig. 3.3: Molecular structure of $[\text{Ca}_2(\text{Odpp})_3][\text{Yb}(\text{Odpp})_4]$, representative of a series of analogous complexes.

The treatment of the magnesium(I) dimer, $[(^{\text{Mes}}\text{Nacnac})\text{MgMg}(^{\text{Mes}}\text{Nacnac})]$ ($^{\text{Mes}}\text{Nacnac} = [\{\text{N}(\text{R})\text{C}(\text{Me})\}_2\text{CH}]^-$, $\text{R} = \text{C}_6\text{H}_2\text{Me}_3\text{-2,4,6}$) with anthracene at ambient temperature in toluene gave a monomeric complex, in which the two $\text{Mg}(^{\text{Mes}}\text{Nacnac})$ fragments bridged by an anthracene dianion (Eqn. 3.2).⁵⁹ However, the connections of the two fragments with the anthracene dianion are significantly different; one Mg centre has a polar covalent interaction with two carbons, and the other displays η^4 -arene interactions with one of the arene rings. Consequently, the molecule seems to have a contact ion pair involving a $[\text{Mg}(^{\text{Mes}}\text{Nacnac})]^+$ cation and a $[(^{\text{Mes}}\text{Nacnac})\text{Mg}(\text{anthracene})]^-$ anion. The Mg-C(π) distances range from 2.382(7)–2.426(6) Å, and the covalent M-C contacts are 2.344(7) and 2.372(7) Å.

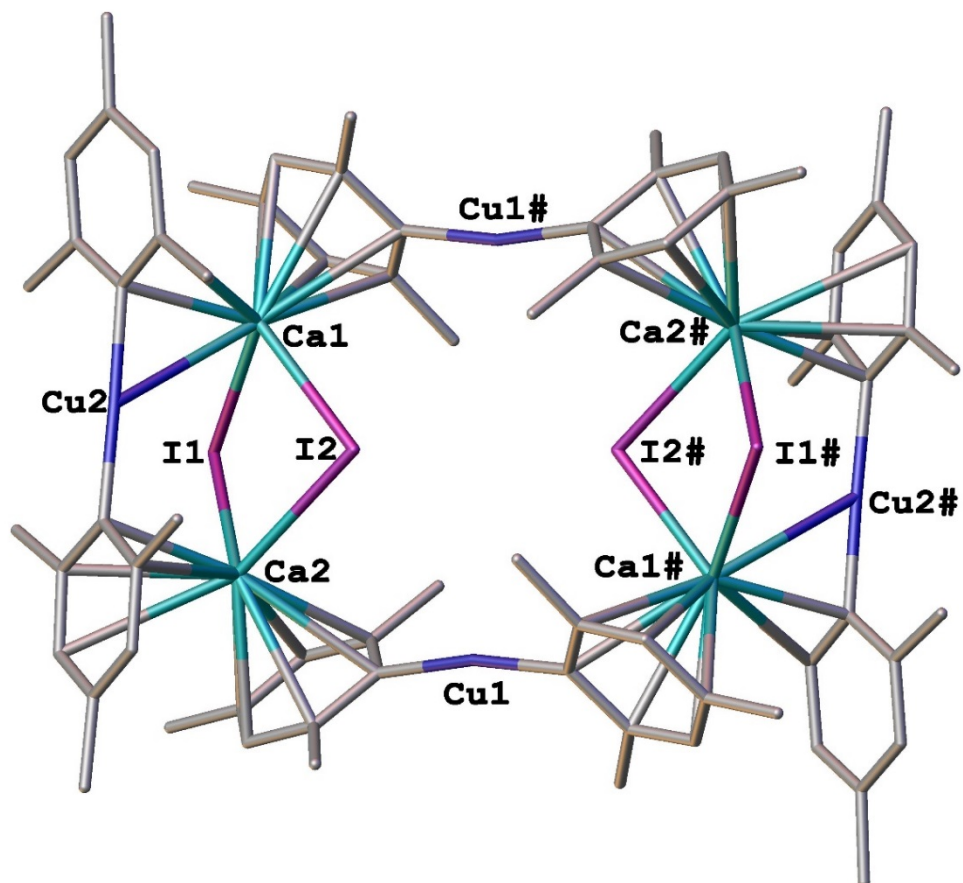
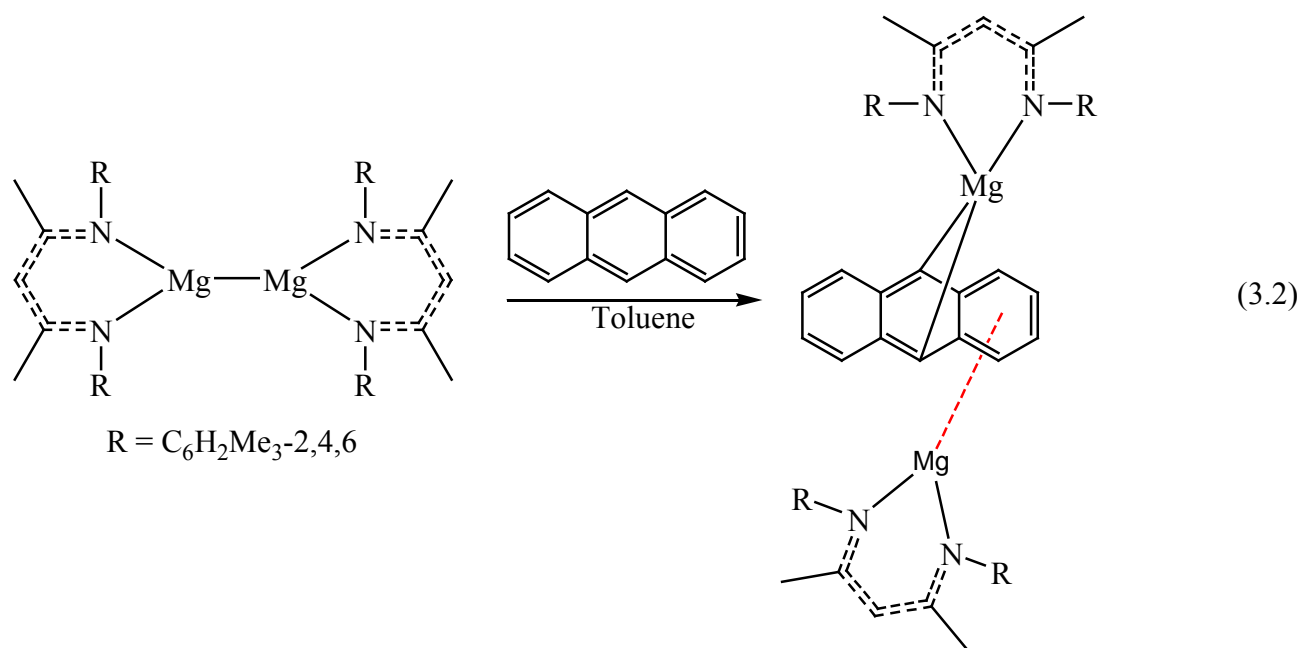


Fig. 3.4: Molecular structure of $[\text{ICa}(\mu\text{-}\eta^1, \eta^6\text{-Mes}_2\text{Cu})_4]$.



Chapter 3

Two separate dimorphs of the barium complex $[(\text{Ba}\{\text{GaCl}_4\}_2)_3 \cdot 2\text{C}_6\text{H}_6]$ (Fig. 3.5) have been synthesised by the reaction of gallium chloride, barium chloride and barium metal in benzene.⁶⁰ The dimorphs have the same structural units; however, one crystallises in the monoclinic space group $C2/c$, and the other belongs to a rhombohedral space group $R\bar{3}$. The crystal structure shows one Ba atom coordinated by two axial benzene molecules in an η^6 -fashion, and the benzene molecules being staggered on opposite sides of Ba. The Ba-C contacts fall in the range from 3.277(7)–3.331(11) and 3.278(10)–3.308(9) Å in the monoclinic and rhombohedral forms, respectively. The Ba atom is surrounded by six Cl^- ions from adjacent, bridging GaCl_4^- groups in a hexagonal planar fashion around the equatorial coordination plane. The Ba-Cl distances range from 3.302(2)–3.377(7) and 3.343(2)–3.344(3) Å in the monoclinic and rhombohedral forms, respectively. Based on hapticity, the coordination number around the Ba atom is 12 (6 with two benzene rings and 6 chloride ions).

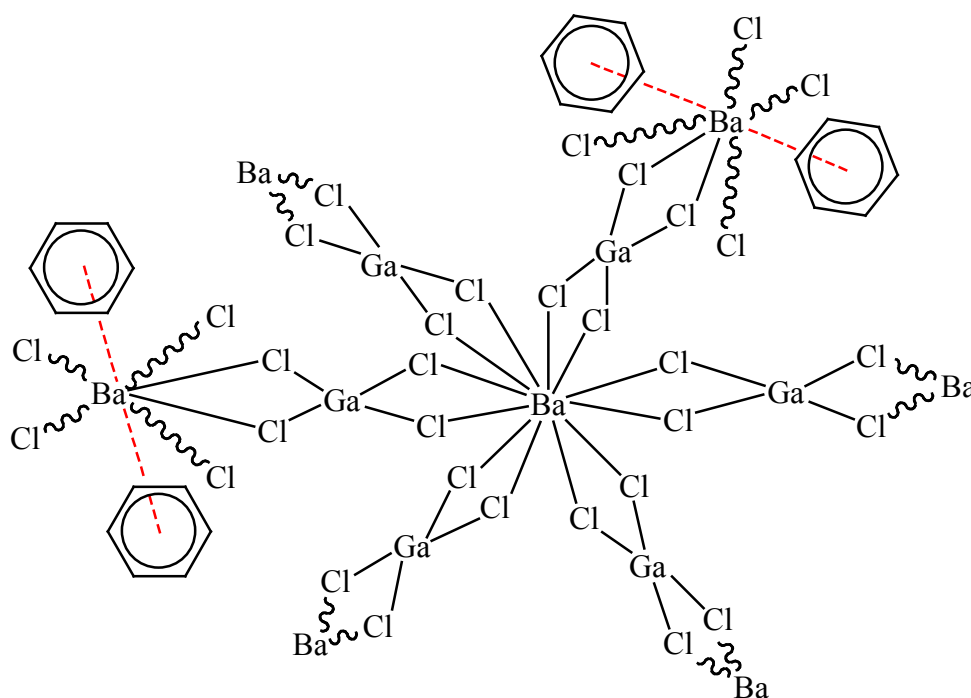


Fig. 3.5: Molecular structure of $[(\text{Ba}\{\text{GaCl}_4\}_2)_3 \cdot 2\text{C}_6\text{H}_6]$.

Chapter 3

The other Ba atom is coordinated to the same GaCl_4^- groups, surrounded by 12 chloride ions in an icosahedral fashion. The Ba-Cl distances range from 3.321(2)–3.440(2) Å in the monoclinic form, and 3.338(2)–3.415(2) Å in the rhombohedral form.

The homoleptic alkaline earth triazenide complex $[\text{Ba}\{\text{N}_3\text{Dmp}(\text{Tph})\}_2]$ [$\text{Dmp} = 2,6\text{-Mes}_2\text{C}_6\text{H}_3$ and $\text{Mes} = 2,4,6\text{-Me}_3\text{C}_6\text{H}_2$; $\text{Tph} = 2\text{-TripC}_6\text{H}_4$ and $\text{Trip} = 2,4,6\text{-}^i\text{Pr}_3\text{C}_6\text{H}_2$] (Fig. 3.6) has been synthesised by the reaction of phenylsilane, bis(pentafluorophenyl)mercury, triazene and excess Ba pieces.⁶¹ The coordination sphere of Ba^{2+} consists of four nitrogen atoms of the two κ^2 -chelated triazenide ligands and π -arene interactions to the two Mes rings of the terphenyl substituents in an η^6 fashion. This gives rise to a distorted octahedral coordination of the Ba centre if we consider the centroid as the binding site.

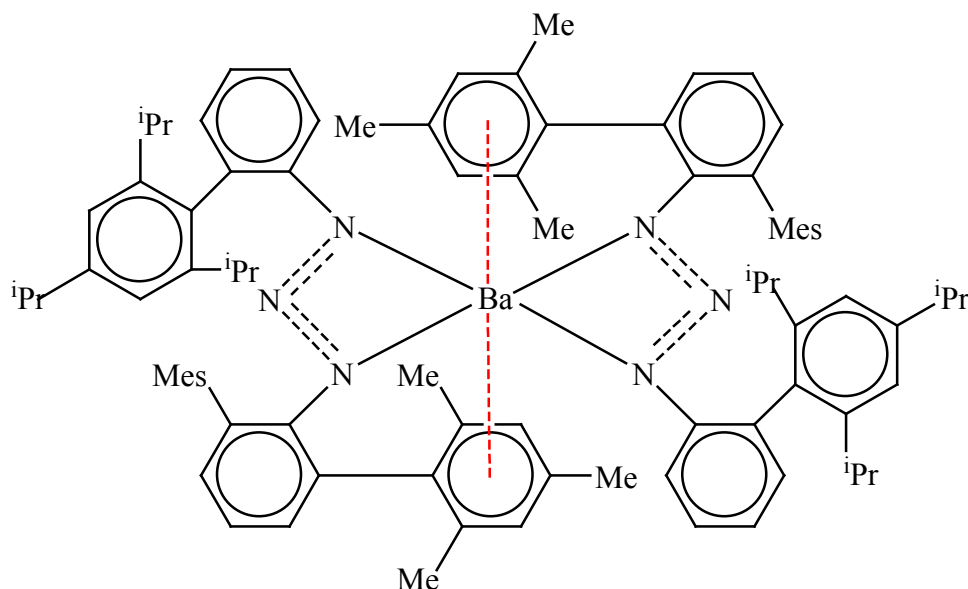


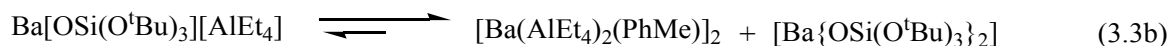
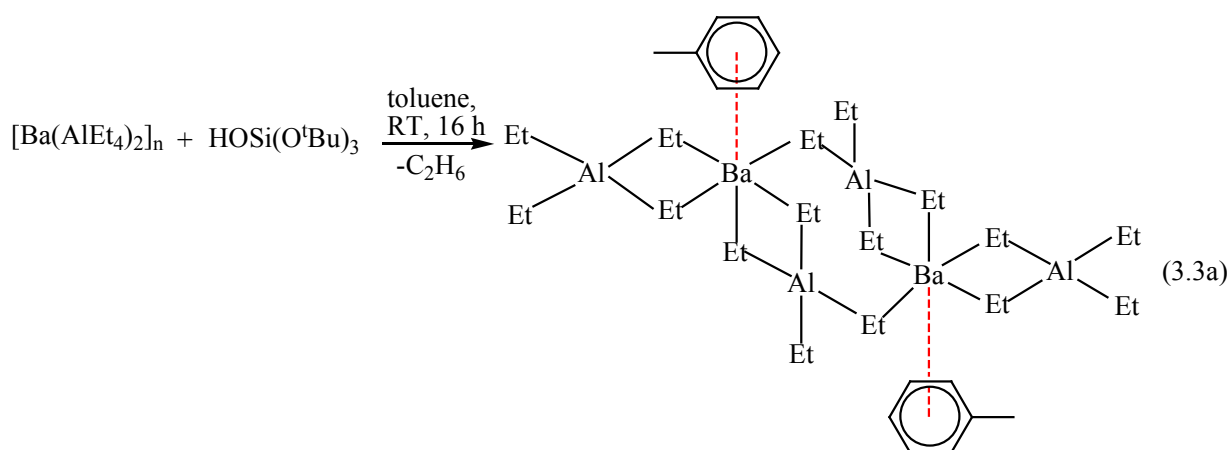
Fig. 3.6: Molecular structure of $[\text{Ba}\{\text{N}_3\text{Dmp}(\text{Tph})\}_2]$, representative of $[\text{Sr}\{\text{N}_3\text{Dmp}(\text{Tph})\}_2]$.

The Ba-C contacts range from 3.312(5)–3.424(5) Å and the Ba-centroid distance is 3.0738(4) Å. The strontium complex $[\text{Sr}\{\text{N}_3\text{Dmp}(\text{Tph})\}_2]$ featuring an analogous structure of barium complex, has also been synthesised by the reaction of phenylsilane, bis(pentafluorophenyl)mercury, triazene and an excess of Sr. However, the Sr- π -arene interactions modes were η^5/η^3 instead of being η^6 . The Sr-C(η^5) distances range from 3.011(4)–3.311(4) Å, and that of Sr-C(η^3) range from 2.980(4)–3.241(4) Å. The Sr-

Chapter 3

Centroid(η^5) and Sr-Centroid(η^3) distances are 2.839 and 2.974 Å, respectively. The geometry of the metal centre of $[\text{Sr}\{\text{N}_3\text{Dmp}(\text{Tph})\}_2]$ can be described as distorted tetrahedral by considering the arene binding sites as one binding site.

The treatment of $[\text{Ba}(\text{AlEt}_4)_2]_n$ with $\text{HOSi}(\text{O}^t\text{Bu})_3$ in toluene resulted in the isolation of the dimeric complex $[\text{Ba}(\text{AlEt}_4)_2(\text{PhMe})]_2$ (Eqn. 3.3a) with κ^2 and $\mu_2:\kappa^2,\eta^1$ coordinating terminal and bridging tetraethylaluminato ligands, respectively.⁶² The existence of a Schlenk equilibrium between $[\text{Ba}\{\text{OSi}(\text{O}^t\text{Bu})_3\}(\text{AlEt}_4)]$, $[\text{Ba}\{\text{OSi}(\text{O}^t\text{Bu})_3\}_2]$ and $[\text{Ba}(\text{AlEt}_4)_2(\text{PhMe})]_2$ (Eqn. 3.3b) was believed and isolated one component of the equilibrium. The average Ba-C(toluene) and Ba-Al distances are 3.535 and 3.311 Å, respectively. An analogous complex $[\text{Ba}(\text{GaEt}_4)_2(\text{PhMe})]_2$ was also isolated by the reaction of $[\text{Ba}(\text{AlEt}_4)_2]_n$ and $\text{GaEt}_3\cdot\text{Et}_2\text{O}$ in toluene and found to be isostructural with $[\text{Ba}(\text{AlEt}_4)_2(\text{PhMe})]_2$ having an average Ba-C(toluene) distance of 3.322 Å.⁶³



The reaction of $[\text{Ba}\{\text{N}(\text{SiHMe}_2)_2\}_2]_n$ with GaMe_3 resulted in the barium oxo complex $[\text{Ba}(\mu_4\text{-O})(\text{GaMe}_3)_2(\text{toluene})]_2$, which features a planar $[\text{Ba}(\mu\text{-O})]_2$ core (Fig. 3.7).⁶⁴ Four GaMe_3 molecules and two η^6 -coordinating toluene molecules shield this Ba_2O_2 moiety. Two GaMe_3 molecules bridge the barium centres by two Ba–CH₃ contacts and one Ga–O bond each. The other two molecules each interact with one barium centre by heterobridged moieties of the type $[\text{Ba}(\mu\text{-CH}_3)(\mu\text{-O})\text{GaMe}_2]$. The average Ba1– and Ba2–centroid distances are 3.010 and 3.013 Å, respectively.

Chapter 3

A dicalcium complex $[\text{Ca}(\text{Dipp-Bian})(\text{thf})]_2$ (Dipp = 2,6-diisopropylphenyl, Bian = acenaphthylene-1,2-diamine) (Fig. 3.8) having two Dipp rings connected to two calcium centres in an η^6 fashion has been reported.⁶⁵ The Ca-C(arene) contacts range from 2.7518(18)-3.0341(19) Å with a Ca-centroid contact being 2.5345(8) Å.

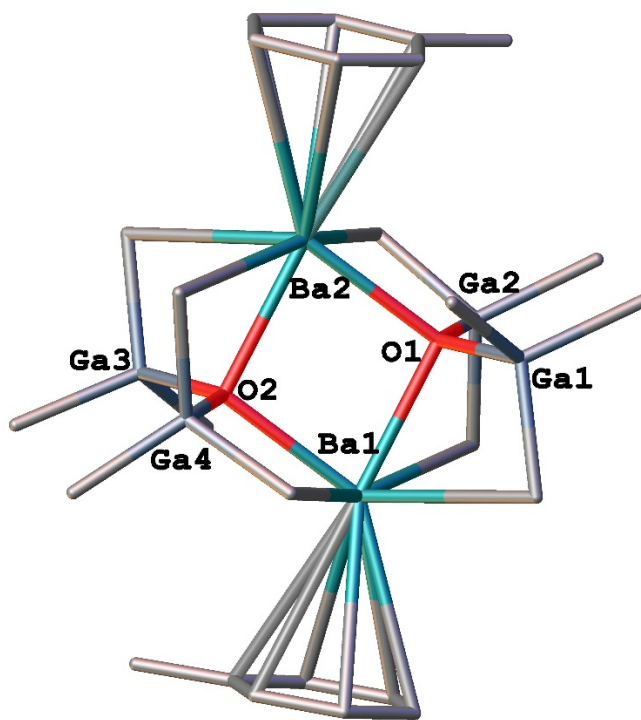


Fig. 3.7: Molecular structure of $[\text{Ba}(\mu_4\text{-O})(\text{GaMe}_3)_2(\text{toluene})]_2$.

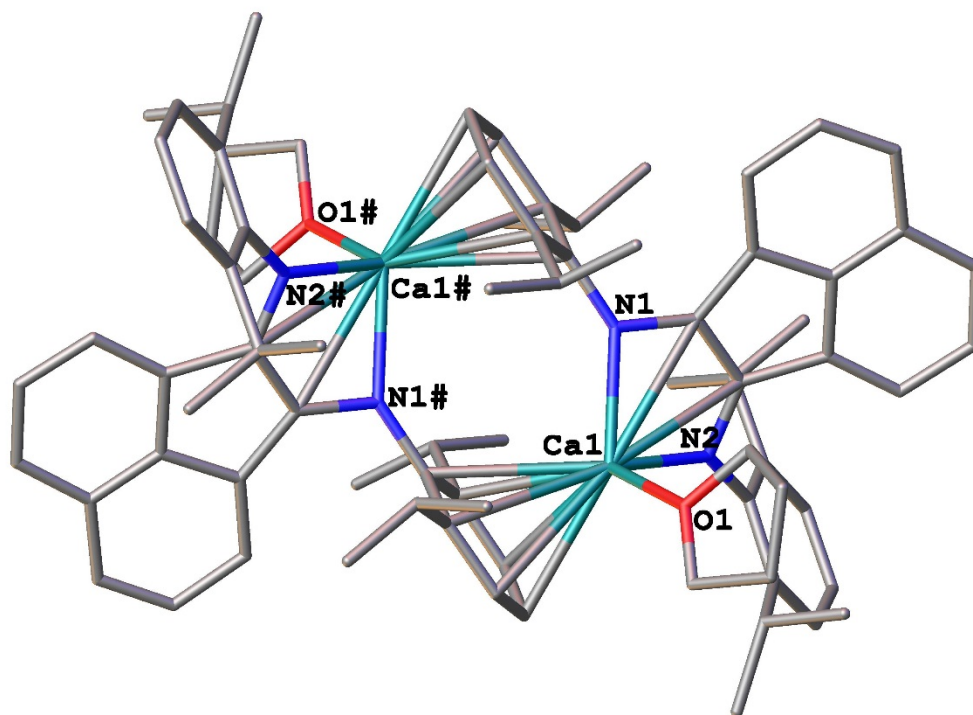
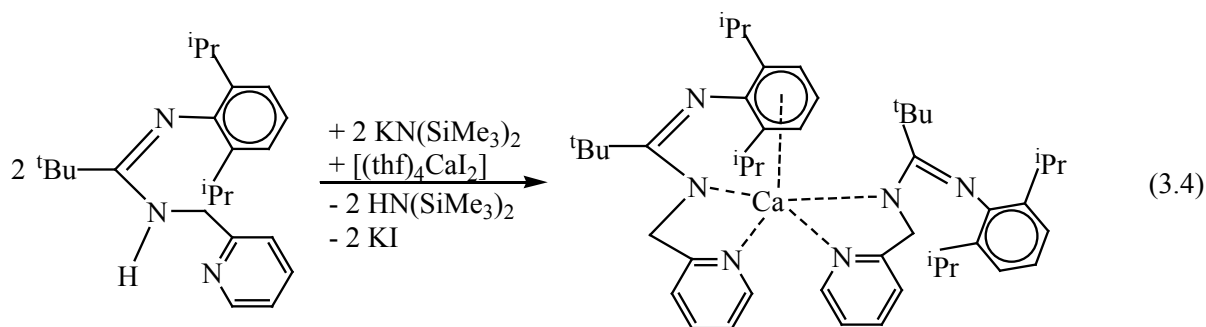


Fig. 3.8: Molecular structure of $[\text{Ca}(\text{Dipp-Bian})(\text{thf})_2]$.

The reaction of $\text{Dipp-N}=\text{C}(\text{tBu})\text{N}(\text{H})\text{CH}_2\text{-Py}$ with CaI_2 and $\text{KN}(\text{SiMe}_3)_2$ in THF resulted in the formation of $[(\text{thf})\text{Ca}\{(\text{Dipp-N})\text{C}(\text{tBu})\text{NCH}_2\text{-Py}\}_2]$ (Eqn. 3.4).⁶⁶ This structure features an intramolecular calcium- π interaction with an aryl group of the ligand. The Ca–C(arene) distances fall in the range from 2.764(2)–3.135(2) Å (average 2.958 Å) with a Ca–centroid distance of 2.609 Å. An analogous complex $[\text{Ca}\{(\text{Dipp-N})\text{C}(\text{tBu})\text{-N-Qu}\}_2]$ (Qu = 8-quinolyl) has also been prepared from the treatment of $\text{Dipp-N}=\text{C}(\text{tBu})\text{N}(\text{H})\text{CH}_2\text{-Qu}$ with $[(\text{thf})_2\text{Ca}\{\text{N}(\text{SiMe}_3)_2\}_2]$ in THF.⁶⁷ The Ca–C(arene) distances span the range from 2.805(2)–3.145(2) Å (average 2.958 Å) with a Ca–centroid distance of 2.662 Å.



Chapter 3

A solution of (Dipp-N=C(^tBu)-N(H)-C₂H₄-Py) and [(thf)₂Ae{N(SiMe₃)₂}₂] (Ae = Ca, Sr) in toluene, stirred at room temperature gave the heteroleptic complexes [{(Me₃Si)₂N} Ae {Dipp-N=C(^tBu)-N-C₂H₄-Py}] (Ae = Ca, Sr) (Fig. 3.9).⁶⁸ The Ca-π interactions span the range from 2.750(3)–3.048(3) Å, relatively smaller than the Sr-π interactions (2.885(3)–3.098(3) Å) leading to distances between the aryl centroid and calcium or strontium atoms of 2.554 and 2.680 Å, respectively.

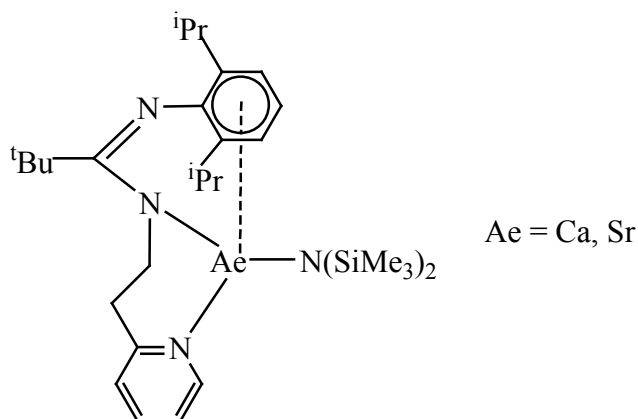


Fig. 3.9: Molecular structure of [{(Me₃Si)₂N} Ae {Dipp-N=C(^tBu)-N-C₂H₄-Py}].

The homoleptic bis(guanidinate) complex of barium [Ba(MesN{C(NCy₂)})₂NMes]₂ (Mes = 2,4,6-Me₃C₆H₂, Cy = cyclohexyl) has been synthesised by the redox transmetallation/ligand exchange reactions of Ba, diphenylmercury and the guanidine MesN{C(NCy₂)})₂N(H)Mes in THF (Fig 3.10).⁶⁹ This is the first example of monomeric barium complex of the NCN ligand family, having the structure stabilised by barium-arene interactions in the solid state. The barium centre is coordinated by two guanidinate ligands through one amide linkage and Ba-π interactions between the metal centre and the nitrogen-bound mesityl substituents. The Ba-C distances between the metal centre and the *ipso*-carbon atoms of the nitrogen-bound mesityl group on each guanidinate ligand are 3.256(2) and 3.157(2) Å. The Ba-C(η⁶) contacts to the other nitrogen-bound mesityl group fall in range from 3.138(2)–3.303(3) and 3.163(2)–3.337(3) Å.

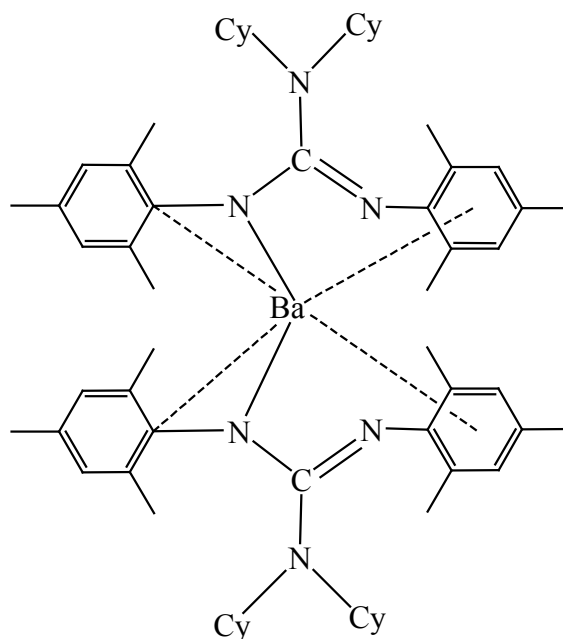


Fig. 3.10: Molecular structure of $[\text{Ba}(\text{MesN}\{\text{C}(\text{NCy}_2)\}\text{NMe})_2]$.

Recently, an unusual solvent-free calcium complex $[\text{AdAm}^{\text{Dipp}}\text{CaN}(\text{SiMe}_3)_2]$ (Ad = 1-adamantyl, Am = amidinate and Dipp = 2,6-diisopropylphenyl) has been reported, in which the coordination sphere of calcium is achieved not only by an η^6 aryl coordination but also by a SiMe-Ca agostic interaction (Fig.3.11).⁷⁰ The Ca-C(η^6) distances range 2.745(2)-2.925(2) and the SiMe-Ca agostic interaction is 2.823(2) Å. The centrosymmetric dimer $[(\text{AdAmDippCaH})_2]$ with bridging hydrides (Fig 3.12) was also reported. The Ca-C(η^6) distances range from 2.739(2)–2.894(2) Å, and compare well with $[\text{AdAm}^{\text{Dipp}}\text{CaN}(\text{SiMe}_3)_2]$.

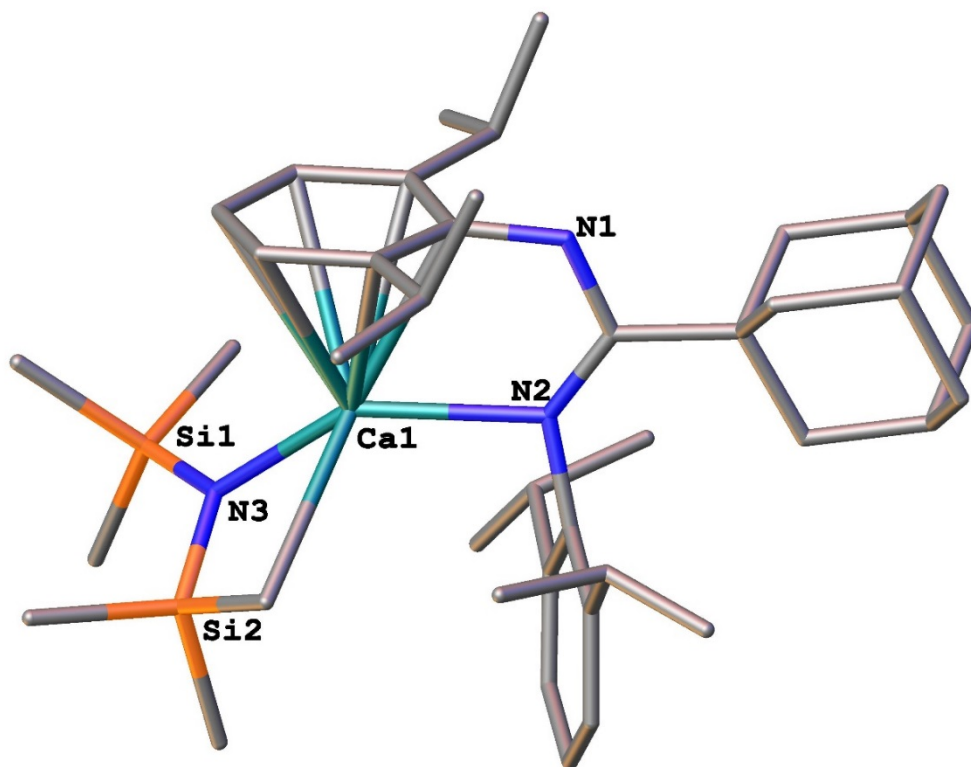


Fig. 3.11: Molecular structure of $[\text{AdAm}^{\text{Dipp}}\text{CaN}(\text{SiMe}_3)_2]$.

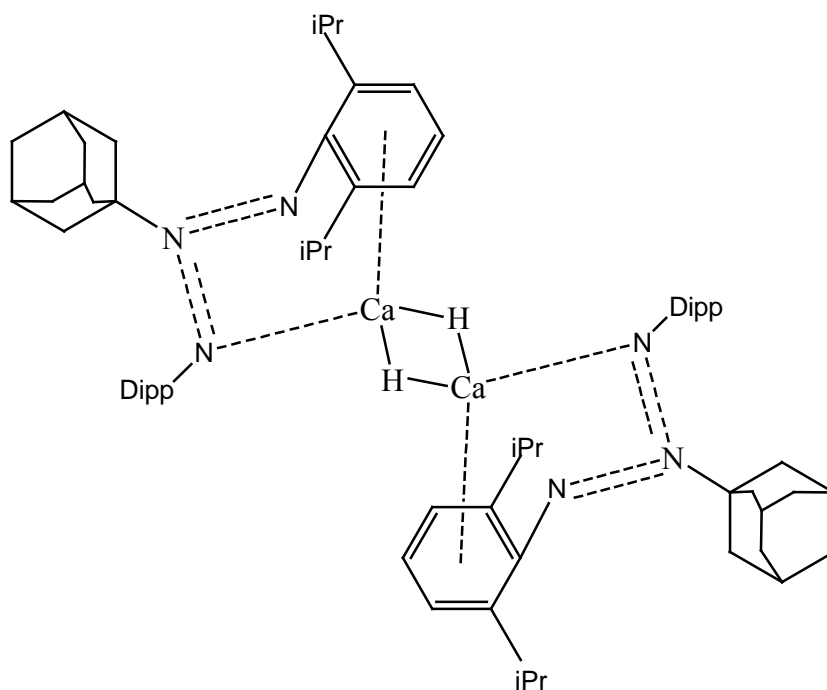


Fig. 3.12: Molecular structure of $[(\text{AdAmDippCaH})_2]$.

3.2 Research Plan

The chemistry of alkaline earth metals is dominated by the oxidation state +2, and they are known as redox-inactive metals.¹¹⁸ Divalent cations of the heavy alkaline earths Ca^{2+} , Sr^{2+} and Ba^{2+} are large, polarisable, and electrophilic with the effective ionic radii of 1.12, 1.26, and 1.42 Å (C. N. = 8), respectively.¹¹⁹ These alkaline earths metals are similar to the divalent Ln metals Sm, Eu and Yb with ionic radii of 1.27, 1.25 and 1.14 Å (C. N. = 8), however, these are redox active. They form d^0 complexes featuring ionic, non-directional bonding without any susceptibility for π -bonding due to the inability to convey $d-\pi^*$ back-donation. Nevertheless, in recent years several compound classes with alkaline earth metals having π -bonding were investigated.

There are several reasons for the interest in arene complexes of alkaline earth elements. (i) Depending on the softness and hardness of the metal cations, the metal cation- π system interactions play an important role in chemistry, pharmacy and biology.¹²⁰⁻¹²³ Calcium cations are considered as quite hard Lewis acids, and the calcium- π interactions have great importance in medicinal and pharmaceutical chemistry.^{124, 125} (ii) In terms of catalysis, arenes are easier to substitute by incoming substrates compared to the negatively charged cyclopentadienyl ligands. (iii) By varying the nature of the ancillary ligands, a variation in the hapticity of the arene ligands could be generated. (iv) These compounds are potential precursors for catalysts such as in hydrogenation and polymerisation reactions. (v) The zero-oxidation-state metal arene complexes can generate the metal in an active form by appropriate displacement reactions, and they are good candidates for the metal organic chemical vapour deposition (MOCVD).¹¹

Computational studies have been done by several groups for the interactions between divalent Ae^{2+} cations and neutral arenes.¹²⁶⁻¹³⁰ However, the Ae-arene complexes remain little explored, and no halogenoaluminate alkaline earth arene complexes have been reported till now. Therefore, this chapter expects to synthesise and characterise a series of iodoaluminate complexes involving Ae- π (arene) interactions. Iodoaluminate complexes of heavy alkaline earths (Ca, Sr and Ba) featuring both half-sandwich and sandwich fashions are synthesised by the deiodination of metal iodide by AlI_3 in alkyl substituted aromatic hydrocarbons of varying steric bulk such as toluene and mesitylene.

Chapter 3

The IR spectra of the complexes have been recorded in Nujol mulls between sodium chloride plates. All the spectra exhibit a similar pattern comprising the presence of C–H aromatic stretches of the coordinated solvent molecule at about 3000 cm^{-1} and sp^3 C-H stretching at around 2900 cm^{-1} comparable to the analogous lanthanoid complexes described in chapter 2.

Microanalysis was performed to determine the percentages of carbon and hydrogen in the complexes and thereby indicating purity, and complexometric titrations using EDTA were performed to determine the metal percentages. The metal and carbon, hydrogen percentages match the compositions found by X-ray diffraction for the complexes $[\text{Ca}(\eta^6\text{-C}_6\text{H}_5\text{Me})(\text{AlI}_4)_2]_{0.5}[\text{Ca}(\eta^6\text{-C}_6\text{H}_5\text{Me})(\text{AlI}_4)_2]_n$, $[\text{Sr}(\eta^6\text{-MeC}_6\text{H}_5)(\text{AlI}_4)_2]_n\cdot\text{PhMe}$ and $[\text{Ba}(\eta^4\text{-C}_6\text{H}_5\text{Me})_2(\text{AlI}_4)_2]$. However, in the complex $[\text{Ca}(\eta^6\text{-Me}_3\text{C}_3\text{H}_5)(\text{AlI}_4)_2]_n$, the carbon percentage was lower than expected. It was reported to get consistent lower carbon in alkaline earth complexes,¹³¹ and the reason may be due to the reaction of the complexes with aluminium crucible used in analysis.¹³² On the other hand, the carbon and hydrogen percentages in $[\text{Sr}(\eta^6\text{-Me}_3\text{C}_3\text{H}_5)(\text{AlI}_4)_2]_n$ were higher than the expected values. This may be due to the residual toluene (ca. 0.5 mole) on the surface of the crystals.

The complexes were insoluble in most non-polar solvents and decomposed in polar organic solvents such as thf. Due to the insolubility of the complexes in common organic solvents, no NMR experiments could be performed.

3.3.2 X-ray Crystal Structures

3.3.2.1 Iodoaluminate Ae(II) complexes in toluene

X-ray crystallography shows $[\text{Ca}(\eta^6\text{-C}_6\text{H}_5\text{Me})(\text{AlI}_4)_2]_{0.5}[\text{Ca}(\eta^6\text{-C}_6\text{H}_5\text{Me})(\text{AlI}_4)_2]_n$ (**1**) crystallises with one and half molecules in the asymmetric unit and the overall structure is polymeric. The half molecule grows to a monomeric structure of $[\text{Ca}(\eta^6\text{-C}_6\text{H}_5\text{Me})(\text{AlI}_4)_2]$, and the other molecule expands as a single strand polymeric structure. (Fig. 3.13a). The coordination sphere around the Ca^{2+} ion in both the monomer and polymer is surrounded by five iodides and an axial arene in an η^6 fashion leading to an octahedral arrangement, if the centroid of the arene is considered a single coordination site. To the best of our knowledge, **1** is the first structure of this kind among the alkaline earths, and is isostructural with the ytterbium complex $[\text{Yb}(\eta^6\text{-MeC}_6\text{H}_5)(\text{AlI}_4)_2]_n$, both having the coordination number of eight around the metal centres. This is mainly due to the hard ion characteristics of Yb^{2+} and Ca^{2+} , giving ionic compounds, and their almost identical size (1.14 Å Yb^{2+} and 1.12 Å for Ca^{2+})

133

The Ca-C bond lengths (polymer) span the range from 2.89(3)-3.09(2) Å (average 2.9650 Å) in **1** whereas, they are 3.072(3)-3.515(3) and 3.014(4)-3.403(4) Å in the calix[4]arene complex $[p\text{-}^t\text{Bu-calix[4]}(\text{OC}_5\text{H}_9)_2(\text{O})_2\text{-Ca}_2\text{I}_2\cdot(\text{MeCN})_2]^{54}$ and 3.015(7)-3.132(7) Å in the calcium triazene complex $[\text{Ca}(\text{C}_6\text{F}_5)(\text{N}_3\text{ArAr}')(\text{thf})]$ ($\text{Ar} = 2,4,6\text{-Me}_3$ and $\text{Ar}' = 2,4,6\text{-}^i\text{Pr}_3$),⁵⁵ are significantly elongated compared to **1**. However, these interactions are considerably stronger in the complexes $[\text{ICa}(\mu\text{-}\eta^1, \eta^6\text{-Mes}_2\text{Cu})_4]^{58}$, $[\text{Ca}(\text{Dipp-Bian})(\text{thf})_2]^{65}$, $[(\text{thf})\text{Ca}\{(\text{Dipp-N})\text{C}(^t\text{Bu})\text{NCH}_2\text{-Py}\}_2]^{66}$, $[\text{Ca}\{(\text{Dipp-N})\text{C}(^t\text{Bu})\text{-N-Qu}\}_2]^{67}$ $[\{(\text{Me}_3\text{Si})_2\text{N}\}\text{-Ca}\{\text{Dipp-N}=\text{C}(^t\text{Bu})\text{-N-C}_2\text{H}_4\text{-Py}\}]^{68}$ $[\text{AdAm}^{\text{Dipp}}\text{CaN}(\text{SiMe}_3)_2]^{70}$, $[(\text{AdAmDippCaH})_2]^{70}$, in which the Ca-C contacts range from 2.792(5)-2.866(6), 2.7518(18)-3.0341(19), 2.764(2)-3.135(2), 2.805(2)-3.145(2), 2.750(3)-3.048(3), 2.745(2) to 2.925(2) and 2.739(2)-2.894(2) Å, respectively. Complex **1** has the Ca-centroid distance of 2.6164(5) Å, and in comparison with the above literature complexes, the Ca-centroid distances are in accord with the Ca-C distances.

Chapter 3

When compared with Ca-C(Cp) distances, where the aromatic Cp is charged, the distances to the neutral arenes are much longer as expected. For example, the average Ca-C(Cp) distances in the cyclopentadienyl complexes are 2.65(4) Å in $[\text{Cp}(\text{SiMe}_3)_3\text{Ca}(\mu\text{-I})(\text{thf})_2]^{79}$, 2.70(1) Å in $[(\text{Me}_5\text{C}_5\text{Ca}(\mu\text{-Me}_3\text{Al.THF}))_2]^{80}$, 2.67 (1) Å in $[(\text{Me}_5\text{C}_5)\text{Ca}(\mu\text{-I})(\text{THF})_2]^{82}$, 2.684(4) Å in $[(\text{C}_5\text{Me}_5)\text{Ca}(\text{OPPh}_3)_3]^+\text{I}^-^{83}$, 2.677(4) Å $[(\text{C}_5(\text{tBu})_3\text{H}_2)_2]\text{CaI}(\text{THF})_2]^{86}$ and 2.63(2) Å in $[\text{C}_5(\text{tBu})_3\text{H}_2]_2\text{CaI}(\text{THF})_2]^{86}$. Furthermore, the Ca-Cp(Centroid) contacts are 2.36(2) Å in $[\text{Cp}(\text{SiMe}_3)_3]\text{Ca}(\mu\text{-I})(\text{thf})_2]^{79}$, 2.429 and 2.423 Å in $[\text{Ca}(\text{C}_5\text{Ph}_4\text{H})_2(\text{thf})]^{91}$, 2.39 Å in $[(\text{C}_5(\text{tBu})_3\text{H}_2)_2]\text{CaI}(\text{THF})_2]^{86}$, 2.34 Å in $[\text{C}_5(\text{tBu})_3\text{H}_2]_2\text{-CaI}(\text{THF})_2]^{86}$ and 2.381(3) Å in *trans*- $\text{Ph}_2(\text{CH}_3)_2\text{C}_2(\eta^5\text{-C}_5\text{H}_4)_2\text{Ca}(\text{DME})^{90}$. Comparing the literature values, it is obvious that both the average Ca-C contacts and the Ca-Centroid contacts in cyclopentadienyl complexes are significantly shorter compared to **1**. The Ca-C interactions are expectedly stronger in charged cyclopentadienyl ligands than that of the charge neutral arene ligands studied here.

Chapter 3

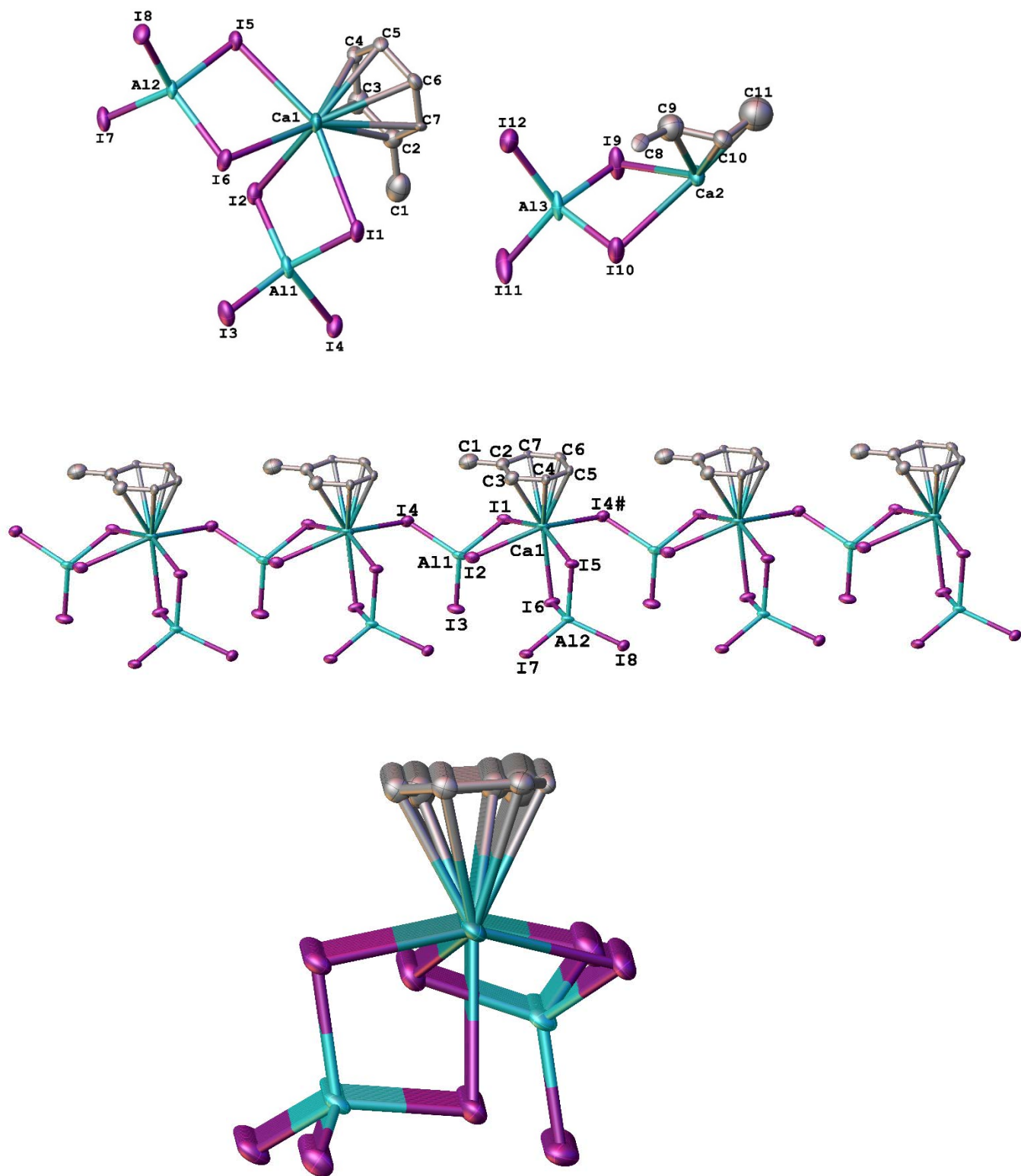


Fig. 3.13a: One and half molecules in the asymmetric unit (top), the one dimensional extended framework for $[\text{Ca}(\eta^6\text{-MeC}_6\text{H}_5)(\text{AlI}_4)_2]_{1.5}$ (1) (middle) and single stranded polymer with two AlI_4^- units (bottom). Hydrogen atoms have been omitted for clarity.

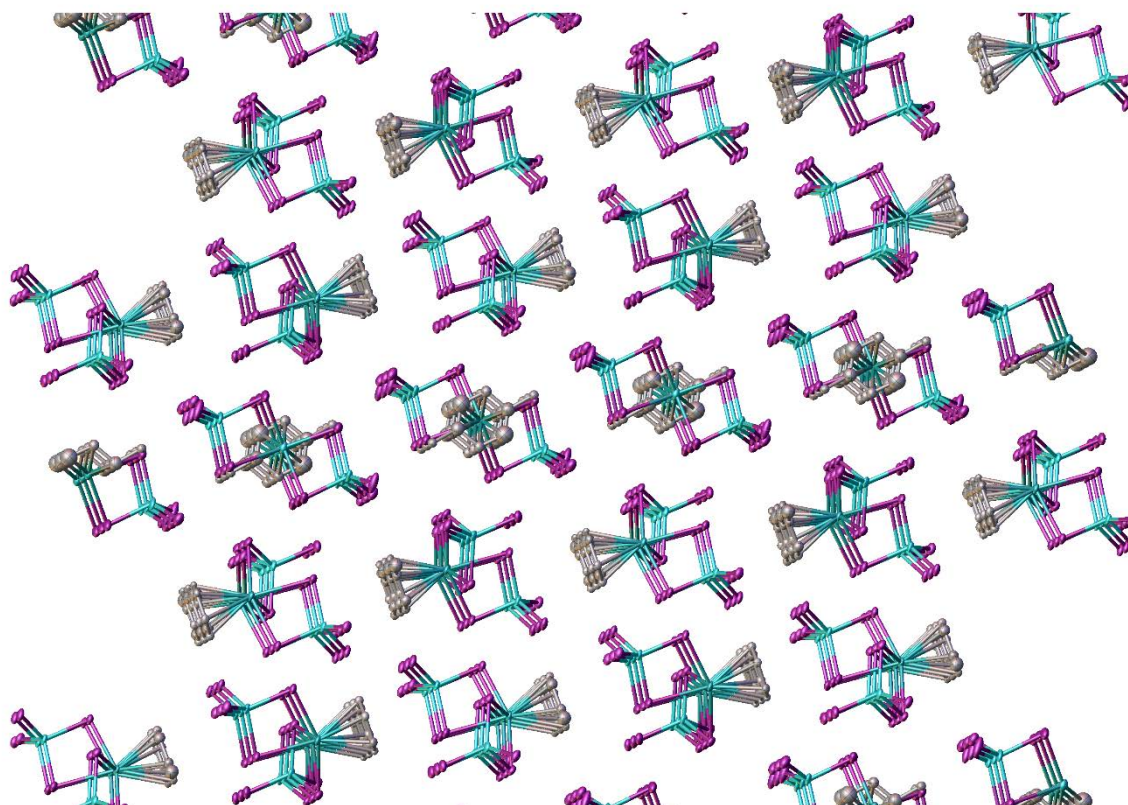


Fig. 3.13b: Packing diagram of **1**. The monomer units are filling up the voids by taking positions in between the polymeric counterparts.

In complex **1**, the Ca-I bond distances range from 3.126(7)-3.316(7) Å with the axial Ca-I contact of 3.316(7) Å. In the ytterbium analogue $[\text{Yb}(\eta^6\text{-MeC}_6\text{H}_5)(\text{AlI}_4)_2]_n \cdot 1/2\text{PhMe}$, the Yb-I contacts are slightly longer and range from 3.1442(10)-3.2917(10) Å, and the axial Yb-I contact is 3.2917(10) (chapter 2). In accordance with the slight differences of the ionic radii of 8-coordinate Ca^{2+} and Yb^{2+} (1.12 and 1.14 Å, respectively)¹³³, interestingly the axial M-I bond is the longest in both the Ca and Yb complexes. The I-Ca-I bond angles range from 78.06(16)-155.9(2)° are comparable to the I-Yb-I angles of 77.19(4) to 155.60(2)°. The I-Al-I angles are close to the idealised tetrahedral angles.

Complex $[\text{Sr}(\eta^6\text{-MeC}_6\text{H}_5)(\text{AlI}_4)_2]_n \cdot \text{PhMe}$ (**2**) (Fig. 3.14a) crystallises in the orthorhombic space group $P2_12_12_1$ (No. 19) with only one molecule in the asymmetric unit. The X-ray crystal structure of complex **2** comprises of a nine coordinate Sr^{2+} centre, which is bound to six (I7 and I8 bridge between monomer units) iodine atoms of the AlI_4^- moieties with a toluene molecule at an axial position, and I6 occupies the other axial position. The

Chapter 3

coordination polyhedron surrounding the Sr²⁺ centre is a distorted pentagonal bipyramid if the centroid of the aromatic ligand is considered as a sole point of coordination, but with a formal coordination number of nine, and is isostructural with its europium analogue [Eu(η^6 -MeC₆H₅)(AlI₄)₂]_n.PhMe (chapter 2).

In complex **2**, the Sr-C(toluene) distances fall in the range from 2.989(12)-3.129(9) Å, which are considerably shorter than that of the Sr-C(mesityl) and Sr-C(triisopropylphenyl) distances in triazene complex [Sr(C₆F₅)(N₃ArAr')] (Ar = 2,4,6-Me₃ and Ar' = 2,4,6-ⁱPr₃)⁵⁵ (3.165–3.306 and 3.078–3.283 Å, respectively). The Sr-C(η^5) distances in [Sr{N₃Dmp(Tph)}₂]⁶¹ [Dmp = 2,6-Mes₂C₆H₃ and Mes = 2,4,6-Me₃C₆H₂; Tph = 2-TripC₆H₄ and Trip = 2,4,6-ⁱPr₃C₆H₂] range from 3.011(4)-3.311(4) Å and are somewhat elongated than those in **2**. Complex [{(Me₃Si)₂N}Sr{Dipp-N=C(^tBu)-N-C₂H₄-Py}]⁶⁸ has significantly shorter Sr-C interactions (2.885(3)–3.098(3) Å) compared to **2**. The Sr-centroid contact in **2** is 2.717(3) Å, significantly shorter than 2.839 Å in [Sr{N₃Dmp(Tph)}₂]⁶¹; however, elongated compared with 2.680 Å in [{(Me₃Si)₂N}Sr{Dipp-N=C(^tBu)-N-C₂H₄-Py}]⁶⁸.

The average Sr-C(Cp) distances in [(Cp(SiMe₃)₃)SrI(thf)₂]₂⁷⁹, (Cp^{TRP})₂Sr(thf) (TRP = 1,2,4-triisopropyl)¹³⁴ and [Sr(thf)₃(η^5 -C₅H₄PPh₂)₂Pt(Me)₂].1.5 thf]⁹³ are 2.87, 2.838 and 2.87(1) Å, respectively, and are significantly shorter than the average Sr-C(toluene) length 3.0497 Å in **2**. Furthermore, the Sr-Cp(centroid) contact in [(Cp(SiMe₃)₃)SrI(thf)₂]₂⁷⁹ 2.604(7) is also shorter than that of the Sr-centroid contact in **2**. The interactions between the negatively charged Cp ligands and strontium are stronger than the neutral arene-Sr interactions as expected.

Complex **2** has Sr-I bond distances ranging from 3.3628(11)-3.6314(12) Å and are comparable to those in the europium complex [Eu(η^6 -MeC₆H₅)(AlI₄)₂]_n.PhMe, where the Eu-I contacts range from 3.3683(14) to 3.6062(14) Å (chapter 2). As the ionic radii of 9-coordinate Sr²⁺ and Eu²⁺ are very similar (1.31 and 1.30 Å, respectively)¹³³, the Sr-I and Eu-I distances in **2** and [Eu(η^6 -MeC₆H₅)(AlI₄)₂]_n.PhMe are expected to be equivalent. The I-Sr-I bond angles range from 68.11(2)-143.92(3)° and are comparable to the I-Eu-I angles of 68.56(3)-142.61(3)°. The I-Al-I angles are close to ideal for tetrahedral geometry.

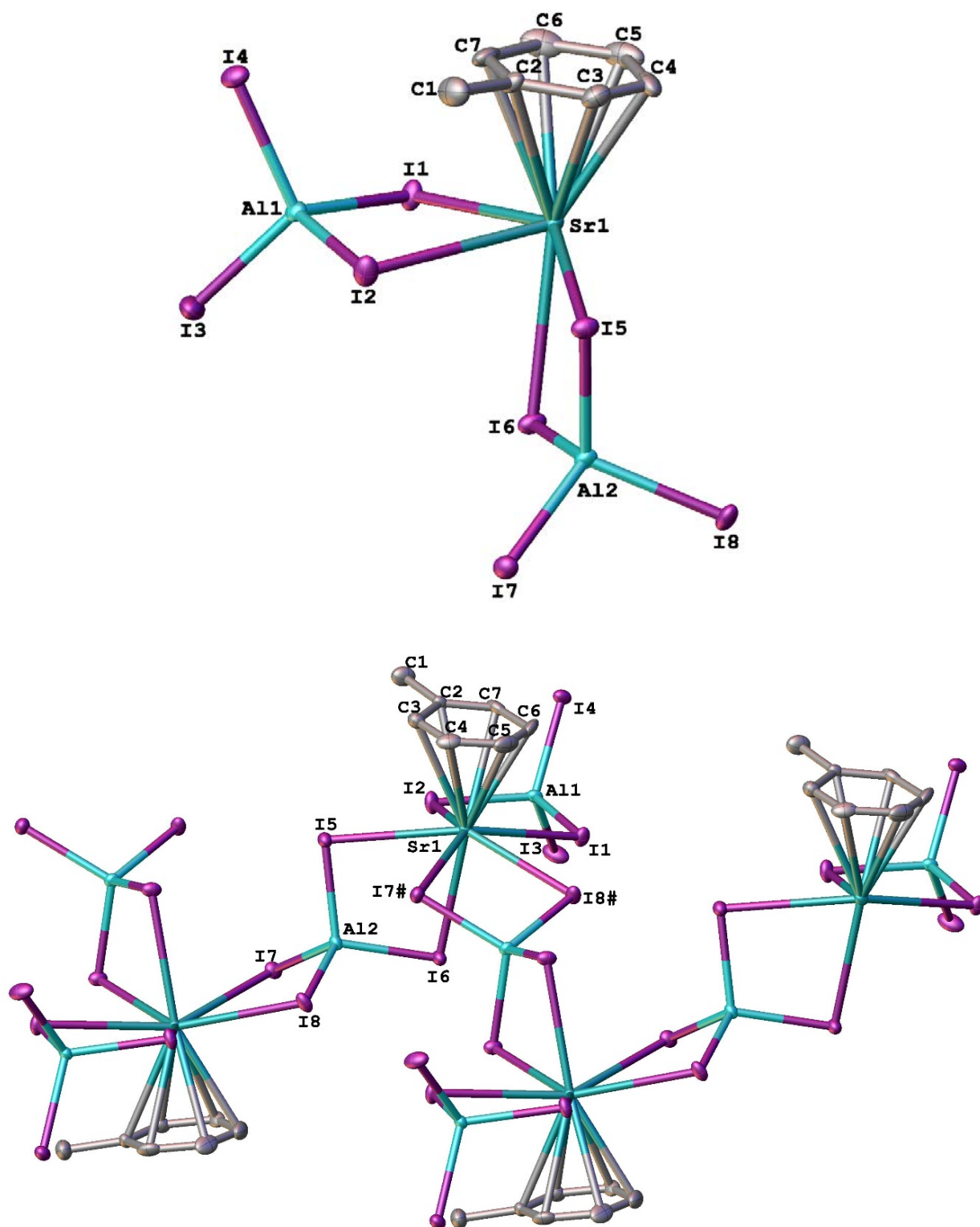


Fig. 3.14a: A monomeric repeat unit (top) and the one dimensional extended zigzag framework for $[\text{Sr}(\eta^6\text{-MeC}_6\text{H}_5)(\text{AlI}_4)_2]_n \cdot \text{PhMe}$ (**2**) (bottom). Hydrogen atoms and the solvent of crystallisation (toluene) have been omitted for clarity.

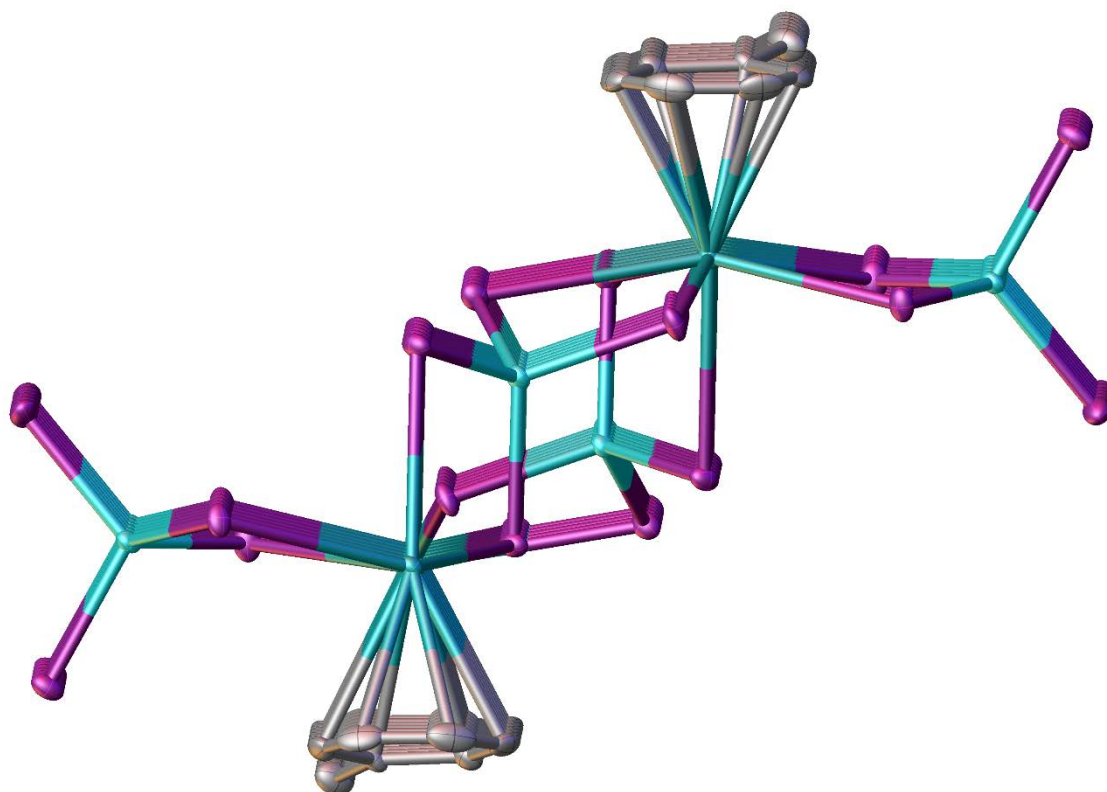


Fig. 3.14b: The Sr-arene double stranded polymer with two bridging AlI_4^- units and two terminal AlI_4^- units for **2**. Hydrogen atoms and the solvent of crystallisation (toluene) have been omitted for clarity.

The X-ray crystal structure of $[\text{Ba}(\eta^4\text{-C}_6\text{H}_5\text{Me})_2(\text{AlI}_4)_2]$ (**3**) (Fig. 3.15) shows an eight coordinate species where the Ba^{2+} centre is sandwiched between a pair of toluene molecules both in an η^4 fashion, as well as with four iodide atoms bridging to two Al centres. This is the first ever-reported sandwich complex of barium having a distorted octahedral arrangement. There is only one molecule in the asymmetric unit.

The Ba-C contacts range from 3.314(9)–3.435(9) Å (average 3.333 Å) with a Ba-centroid contact for both arenes of 3.087(4) Å. Significantly elongated Ba-C distances are available in the literature compared with **3** e.g. $[\text{Ba}(\eta^6\text{-C}_6\text{H}_5\text{Me})(\text{Sn}_3(\text{PSi}^i\text{Bu}_3)_4)]^{52}$ (3.36–3.48 Å), triazene complex $[\text{Ba}(\text{C}_6\text{F}_5)(\text{N}_3\text{ArAr}')]^55$ (Ar = 2,4,6-Me₃ and Ar' = 2,4,6-ⁱPr₃) (Ba-C(mesityl) distances 3.327–3.430 Å and Ba-C(triisopropylphenyl) 3.286–3.406 Å). However, the values for **3** are comparable with $[(\text{Ba}\{\text{GaCl}_4\}_2)_3 \cdot 2\text{C}_6\text{H}_6]^{60}$ (3.277(7)–3.331(11) and 3.278(10)–3.308(9) Å), $[\text{Ba}\{\text{N}_3\text{Dmp}(\text{Tph})\}_2]^{61}$ (3.312(5)–3.424(5) Å) and

Chapter 3

[Ba(MesN{C(NC_y2)}NMe_s)₂]⁶⁹ (3.138(2)–3.303(3) and 3.163(2)–3.337(3) Å). The Ba-centroid contact in [Ba{N₃Dmp(Tph)}₂]⁶¹ is 3.0738(4) Å and the Ba1– and Ba2–centroid distances in [Ba(μ₄-O)(GaMe₃)₂(toluene)]⁶⁴ are 3.010 and 3.013 Å, respectively. The Ba-centroid distances for the literature compounds compare well with the complex **2**.

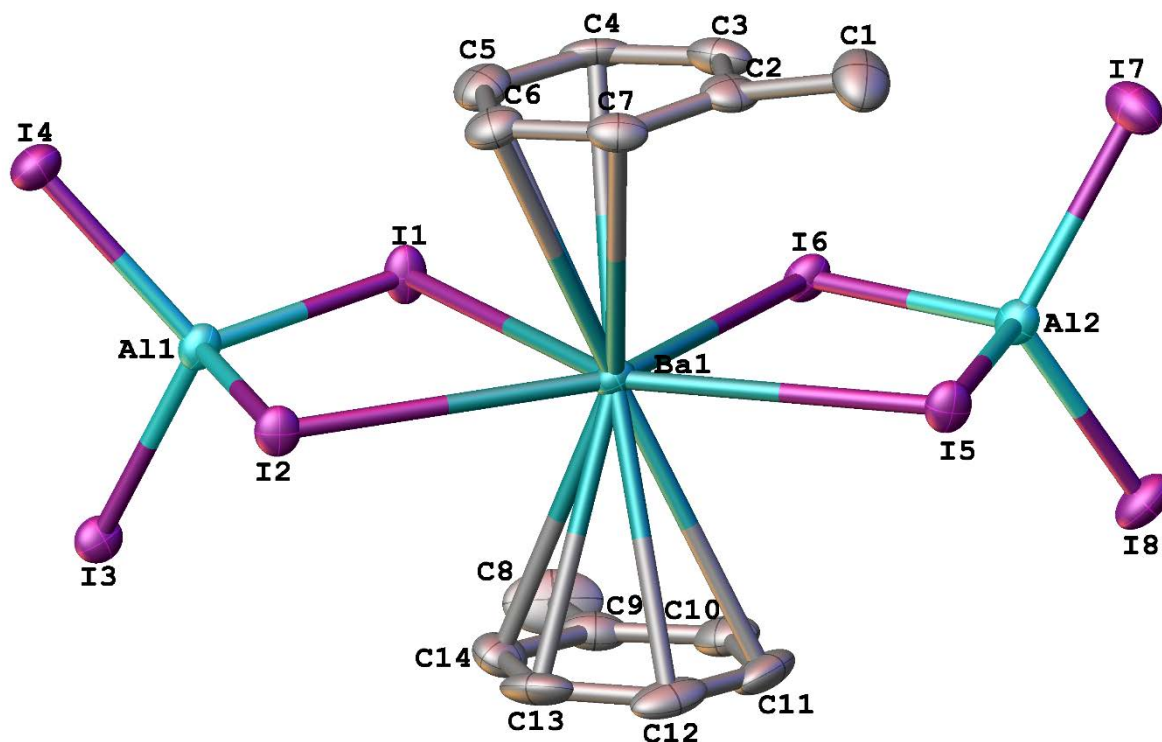


Fig. 3.15: Molecular structure of Ba(η^4 -C₆H₅Me)₂(AlI₄)₂ (**3**). Hydrogen atoms have been omitted for clarity.

The Ba-centroid(Cp) contact in the cyclopentadienyl complex [{(C₅H₂R₃-1,2,4)BaI(THF)₂}_∞] (R = CMe₃) is 2.762 Å and that of 2.72 and 2.73 Å for the two barium centres in [{(C₅HR₄)BaI(THF)₂}₂] (R = CHMe₂).⁷⁸ [(C₅SiMe₃)₃H₂)BaI(thf)₂].1/2C₇H₈}_∞ has the Ba-centroid(Cp) distance of 2.76(1) Å.⁷⁹ Due to the strong interactions between the negatively charged cyclopentadienyl rings and barium centre, the Ba-centroid(Cp) contacts are significantly shorter, as expected compared to the Ba-centroid(toluene) contacts in **3** where the arene is uncharged.

Chapter 3

In complex **3**, the Ba-I contacts range from 3.5071(9)-3.5896(11) Å (average 3.544 Å) and are comparable (considering the ionic radii of metals¹³³) to the corresponding samarium and europium complexes, where the average Ln-I contacts are 3.4455 and 3.4529 Å, respectively (chapter 2). The Ba-I distances in the cyclopentadienyl complexes $\{[(C_5SiMe_3)_3H_2]BaI(thf)_2\} \cdot 1/2C_7H_8\}_\infty$ ⁷⁹ and $[\{(C_5H_2R_{3-1,2,4})BaI(THF)_2\}_\infty]$ ⁷⁸ range from 3.390(1)-3.475(2) and 3.4457(5)-3.4466(6) Å, respectively, slightly shorter than those in **3**. The I-Ba-I angles range from 69.718(18)-147.52(2)° are comparable to the I-Sm-I angles of 68.30(3) to 143.20(3)°. The I-Al-I angles are close to ideal for tetrahedral geometry.

The average Ae-C distances as well as the Ae-C(centroid) distances in the iodoaluminate alkaline earth complexes show a gradual increase (Fig. 3.16a and 3.16b) from calcium to barium due to the increase of ionic radii.

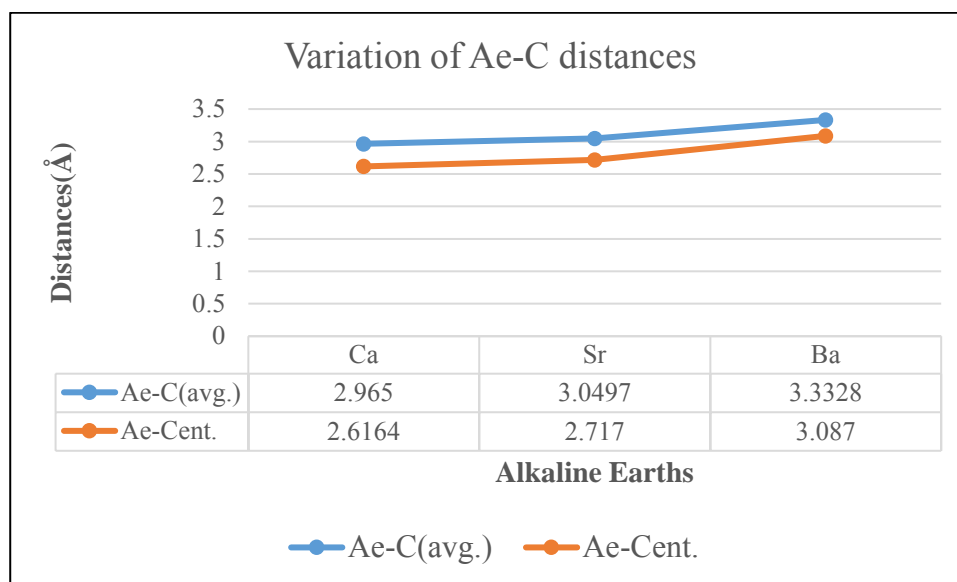


Fig. 3.16a: Changes of the metal-arene distances in the iodoaluminate complexes of alkaline earths.

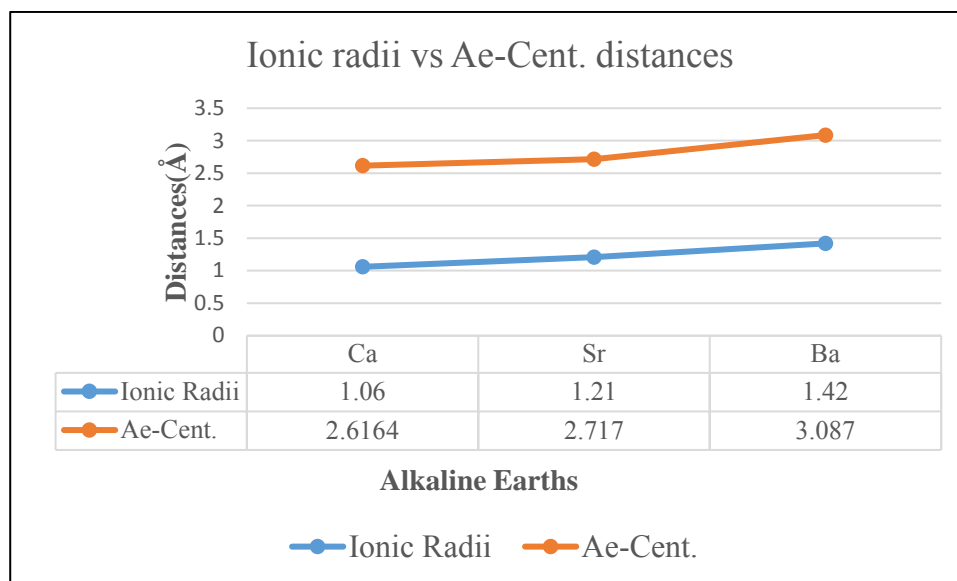


Fig. 3.16b: Changes of the metal-centroid(arene) distances with the ionic radii in the iodoaluminate complexes of alkaline earths.

3.3.2.2 Iodoaluminate Ae(II) complexes in mesitylene

The more highly substituted (trimethyl benzene) arene has been used to synthesise the iodoaluminate Ae(II) analogues of the toluene adducts. Calcium and strontium complexes have been synthesised and characterised successfully. The complex $[\text{Ca}(\eta^6\text{-Me}_3\text{C}_3\text{H}_5)(\text{AlI}_4)_2]_n$ (**4**) (Fig. 3.17a) crystallises in the orthorhombic space group $Pn2_1a$ (No. 33) featuring only one independent molecule in the asymmetric unit. The geometry around the metal centre and the Ca-I contacts (range 3.146(4)-3.4359(17) Å) are analogous to **1**. However, the average Ca-C and Ca-centroid distances (2.9302 and 2.574(3) Å, respectively) in **4** are slightly shorter than those in **1**. This is due the stronger Ca-mesitylene interactions than Ca-toluene interactions. The electron donating methyl groups make the mesitylene ring more electron dense compared to toluene. The I-Ca-I angles are comparable with **1**, and the I-Al-I angles are close to an idealised tetrahedron.

Chapter 3

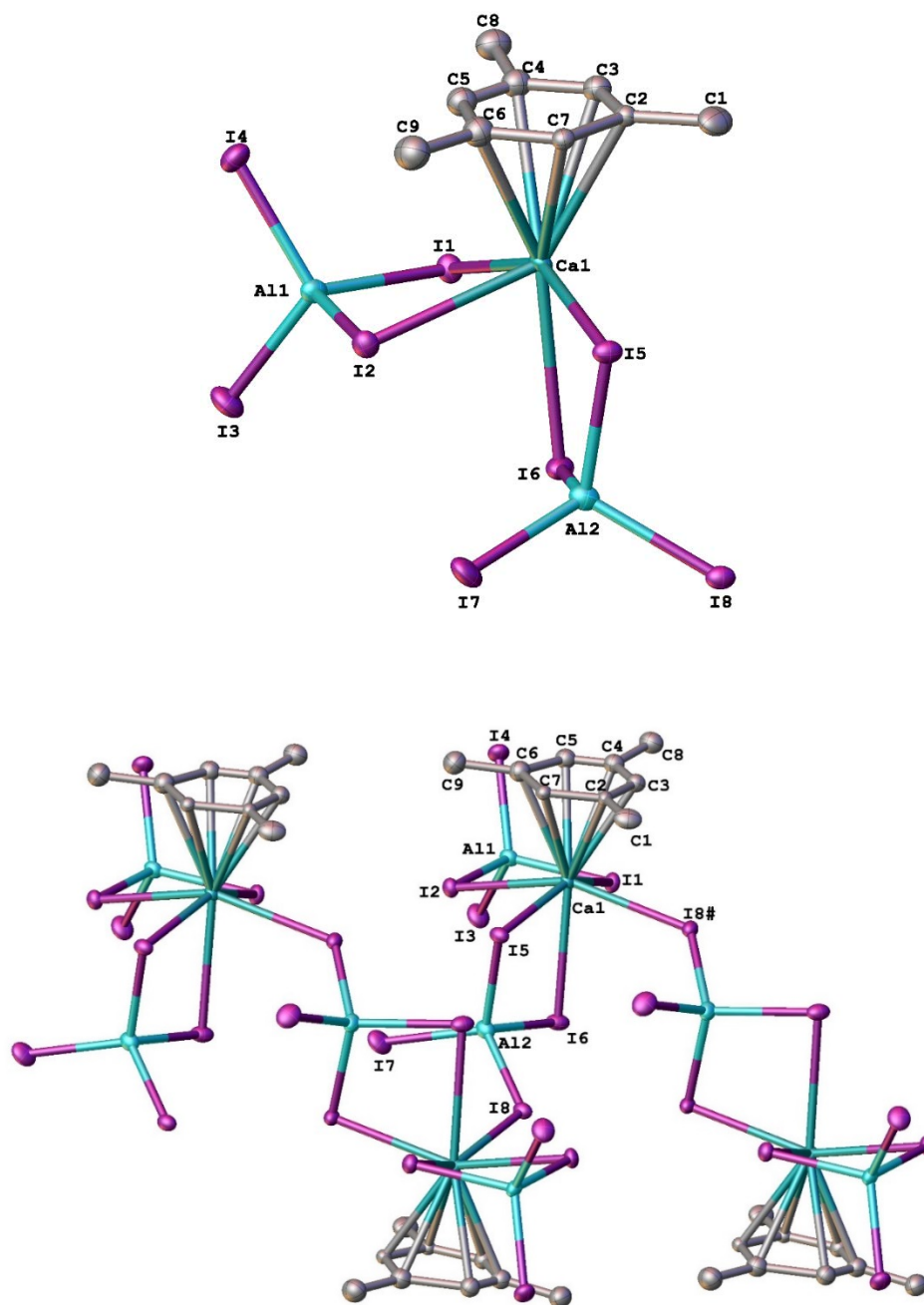


Fig. 3.17a: A monomeric repeat unit (top) and the one dimensional extended zigzag framework for $[\text{Ca}(\eta^6\text{-Me}_3\text{C}_3\text{H}_5)(\text{AlI}_4)_2]_n$ (**4**) (bottom). Hydrogen atoms have been omitted for clarity.

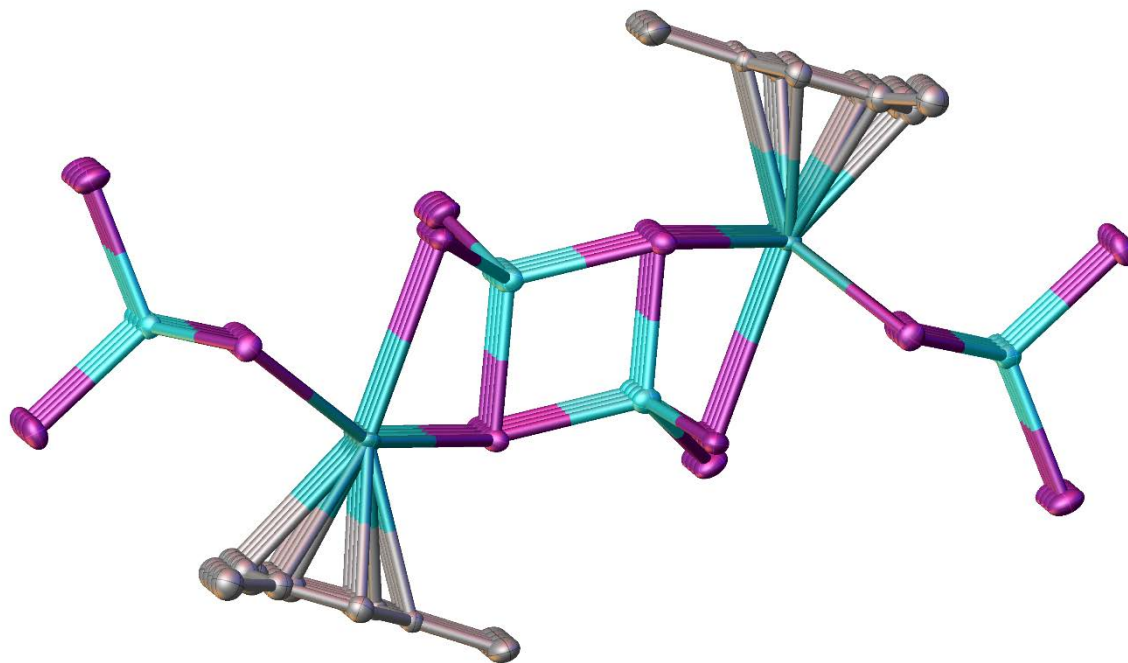


Fig. 3.17b: The Ca-arene double stranded polymer with two bridging AlI_4^- units and two terminal AlI_4^- units for **4**. Hydrogen atoms have been omitted for clarity.

The complex $[\text{Sr}(\eta^6\text{-Me}_3\text{C}_3\text{H}_5)(\text{AlI}_4)_2]_n$ (**5**) (Fig. 3.18a) crystallises in the monoclinic space group $C2/c$ (No. 15) and are isostructural with **2** and **4**. Both the average Sr-C and Sr-centroid distances in **5** (3.1065 and 2.7735(12), respectively) are slightly elongated compared to **2**. The bond lengths (\AA) and bond angles ($^\circ$) for complexes **1-5** are listed in Table 3.1 and 3.2, respectively.

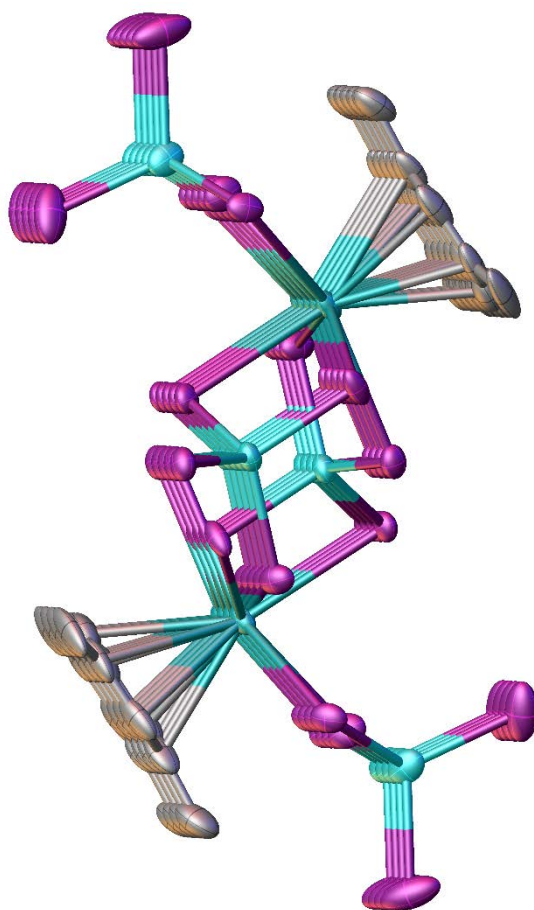


Fig. 3.18b: The Sr-arene double stranded polymer with two bridging AlI_4^- units and two terminal AlI_4^- units for **5**. Hydrogen atoms have been omitted for clarity.

Chapter 3

Table 3.1: The selected bond lengths (Å) for 1, 2, 3, 4 and 5.

A =	Ca (1)	Sr (2)	Ba (3)	Ca (4)	Sr (5)
Ae(1)-I(1)	3.212(7)	3.3628(11)	3.5896(11)	3.188(3)	3.4092(16)
Ae(1)-I(2)	3.239(8)	3.4584(11)	3.5575(10)	3.193(3)	3.4971(17)
Ae(1)-I(4) ¹	3.275(8)				
Ae(1)-I(5)	3.126(7)	3.4210(12)	3.5203(10)	3.147(4)	3.4228(14)
Ae(1)-I(6)	3.316(7)	3.4033(11)	3.5071(9)	3.4359(17)	3.4181(14)
Ae(1) ¹ -I(7)		3.6314(12)			3.4270(2)
Ae(1) ¹ -I(8)		3.4893(12)			3.6004(15)
Ae(1)-I(8) ¹				3.146(4)	
Ae(1)-C(2)	3.09(4)	3.129(9)		2.955(8)	3.104(14)
Ae(1)-C(3)	2.97(4)	3.100(10)		2.938(14)	3.057(13)
Ae(1)-C(4)	2.91(3)	3.027(10)	3.315(9)	2.948(16)	3.085(15)
Ae(1)-C(5)	2.89(3)	3.006(12)	3.267(10)	2.888(9)	3.088(14)
Ae(1)-C(6)	2.92(3)	2.989(12)	3.314(9)	2.920(17)	3.176(12)
Ae(1)-C(7)	3.01(3)	3.051(10)	3.435(9)	2.932(12)	3.129(16)
Ae(1)-C(avg.)	2.9650	3.0497	3.3328	2.9302	3.1065
Ae(1)-C(cent.)	2.6164(5)	2.717(3)	3.087(4)	2.574(3)	2.7735(12)
Al(1)-I(1)	2.579(10)	2.544(3)	2.550(3)	2.571(6)	2.567(5)
Al(1)-I(2)	2.538(11)	2.557(3)	2.540(3)	2.586(6)	2.556(4)
Al(1)-I(3)	2.482(10)	2.508(3)	2.560(3)	2.504(2)	2.517(6)
Al(1)-I(4)	2.582(12)	2.504(3)	2.490(3)	2.498(2)	2.504(5)
Al(2)-I(5)	2.576(9)	2.544(3)	2.570(3)	2.567(4)	2.543(3)
Al(2)-I(6)	2.567(10)	2.552(3)	2.578(3)	2.625(4)	2.541(4)
Al(2)-I(7)	2.474(10)	2.531(3)	2.487(3)	2.572(4)	2.536(4)
Al(2)-I(8)	2.521(11)	2.528(3)	2.507(3)	2.536(4)	2.527(4)

(1) ¹+x,-1+y,+z; (2) ¹1/2+x,3/2-y,1-z; (4) ¹1-x,1/2+y,-z; (5) ¹1/2-X,-1/2+Y,1/2-Z

Chapter 3

Table 3.2: The selected bond angles (°) for 1, 2, 3, 4 and 5.

Ae =	Ca (1)	Sr (2)	Ba (3)	Ca (4)	Sr (5)
Centroid-Ae-I(axial)/centroid	178.40(3)	172.30(4)	178.238(17)	174.78(4)	169.03(4)
I(1)-Ae(1)-I(2)	78.11(17)	71.54(3)	69.718(18)	78.66(4)	71.07(4)
I(1)-Ae(1)-I(5)	155.9(2)	140.94(3)	142.76(2)	151.10(7)	143.04(4)
I(1)-Ae(1)-I(6)	80.79(16)	84.68(3)	69.88(2)	76.44(6)	86.38(4)
I(1)-Ae(1)-I(7) ²		135.26(3)			134.23(4)
I(1)-Ae(1)-I(8) ²		68.34(2)		84.75(11)	66.09(3)
I(2)-Ae(1)-I(7) ²		143.92(3)			146.14(4)
I(2)-Ae(1)-I(8) ²		137.23(3)		150.99(7)	134.59(4)
I(5)-Ae(1)-I(2)	88.49(17)	72.21(3)	147.52(2)	85.03(11)	74.59(4)
I(5)-Ae(1)-I(7) ²		73.90(2)			73.85(4)
I(5)-Ae(1)-I(8) ²		138.50(3)		99.03(5)	139.16(4)
I(6)-Ae(1)-I(2)	79.34(15)	76.91(3)	139.41(2)	76.02(5)	76.83(4)
I(6)-Ae(1)-I(5)	77.10(15)	73.41(2)	72.92(2)	76.55(6)	72.74(3)
I(6)-Ae(1)-I(7) ²		81.96(3)			82.40(4)
I(6)-Ae(1)-I(8) ²		85.15(2)		77.05(6)	86.03(3)
I(8) ² -Ae(1)-I(7) ²		68.11(2)			68.95(3)
I(4) ¹ -Ae(1)-I(1)	78.06(16)				
I(4) ¹ -Ae(1)-I(2)	150.1(2)				
I(4) ¹ -Ae(1)-I(5)	106.7(2)				
I(4) ¹ -Ae(1)-I(6)	79.23(17)				
I(1)-Al(1)-I(2)	105.2(4)	102.86(10)	106.76(10)	103.29(8)	103.21(17)
I(3)-Al(1)-I(1)	110.6(4)	110.25(11)	106.89(10)	110.4(2)	108.11(16)
I(3)-Al(1)-I(2)	116.9(4)	110.72(11)	108.73(10)	109.27(19)	111.5(2)
I(4)-Al(1)-I(1)	102.9(3)	110.71(11)	114.28(11)	111.2(2)	109.2(2)
I(4)-Al(1)-I(2)	109.3(4)	110.21(11)	108.36(10)	110.6(2)	110.81(16)
I(4)-Al(1)-I(3)	110.9(4)	111.76(11)	111.61(10)	111.75(9)	113.44(19)
I(5)-Al(2)-I(6)	102.7(3)	106.33(10)	108.43(10)	103.76(12)	105.87(13)
I(7)-Al(2)-I(5)	109.7(4)	110.44(11)	108.45(10)	109.82(13)	108.96(14)
I(7)-Al(2)-I(6)	113.3(4)	114.37(11)	107.84(10)	116.85(13)	113.99(13)
I(8)-Al(2)-I(5)	108.7(4)	111.56(11)	108.23(10)	108.74(13)	112.27(13)
I(8)-Al(2)-I(6)	109.3(4)	110.16(11)	107.40(10)	104.82 (12)	112.22(14)
I(8)-Al(2)-I(7)	112.7(3)	104.09(10)	116.26(11)	112.26(13)	103.66(13)

(1) ¹+x,-1+y,+z; (2) ²-1/2+x,3/2-y,1-z; (4) ²1-x,1/2+y,-z' (5) ²1/2-X,1/2+Y,1/2-Z

3.3.3 Discussion

A series of heavy alkaline earth iodoaluminate complexes ($[\text{Ca}(\eta^6\text{-C}_6\text{H}_5\text{Me})(\text{AlI}_4)_2]_{0.5}$, $[\text{Ca}(\eta^6\text{-C}_6\text{H}_5\text{Me})(\text{AlI}_4)_2]_n$, $[\text{Sr}(\eta^6\text{-MeC}_6\text{H}_5)(\text{AlI}_4)_2]_n$.PhMe, $\text{Ba}(\eta^4\text{-C}_6\text{H}_5\text{Me})_2(\text{AlI}_4)_2$ and $[\text{Ae}(\eta^6\text{-Me}_3\text{C}_3\text{H}_5)(\text{AlI}_4)_2]_n$ (Ae = Ca, Sr)) have been synthesised and characterised. The calcium and strontium complexes were isolated from two different solvents, toluene and mesitylene. The Ca-centroid and the average Ca-C distances in the mesitylene complex are somewhat reduced than that of toluene complex. This fact suggests stronger Ca-arene interactions in mesitylene complex than in the toluene analogue, presumably due to the electron donating effect of three methyl groups in mesitylene molecule (only one in toluene). Both complexes have a zigzag polymer structure. The strontium complex is isostructural with the samarium and europium complexes reported in chapter 2.

The barium complex ($\text{Ba}(\eta^4\text{-C}_6\text{H}_5\text{Me})_2(\text{AlI}_4)_2$) comes with a different structure than the other alkaline earth complexes. Barium centre is sandwiched between two toluene molecules both in an η^4 fashion giving barium centre eight coordination. In contrary, the other complexes have only one toluene/mesitylene molecule bonded to the metal centres. The Ba-I, Ba-C contacts are comparable with other analogous complexes considering the ionic radii of metals and iodide.

3.4 Conclusions

Compounds **1-5** extend the structural diversity attainable within the iodoaluminate complexes of heavy alkaline earths. These are the first ever-reported bimetallic complexes of alkaline earths featuring metal- π arene interactions. All the complexes were synthesised by the reaction of in situ prepared aluminium iodide and alkaline earth iodides in a one-pot reaction, leading to the isolation of various complexes by a convenient reaction scheme.

3.5 Experimental

For general procedures, see Appendix 2. Combustion analyses consistently gave variable results, and are therefore presented only in Appendix 2. Metal analyses were generally more accurate and are presented here.



Toluene (30 mL) was taken in a Schlenk flask and charged with an excess of Al powder (0.162 g, 6 mmol) and I₂ granules (1.90 g, 7.5 mmol). The mixture was heated with stirring at 100°C in an oil bath for a couple of hours. The solution became colourless from red indicating the consumption of all iodine. After cooling the solution to room temperature, Ca pieces (0.1 g, 2.5 mmol) and ICH₂CH₂I (0.704g, 2.5 mmol) were added to the solution under nitrogen atmosphere in the glove box. Heating the solution at 100°C overnight gave a light yellow solution, which was filtered and stored at room temperature. Light yellow crystals were developed in two days (1.46 g, 32%). Metal analysis (C_{10.5}H₁₂Al₃Ca_{1.5}I₁₂); cal. (%) Ca 3.34; found Ca 3.29. IR (Nujol, v/cm⁻¹): 2923 (s), 2725 (w), 1608 (w), 1592 (w), 1463 (m), 1377 (m), 1170 (w), 984 (w), 861 (w), 831 (w), 806 (w), 767 (w), 694 (w).



Following the procedure in **1**, Sr pieces (0.219 g, 2.5 mmol) and ICH₂CH₂I (0.704g, 2.5 mmol) were added to the solution under nitrogen atmosphere in the glove box. Heating the solution at 100°C overnight gave a light yellow solution, which was filtered and stored at room temperature. Light yellow crystals were developed in two days (0.92 g, 27%). Metal analysis (C₁₄H₁₆Al₂I₈Sr); cal. (%) Sr 6.53; found Sr 6.48. IR (Nujol, v/cm⁻¹): 2925 (s), 2854 (s), 2726 (w), 1605 (w), 1462 (s), 1260 (w), 1081 (w), 1020 (w), 799 (w), 769 (w), 727 (w), 694 (w).



Following the procedure in **1**, Ba pieces (0.343 g, 2.5 mmol) and ICH₂CH₂I (0.704g, 2.5 mmol) were added to the solution under nitrogen atmosphere in the glove box. Heating the

Chapter 3

solution at 100°C overnight gave a light yellow solution, which was filtered and stored at room temperature. Light yellow crystals were developed in two days (0.79 g, 23%). Metal analysis ($C_{14}H_{16}Al_2BaI_8$); cal. (%) Ba 9.87; found Ba 9.79. IR (Nujol, ν/cm^{-1}): 2923 (s), 2857 (s), 2722 (w), 1592 (w), 1463 (s), 1377 (m), 1023 (w), 755 (w), 723 (w), 696 (w).



A Schlenk flask was charged with 40 mL mesitylene, and an excess of Al powder (0.162 g, 6 mmol) and I_2 granules (1.90 g, 7.5 mmol) was added into it. The mixture was heated with stirring at 100°C in an oil bath for a couple of hours. The solution became colourless from red indicating the consumption of all iodine. After cooling the solution to room temperature, Ca pieces (0.1 g, 2.5 mmol) and ICH_2CH_2I (0.704g, 2.5 mmol) were added to the solution under nitrogen atmosphere in the glove box. Heating the solution at 100°C overnight gave a light yellow solution, which was filtered and stored at room temperature. Light yellow crystals were developed in two days (1.28 g, 42%). Metal analysis ($C_9H_{12}Al_2CaI_8$); cal. (%) Ca 3.26; found Ca 3.31. IR (Nujol, ν/cm^{-1}): 2925 (s), 2854 (s), 2730 (w), 1593 (w), 1463(s), 1377 (m), 1261 (w), 1034 (w), 867 (w), 722 (w), 723 (w), 689 (w).



Following the procedure in **4**, Sr pieces (0.219 g, 2.5 mmol) and ICH_2CH_2I (0.704g, 2.5 mmol) were added to the solution under nitrogen atmosphere in the glove box. Heating the solution at 100°C overnight gave a light yellow solution, which was filtered and stored at room temperature. Light yellow crystals were developed in two days (0.79 g, 23%). Metal analysis ($C_9H_{12}Al_2I_8Sr$); cal. (%) Sr 6.86; found Sr 6.82. IR (Nujol, ν/cm^{-1}): 2924 (s), 2725 (w), 1608 (w), 1592 (w), 1464 (m), 1377 (m), 1030 (w), 861 (w), 834 (w), 806 (w), 723 (w), 690 (w).

3.6 X-ray crystal data

For general procedures, see Appendix 2.

[Ca(η^6 -C₆H₅Me)(AlI₄)₂]_{1.5} (1)

C_{10.5}H₁₂Al₃Ca_{1.5}I₁₂, $M_r = 1802.06$ g/mol, monoclinic, space group $C2/c$ (No. 15), $a = 45.393(9)$ Å, $b = 8.0140(16)$ Å, $c = 20.304(4)$ Å, $\beta = 98.12(3)^\circ$, $\alpha = \gamma = 90^\circ$, $V = 7312(3)$ Å³, $T = 173(2)$ K, $Z = 8$, $Z' = 1$, $\mu(\text{MoK}\alpha) = 10.450$ mm⁻¹, $D_{\text{calc}} = 3.274$ gcm⁻³, 31284 reflections measured, 6303 unique ($R_{\text{int}} = 0.0772$) which were used in all calculations. The final wR_2 was 0.2858 (all data) and R_I was 0.1299 ($I > 2\sigma(I)$).

[Sr(η^6 -MeC₆H₅)(AlI₄)₂]_n.PhMe (2)

C₁₄H₁₆Al₂I₈Sr, $M_r = 1341.05$ g/mol, orthorhombic, space group $P2_12_12_1$ (No. 19), $a = 11.035(2)$ Å, $b = 14.468(3)$ Å, $c = 18.966(4)$ Å, $\alpha = \beta = \gamma = 90^\circ$, $V = 3028.0(10)$ Å³, $T = 173(2)$ K, $Z = 4$, $Z' = 1$, $\mu(\text{MoK}\alpha) = 9.996$ mm⁻¹, $D_{\text{calc}} = 2.942$ gcm⁻³, 47978 reflections measured, 8478 unique ($R_{\text{int}} = 0.0461$) which were used in all calculations. The final wR_2 was 0.0821 (all data) and R_I was 0.0335 ($I > 2\sigma(I)$).

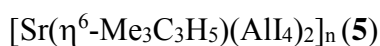
Ba(η^4 -C₆H₅Me)₂(AlI₄)₂ (3)

C₁₄H₁₆Al₂BaI₈, $M_r = 1390.77$ g/mol, monoclinic, space group $P2_1/c$ (No. 14), $a = 10.166(2)$ Å, $b = 21.721(4)$ Å, $c = 13.988(3)$ Å, $\beta = 96.62(3)^\circ$, $\alpha = \gamma = 90^\circ$, $V = 3068.2(11)$ Å³, $T = 173(2)$ K, $Z = 4$, $Z' = 1$, $\mu(\text{MoK}\alpha) = 9.402$, 36872 reflections measured, 5382 unique ($R_{\text{int}} = 0.0479$) which were used in all calculations. The final wR_2 was 0.0785 (all data) and R_I was 0.0362 ($I > 2\sigma(I)$).

Chapter 3



C₉H₁₂Al₂CaI₈, $M_r = 1229.43$ g/mol, orthorhombic, space group $Pn2_1a$ (No. 33), $a = 17.374(4)$ Å, $b = 8.9230(18)$ Å, $c = 17.273(4)$ Å, $\alpha = \beta = \gamma = 90^\circ$, $V = 2677.8(9)$ Å³, $T = 298(2)$ K, $Z = 4$, $Z' = 1$, $\mu(\text{MoK}\alpha) = 9.515$, 21970 reflections measured, 5308 unique ($R_{int} = 0.0414$) which were used in all calculations. The final wR_2 was 0.0784 (all data) and R_1 was 0.0313 ($I > 2\sigma(I)$).



C₉H₁₂Al₂I₈Sr, $M_r = 1276.97$ g/mol, monoclinic, space group $C2/c$ (no. 15), $a = 28.863(6)$ Å, $b = 11.000(2)$ Å, $c = 21.017(4)$ Å, $\beta = 111.82(3)^\circ$, $V = 6194(2)$ Å³, $Z = 8$, $T = 293(2)$ K, $\mu(\text{MoK}\alpha) = 9.765$ mm⁻¹, $D_{calc} = 2.738$ gcm⁻³, 51768 reflections measured ($4.002^\circ \leq 2\Theta \leq 63.908^\circ$), 8613 unique ($R_{int} = 0.0950$, $R_{sigma} = 0.0617$) which were used in all calculations. The final R_1 was 0.0923 ($I > 2\sigma(I)$) and wR_2 was 0.2309 (all data).

Chapter 3

3.7 References

1. E. O. Fischer and W. Hafner, *Z. Naturforsch., B: Chem. Sci.*, 1955, **10**, 665-668.
2. E. L. Muetterties, J. R. Bleeke and A. C. Sievert, *J. Organomet. Chem.*, 1979, **178**, 197-216.
3. A. Sievert and E. Muetterties, *Inorg. Chem.*, 1981, **20**, 489-501.
4. S. Troyanov, *J. Organomet. Chem.*, 1994, **475**, 139-147.
5. H. Le Bozec, D. Touchard and P. H. Dixneuf, *Adv. Organomet. Chem.*, 1989, **29**, 163-247.
6. K. Jonas, *Pure Appl. Chem.*, 1990, **62**, 1169-1174.
7. E. Uhlig, *Organometallics*, 1993, **12**, 4751-4756.
8. H. Schmidbaur, *Angew. Chem. Int. Ed.*, 1985, **24**, 893-904.
9. E. Muetterties, J. Bleeke, E. Wucherer and T. Albright, *Chem. Rev.*, 1982, **82**, 499-525.
10. F. Calderazzo and G. Pampaloni, *J. Organomet. Chem.*, 1992, **423**, 307-328.
11. F. Calderazzo and G. Pampaloni, *J. Organomet. Chem.*, 1995, **500**, 47-60.
12. M. Cesari, U. Pedretti, Z. Zazzetta, G. Lugli and W. Marconi, *Inorg. Chim. Acta*, 1971, **5**, 439-444.
13. F. A. Cotton and W. Schwotzer, *Organometallics*, 1985, **4**, 942-943.
14. F. A. Cotton, W. Schwotzer and C. Q. Simpson, *Angew. Chem. Int. Ed.*, 1986, **25**, 637-639.
15. F. A. Cotton and W. Schwotzer, *Organometallics*, 1987, **6**, 1275-1280.
16. G. C. Campbell, F. A. Cotton, J. F. Haw and W. Schwotzer, *Organometallics*, 1986, **5**, 274-279.

Chapter 3

17. H. Schumann, J. A. Meese-Marktscheffel and L. Esser, *Chem. Rev.*, 1995, **95**, 865-986.
18. G. B. Deacon and Q. Shen, *J. Organomet. Chem.*, 1996, **511**, 1-17.
19. M. N. Bochkarev, *Chem. Rev.*, 2002, **102**, 2089-2118.
20. F. G. N. Cloke, *Chem. Soc. Rev.*, 1993, **22**, 17-24.
21. M. N. Bochkarev, *Russ. Chem. Rev.*, 2000, **69**, 783-794.
22. F. A. Cotton, *Inorg. Chem.*, 2002, **41**, 643-658.
23. F. T. Edelmann, D. M. M. Freckmann and H. Schumann, *Chem. Rev.*, 2002, **102**, 1851-1896.
24. F. Barbotin, R. Spitz and C. Boisson, *Macromol. Rapid Commun.*, 2001, **22**, 1411-1414.
25. T. Hayakawa, Y. Nakayama and H. Yasuda, *Polym. Int.*, 2001, **50**, 1260-1264.
26. A. Fischbach and R. Anwander, in *Neodymium Based Ziegler Catalysts—Fundamental Chemistry*, Springer, 2006, pp. 155-281.
27. F. A. Cotton and W. Schwotzer, *J. Am. Chem. Soc.*, 1986, **108**, 4657-4658.
28. F. A. Cotton and W. Schwotzer, *Organometallics*, 1987, **6**, 1275-1280.
29. B. Fan, Q. Shen and Y. Lin, *Chin. J. Org. Chem.*, 1989, **9**, 414-414.
30. B. Fan, Q. Shen and Y. Lin, *J. Organomet. Chem.*, 1989, **376**, 61-66.
31. B. Fan, Q. Shen and Y. Lin, *J. Organomet. Chem.*, 1989, **377**, 51-58.
32. B. Fan, S. Jin, Q. Shen and Y. Lin, *Chin. Sci. Bull.*, 1991, **36**, 84-85.
33. B. Fan, Q. Shen and Y. Lin, *Chin. J. Inorg. Chem.*, 1991, **7**, 143.
34. B. Fan, Y. Lin and Q. Shen, *Chin. J. Appl. Chem.*, 1990, **7**, 23.

Chapter 3

35. H.-Z. Liang, J.-W. Guan, Y.-H. Lin and Q. Shen, *Chin. J. Org. Chem.*, 1994, **14**, 380-382.
36. P. Biagini, G. Lugli and R. Millini, *Gazz. Chim. Ital.*, 1994, **124**, 217-225.
37. H. Liang, Q. Shen, J. Guan and Y. Lin, *J. Organomet. Chem.*, 1994, **474**, 113-116.
38. Q. Liu, Y.-H. Lin and Q. Shen, *Acta Cryst.*, 1997, **C53**, 1579-1580.
39. Y.-M. Yao, Y. Zhang, Q. Shen, Q.-C. Liu, Q.-J. Meng and Y.-H. Lin, *Chin. J. Chem.*, 2001, **19**, 588-592.
40. Q. Liu, Q. Shen, Y. Lin and Y. Zhang, *Chin. J. Inorg. Chem.*, 1998, **14**, 194-198.
41. P. Biagini, G. Lugli and R. Millini, *New J. Chem.*, 1995, **19**, 713-722.
42. S. Jin, J. Guan, H. Liang and Q. Shen, *J. Catal.*, 1993, **14**, 159-162.
43. J. Hu, H. Tian, Q. Shen and L. Liang, *Chin. Sci. Bull.*, 1992, **37**, 566.
44. J. Hu, L. Liang and Q. Shen, *J. Rare Earths*, 1993, **11**, 302.
45. H. Liang, Q. Shen, S. Jin and Y. Lin, *J. Chin. Rare Earth Soc.*, 1994, **12**, 193-196.
46. H. Liang, Q. Shen, S. Jin and Y. Lin, *Chem. Commun.*, 1992, 480-481.
47. A. A. Fagin, M. N. Bochkarev, S. A. Kozimor, J. W. Ziller and W. J. Evans, *Z. Anorg. Allg. Chem.*, 2005, **631**, 2848-2853.
48. A. S. Filatov, A. Y. Rogachev and M. A. Petrukhina, *J. Mol. Struct.*, 2008, **890**, 116-122.
49. A. S. Filatov, S. N. Gifford, D. K. Kumar and M. A. Petrukhina, *Acta Cryst.*, 2009, **E65**, m286-m287.
50. S.-S. Liu, J. W. Ziller, Y.-Q. Zhang, B.-W. Wang, W. J. Evans and S. Gao, *Chem. Commun.*, 2014, **50**, 11418-11420.
51. M. F. Zuniga, G. B. Deacon and K. Ruhlandt-Senge, *Inorg. Chem.*, 2008, **47**, 4669-4681.

Chapter 3

52. M. Westerhausen, M. Krofta, N. Wiberg, J. Knizek, H. Nöth and A. Pfitzner, *Z. Naturforsch., B: Chem. Sci.*, 1998, **53**, 1489-1493.
53. L. Bonomo, E. Solari, R. Scopelliti and C. Floriani, *Chem. Eur. J.*, 2001, **7**, 1322-1332.
54. G. Guillemot, E. Solari, C. Rizzoli and C. Floriani, *Chem. Eur. J.*, 2002, **8**, 2072-2080.
55. S. O. Hauber, F. Lissner, G. B. Deacon and M. Niemeyer, *Angew. Chem. Int. Ed.*, 2005, **44**, 5871-5875.
56. S. Krieck, H. Görls, L. Yu, M. Reiher and M. Westerhausen, *J. Am. Chem. Soc.*, 2009, **131**, 2977-2985.
57. G. B. Deacon, P. C. Junk, G. J. Moxey, K. Ruhlandt-Senge, C. St. Prix and M. F. Zuniga, *Chem. Eur. J.*, 2009, **15**, 5503-5519.
58. S. Krieck, H. Görls and M. Westerhausen, *Chem. Asian J.*, 2010, **5**, 272-277.
59. C. Jones, L. McDyre, D. M. Murphy and A. Stasch, *Chem. Commun.*, 2010, **46**, 1511-1513.
60. M. Lindsjo, A. Fischer and L. Kloo, *Dalton Trans.*, 2010, **39**, 1467-1469.
61. H. S. Lee and M. Niemeyer, *Inorg. Chem.*, 2010, **49**, 730-735.
62. O. Michel, S. König, K. W. Törnroos, C. Maichle-Mössmer and R. Anwander, *Chem. Eur. J.*, 2011, **17**, 11857-11867.
63. O. Michel, K. W. Törnroos, C. Maichle-Mössmer and R. Anwander, *Chem. Eur. J.*, 2011, **17**, 4964-4967.
64. O. Michel, K. W. Törnroos, C. Maichle-Mössmer and R. Anwander, *Eur. J. Inorg. Chem.*, 2012, **2012**, 44-47.
65. I. L. Fedushkin, A. A. Skatova, N. L. Bazyakina, V. A. Chudakova, N. M. Khvoinova, A. S. Nikipelov, O. V. Eremenko, A. V. Piskunov, G. K. Fukin and K. A. Lyssenko, *Russ. Chem. Bull.*, 2013, **62**, 1815-1828.

Chapter 3

66. C. Loh, S. Seupel, H. Görls, S. Krieck and M. Westerhausen, *Organometallics*, 2014, **33**, 1480-1491.
67. C. Loh, S. Seupel, A. Koch, H. Görls, S. Krieck and M. Westerhausen, *Dalton Trans.*, 2014, **43**, 14440-14449.
68. D. Kalden, A. Oberheide, C. Loh, H. Görls, S. Krieck and M. Westerhausen, *Chem. Eur. J.*, 2016, **22**, 10944-10959.
69. G. J. Moxey, A. J. Blake, W. Lewis and D. L. Kays, *Eur. J. Inorg. Chem.*, 2015, **2015**, 5892-5902.
70. A. Causero, G. Ballmann, J. Pahl, H. Zijlstra, C. Färber and S. Harder, *Organometallics*, 2016, **35**, 3350-3360.
71. T. P. Hanusa, *Chem. Rev.*, 1993, **93**, 1023-1036.
72. H. Schumann, S. Schutte, H. J. Kroth and D. Lentz, *Angew. Chem. Int. Ed.*, 2004, **43**, 6208-6211.
73. M. Wiecko, C. Eidamshaus, R. Köppe and P. W. Roesky, *Dalton Trans.*, 2008, 4837-4839.
74. M. J. Harvey, T. P. Hanusa and J. V. G. Young, *Angew. Chem. Int. Ed.*, 1999, **38**, 217-219.
75. P. Jochmann, T. S. Dols, T. P. Spaniol, L. Perrin, L. Maron and J. Okuda, *Angew. Chem. Int. Ed.*, 2009, **48**, 5715-5719.
76. P. Jochmann, T. S. Dols, T. P. Spaniol, L. Perrin, L. Maron and J. Okuda, *Angew. Chem. Int. Ed.*, 2010, **49**, 7795-7798.
77. R. Goddard, J. Akhtar and K. B. Starowieyski, *J. Organomet. Chem.*, 1985, **282**, 149-154.
78. H. Sitzmann, F. Weber, M. D. Walter and G. Wolmershäuser, *Organometallics*, 2003, **22**, 1931-1936.
79. M. J. Harvey and T. P. Hanusa, *Organometallics*, 2000, **19**, 1556-1566.

Chapter 3

80. P. S. Tanner, R. A. Williams and T. P. Hanusa, *Inorg. Chem.*, 1993, **32**, 2234-2235.
81. M. Westerhausen, M. H. Digeser, C. Gückel, H. Nöth, J. Knizek and W. Ponikwar, *Organometallics*, 1999, **18**, 2491-2496.
82. M. J. McCormick, S. C. Sockwell, C. E. Davies, T. P. Hanusa and J. C. Huffman, *Organometallics*, 1989, **8**, 2044-2049.
83. K. C. Jayaratne, L. S. Fitts, T. P. Hanusa and V. G. Young, *Organometallics*, 2001, **20**, 3638-3640.
84. D. J. Burkey, E. K. Alexander and T. P. Hanusa, *Organometallics*, 1994, **13**, 2773-2786.
85. D. Naglav, B. Tobey, A. Neumann, D. Bläser, C. Wölper and S. Schulz, *Organometallics*, 2015, **34**, 3072-3078.
86. M. J. Harvey, T. P. Hanusa and V. G. Young, *J. Organomet. Chem.*, 2001, **626**, 43-48.
87. J. Vollet, J. R. Hartig, K. Baranowska and H. Schnöckel, *Organometallics*, 2006, **25**, 2101-2103.
88. R. E. Cramer, P. N. Richmann and J. W. Gilje, *J. Organomet. Chem.*, 1991, **408**, 131-136.
89. A. Xia, J. E. Knox, M. J. Heeg, H. B. Schlegel and C. H. Winter, *Organometallics*, 2003, **22**, 4060-4069.
90. B. Twamley, G. J. Matare, P. J. Shapiro and A. Vij, *Acta Cryst.*, 2001, **E57**, m402-m403.
91. G. B. Deacon, F. Jaroschik, P. C. Junk and R. P. Kelly, *Organometallics*, 2015, **34**, 2369-2377.
92. H. Li, B. Wei, L. Xu, W.-X. Zhang and Z. Xi, *Angew. Chem. Int. Ed.*, 2013, **52**, 10822-10825.

Chapter 3

93. D. P. Daniels, G. B. Deacon, D. Harakat, F. Jaroschik and P. C. Junk, *Dalton Trans.*, 2012, **41**, 267-277.
94. B. Blom, G. Klatt, D. Gallego, G. Tan and M. Driess, *Dalton Trans.*, 2015, **44**, 639-644.
95. C. Ruspic, J. R. Moss, M. Schürmann and S. Harder, *Angew. Chem. Int. Ed.*, 2008, **47**, 2121-2126.
96. G. B. Deacon, C. M. Forsyth, F. Jaroschik, P. C. Junk, D. L. Kay, T. Maschmeyer, A. F. Masters, J. Wang and L. D. Field, *Organometallics*, 2008, **27**, 4772-4778.
97. M. del Mar Conejo, R. Fernández, E. Carmona, R. A. Andersen, E. Gutiérrez-Puebla and M. A. Monge, *Chem. Eur. J.*, 2003, **9**, 4462-4471.
98. D. Naglav, M. R. Buchner, G. Bendt, F. Kraus and S. Schulz, *Angew. Chem. Int. Ed.*, 2016, **55**, 10562-10576.
99. K. Yasushi, K. Nobuko, M. Kunio, K. Nobutami, M. Kazushi, Y. Hajime and N. Akira, *Chem. Lett.*, 1982, **11**, 1277-1280.
100. N. A. Bell, I. W. Nowell and H. M. M. Shearer, *Chem. Commun.*, 1982, 147-148.
101. M. Arrowsmith, M. R. Crimmin, M. S. Hill, S. L. Lomas, D. J. MacDougall and M. F. Mahon, *Organometallics*, 2013, **32**, 4961-4972.
102. A. G. Barrett, M. R. Crimmin, M. S. Hill, P. B. Hitchcock, S. L. Lomas, P. A. Procopiou and K. Suntharalingam, *Chem. Commun.*, 2009, 2299-2301.
103. M. Westerhausen, M. H. Digeser, H. Nöth, T. Seifert and A. Pfitzner, *J. Am. Chem. Soc.*, 1998, **120**, 6722-6725.
104. A. Stasch, S. P. Sarish, H. W. Roesky, K. Meindl, F. Dall'Antonia, T. Schulz and D. Stalke, *Chem. Asian J.*, 2009, **4**, 1451-1457.
105. K.-C. Yang, C.-C. Chang, J.-Y. Huang, C.-C. Lin, G.-H. Lee, Y. Wang and M. Y. Chiang, *J. Organomet. Chem.*, 2002, **648**, 176-187.
106. S. I. Troyanov, V. Varga and K. Mach, *Organometallics*, 1993, **12**, 2820-2824.

Chapter 3

107. V. Varga, K. Mach, J. Heyrovský, G. Schmid and U. Thewalt, *J. Organomet. Chem.*, 1994, **475**, 127-137.
108. U. H. Verkerk, R. McDonald and J. M. Stryker, *Can. J. Chem.*, 2005, **83**, 922-928.
109. M. A. Guino-o, C. F. Campana and K. Ruhlandt-Senge, *Chem. Commun.*, 2008, 1692-1694.
110. G. Bender, T. Wiegand, H. Eckert, R. Fröhlich, C. G. Daniliuc, C. Mück-Lichtenfeld, S. Ndambuki, T. Ziegler, G. Kehr and G. Erker, *Angew. Chem. Int. Ed.*, 2012, **51**, 8846-8849.
111. J. L. Atwood and K. D. Smith, *J. Am. Chem. Soc.*, 1974, **96**, 994-998.
112. A. Jaenschke, F. Olbrich and U. Behrens, *Z. Anorg. Allg. Chem.*, 2009, **635**, 2550-2557.
113. Y. Liu, Y. Zhao, X.-J. Yang, S. Li, J. Gao, P. Yang, Y. Xia and B. Wu, *Organometallics*, 2011, **30**, 1599-1606.
114. M. Fujita, O. C. Lightbody, M. J. Ferguson, R. McDonald and J. M. Stryker, *J. Am. Chem. Soc.*, 2009, **131**, 4568-4569.
115. V. Varga, K. Mach, G. Schmid and U. Thewalt, *J. Organomet. Chem.*, 1993, **454**, C1-C4.
116. M. Westerhausen, N. Makropoulos, B. Wieneke, K. Karaghiosoff, H. Nöth, H. Schwenk-Kircher, J. Knizek and T. Seifert, *Eur. J. Inorg. Chem.*, 1998, **1998**, 965-971.
117. M. M. Olmstead, W. J. Grigsby, D. R. Chacon, T. Hascall and P. P. Power, *Inorg. Chim. Acta*, **251**, 273-284.
118. S. Kriek, L. Yu, M. Reiher and M. Westerhausen, *Eur. J. Inorg. Chem.*, 2010, **2010**, 197-216.
119. S.-C. Roşca, E. Caytan, V. Dorcet, T. Roisnel, J.-F. Carpentier and Y. Sarazin, *Organometallics*, 2017, **36**, 1269-1277.

Chapter 3

120. D. A. Dougherty, *Science*, 1996, **271**, 163-168.
121. J. C. Ma and D. A. Dougherty, *Chem. Rev.*, 1997, **97**, 1303-1324.
122. A. S. Mahadevi and G. N. Sastry, *Chem. Rev.*, 2012, **113**, 2100-2138.
123. D. A. Dougherty, *Acc. Chem. Res.*, 2013, **46**, 885-893.
124. R. C. Dunbar, J. D. Steill and J. Oomens, *J. Am. Chem. Soc.*, 2011, **133**, 9376-9386.
125. S. Tetreault and V. S. Ananthanarayanan, *J. Med. Chem.*, 1993, **36**, 1017-1023.
126. A. Gapeev and R. C. Dunbar, *J. Phys. Chem. A*, 2000, **104**, 4084-4088.
127. Y.-H. Cheng, L. Liu, Y. Fu, R. Chen, X.-S. Li and Q.-X. Guo, *J. Phys. Chem. A*, 2002, **106**, 11215-11220.
128. A. S. Reddy and G. N. Sastry, *J. Phys. Chem. A*, 2005, **109**, 8893-8903.
129. M. Westerhausen, M. Gärtner, R. Fischer, J. Langer, L. Yu and M. Reiher, *Chem. Eur. J.*, 2007, **13**, 6292-6306.
130. A. S. Reddy, H. Zipse and G. N. Sastry, *J. Phys. Chem. B*, 2007, **111**, 11546-11553.
131. L. M. Engelhardt, P. C. Junk, C. L. Raston and A. H. White, *J. Chem. Soc., Chem. Commun.*, 1988, 1500-1501.
132. A. W. Duff, P. B. Hitchcock, M. F. Lappert, R. G. Taylor and J. A. Segal, *J. Organomet. Chem.*, 1985, **293**, 271-283.
133. R. Shannon, *Acta Cryst.*, 1976, **A32**, 751-767.
134. D. J. Burkey and T. P. Hanusa, *Acta Cryst.*, 1996, **C52**, 2452-2454.

CHAPTER 4

FORMAMIDINATE CHEMISTRY OF DIVALENT AND TRIVALENT LANTHANOIDS

4.1 Introduction

In order to get alternative N-donor based ligand systems to the ubiquitous cyclopentadienyl type ligands,¹⁻¹² our group has focused on the versatile and readily available N, N'-bis(aryl)formamidine ligands (Fig. 4.1) to explore the chemistry of rare earth complexes.¹³⁻²⁹ Recently, the formamidinate chemistry of lanthanoids has extensively been reviewed by us.³⁰ The common synthetic methods of the complexes involve metathesis or salt elimination, direct metalation, protolysis, redox transmetallation and redox transmetallation/protolysis or RTP reactions. The general synthetic procedures have been described in chapter one.

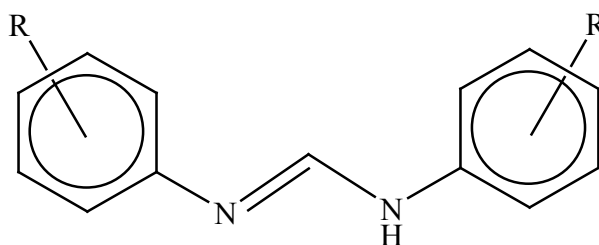
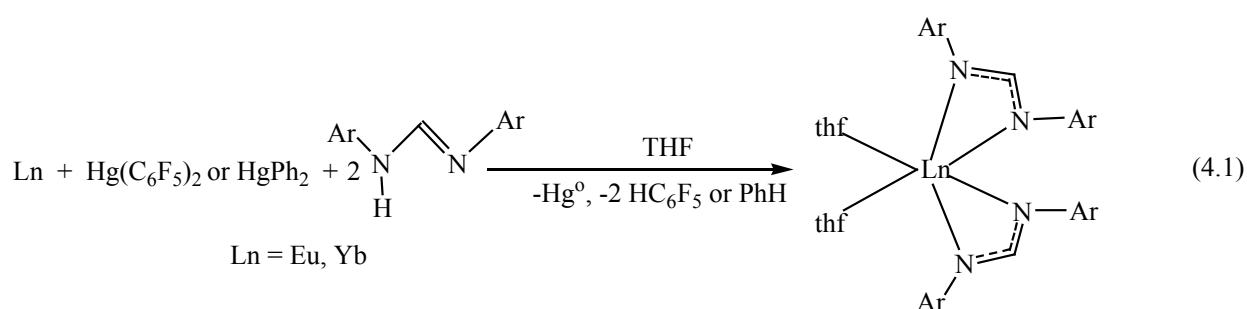


Fig. 4.1: N, N'- bis(aryl)formamidine ligands; = *o*-MeC₆H₄ (*o*-TolFormH), 2,6-Me₂C₆H₃ (XylFormH), 2,4,6-Me₃C₆H₂ (MesFormH), 2,6-Et₂C₆H₃ (EtFormH), *o*-PhC₆H₄ (*o*-PhPhFormH), 2,6-ⁱPr₂C₆H₃ (DippFormH), *o*-HC₆F₄ (TFFormH), FC₆H₄ (FFormH).

A series of reactive, monomeric divalent lanthanoid formamidinates [Yb(Form)₂(thf)₂] (Form = [RNCHNR]; R = *o*-MeC₆H₄ (*o*-TolForm), 2,6-Me₂C₆H₃ (XylForm), 2,4,6-Me₃C₆H₂ (MesForm), 2,6-Et₂C₆H₃ (EtForm), *o*-PhC₆H₄ (*o*-PhPhForm), 2,6-ⁱPr₂C₆H₃ (DippForm), *o*-HC₆F₄ (TFForm), FC₆H₄ (FForm), [Sm(DippForm)₂(thf)₂] and [Eu(DippForm)₂(thf)₂] have been synthesised by the redox transmetallation/protolysis (RTP) reactions between an excess of a lanthanoid metal, Hg(C₆F₅)₂ and the corresponding formamidine (HForm) (Eqn. 4.1).^{13, 14} The complexes feature chelating N, N'-Form ligands and two *cis*-thf donors. [Sm(DippForm)₂(thf)₂] was also synthesised by the metathesis/salt elimination reaction between NaDippForm and [Sm(I)₂(thf)₂] in thf.¹⁵

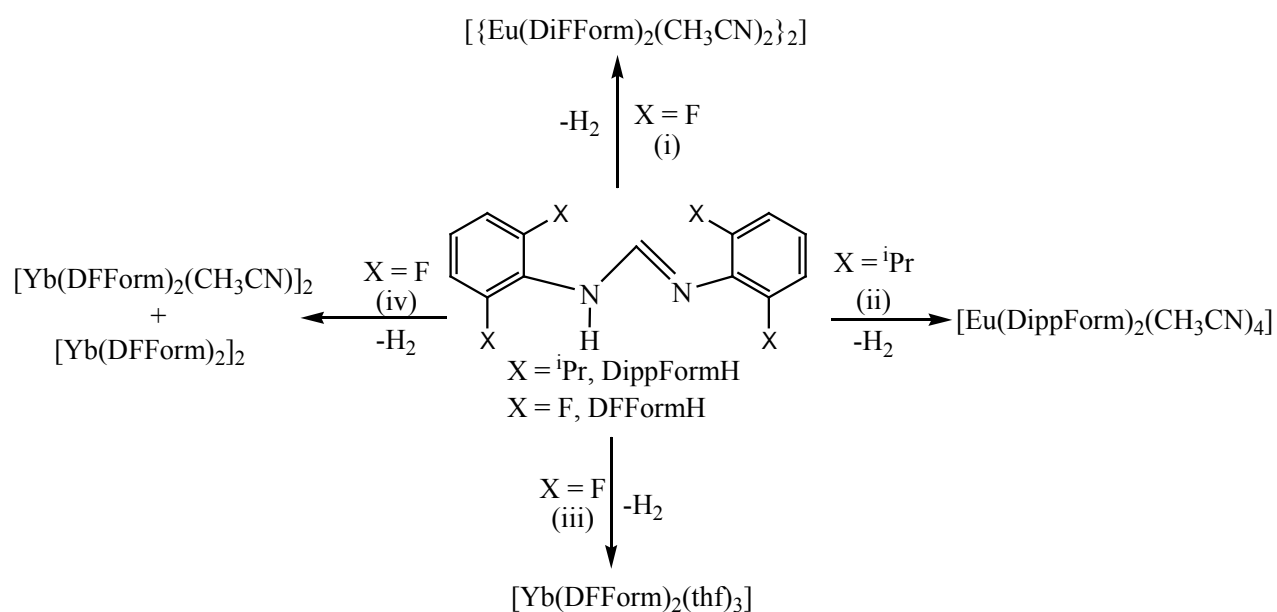
Chapter 4

Syntheses by direct metalation reactions, without the requirement of an organomercurial co-oxidant as in RTP reactions have been introduced recently for the synthesis of divalent lanthanoid complexes.¹⁶ This approach was successful for the synthesis of some divalent europium and ytterbium complexes using acetonitrile as a solvent (Scheme 4.1). However, the ytterbium metal required activation by two drops of Hg^0 to initiate the reactions. Some other divalent compounds of ytterbium such as $[\text{Yb}(\text{DippForm})_2(\text{thf})]$, $[\text{Yb}(\text{DippForm})_2(\text{CH}_3\text{CN})_3]$, $[\text{Yb}(\text{DippForm})_2(\text{CH}_3\text{CN})_2]$, $[\text{Yb}(\text{FForm})_2(\text{thf})_2]$ and $[\text{Yb}(\text{DFForm})_2(\text{dme})]$ have been synthesised by RTP reactions followed by crystallisation in solvents other than thf.^{14, 16}

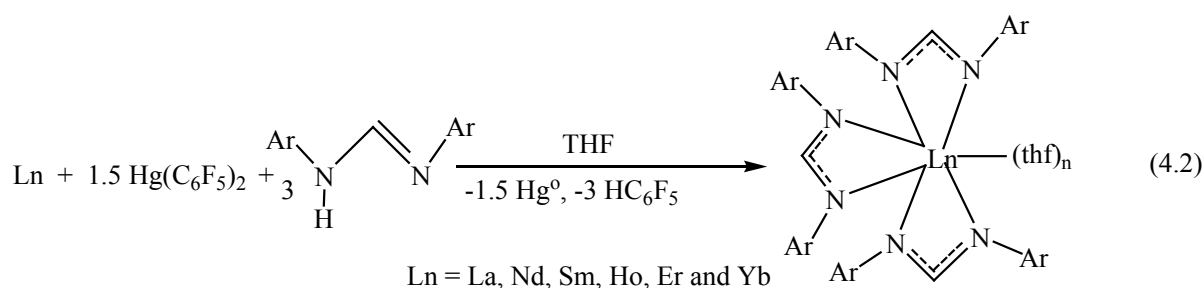


A series of tris(formamidinato)lanthanoid(III) complexes, $[\text{Ln}(\text{Form})_3(\text{thf})_n]$, viz. $[\text{La}(o\text{-TolForm})_3(\text{thf})_2]$, $[\text{Er}(o\text{-TolForm})_3(\text{thf})]$, $[\text{La}(\text{XylForm})_3(\text{thf})]$, $[\text{Sm}(\text{XylForm})_3]$, $[\text{Ln}(\text{MesForm})_3]$ ($\text{Ln} = \text{La, Nd, Sm}$ and Yb), $[\text{Ln}(\text{EtForm})_3]$ ($\text{Ln} = \text{La, Nd, Sm, Ho}$ and Yb), and $[\text{Ln}(o\text{-PhPhForm})_3]$ ($\text{Ln} = \text{La, Nd, Sm}$ and Er) complexes has been synthesised by RTP reactions between N, N'-bis(aryl)formamidines, an excess of lanthanoid metal and bis(pentafluorophenyl) mercury ($\text{Hg}(\text{C}_6\text{F}_5)_2$) in thf (Eqn. 4.2).¹⁷ On the contrary, $[\{\text{Yb}(o\text{-TolForm})_2(\mu\text{-OH})(\text{thf})\}_2]$ was isolated unexpectedly from the analogous attempts to prepare $[\text{Yb}(o\text{-TolForm})_3]$ by the RTP reaction. $[\text{Yb}(o\text{-TolForm})_3(\text{thf})]$ was isolated from a metathesis reaction of YbCl_3 and $o\text{-TolFormLi}$ in thf. The bulkier formamidine, DippFormH gave $[\text{Ln}(\text{DippForm})_2\text{F}(\text{thf})]$ ($\text{Ln} = \text{La, Ce, Nd, Sm}$ and Tm) featuring C-F activation of the implied $[\text{Ln}(\text{DippForm})_2\text{C}_6\text{F}_5]$ intermediates. The reaction of bis(phenylethynyl)mercury ($\text{Hg}(\text{C}\equiv\text{CPh})_2$), Nd metal and DippFormH in thf resulted in the formation of $[\text{Nd}(\text{DippForm})_2(\text{C}\equiv\text{CPh})(\text{thf})]$ with a rare (for Ln) terminal $\text{C}\equiv\text{CPh}$ group. The oxidation of $[\text{Sm}(\text{DippForm})_2(\text{thf})_2]$ with $\text{Hg}(\text{C}\equiv\text{CPh})_2$ afforded the similar complex involving samarium, $[\text{Sm}(\text{DippForm})_2(\text{C}\equiv\text{CPh})(\text{thf})]$.

Chapter 4



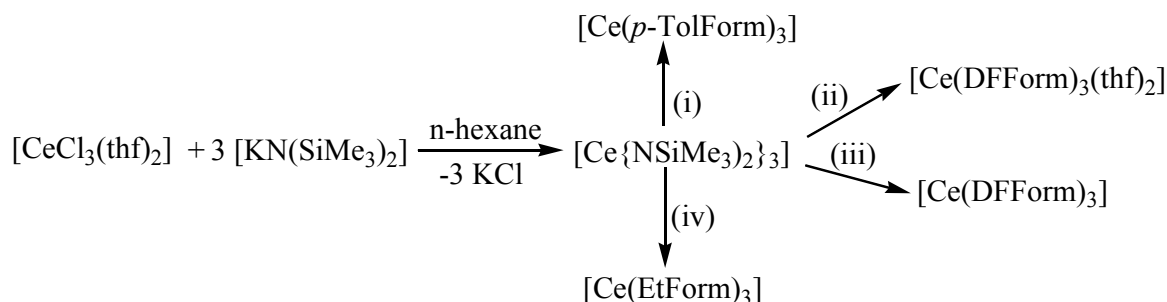
Scheme 4.1: Direct metalation synthesis of divalent rare-earth ArForm complexes (i) Eu^0 , CH_3CN , 16 h, room temperature; (ii) Eu^0 , CH_3CN , 24 h, 60 °C; (iii) Yb^0 , Hg^0 (two drops), thf/CH_3CN , 24 h, 50 °C; (iv) Yb^0 , Hg^0 (one drop), CH_3CN , 10 h, room temperature, crystallised from toluene.



RTP reactions between rare-earth metals, $Hg(C_6F_5)_2$, and N, N'-bis(4-methylphenyl)-formamidine (*p*-TolFormH) in *thf* followed by the addition of non-coordinating solvents (hexane or toluene) afforded unsolvated dimeric complexes $[Ln(p\text{-TolForm})_3]_2$ [$Ln = La, Ce, Nd, Sm$], containing rare $\mu\text{-}1\kappa(N, N'):2\kappa(N, N')$ formamidinate ligands bridging between the two metal centres. However, the smaller lutetium analogue $[Lu(p\text{-TolForm})_3(thf)]$ remains solvated with a seven-coordinate monomeric structure. In order to examine the reactivity of $[Sm(p\text{-TolForm})_3]_2$, it has been treated with triphenylphosphine oxide, DFFormH and $[K(p\text{-TolForm})(18\text{-Crown-}6)]$ producing $[Sm(p\text{-TolForm})_3(Ph_3PO)_2]$,

Chapter 4

Protolysis reactions between $[\text{Ce}\{\text{N}(\text{SiMe}_3)_2\}_3]$ and a stoichiometric amount of the corresponding formamidine ligands DFFormH, EtFormH, and *p*-TolFormH gave the trivalent cerium complexes $[\text{Ce}(\text{DFForm})_3(\text{thf})_2]$ and $[\text{Ce}(\text{DFForm})_3]$, $[\text{Ce}(\text{EtForm})_3]$, and $[\text{Ce}(p\text{-TolForm})_3]$, respectively (Scheme 4.3).²⁰ A bimetallic cerium/lithium complex $[\text{LiCe}(\text{DFForm})_4]$ was also synthesised by the treatment of the mixture of $[\text{Ce}\{\text{N}(\text{SiHMe}_2)_2\}_3(\text{thf})_2]$, $[\text{Li}\{\text{N}(\text{SiHMe}_2)_2\}]$ and DFFormH in toluene. Attempted oxidation of $[\text{Ce}(\text{DFForm})_3(\text{thf})_2]$ and $[\text{Ce}(\text{EtForm})_3]$ with Ph_3CCl resulted in $[\text{Ce}_3\text{Cl}_5(\text{DFForm})_4(\text{thf})_4]$ and $[\text{Ce}(\text{EtForm})\text{Cl}_2(\text{thf})_3]$, respectively. The cerium(III) formamidinate complex $[\{\text{Ce}(p\text{-TolForm})_3\}_2]$ was also prepared by the protolysis reaction between $[\text{Ce}\{\text{N}(\text{SiMe}_3)_2\}_3]$ and *p*-TolFormH which was previously reported by an alternative RTP synthesis. Moreover, the first structurally characterised homoleptic cerium(IV) formamidinate complex $[\text{Ce}(p\text{-TolForm})_4]$ (Fig. 4.3) was achieved by protolysis reaction between $[\text{Ce}\{\text{N}(\text{SiHMe}_2)_2\}_4]$ and four equivalents of *p*-TolFormH. The cerium(IV) silylamide complex $[\text{Ce}\{\text{N}(\text{SiMe}_3)_2\}_3(\text{bda})_{0.5}]_2$ (bda = 1,4-benzenediolato) was synthesised by treating $[\text{Ce}\{\text{N}(\text{SiMe}_3)_2\}_3]$ and half an equivalent of 1,4-benzoquinone.



Scheme 4.3: Reaction time for each complex: 16 h. In each reaction three equivalents of $\text{HN}(\text{SiMe}_3)_2$ were produced and removed by vacuum drying (2–5 h). (i) 3 *p*-TolFormH, toluene or diethyl ether; (ii) 3 DFFormH, thf; (iii) 3 DFFormH, toluene; (iv) 3 EtFormH, thf.

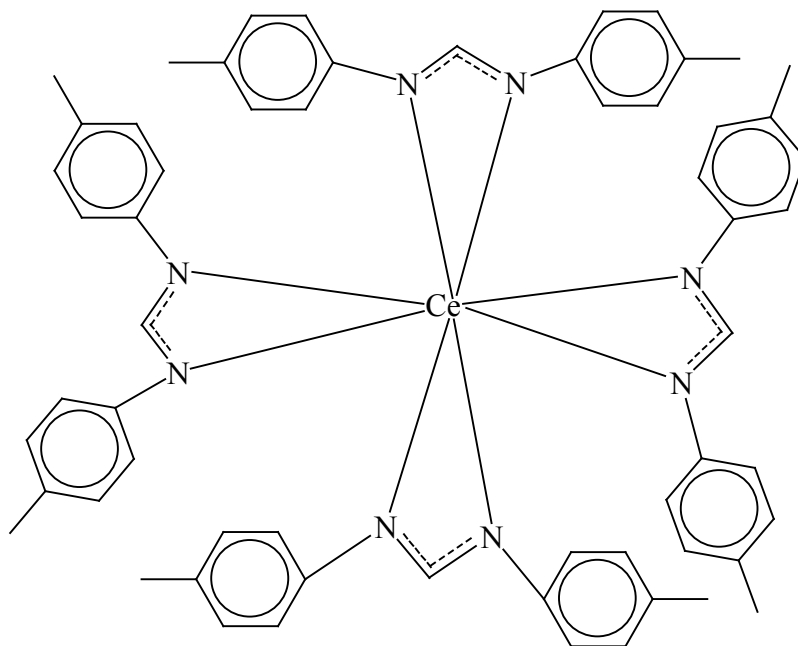
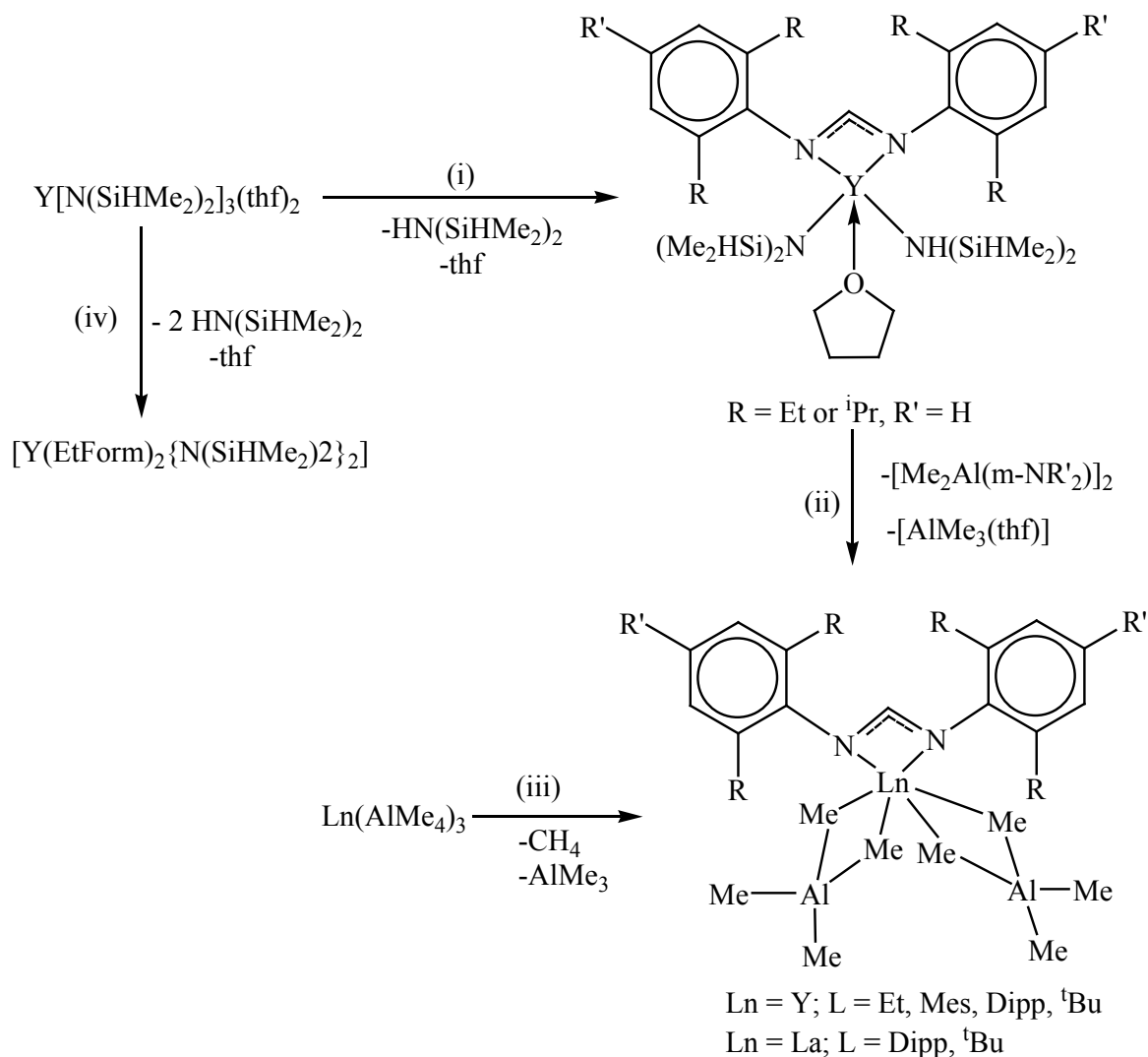


Fig. 4.3. Molecular structure of [Ce(*p*-TolForm)₄].

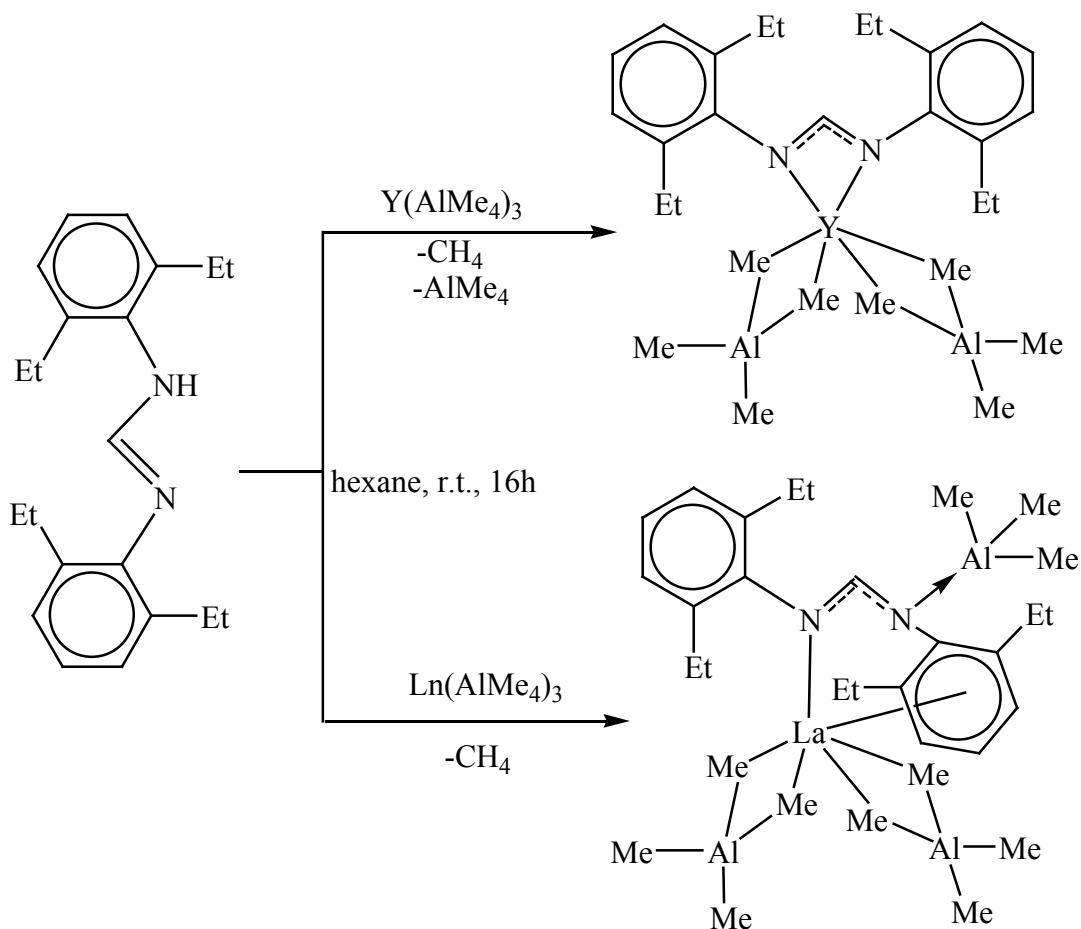
Rare earth tetramethylaluminate complexes bearing formamidinato N-ancillary ligands have been synthesised and the catalytic activity of the complexes for isoprene polymerisation has been tested. Protolysis reactions of [Y{N(SiHMe₂)₂}₃(thf)₂] with EtFormH and DippFormH produced the corresponding [Y(Form){N(SiHMe₂)₂}₂(thf)] complexes, subsequently provide [Y(Form)(AlMe₄)₂] complexes after treatment with AlMe₃ (Scheme 4.4). An unsolvated product [Y(EtForm)₂{N(SiHMe₂)₂}₂] was also isolated by a double protolysis of [Y{N(SiHMe₂)₂}₃(thf)₂] in hexane. The bimetallic formamidinate complexes, [Ln(Form)(AlMe₄)₂] (Ln = Y, Form = EtForm, MesForm, DippForm, ^tBuForm (Ar = 2-^tBuC₆H₄); Ln = La, Form = DippForm, ^tBuForm) have been synthesised by the protolysis reactions of formamidines and homoleptic rare earth metal tetramethylaluminates Ln(AlMe₄)₃ in high yield (Scheme 4.4). These complexes have a distorted-octahedral geometry with the six coordinate metal ligated by two nitrogen atoms of the formamidinato ligand and two methyl carbons of each of the η²-coordinated tetramethylaluminate moieties.²¹

Chapter 4



Scheme 4.4: (i) Et- or DippFormH, hexane, r.t., 16 h; (ii) 4AlMe₃, C₆D₆, r.t., 1 h; (iii) LFormH, hexane, r.t., 16h; (iv) 2 EtFormH, hexane, r.t., 16 h.

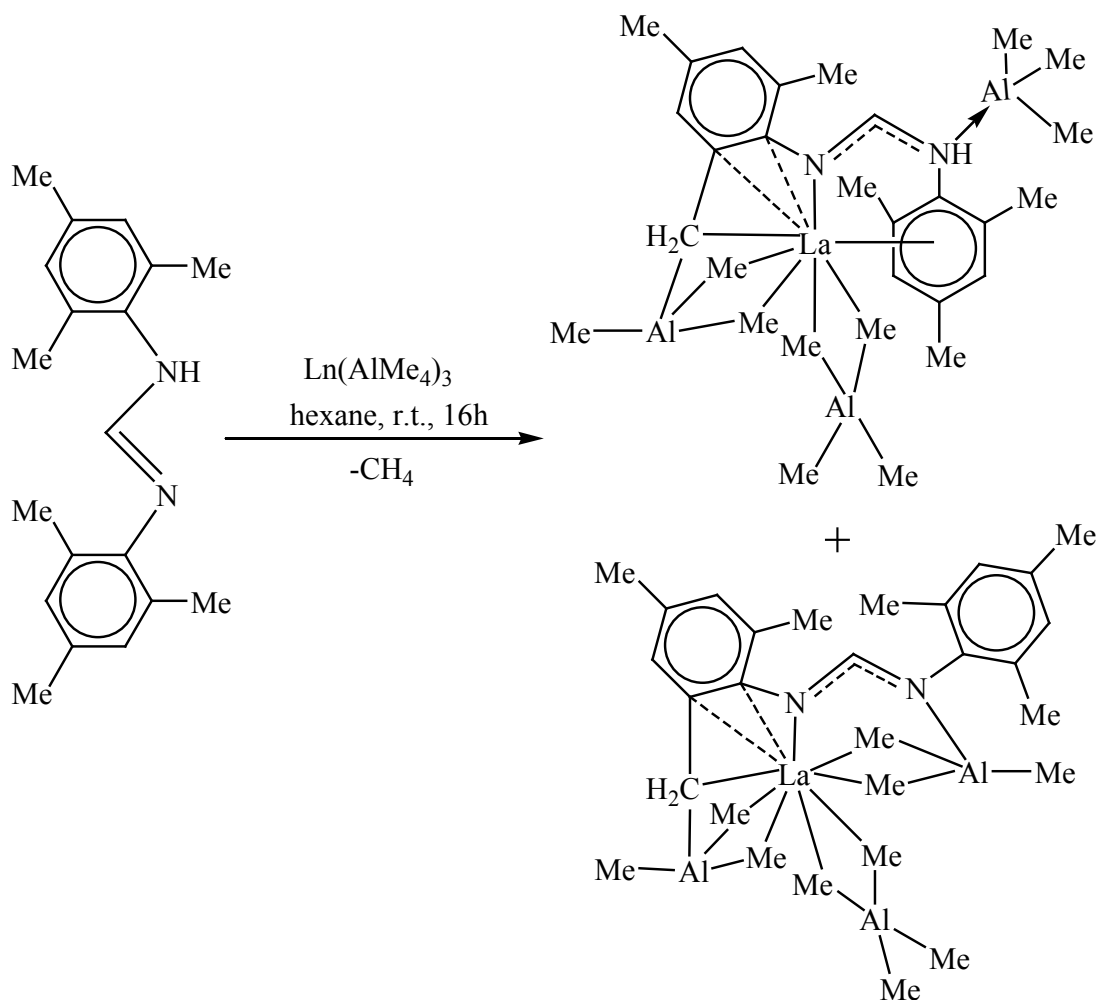
A protolysis reaction between La(AlMe₄)₃ and EtFormH resulted in a compound, [La(EtFormAlMe₃)(AlMe₄)₂](C₇H₈)_{1.5} containing a metal- π -arene interaction. In contrast to the six-coordinate [Ln(Form)(AlMe₄)₂], an eight-coordinate configuration in [La(EtFormAlMe₃)(AlMe₄)₂](C₇H₈)_{1.5} resulted from the coordination of one nitrogen of EtForm and one aryl substituent to the lanthanum atom in an $\eta^1(\text{N})\text{:}\eta^6(\text{arene})$ manner (Scheme 4.5).



Scheme 4.5: Syntheses of lanthanoid-aluminium complexes.

The reaction of the homoleptic precursor $\text{La(AlMe}_4)_3$ with one equivalent of MesFormH in hexane formed $[\text{La}(\text{Me}_2\text{CH}_2\text{FormAlMe}_3)(\text{AlMe}_3)(\text{AlMe}_4)]$ ($\text{Me}_2\text{CH}_2\text{Form} = \text{MesForm-H}(o\text{-Me})$) having a C–H bond activation of an *o*-methyl group of the mesityl moiety (Scheme 4.6). The high mobility of the aluminate methyl groups facilitated the C–H activation reactions.

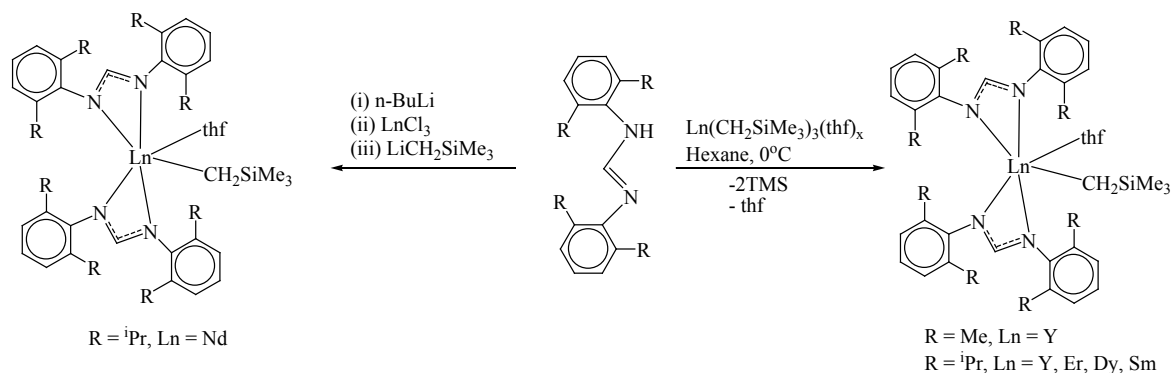
The catalytic activity of the compounds $[\text{Ln}(\text{Form})(\text{AlMe}_4)_2]$ ($\text{Ln} = \text{Y, La}$; $\text{Form} = \text{EtForm, DippForm}$) in isoprene polymerisation were investigated by activating them with $[\text{Ph}_3\text{C}][\text{B}(\text{C}_6\text{F}_5)_4]$ or $[\text{PhNMe}_2\text{H}][\text{B}(\text{C}_6\text{F}_5)_4]$. At ambient temperature, polyisoprene of narrow molecular weight distribution ($\text{PDI} < 1.2$) was produced. The cocatalysts were stereoselective; trityl borate gave *trans*-1,4-selectivity (maximum 87%), while the anilinium borate favors *cis*-1,4-selectivity (maximum 82%).²¹



Scheme 4.6: Syntheses of lanthanoid-aluminium complexes.

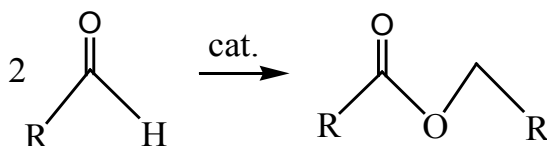
Alkyl elimination or salt metathesis reactions afforded a series of rare-earth metal monoalkyl complexes supported by the N, N'-di(2,6-dialkylphenyl)formamidine ligand $[\text{LnL}_2\text{CH}_2\text{SiMe}_3\cdot\text{thf}]$ [$\text{L} = \text{HC}(\text{N}-2,6\text{-Me}_2\text{C}_6\text{H}_3)_2$, $\text{Ln} = \text{Y}$, $\text{L} = \text{HC}(\text{N}-2,6\text{-}^i\text{Pr}_2\text{C}_6\text{H}_3)_2$; $\text{Ln} = \text{Y}$, Er, Dy, Sm, and Nd] in good yields (Scheme 4.7). These compounds were combined with $[\text{Ph}_3\text{C}][\text{B}(\text{C}_6\text{F}_5)_4]$ and alkylaluminum to test the catalytic activity for isoprene polymerisation. The catalytic activity towards isoprene polymerisation was good and polyisoprenes with high molecular weight ($M_n > 10^4$) and narrow molecular distribution ($\text{PDI} < 2.0$) were obtained. If the catalysts were added in the order $[\text{RE}]/[\text{alkylaluminum}]/[\text{borate}]$, 1,4- regioselectivity was reported as high as 98%.³¹

Chapter 4



Scheme 4.7: Alkyl elimination reactions for syntheses of rare-earth metal monoalkyl complexes.

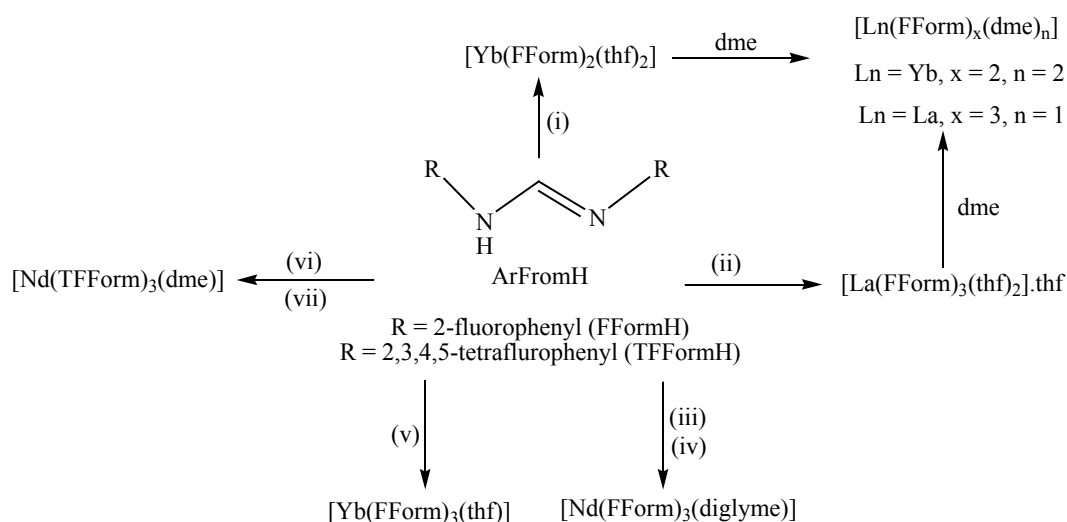
Moreover, the catalytic activity of some tris(formamidinato)lanthanum(III) complexes for the Tishchenko reaction has been reported. The dimerisation of an aldehyde to the corresponding carboxylic ester (Scheme 4.8) is commonly known as the industrially important Tishchenko reaction. $[La(o-TolForm)_3(thf)_2]$, $[La(XylForm)_3(thf)]$, and $[La(EtForm)_3]$ were examined as precatalysts for the Tishchenko reaction and the first compound was found as the most efficient catalyst ever reported. The catalytic activity of these compounds is due to their high Lewis acidity and easily interchangeable ligand spheres.²²



Scheme 4.8: Tishchenko reaction.

RTP reactions involving Ln (Ln = Yb, La, Nd), $Hg(C_6F_5)_2$ and the FFormH ligand produced the trivalent complexes $[Yb(FForm)_3(thf)]$, $[La(FForm)_3(thf)_2].thf$ and $[Nd(FForm)_3(thf)_x]$ ($x = 1-2$). Further recrystallisations of the complexes from either dme or diglyme/hexane gave $[La(FForm)_3(dme)]$ and $[Nd(FForm)_3(diglyme)].diglyme$ complexes suitable for X-ray crystallography. Moreover, an RTP reaction involving TFormH and Nd followed by crystallisation from dme resulted in $[Nd(TFForm)_3(dme)]$. The heat treatment of the divalent $[Yb(TFForm)_2(thf)_3]$ in PhMe and diglyme yielded the complexes $[Yb(TFForm)_3(thf)_2]$ and $[Yb(TFForm)(diglyme)_2][Yb(TFForm)_4]$, respectively. The syntheses of these complexes are illustrated in scheme 4.9.¹⁴

Chapter 4

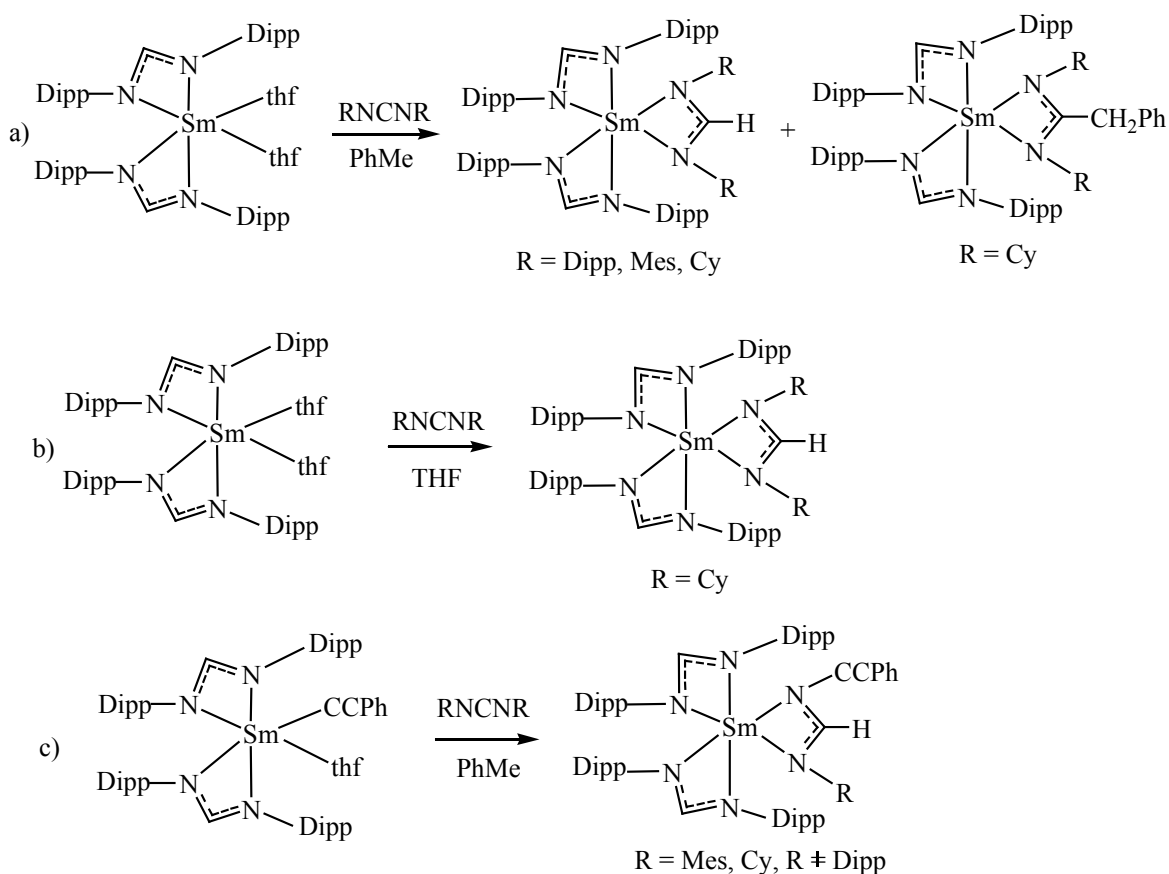


Scheme 4.9: (i) Yb^0 (excess), $\text{Hg}(\text{C}_6\text{F}_5)_2$, 2 FFormH, thf, sonication 1 d, $-\text{Hg}^0$, $-2 \text{C}_6\text{F}_5\text{H}$; (ii) La^0 , 1.5 $\text{Hg}(\text{C}_6\text{F}_5)_2$, 3 FFormH, thf, 60 °C 2 d, -1.5Hg^0 , $-3 \text{C}_6\text{F}_5\text{H}$; (iii) Nd^0 , 1.5 $\text{Hg}(\text{C}_6\text{F}_5)_2$, 3 FFormH, thf, sonication 2 d, -1.5Hg^0 , $-3 \text{C}_6\text{F}_5\text{H}$; (iv) diglyme/hexane; (v) Yb^0 (slight excess), 1.5 $\text{Hg}(\text{C}_6\text{F}_5)_2$, 3 FFormH, thf, room temperature, 2 d, -1.5Hg^0 , $-3 \text{C}_6\text{F}_5\text{H}$; (vi) Nd^0 , 1.5 $\text{Hg}(\text{C}_6\text{F}_5)_2$, 3 TFFormH, thf, sonication 2 d, -1.5Hg^0 , $-3 \text{C}_6\text{F}_5\text{H}$; (vii) evaporation followed by crystallisation from dme/PhMe.

Highly crowded samarium complexes, $[\text{Sm}(\text{L})_3]$ and $[\text{Sm}(\text{L})_2(\text{L}')] (L = \text{formamidinate and } L' = \text{formamidinate or amidinate})$ have been synthesised by the oxidation of divalent $[\text{SmL}_2(\text{thf})_2]$ species or the insertion reactions of trivalent $[\text{Sm}(\text{L})_2(\text{C}\equiv\text{CPh})(\text{thf})]$ complexes with carbodiimides (RNCNR ; $\text{R} = \text{Cy, Mes, Dipp}$). It was noticed that the size of the R substituent on the carbodiimide influenced the reaction outcomes significantly. The homoleptic tris(formamidinato)samarium(III) complex, $[\text{Sm}(\text{L})_3]$ (Scheme 4.10a) was obtained by the oxidation of $[\text{SmL}_2(\text{thf})_2]$ with *N,N'*-di(2,6-diisopropylphenyl)carbodiimide (DippNCNDipp) in PhMe in good yield. This compound was previously isolated by a different reaction route¹⁵; however, the current route was described as a simpler one with improved yield. The heteroleptic complex, $[\text{Sm}(\text{L})_2(\text{MesNC}(\text{H})\text{NMe})]$ (Scheme 4.10a) was obtained from the same reaction of $[\text{SmL}_2(\text{thf})_2]$ with RNCNR ($\text{R} = \text{Mes}$) but this reaction with $\text{R} = \text{Cy}$ gave a mixture of products. Fractional crystallisation of that mixture afforded two complexes, $[\text{SmL}_2(\text{CyNC}(\text{CH}_2\text{Ph})\text{NCy})]$ and $[\text{SmL}_2(\text{CyNC}(\text{H})\text{NCy})]$. In contrast, pure $[\text{SmL}_2(\text{CyNC}(\text{H})\text{NCy})]$ was isolated solely by using thf as solvent (Scheme 4.10b). Treatment of $[\text{Sm}(\text{L})_2(\text{C}\equiv\text{CPh})(\text{thf})]$ and carbodiimides RNCNR ($\text{R} = \text{Cy, Mes}$) resulted in $[\text{Sm}(\text{L})_2(\text{RNC}(\text{C}\equiv\text{CPh})\text{NR})]$ ($\text{R} = \text{Cy or Mes}$) and are analogues of

Chapter 4

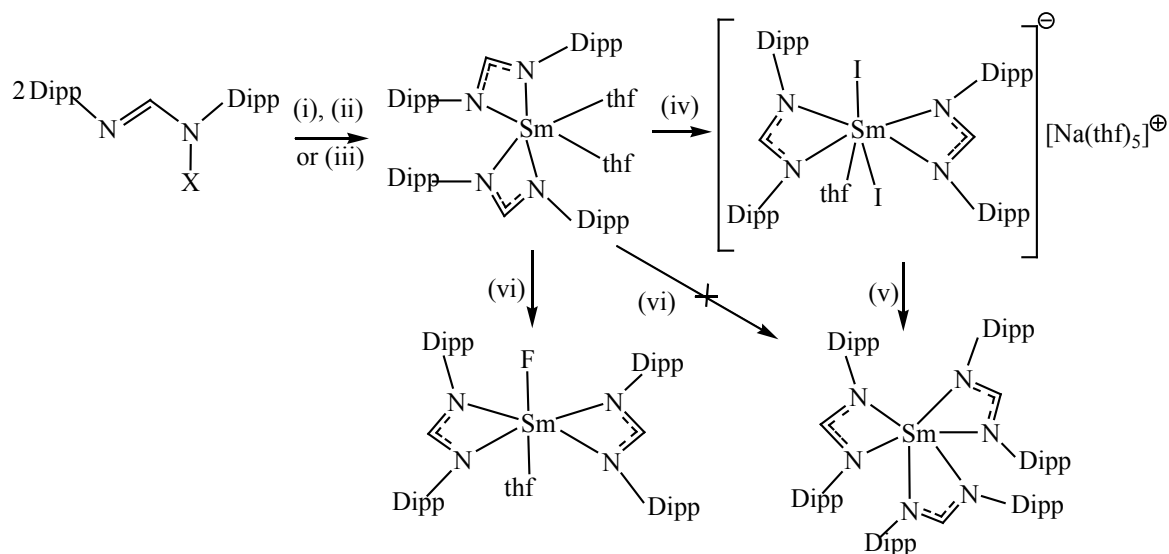
$[\text{SmL}_2(\text{CyNC}(\text{CH}_2\text{Ph})\text{NCy})]$ but no product was obtained from the reaction of $[\text{Sm}(\text{L})_2(\text{C}\equiv\text{CPh})(\text{thf})]$ with DippNCNDipp (Scheme 4.10c).²³



Scheme 4.10: Syntheses of highly crowded samarium complexes.

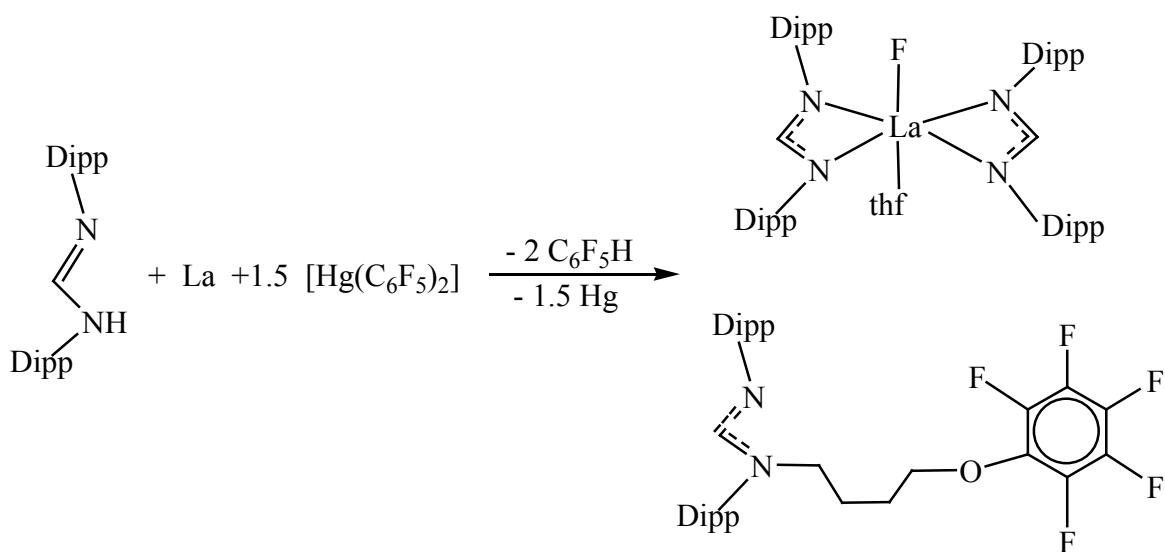
The synthesis of the dark green $[\text{Sm}(\text{DippForm})_2(\text{thf})_2]$ complex was accomplished by three different synthetic routes (Scheme 4.11). From the structural data, it was observed that $[\text{Sm}(\text{DippForm})_2(\text{thf})_2]$ is hexacoordinated and isomorphous with the related strontium and barium amidinates. During the synthesis of the divalent product of samarium, a colourless crystalline trivalent samarium compound was isolated as co-product and confirmed by single crystal X-ray diffraction as the samarate $[\text{Na}(\text{thf})_5][\text{Sm}(\text{I})_2(\text{DippForm})_2(\text{thf})]$. Dissolution of this product in hexane gave homoleptic $[\text{Sm}(\text{DippForm})_3]$ with simultaneous precipitation of NaI and $[\text{Sm}(\text{I})_3(\text{thf})_{3.5}]$. Moreover, the monofluoro-bis(amidinate) $[\text{SmF}(\text{DippForm})_2(\text{thf})]$ has been isolated from a reaction mixture that underwent C-F activation.¹⁵

Chapter 4



Scheme 4.11: (i) X = Na, $\text{SmI}_2(\text{thf})_2$; (ii) X = H, $\text{Sm}/\text{Hg}(\text{C}_6\text{F}_5)_2$; (iii) X = H, $\text{Sm}[\text{N}(\text{SiMe}_3)_2]_2(\text{thf})_2$; (iv) $\text{SmI}_2(\text{thf})_2/\text{NaI}$; (v) Dissolution in hexane; (vi) DippFormH , $\text{Hg}(\text{C}_6\text{F}_5)_2$.

The lanthanoid-formamidinate complex, $[\text{LaF}\{\text{DippForm}\}_2(\text{thf})]$ with a rare terminal La–F bond has been synthesised by the reaction of elemental lanthanum with $\text{Hg}(\text{C}_6\text{F}_5)_2$ and DippFormH in thf (Scheme 4.12). A novel functionalised formamidinate was found as a by-product of this reaction, which resulted from the ring opening of thf. X-ray crystal structure confirmed the six coordinate lanthanum centre with *cisoid* DippForm ligands.²⁴



Scheme 4.12: Lanthanoid-formamidinate complex with a terminal La–F bond.

Chapter 4

The samarium complex $[\{(Me_3Si)_2N\}_2Sm\{\mu-(RNC(H)N(Ar-Ar)NC(H)NR)\}Sm\{N(SiMe_3)_2\}_2]$ ($R = C_6H_3-2,6-iPr_2$; $Ar-Ar = C_6H_3-2-iPr-6-C(CH_3)_2C(CH_3)_2-6'-C_6H_3-2'-iPr$) featuring a coupled bis(formamidinate) ligand was synthesised by the reaction of N,N' -bis(2,6-diisopropylphenyl)carbodiimide and $[Sm\{N(SiMe_3)_2\}_2(thf)_2]$ in hexane (Fig. 4.4).²⁵ Moreover, treating $Li(DippForm)$ with anhydrous samarium trichloride and $Li_2(COT'')$ [$COT'' = 1,4$ -bis(trimethylsilyl)cyclooctatetraenyl] in thf afforded the complex N, N' -bis(2,6-diisopropylphenyl) formamidinato][η^8 -1,4-bis(trimethylsilyl)cyclooctatetraenyl](tetrahydrofuran)samarium(III).³² Following a similar method, $[Yb(DippForm)(COT'')(thf)]$ has also been synthesised (Scheme 4.13).³³

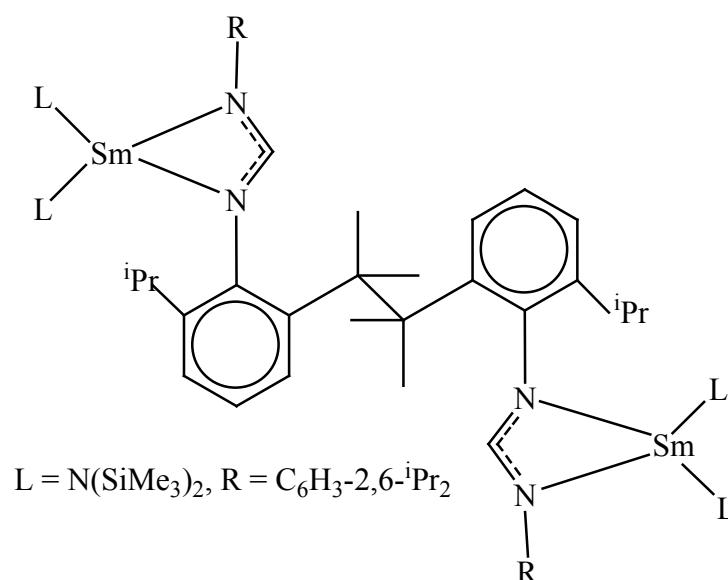
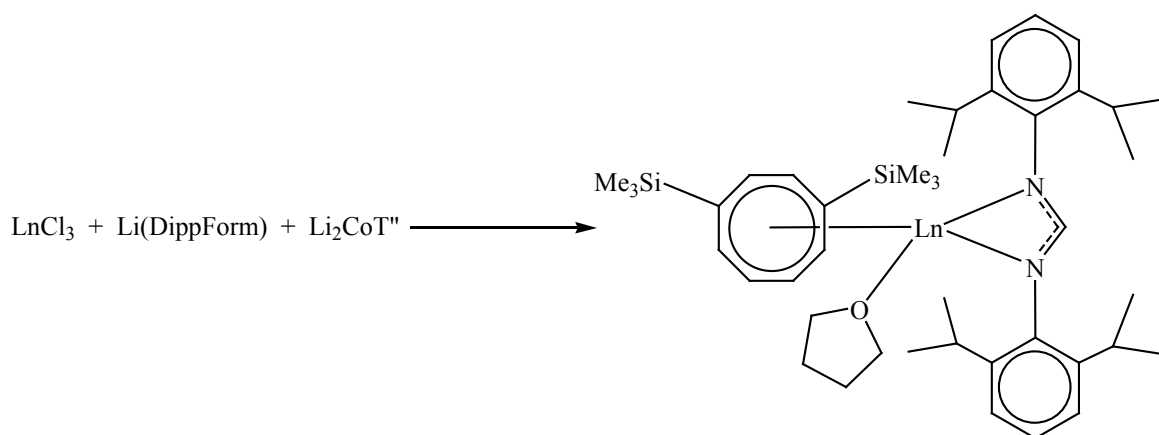


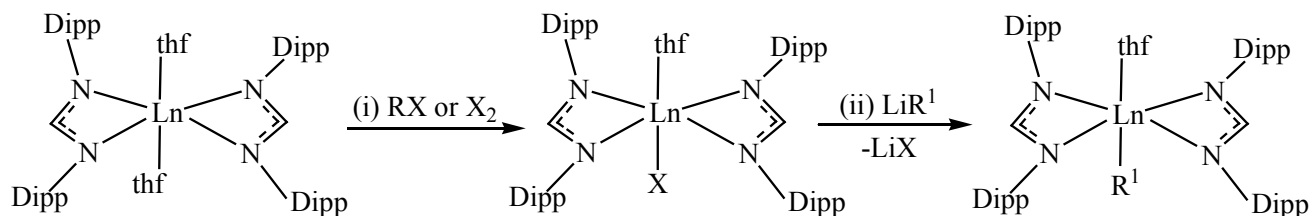
Fig. 4.4: Molecular structure of $[\{(Me_3Si)_2N\}_2Sm\{\mu-(RNC(H)N(Ar-Ar)NC(H)NR)\}Sm\{N(SiMe_3)_2\}_2]$.



Scheme 4.13: Syntheses of $[Ln(DippForm)(COT'')(thf)]$ complexes ($Ln = Sm, Yb$).

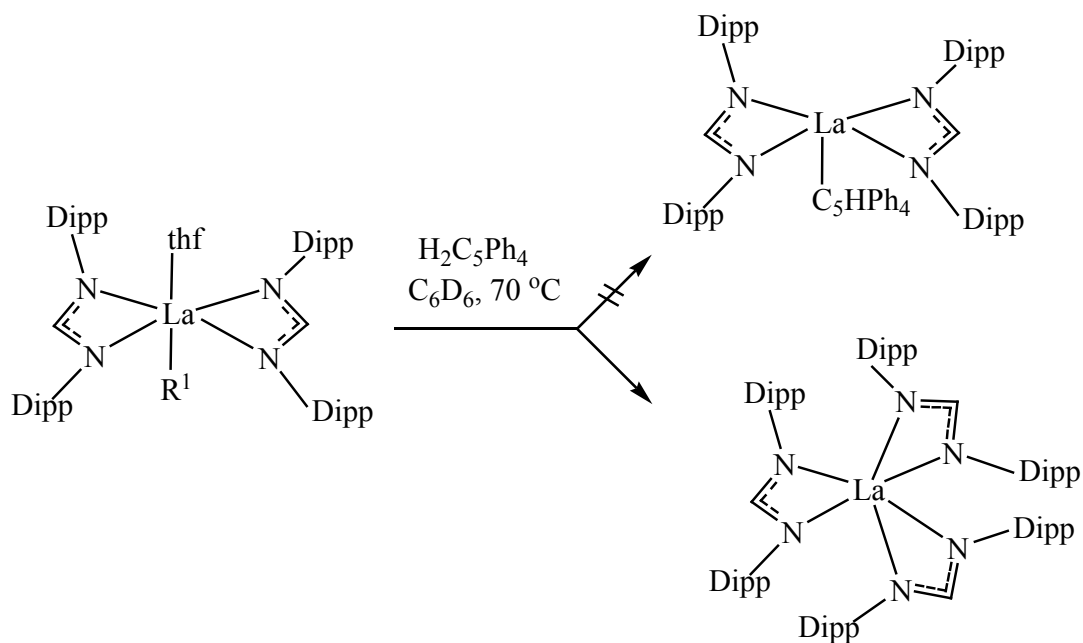
Chapter 4

A series of bulky formamidinate supported samarium(III) halide complexes, $[\text{Sm}(\text{DippForm})_2\text{X}(\text{thf})]$ ($\text{X} = \text{Cl}$, $\text{X} = \text{Br}$, $\text{X} = \text{I}$) have been synthesised by the oxidation of $[\text{Sm}(\text{DippForm})_2(\text{thf})_2]$ with *tert*-butyl chloride, 1,2-dibromoethane, and iodine, respectively, at ambient temperature (Scheme 4.14). Compounds with a rare terminal La-Me species, $[\text{Ln}(\text{DippForm})_2\text{Me}(\text{thf})]$ ($\text{Ln} = \text{Sm}$, $\text{Ln} = \text{La}$) and $[\text{Sm}(\text{DippForm})_2(\text{CH}_2\text{SiMe}_3)(\text{thf})]$ have been synthesised by the subsequent metathesis reactions of lanthanoid halides $[\text{Ln}(\text{DippForm})_2\text{X}(\text{thf})]$ ($\text{Ln} = \text{Sm}$, La ; $\text{X} = \text{Cl}$, F) with lithium reagents LiMe and $\text{LiCH}_2\text{SiMe}_3$, respectively at ambient temperature in toluene (Scheme 4.14). The homoleptic tris(formamidinato)lanthanum complex, $[\text{La}(\text{DippForm})_3]$ resulted unexpectedly from the reaction of $[\text{La}(\text{DippForm})_2\text{Me}(\text{thf})]$ with 1,2,3,4-tetraphenylcyclopentadiene in very low yield (Scheme 4.15). The mono(formamidinato)samarium(III) complex $[\text{Sm}(\text{DippForm})\text{Br}_2(\text{thf})_3]$ formed as a coproduct with the bis(formamidinate), $[\text{Sm}(\text{DippForm})_2\text{Br}(\text{thf})]$ from the redox transmetallation/protolysis reaction of samarium metal with bis(2-bromo-3,4,5,6-tetrafluorophenyl)mercury and DippFormH in *thf* (Scheme 4.16). The ethenolate complex $[\text{Sm}(\text{DippForm})_2(\text{OCH}=\text{CH}_2)(\text{thf})]$ (instead of the target $\text{Sm}-\text{Ph}$ complex) formed from the redox reaction of the divalent samarium complex $[\text{Sm}(\text{DippForm})_2(\text{thf})_2]$ with diphenylmercury (Scheme 4.16).²⁶

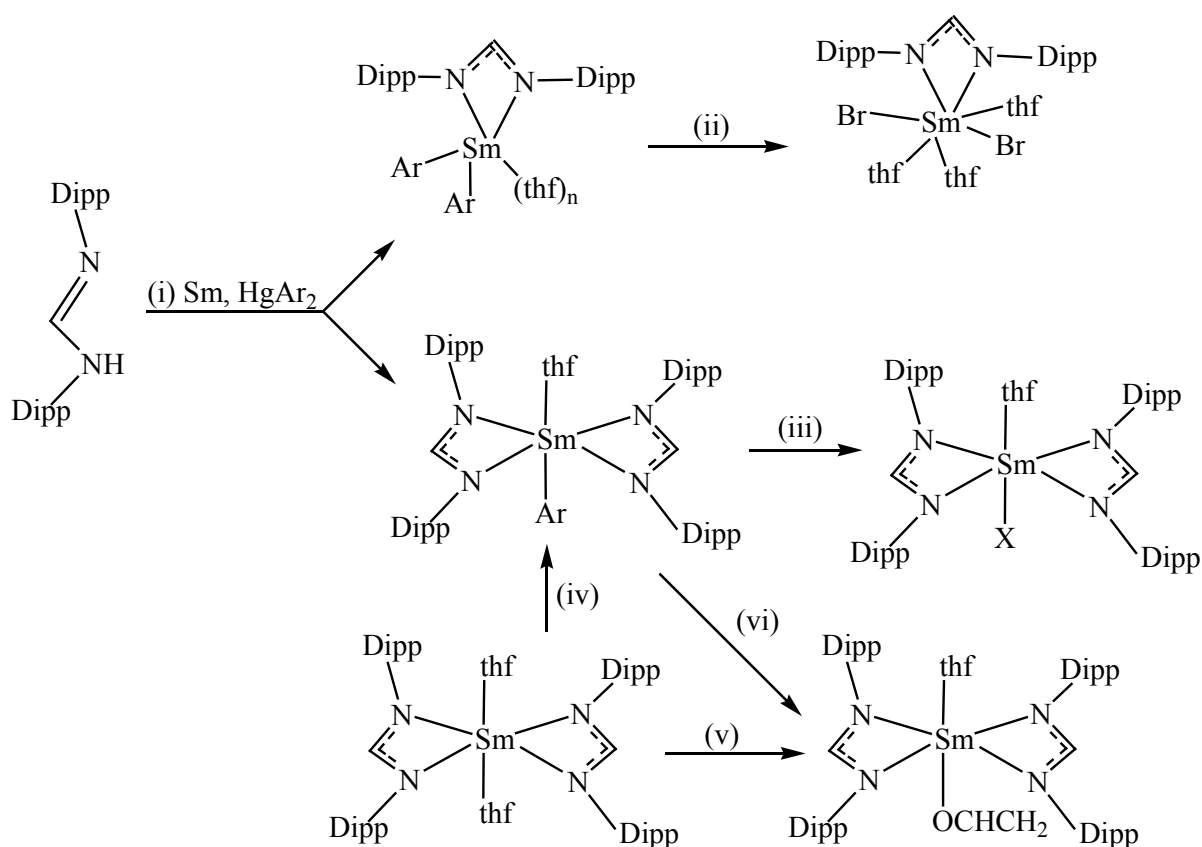


Scheme 4.14: (i) $\text{Ln} = \text{Sm}$, $\text{R} = \text{}^t\text{Bu}$, $\text{X} = \text{Cl}$; $\text{R} = \text{BrC}_2\text{H}_4$ or $2\text{-HC}_6\text{F}_4$, $\text{X} = \text{Br}$, $\text{X}_2 = \text{I}_2$; (ii) $\text{Ln} = \text{Sm}$, $\text{X} = \text{Cl}$, $\text{R}^1 = \text{Me}$; $\text{R}^1 = \text{CH}_2\text{SiMe}_3$; $\text{Ln} = \text{La}$, $\text{X} = \text{F}$, $\text{R}^1 = \text{Me}$.

Chapter 4



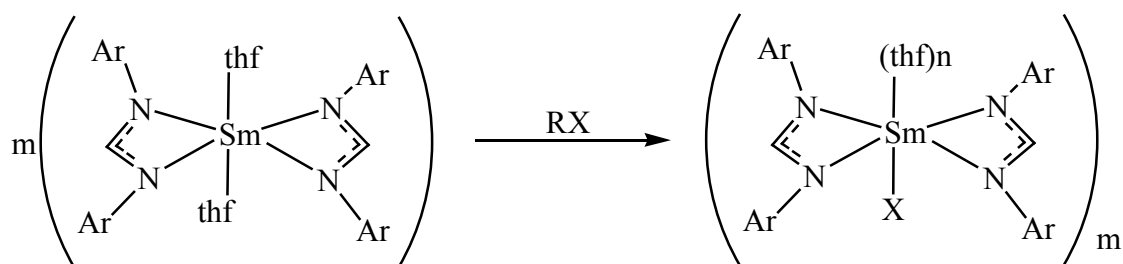
Scheme 4.15: Synthesis of homoleptic tris(formamidinato)lanthanum complex.



Scheme 4.16: (i) Ar = C₆F₅, 2-BrC₆F₄ (ii) Ar = 2-BrC₆F₄, X = Br (iii) Ar = C₆F₅, 2-BrC₆F₄; X = F, Br (iv) HgPh₂, PhMe, 110 °C, Ar = Ph (v) HgPh₂, PhMe, 110 °C (vi) thf, Ar = Ph.

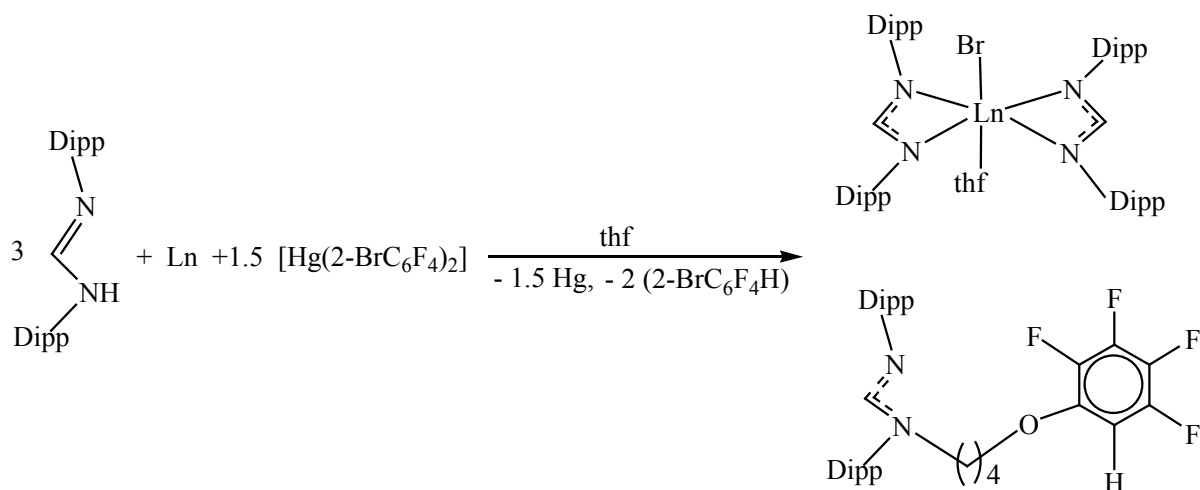
Chapter 4

The trivalent ytterbium–fluoride complexes $[\{Yb(EtForm)_2(\mu_2-F)\}_2]$ and $[\{Yb(o-PhPhForm)_2(\mu_2-F)\}_2]$ were obtained by the oxidation of compounds $[Yb(EtForm)_2(thf)_2]$ and $[Yb(o-PhPhForm)_2(thf)_2]$ with perfluorodecalin in thf at ambient temperature (Scheme 4.17). On the other hand, the oxidation of $[Yb(o-PhPhForm)_2(thf)_2]$ and $[Yb(DippForm)_2(thf)_2] \cdot 2THF$ with hexachloroethane and 1,2-dichloroethane in thf or toluene at room temperature gave $[Yb(o-PhPhForm)_2Cl(thf)_2] \cdot 2THF$ and $[Yb(DippForm)_2Cl(thf)] \cdot THF$, respectively (Scheme 4.17). An analogous terbium compound $[Tb(DippForm)_2Cl(thf)_2]$ was obtained by the metathesis reaction between $TbCl_3$ and $Na(DippForm)$. The reactions between excess Ln metal, $Hg(2-BrC_6F_4)_2$, and $DippFormH$ in thf at room temperature followed by crystallisation from toluene (Ln = La, Nd) or diethyl ether (Ln = Yb) yielded the complexes $[Ln(DippForm)_2Br(thf)] \cdot solv$ (Ln = La, Nd); solv = none; Ln = Yb, solv = Et_2O) (Scheme 4.18) with C-Br activation. $[Yb(DippForm)_2Br(thf)] \cdot Et_2O$ was synthesised by the treatment of $[Yb(DippForm)_2(thf)_2] \cdot 2THF$ and 1-bromo-2,3,4,5-tetrafluorobenzene (Scheme 4.17).¹³



Scheme 4.17: Ar = EtForm, RX = $C_{10}F_{18}$, X = F, n = 0, m = 2; Ar = *o*-PhPhForm, RX = $C_{10}F_{18}$, X = F, n = 0, m = 2; Ar = *o*-PhPhForm, RX = C_2Cl_6 , X = Cl, n = 2, m = 1; Ar = DippForm, RX = 1,2- $Cl_2C_2H_4$, X = Cl, n = 2, m = 1; Ar = DippForm, RX = *o*-HBrC₆F₄, X = Br, n = 1, m = 1.

Chapter 4



Scheme 4.18: Ln = La, Nd, Yb.

A heterobimetallic samarium(II)formamidinate complex has been synthesised, and selected reactions of samarium(II) complexes and one samarium(III) formamidinate complex with benzophenone or CS_2 have been reported. The heterobimetallic formamidinate samarium(II)/potassium complex $[\text{KSm}(\text{DippForm})_3]$ has been synthesised by the treatment of $[\text{Sm}(\text{DippForm})_3]$ and potassium graphite in toluene at elevated temperature (Fig. 4.5). In this complex, samarium is five coordinated by two chelating $\kappa(\text{N}, \text{N}')$ formamidinate ligands and a one 1κ formamidinate ligand having a link to potassium by an $\eta^6\text{-2,6}$ -diisopropylphenyl group and the other N atom. The reaction of $[\text{Sm}(\text{DippForm})_2(\text{thf})_2]$ with benzophenone resulted in the highly unusual $[\text{Sm}(\text{DippForm})_2(\text{thf})\{\mu\text{-OC}(\text{Ph})=(\text{C}_6\text{H}_5)\text{-C}(\text{Ph})_2\text{O}\}\text{Sm}(\text{DippForm})_2]$ ($\text{C}_6\text{H}_5 = 1,4\text{-cyclohexadiene-3-yl-6-ylidene}$) compound. This compound features a C-C coupling between a carbonyl carbon and the carbon at the *p*-position of a phenyl group of the OCPh_2 fragment. An isostructural complex $[(\text{DippForm})_2(\text{thf})\text{Yb}\{\mu\text{-OC}(\text{Ph})=(\text{C}_6\text{H}_5)\text{C}(\text{Ph})_2\text{O}\}\text{Yb}(\text{DippForm})_2]$ was also isolated from an analogous reaction of $[\text{Yb}(\text{DippForm})_2(\text{thf})_2]$ and benzophenone (Scheme 4.19).²⁷

The reaction of $[\text{Sm}(\text{DippForm})_2(\text{thf})_2]$ with carbon disulfide to form a dinuclear formamidinatosamarium(III) complex $[\{\text{Sm}(\text{DippForm})_2(\text{thf})\}_2(\mu\text{-}\eta^2(\text{C}, \text{S}):\kappa(\text{S}', \text{S}'')\text{-CSCS}_2)]$ (Scheme 4.20) having a rare thioformylcarbonotrithioate ($(\text{SCSCS}_2)^{2-}$) bridging ligand. The C=O bond of benzophenone has been activated by the trivalent $[\text{Sm}(\text{DippForm})_2(\text{CCPh})(\text{thf})]$ forming $[\text{Sm}(\text{DippForm})_2\{\text{OC}(\text{Ph})_2\text{C}_2\text{Ph}\}(\text{thf})]$ as a major product and the unsolvated $[\text{Sm}(\text{DippForm})_2\{\text{OC}(\text{Ph})_2\text{C}_2\text{Ph}\}]$ as a minor product (Fig. 4.6).²⁷

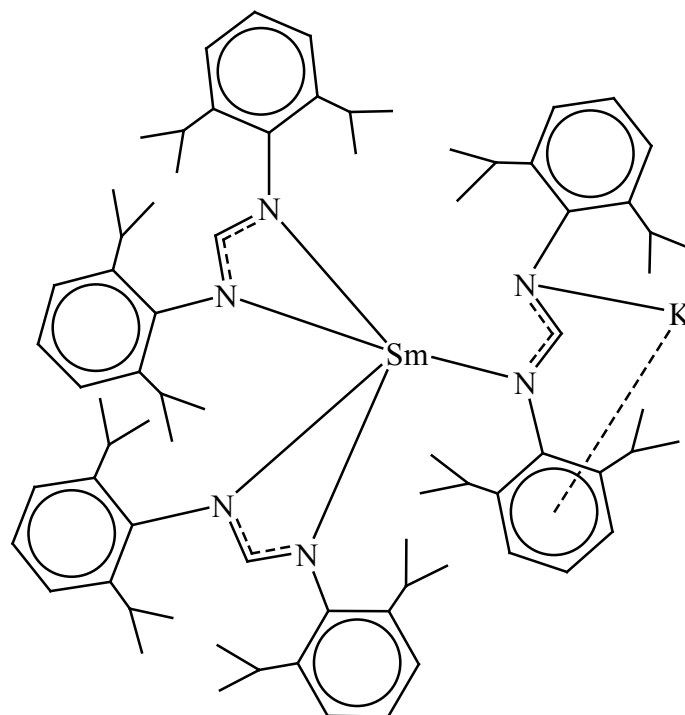
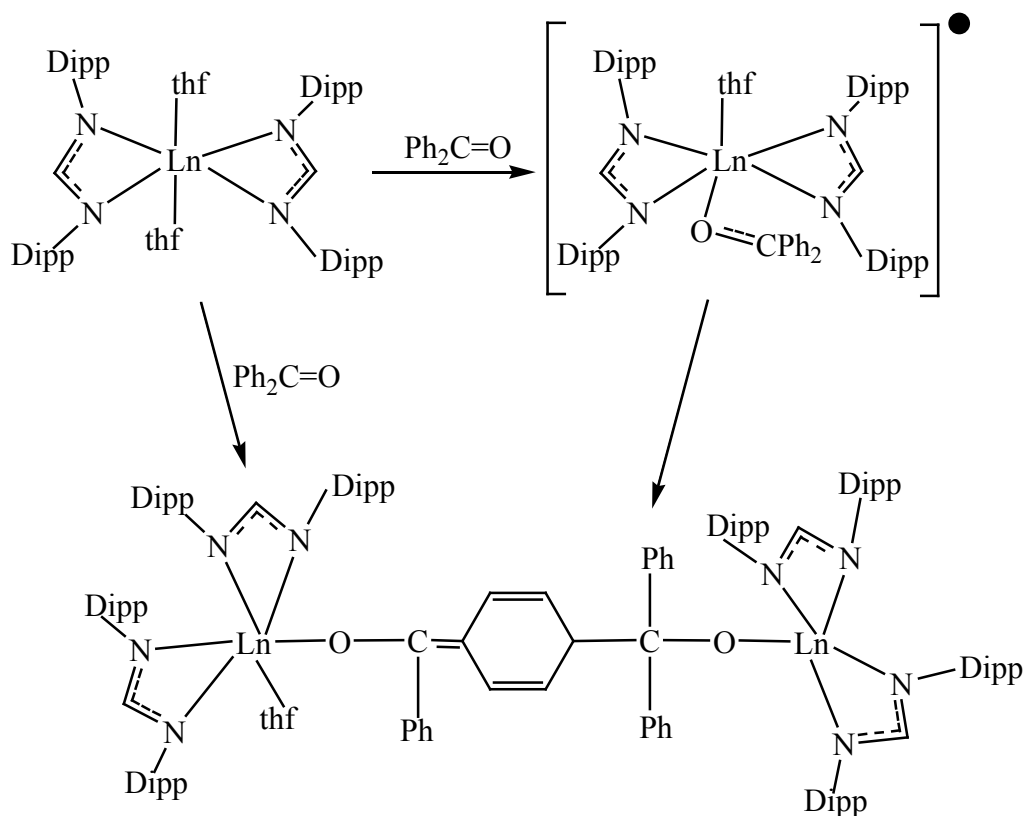
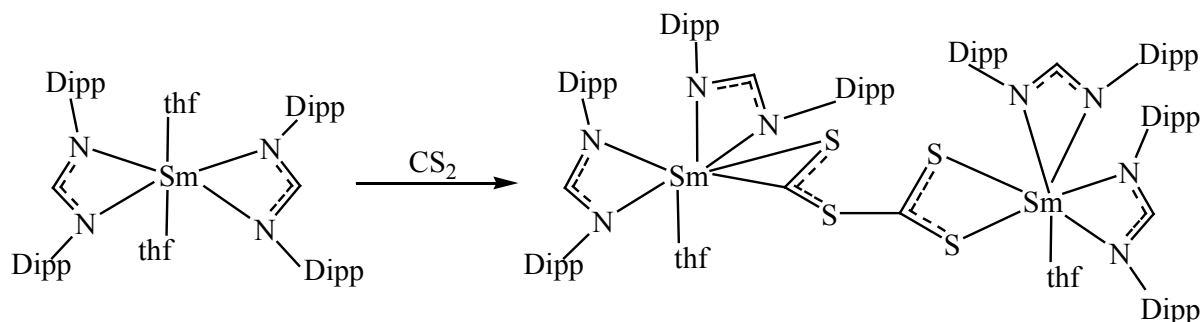


Fig. 4.5: Molecular structure of $[\text{KSm}(\text{DippForm})_3]$.



Scheme 4.19: Synthesis of $[\text{Ln}(\text{DippForm})_2(\text{thf})\{\mu\text{-OC}(\text{Ph})=\text{C}_6\text{H}_4(\text{Ph})_2\text{O}\}\text{Ln}(\text{DippForm})_2]$ ($\text{Ln} = \text{Sm}, \text{Yb}$).

Chapter 4



Scheme 4.20: Synthesis of $[\{\text{Sm}(\text{DippForm})_2(\text{thf})\}_2(\mu\text{-}\eta^2(\text{C},\text{S}):\kappa(\text{S}',\text{S}'')\text{SCSCS}_2)]$.

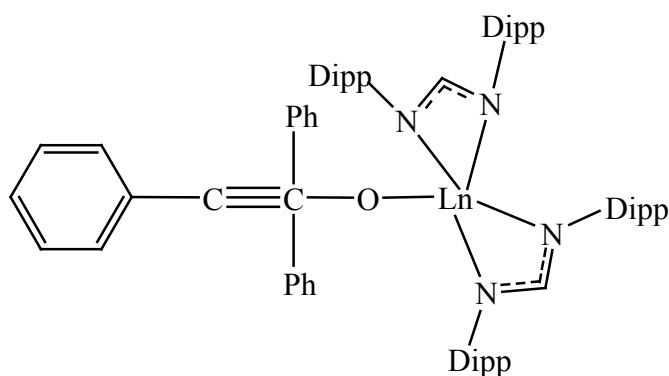
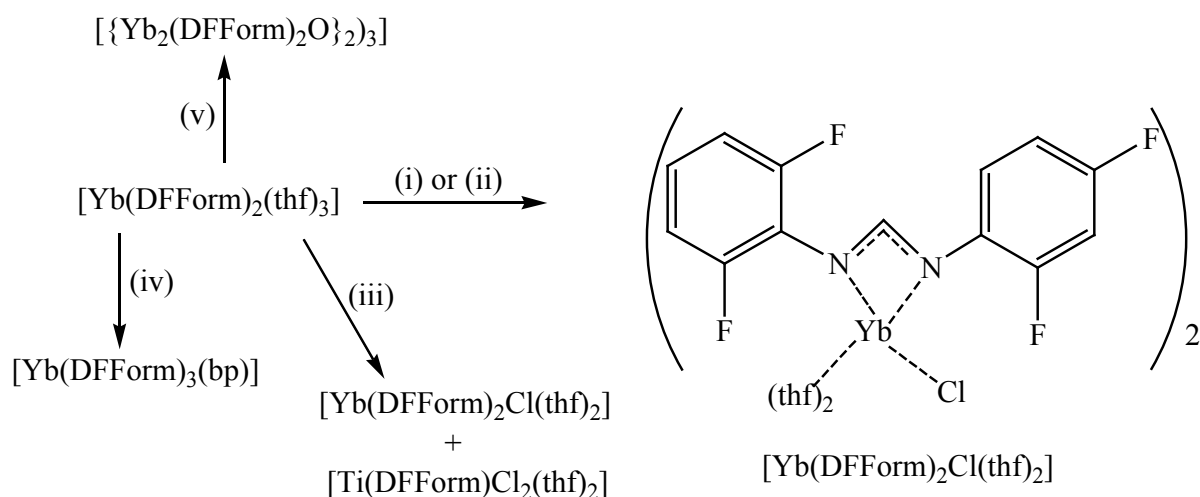


Fig. 4.6: Molecular structure of $[\text{Sm}(\text{DippForm})_2\{\text{OC}(\text{Ph})_2\text{C}_2\text{Ph}\}]$.

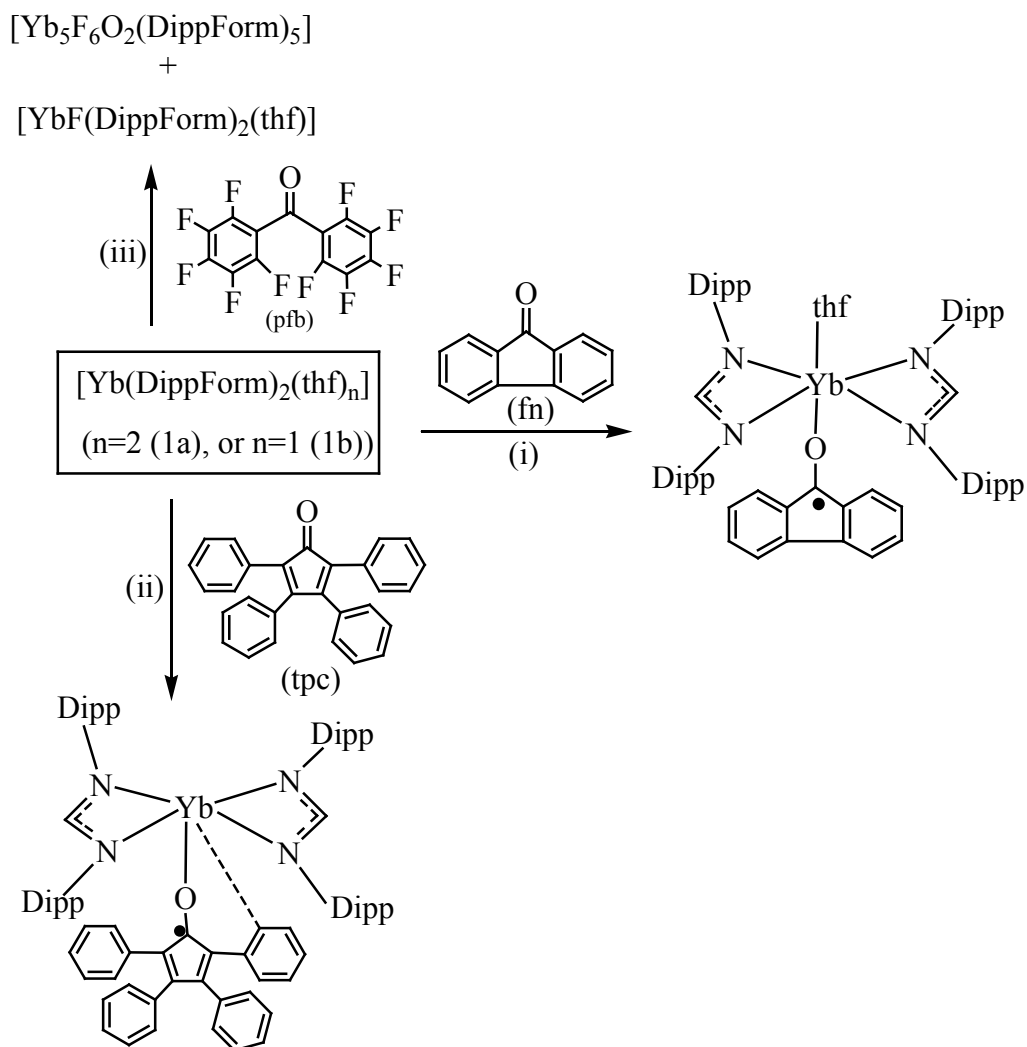
The oxidation of divalent $[\text{Yb}(\text{DFForm})_2(\text{thf})_3]$ by benzophenone (bp) and a halogenating agent ($\text{TiCl}_4(\text{thf})_2$, Ph_3CCl or C_2Cl_6) formed the complexes $[\text{Yb}(\text{DFForm})_3(\text{bp})]$ and $[\text{Yb}(\text{DFForm})_2\text{Cl}(\text{thf})_2]$, respectively (Scheme 4.21).¹⁶ Moreover, the trivalent complex $[\text{Yb}(\text{DFForm})_3(\text{thf})]$ was obtained from an RTP reaction between Yb^0 (slight excess), 1.5 $\text{Hg}(\text{C}_6\text{F}_5)_2$, 3 DFFormH in thf at room temperature. The tetrametallic oxide species $\{\text{Yb}_2(\text{DFForm})_4(\text{O})\}_2$ was also synthesised by exposing $[\text{Yb}(\text{DFForm})_2(\text{thf})_3]$ to trace amounts of O_2 . The sonication of the mixture of DFFormH and europium metal in thf followed by heating gave crystals of a hydroxide species $[\{\text{Eu}(\text{DFForm})_2\text{OH}(\text{thf})\}_2]$. The formation of $[\{\text{Eu}(\text{DFForm})_2\text{OH}(\text{thf})\}_2]$ probably involves a trace amount of water.¹⁶



Scheme 4.21: Reactivity of $[Yb(DFForm)_2(thf)_3]$ towards oxidising agents (i) $\frac{1}{2} C_2Cl_6$ in thf, $-1/2C_2Cl_4$; (ii) Ph_3CCl in thf, $-(Ph_3C)_2$; (iii) $1/2 TiCl_4(thf)_2$ in thf; (iv) bp in DME; (v) trace amounts of adventitious O_2 , toluene.

Recently, two ketyl complexes $[Yb(DippForm)_2(fn^{\cdot-}CO)(thf)]$, and $[Yb(DippForm)_2(tpc^{\cdot-}O)]$ have been synthesised by the treatment of the divalent complexes $[Yb(DippForm)_2(thf)_n]$ ($n = 1$ or 2) with the ketones 9-fluorenone (fn), or 2,3,4,5-tetraphenylcyclopentadienone (tpc, tetracyclone), respectively (ketyl = a radical anion containing a $C^{\cdot-}O^{\ominus}$ group) (Scheme 4.22).²⁸ However, the treatment of **1a** or **1b** with perfluorobenzophenone (pfb) resulted in the formation of C-F activated complex $[YbF(DippForm)_2(thf)]$ and a highly unusual fluoride/oxide-bridged species $[Yb_5F_6O_2(DippForm)_5]$.

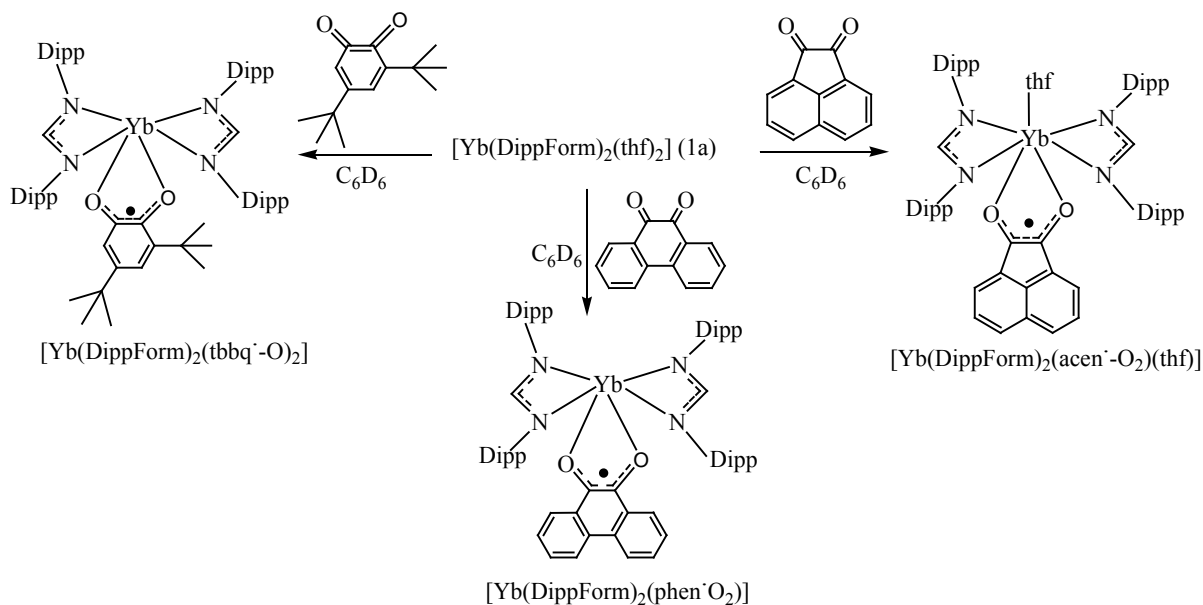
Chapter 4



Scheme 4.22: Reactions of $[\text{Yb}(\text{DippForm})_2(\text{thf})_n]$ (n=2 (**1a**), or n=1 (**1b**)) with (i) 9-fluorenone; (ii) 2,3,4,5-tetraphenylcyclopentadienone; (iii) perfluorobenzophenone.

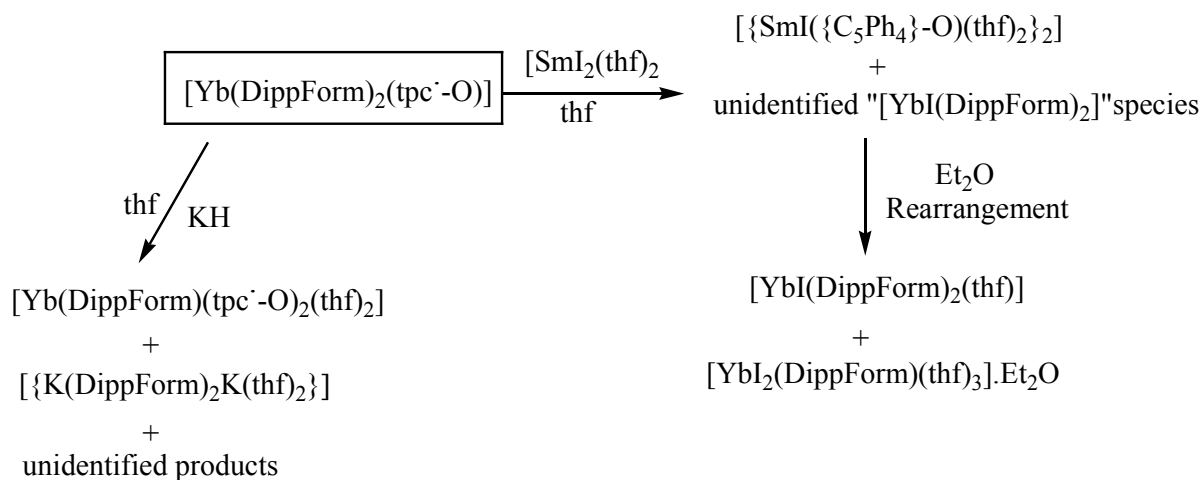
The ketyl complexes $[\text{Yb}(\text{DippForm})_2(\text{tbbq}^{\cdot-}\text{O}_2)]$, $[\text{Yb}(\text{DippForm})_2(\text{phen}^{\cdot-}\text{O}_2)]$, and $[\text{Yb}(\text{DippForm})_2(\text{acen}^{\cdot-}\text{O}_2)(\text{thf})]$ have also been synthesised by the reduction of diketones 3,5-di-tert-butyl-1,2-benzoquinone (tbbq), 9,10-phenanthrenequinone (phen), or 1,2-acenaphthenequinone (acen) (Scheme 4.23). Moreover, an unsolvated derivative of $[\text{Yb}(\text{DippForm})_2(\text{acen}^{\cdot-}\text{O}_2)(\text{thf})]$, viz. $[\text{Yb}(\text{DippForm})_2(\text{acen}^{\cdot-}\text{O}_2)]$ was isolated from toluene.²⁸

Chapter 4



Scheme 4.23: Single-electron-transfer reactions of $[\text{Yb}(\text{DippForm})_2(\text{thf})_2]$ (1a) with 1,2-diketones: tbbq, phen, and acen.

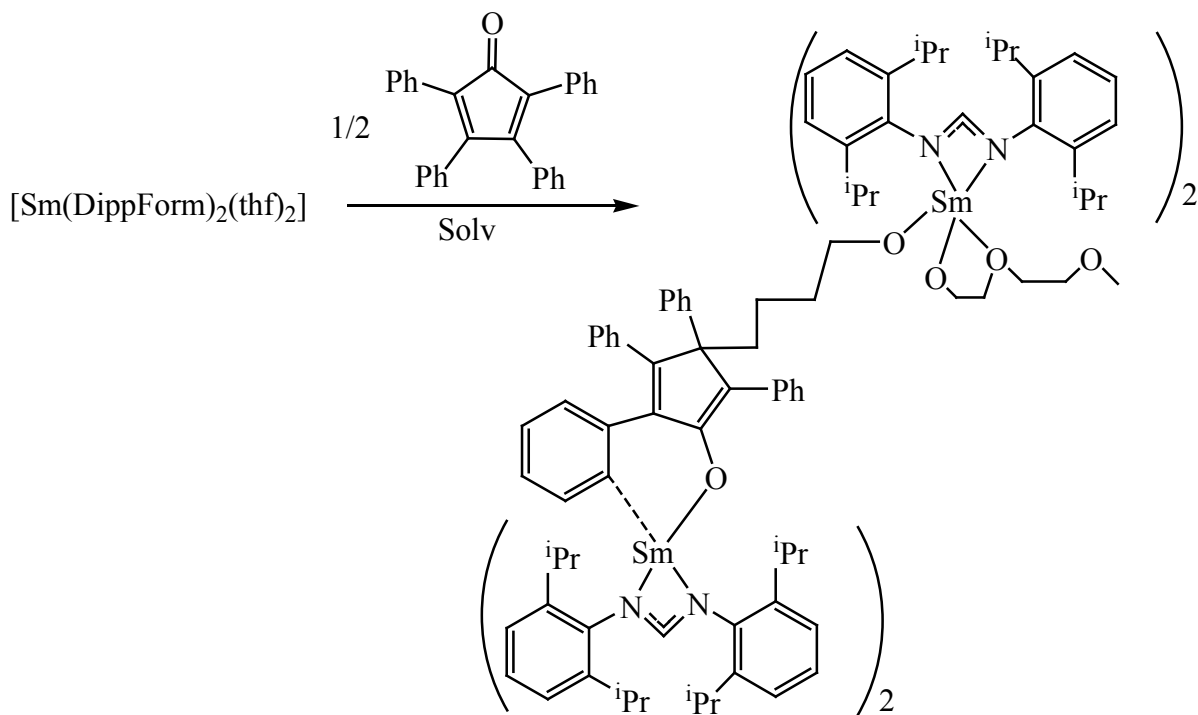
An unusual diketyl species $[\text{Yb}(\text{DippForm})(\text{tpc}'\text{-O})_2(\text{thf})_2]$ featuring two *cisoid* $\text{tpc}'\text{-O}^-$ ligands in very close proximity has been synthesised by the treatment of $[\text{Yb}(\text{DippForm})_2(\text{tpc}'\text{-O})]$ with KH. Upon further treatment with $[\text{SmI}_2(\text{thf})_2]$, the $\text{tpc}'\text{-O}^-$ ketyl was reduced to a dianion (1-oxido-2,3,4,5-tetraphenylcyclopentadienide²⁻), $(\{\text{C}_5\text{Ph}_4\}\text{-O})^{2-}$ by $[\text{SmI}_2(\text{thf})_2]$, giving dimeric $[\{\text{SmI}(\{\text{C}_5\text{Ph}_4\}\text{-O})(\text{thf})_2\}_2]$ and monomeric complexes $[\text{YbI}(\text{DippForm})_2(\text{thf})]$ and $[\text{YbI}_2(\text{DippForm})(\text{thf})_2]$ (Scheme 4.24).²⁸



Scheme 4.24: Reactions of $[\text{Yb}(\text{DippForm})_2(\text{tpc}'\text{-O})]$ with KH, and $[\text{SmI}_2(\text{thf})_2]$.

Chapter 4

The reaction of free-tpc with two equivalents of $[\text{Sm}(\text{DippForm})_2(\text{thf})_2]$ in toluene followed by crystallisation from a diglyme/hexane mixture afforded the formation of a ring-opened thf species, $[\{\text{Sm}(\text{DippForm})_2\}_2(\mu\text{-O-C}_5\text{Ph}_4\text{-(CH}_2\text{)}_4\text{-O)}(\text{diglyme})] \cdot \text{Solv}$ (Solv = hexane, 1/2 diglyme) (Scheme 4.25).²⁸



Scheme 4.25: Reaction performed in toluene, crystals were obtained from a diglyme/hexane mixture.

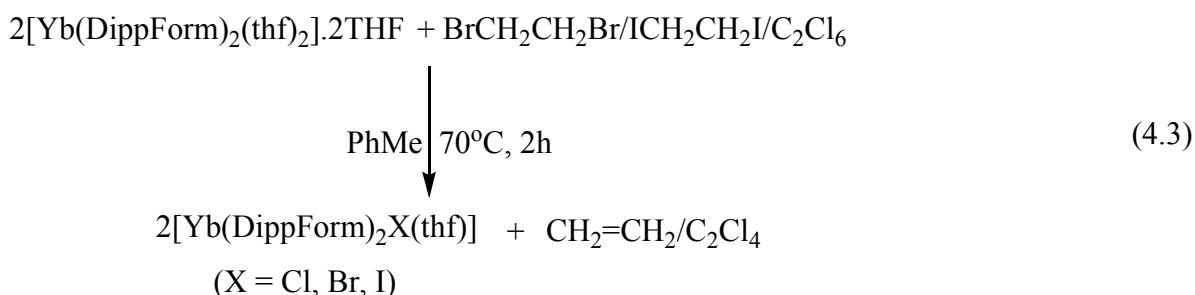
4.2 Research Plan

After perusing the relevant literature, it was obvious that a significant amount of research has been performed on the divalent and trivalent lanthanoid formamidates.³⁰ However, the redox chemistry of divalent lanthanoid formamidates has not been explored extensively. Moreover, no lanthanoid cationic complexes of formamidates had been reported. Therefore, our intention was to synthesise a range of trivalent halide complexes, L_2LnX (L = formamidates) from the oxidation of divalent complexes. Following the synthesis of trivalent halide complexes, we intended to synthesise lanthanoid cationic complexes of formamidates $[L_2Ln]^+[AlX_4/BPh_4/SbCl_6]^-$ by halide abstraction reactions with AlX_3 , $AgBPh_4$ and $SbCl_5$.

4.3 Results and Discussion

4.3.1 Synthesis and Characterisation

Ytterbium(II) formamidates of varying steric bulk, $\text{Yb}(\text{Form})_2(\text{thf})_2$ (Form = [RNCHNR]; R = 2,6-Me₂ (XylForm); 2,4,6-Me₃ (MesForm); 2,6-Et₂ (EtForm); 2,6-ⁱPr₂ (DippForm)) have been synthesised by literature procedures.¹³ Subsequently, the divalent complexes have been oxidised to trivalent ytterbium(III) formamidates by using different oxidants such as hexachloroethane (Cl₃CCCl₃), dibromoethane (BrCH₂CH₂Br) and diiodoethane (ICH₂CH₂I). The most sterically demanding formamidate complex [Yb(DippForm)₂(thf)₂] has been oxidised to the respective trivalent halide complexes [Yb(DippForm)₂X(thf)] (X = Cl, Br and I) (Eqn. 4.3) However, the chloride complex [Yb(DippForm)₂Cl(thf)].THF has been reported, synthesised by the oxidation of [Yb(DippForm)₂(thf)₂] with 1,2-dichloroethane in toluene.¹³



On the other hand, the least sterically demanding formamidate complexes [Yb(Form)₂(thf)₂] (Form = XylForm, MesForm and EtForm) were oxidised to the trivalent homoleptic formamidate complexes instead of forming halide complexes (Eqn. 4.4); however, trivalent homoleptic formamidate complexes of MesForm and EtForm have been reported, synthesised by the RTP reactions.³⁴ Moreover, the reactions of [Yb(Form)₂(thf)₂] (Form = XylForm, MesForm and EtForm) with benzophenone gave trivalent homoleptic complexes; however, Yb(DippForm)₂(thf)₂ gave a ketyl complex.²⁷

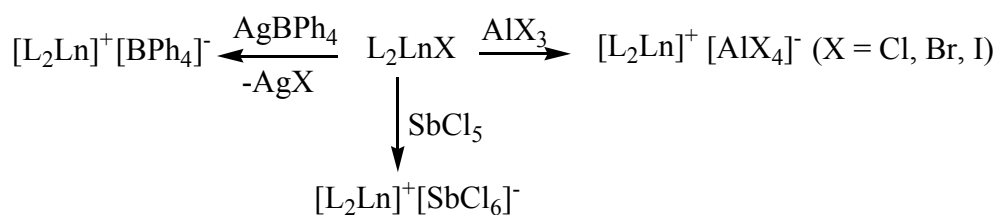
Chapter 4



(Form = XylForm, MesForm and EtForm)

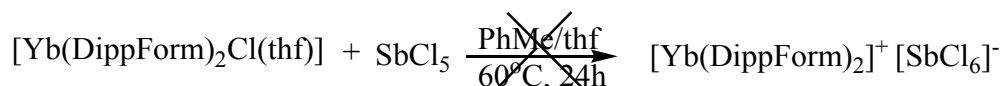
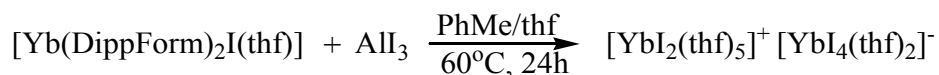


Halide abstraction reactions (Scheme 4.26a) have been performed between previously synthesised trivalent halide complexes $[\text{Yb}(\text{DippForm})_2\text{X}(\text{thf})]$ ($\text{X} = \text{Cl}, \text{Br}, \text{I}$) and a number of halide abstracting reagents such as AlX_3 ($\text{X} = \text{Cl}, \text{Br}, \text{I}$), SbCl_5 and AgBPh_4 with the intention of the isolation of cationic complexes $[\text{L}_2\text{Ln}]^+[\text{AlX}_4/\text{BPh}_4/\text{SbCl}_6]^-$. AgBPh_4 was prepared from silver nitrate and sodium tetraphenylborate by the literature procedure³⁵ and AlX_3 , SbCl_5 were used as received from the supplier. Surprisingly, all attempts to prepare cationic complexes from the halide abstraction reactions (Scheme 4.26b) consistently ended up with only isolation of ligand; however, on one occasion we isolated $[\text{YbI}_2(\text{thf})_5]^+[\text{YbI}_4(\text{thf})_2]^-$, which was reported before by a different synthetic route.³⁶ All reactions to obtain cationic complexes from the halide abstraction route have been unsuccessful at this stage. In one reaction involving $[\text{Yb}(\text{DippForm})_2\text{Cl}(\text{thf})]$ and AgBPh_4 the silver complex $[\text{Ag}(\text{DippForm})]_2$ was isolated instead of the expected cationic complex $[\text{Yb}(\text{DippForm})_2]^+[\text{BPh}_4]^-$.



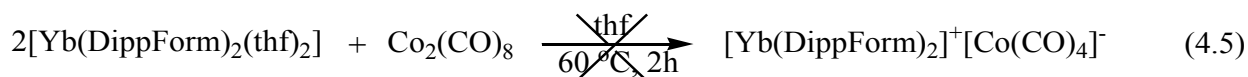
Scheme 4.26a: Prospective halide abstraction reactions to synthesise cationic complexes.

Chapter 4

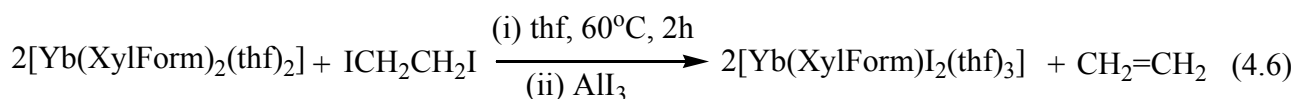


Scheme 4.26b: Halide abstraction reactions to synthesise cationic complexes.

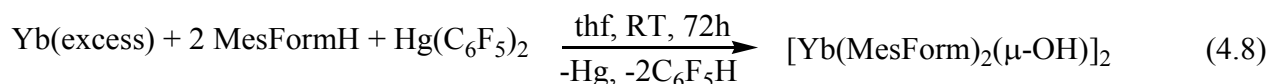
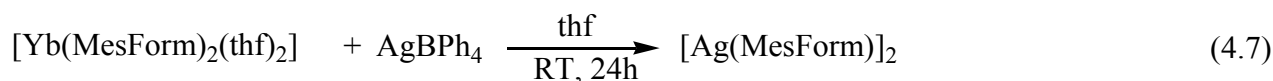
In an attempt to synthesise a cationic complex $[\text{Yb}(\text{DippForm})_2]^+[\text{Co}(\text{CO})_4]^-$ (Eqn. 4.5), the divalent formamidinate complex $[\text{Yb}(\text{DippForm})_2(\text{thf})_2]$ was treated with cobalt carbonyl at 60 °C in thf for 2h.³⁷ However, this reaction was also unsuccessful in isolating the desired cationic complex and we isolated the cobalt complex $[\text{Co}(\text{DippFormCO})(\text{CO})_3] \cdot \text{THF}$ instead.



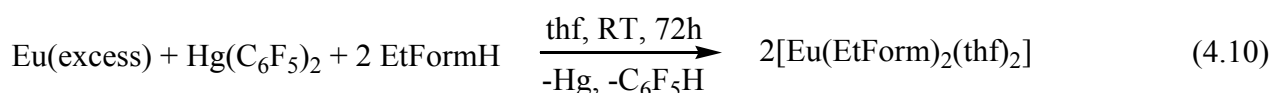
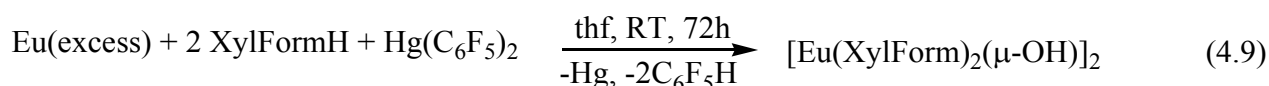
The treatment of $[\text{Yb}(\text{XylForm})_2(\text{thf})_2]$ with $\text{ICH}_2\text{CH}_2\text{I}$ in thf for 2h at 60 °C followed by the addition of AlI_3 in the reaction mixture and further heating for a couple of hours afforded the complex $[\text{Yb}(\text{XylForm})\text{I}_2(\text{thf})_3]$ (Eqn. 4.6). Moreover, the reaction between $[\text{Yb}(\text{MesForm})_2(\text{thf})_2]$ and AgBPh_4 in thf at ambient temperature for 24h gave the silver complex $[\text{Ag}(\text{MesForm})]_2$ (Eqn. 4.7). The redox transmetallation reaction between an excess of ytterbium metal, $\text{Hg}(\text{C}_6\text{F}_5)_2$ and the formamidine MesFormH in thf afforded the complex $[\text{Yb}(\text{MesForm})_2(\mu\text{-OH})]_2$ (Eqn. 4.8). The formation of $[\text{Yb}(\text{MesForm})_2(\mu\text{-OH})]_2$ probably involves a trace amount of water.



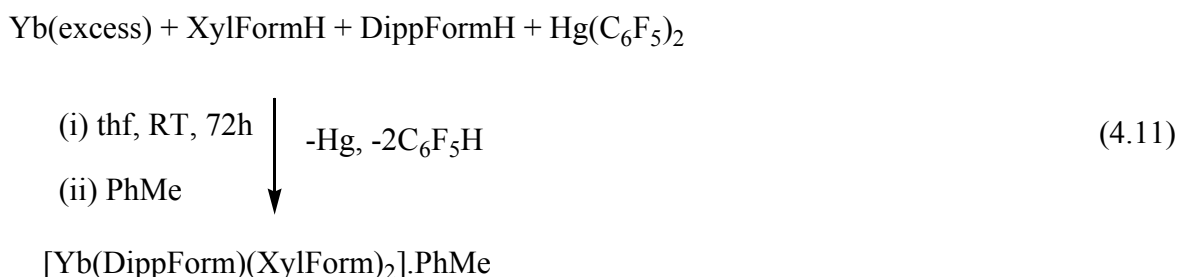
Chapter 4



The redox transmetallation reactions between an excess of europium metal, $\text{Hg}(\text{C}_6\text{F}_5)_2$ and the formamidines XylFormH and EtFormH in thf gave the complexes $[\text{Eu}(\text{XylForm})_2(\mu\text{-OH})(\text{thf})]_2$ and $[\text{Eu}(\text{EtForm})_2(\text{thf})_2]$, respectively (Eqn. 4.9 and 4.10). The formation of $[\text{Eu}(\text{MesForm})_2(\mu\text{-OH})(\text{thf})]_2$ perhaps involves a trace amount of water. The presence of hydroxyl group was further confirmed from infrared spectra.



A heteroleptic trivalent formamidinate complex of ytterbium $[\text{Yb}(\text{DippForm})(\text{XylForm})_2].\text{PhMe}$ was synthesised by the RTP reaction between an excess of Yb metal, $\text{Hg}(\text{C}_6\text{F}_5)_2$, XylFormH and DippFormH in thf followed by crystallisation from toluene (Eqn. 4.11).



The IR spectra of the complexes were recorded in nujol mulls between sodium chloride plates. Due to the extreme sensitivity of complexes to moisture and air, slight decomposition (on transit from the glovebox to the infrared spectrometer) could be observed in the IR spectra of some of the complexes. The absence of a $\nu(\text{N-H})$ absorption in the infrared spectra

(at around 3350 cm^{-1})¹³ indicates the complete deprotonation of the N,N'-bis(aryl)formamidine reagents in the isolated complexes. Strong $\nu(\text{C-N})$ stretching bands were observed in the region of $1675\text{--}1643\text{ cm}^{-1}$ for all spectra. A strong $\nu(\text{O-H})$ band at 3663 cm^{-1} supports the presence of a hydroxyl group in the complex $[\text{Yb}(\text{MesForm})_2(\mu\text{-OH})_2]$. The paramagnetic ytterbium complexes gave broadened NMR spectra and could not be satisfactorily integrated. Microanalysis was performed to determine purity and to confirm the composition of bulk material was similar to the X-ray crystal structure composition. The EDTA complexometric titration was performed to determine the metal composition. The lower percentages of carbon in some complexes are presumably due to the reaction of the complexes with aluminium crucible used in analysis.³⁸ The higher percentages of hydrogen in some complexes may be because of the exposure of moisture to the complexes.

4.3.2 X-ray Crystal Structures

[Yb(DippForm)₂Br(thf)] (1) and [Yb(DippForm)₂I(thf)] (2)

Complexes **1** and **2** (Fig. 4.7) crystallise in the triclinic space group *P*-1 (no. 2) with one molecule within the asymmetric unit. The ytterbium centre is a trivalent, six coordinate complex with O1 *cis* to Br1 or I1 and the geometry for both complexes is best described as trigonal prismatic. The Yb-N bond lengths in complexes **1** and **2** range from 2.315(2) to 2.371(2) and 2.304(3) to 2.391(2) Å, respectively and are comparable to the complexes $[\text{Yb}(\text{DippForm})_2\text{Cl}(\text{thf})]\cdot\text{THF}$ and $[\text{Yb}(\text{DippForm})_2\text{Br}(\text{thf})]\cdot\text{Et}_2\text{O}$.¹³ The Yb-O distances in the complexes **1** and **2** are similar (2.353(2) and (2.352(2) Å, respectively); however slightly longer than in $[\text{Yb}(\text{DippForm})_2\text{Cl}(\text{thf})]\cdot\text{THF}$ (2.3291(17) Å) and $[\text{Yb}(\text{DippForm})_2\text{Br}(\text{thf})]\cdot\text{Et}_2\text{O}$ (2.343(2) Å).¹³

The Yb-Br distances in **1** and $[\text{Yb}(\text{DippForm})_2\text{Br}(\text{thf})]\cdot\text{Et}_2\text{O}$ are similar; however are longer than the Yb-Cl distance in $[\text{Yb}(\text{DippForm})_2\text{Cl}(\text{thf})]\cdot\text{THF}$ by approximately 0.15 Å, which is similar to the difference in the appropriate ionic radii (1.81 Å for Br and 1.96 Å for Cl).³⁹ In complex **2**, the Yb-I distance is 2.8970(7) Å, which is significantly elongated compared to the Y-Br distances in **1** and $[\text{Yb}(\text{DippForm})_2\text{Br}(\text{thf})]\cdot\text{Et}_2\text{O}$ and the Yb-Cl distance in $[\text{Yb}(\text{DippForm})_2\text{Cl}(\text{thf})]\cdot\text{THF}$. These differences in the Yb-Cl, Y-Br and Yb-I distances are expected due to the differences in the ionic radii of Cl, Br and I.³⁹

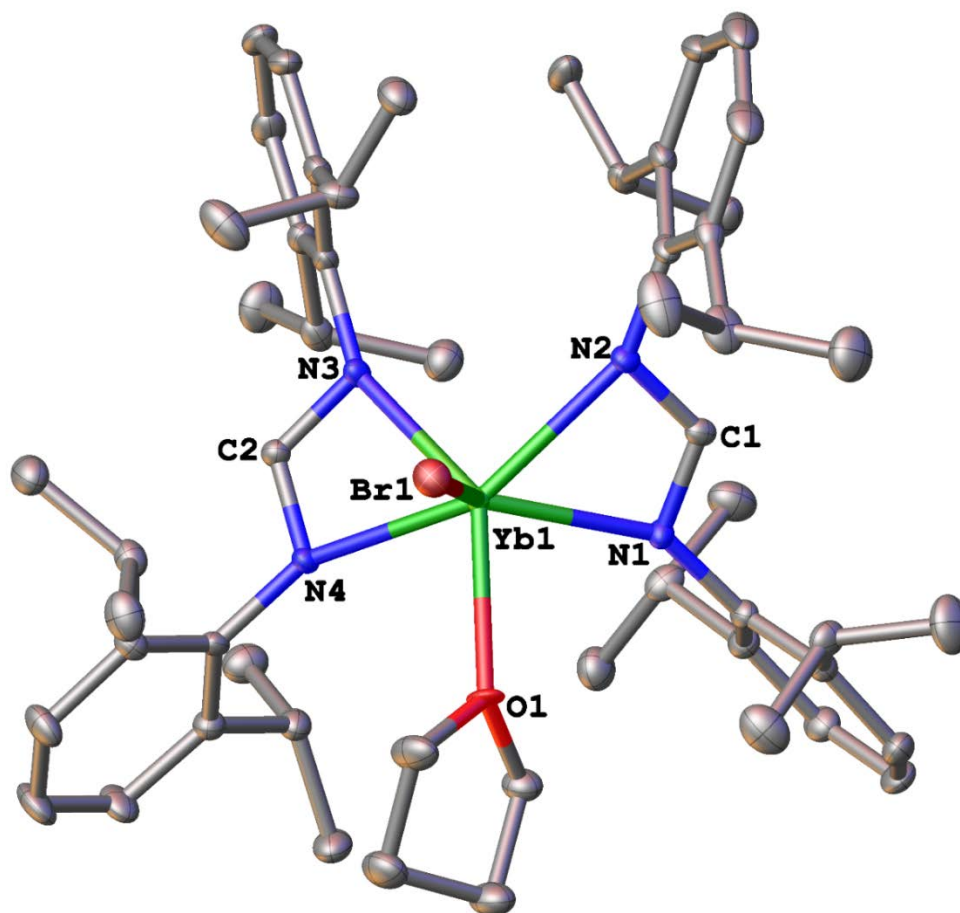


Fig. 4.7: Molecular structure of $\text{Yb}(\text{DippForm})_2\text{Br}(\text{thf})$ (**1**), representative of the isostructural complex $\text{Yb}(\text{DippForm})_2\text{I}(\text{thf})$ (**2**). Ellipsoids have been shown at 50% probability and hydrogen atoms have been omitted for clarity. Selected bond lengths (\AA) and angles ($^\circ$) for **1**: Yb1-Br1 : 2.6617(7), Yb1-O1 : 2.353(2), Yb1-N1 : 2.315(2), Yb1-N2 : 2.371(2), Yb1-N3 : 2.349(2), Yb1-N4 : 2.354(2), N1-Yb1-N2 : 57.97(8), N3-Yb1-N4 : 57.73(8), N1-C1-N2 : 117.4(2), N3-C2-N4 : 117.2(2). Selected bond lengths (\AA) and angles ($^\circ$) for **2**: Yb1-I1 : 2.8970(7), Yb1-O1 : 2.352(2), Yb1-N1 : 2.359(3), Yb1-N2 : 2.340(3), Yb1-N3 : 2.391(2), Yb1-N4 : 2.304(3), N1-Yb1-N2 : 57.71(8), N3-Yb1-N4 : 57.98(8), N1-C1-N2 : 117.2(3), N3-C2-N4 : 118.1(3).

Chapter 4

[Yb(XylForm)₃] (3), [Yb(MesForm)₃] (4) and [Yb(EtForm)₃].2THF (5)

Complex **3** (Fig. 4.8) crystallises in the orthorhombic space group $P2_12_12_1$ (no. 19) with one molecule within the asymmetric unit, and complexes **4** and **5** crystallise in the triclinic space group $P-1$ (no. 2) with one and two molecules within the asymmetric unit, respectively. The ytterbium centre in all three complexes is six coordinated with trigonal prismatic arrangements. The Yb-N contacts in **3**, **4** and **5** range from 2.336(9) to 2.363(9), 2.337(5) to 2.362(4) and 2.330(3) to 2.358(3) Å, respectively. These compare reasonably well with the bond lengths found in the literature complexes $[Yb(MesForm)_3]$ and $[Yb(EtForm)_3].2THF$, synthesised by the RTP reactions.³⁴

[[Ag(MesForm)₂].PhMe (6) and [[Ag(DippForm)₂].2THF (7)

Complex **6** (Fig. 4.9) crystallises in the triclinic space group $P-1$ (No. 2), whereas complex **7** crystallises in the monoclinic space group $P2_1/c$ (no. 14). However, both complexes consist of two independent half molecules in the asymmetric unit. X-ray crystallography shows an inversion centre through the midpoint of the Ag–Ag interaction in the dinuclear complexes **6** and **7**. The Ag–Ag bond contacts in **6** and **7** are 2.7487(6) and 2.7532(10) Å, respectively and are well compared with the reported complexes $Ag_2[(2,6-Me_2C_6H_3N)_2C(H)]_2$ (2.7544(6) Å)⁴⁰, silver(I) tert-butyl-imino-2,2-dimethylpyrrolidinate (2.677(3) Å)⁴¹, $[Ag(4-MePh)_2N_2C(H)]_2$ (2.705(1) Å)⁴², $[Ag(Pr^i)_2N_2C(Me)]_2$ (2.645 Å)⁴³, $[Ag(2-OMePh)_2N_2C(H)]_2$ (2.780 Å)⁴⁴ and $[Ag(Me_3SiN)_2C(Ph)]_2$ (2.655 Å)⁴⁵. The Ag–Ag bond distances are slightly shorter than the sum of the van der Waals radii (1.72 Å for Ag) indicating strong Ag–Ag interactions.⁴⁶

The Ag–N distances in **6** and **7** are from 2.089(3) to 2.096(3) Å and 2.087(5) to 2.089(5), respectively, and are comparable to the complex $[Ag_2[(2,6-Me_2C_6H_3N)_2C(H)]_2]$ (2.110(3) Å)⁴⁰. The N1–Ag1–N2[#] angle in **6** and **7** are (168.83(12) and 168.6(2)°, respectively) slightly bent from linear and are comparable to the above reported complex.⁴⁰

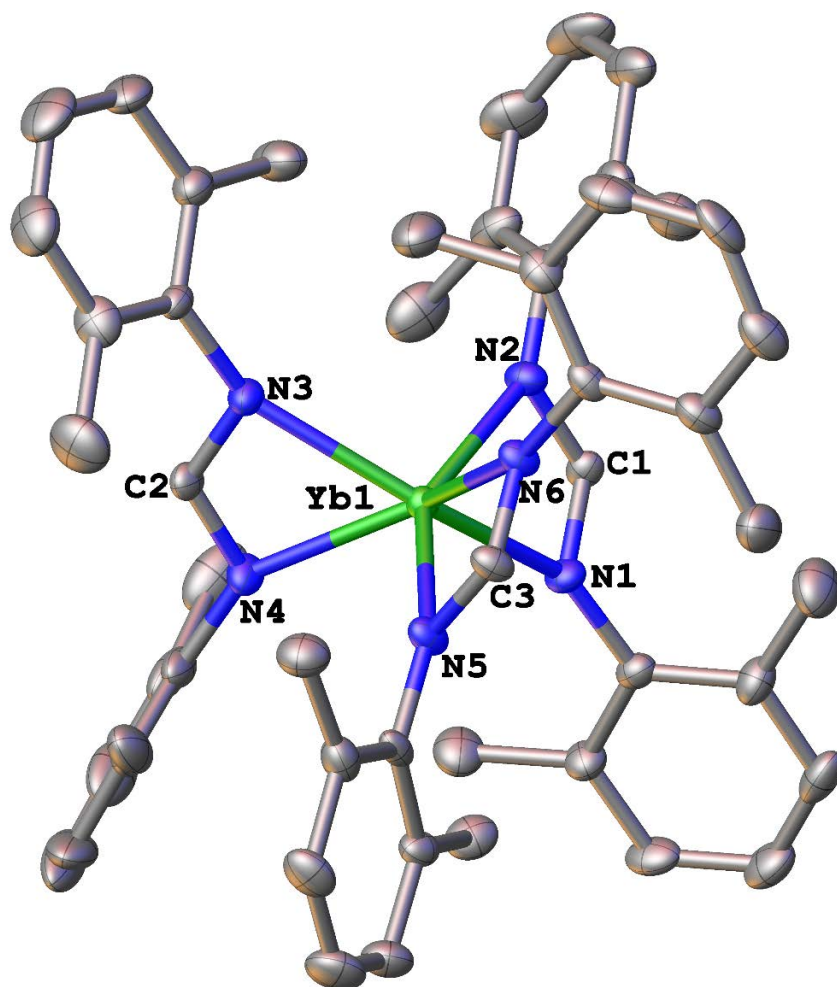


Fig. 4.8: Molecular structure of $\text{Yb}(\text{XylForm})_3$ (**3**), representative of the isostructural complexes $\text{Yb}(\text{MesForm})_3$ (**4**) and $[\text{Yb}(\text{EtForm})_3] \cdot 2\text{THF}$ (**5**). Ellipsoids have been shown at 50% probability; hydrogen atoms (and solvent of crystallisation for **5**) have been omitted for clarity. Selected bond lengths (\AA) and angles ($^\circ$) for **3**: Yb1-N1: 2.357(10), Yb1-N2: 2.344(9), Yb1-N3: 2.336(9), Yb1-N4: 2.356(10), Yb1-N5: 2.337(9), Yb1-N6: 2.363(9), N1-Yb1-N2: 57.8(3), N3-Yb1-N4: 58.4(3), N5-Yb1-N6: 57.8(3), N1-C1-N2: 119.0(11), N3-C2-N4: 119.3(10), N5-C3-N6: 118.4(11). Selected bond lengths (\AA) and angles ($^\circ$) for **4**: Yb1-N1: 2.350(5), Yb1-N2: 2.359(4), Yb1-N3: 2.362(4), Yb1-N4: 2.337(5), Yb1-N5: 2.339(4), Yb1-N6: 2.360(5), N1-Yb1-N2: 58.01(17), N3-Yb1-N4: 57.94(16), N5-Yb1-N6: 57.54(15), N1-C1-N2: 117.8(5), N3-C2-N4: 118.4(5), N5-C3-N6: 118.6(5). Selected bond lengths (\AA) and angles ($^\circ$) for **5**: Yb1-N1: 2.343(3), Yb1-N2: 2.330(3), Yb1-N3: 2.356(3), Yb1-N4: 2.342(3), Yb1-N5: 2.358(3), Yb1-N6: 2.344(2), N1-Yb1-N2: 58.58(9), N3-Yb1-N4: 57.96(10), N5-Yb1-N6: 57.97(9), N1-C1-N2: 118.2(3), N3-C2-N4: 118.2(3), N5-C3-N6: 118.4(3).

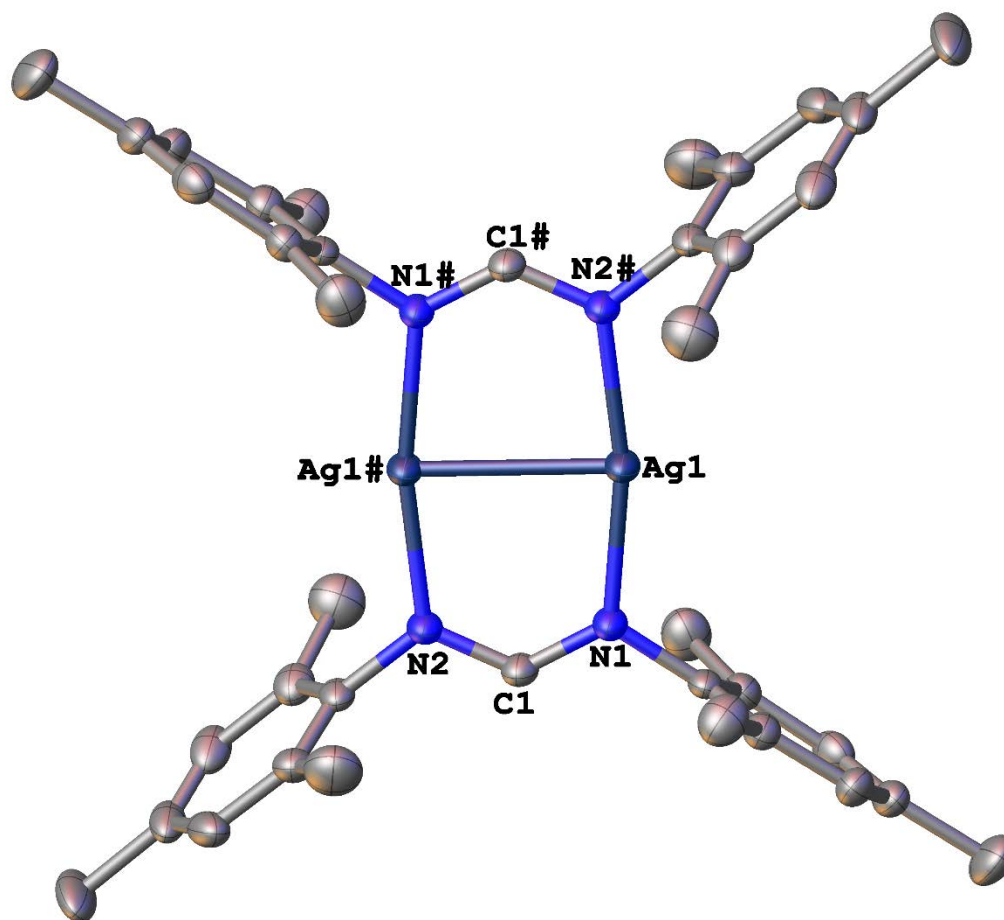


Fig. 4.9: Molecular structure of $[\{\text{Ag}(\text{MesForm})\}_2]\cdot\text{PhMe}$ (**6**), representative of the isostructural complex $[\{\text{Ag}(\text{DippForm})\}_2]\cdot 2\text{THF}$ (**7**). Ellipsoids have been shown at 50% probability; hydrogen atoms and solvent of crystallisation have been omitted for clarity. Selected bond lengths (Å) and angles (°) for **6**: Ag1-N1: 2.089(3), Ag1-N2#: 2.096(3), Ag1-Ag1#: 2.7487(6), N1-Ag1-N2#: 168.83(12), N1-Ag1-Ag1#: 83.32(8), N1-C1-N2: 126.7(4). Selected bond lengths (Å) and angles (°) for **7**: Ag1-N1: 2.089(5), Ag1-N2#: 2.087(5), Ag1-Ag1#: 2.7532(10), N1-Ag1-N2#: 168.6(2), N1-Ag1-Ag1#: 84.02(15) N1-C1-N2: 125.9(6).

Yb(XylForm)I₂(thf)₃ (**8**)

Complex **8** (Fig. 4.10) crystallises in the triclinic space group *P*-1 (no. 2), with two $[\text{Yb}(\text{XylForm})\text{I}_2(\text{thf})_3]$ molecules in the asymmetric unit. The X-ray crystal structure of **8** comprises of a seven coordinate Yb centre, which is bound to two iodides, two nitrogens of the formamidates and three thf molecules. The coordination polyhedron surrounding the Yb centre is best described as a distorted pentagonal bipyramid with the two iodides at the

Chapter 4

axial positions (I1-Yb1-I2: 170.37(6)). The Yb-O distances range from 2.332(13)-2.370(15) Å, comparable to the complexes **1**, **2** (2.353(2) and (2.352(2) Å, respectively) and [Yb(DippForm)₂Cl(thf)]·THF (2.3291(17) Å) and [Yb(DippForm)₂Br(thf)]·Et₂O (2.343(2) Å).¹³

The Yb-N distances in **8** are 2.326(18) and 2.375(15) Å, are comparable with complexes **1**, **2**, **3**, **4**, **5** as well as with the relevant complexes in literature.^{13, 34} The Yb-I distances fall in the range from 2.987(2) to 3.0090(19) Å and are slightly elongated than 2.8970(7) Å in complex **2**. However, Yb-I distances in **8** are slightly shorter than in the dinuclear complexes [{(κ²-N,N'-Priso)Yb(THF)(μ-I)}₂] (Priso = [(ArN)₂CNPrⁱ₂]-, Ar = 2,6-diisopropylphenyl)⁴⁷ and [Yb(Giso)₂] (Giso = [(ArN)₂CN(C₆H₁₁)₂]-, Ar = C₆H₃Prⁱ_{2-2,6})⁴⁸, where the Yb-I distances are 3.0946(14) and 3.1424(9) Å, respectively.

[Co(DippFormCO)(CO)₃].THF (9)

Complex **9** (Fig. 4.11) crystallises in the monoclinic space group *P*2₁/*n* (no. 14), with one molecule in the asymmetric unit. This complex consists of a five-coordinate cobalt centre, connected to four carbonyl groups and a nitrogen atom from the N-C-N backbone of the formamidinate ligand. The C26-Co1-C29 angle is 176.1(2)°, and therefore, the coordination polyhedron surrounding the Co centre is best described as a distorted trigonal bipyramid with the two CO groups at the axial positions. The Co-N length is 1.968(3) Å which is approximately 0.1 Å shorter than the Co-N contact in [Co₂[μ-κ²Ge,N-{Ge(ⁱPr₂bzam)(HMDS)}(μ-CO)(CO)₅] (ⁱPr₂bzam = diisopropyl benzamidinate, HMDS = N(SiMe₃)₂).⁴⁹ The Co-C contacts in **9** fall in the range from 1.755(6) to 1.930(4) Å, and are slightly shorter than the Co-C lengths 1.767(2) to 1.994(18) Å in [Co₂[μ-κ²Ge,N-{Ge(ⁱPr₂bzam)(HMDS)}(μ-CO)(CO)₅] (ⁱPr₂bzam = diisopropyl benzamidinate, HMDS = N(SiMe₃)₂).⁴⁹

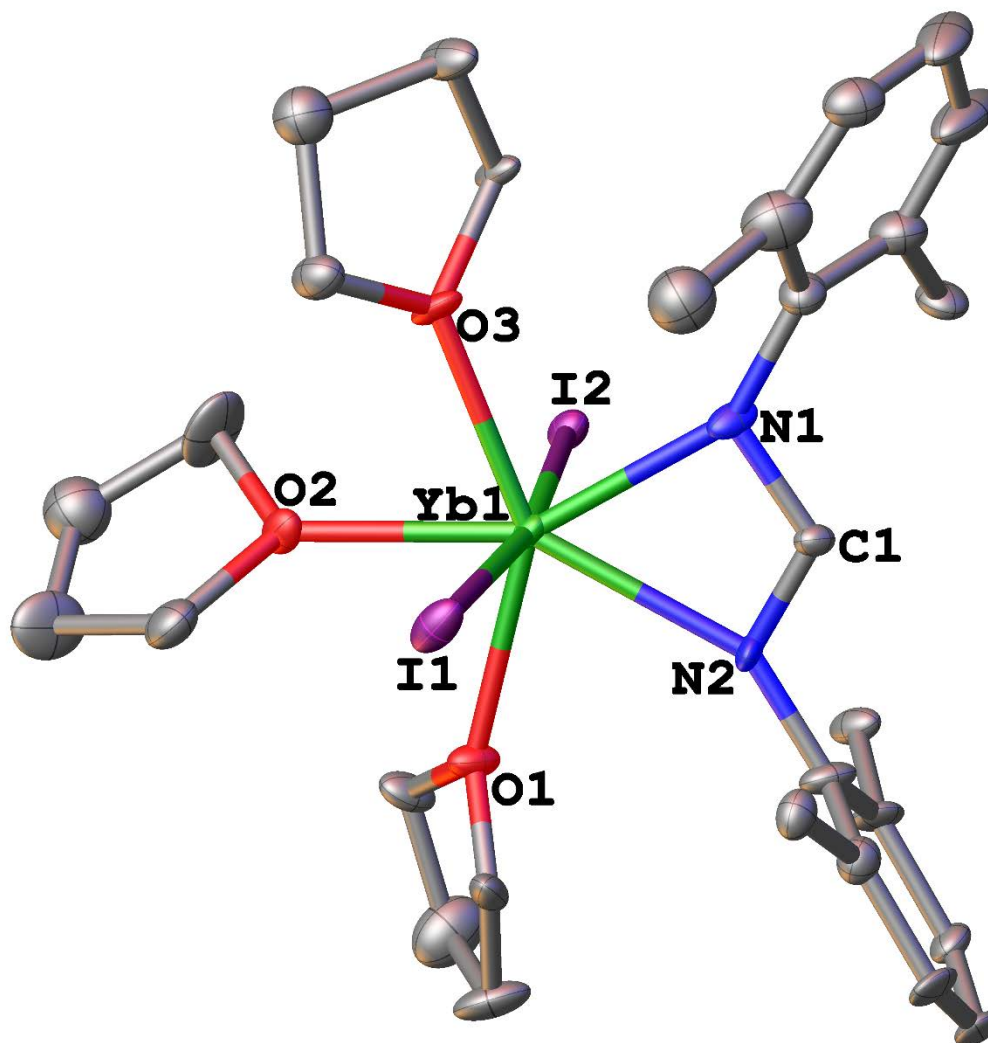


Fig. 4.10: Molecular structure of $\text{Yb}(\text{XylForm})\text{I}_2(\text{thf})_3$ (**8**). Ellipsoids have been shown at 50% probability; hydrogen atoms have been omitted for clarity. Selected bond lengths (\AA) and angles ($^\circ$) for **8**: Yb1-N1: 2.326(18), Yb1-N2: 2.375(15), Yb1-I1: 2.987(2), Yb1-I2: 3.0090(19), Yb1-O1: 2.332(13), Yb1-O2: 2.370(15), Yb1-O3: 2.339(11), N1-Yb1-N2: 58.5(5), I1-Yb1-I2: 170.37(6), O1-Yb1-O2: 74.0(5), O2-Yb1-O3: 71.2(5), O1-Yb1-O3: 145.2(6).

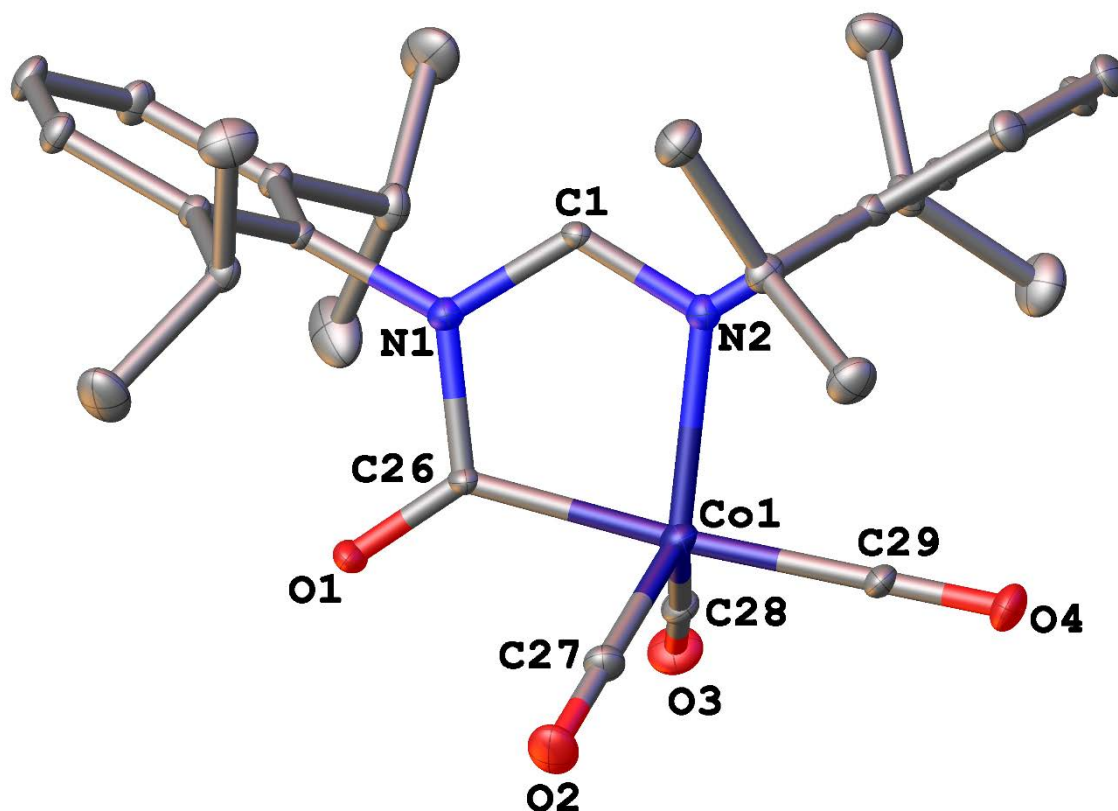


Fig. 4.11: Molecular structure of $[\text{Co}(\text{DippFormCO})(\text{CO})_3]\cdot\text{THF}$ (**9**). Ellipsoids have been shown at 50% probability; hydrogen atoms and solvent of crystallisation have been omitted for clarity. Selected bond lengths (\AA) and angles ($^\circ$) for **9**: Co1-N2: 1.968(3), Co1-C26: 1.930(4), Co1-C27: 1.755(6), Co1-C28: 1.755(6), Co1-C29: 1.799(5), C26-Co1-N2: 82.67(16), C27-Co1-N2: 121.6(2), C28-Co1-N2: 117.70(19), C29-Co1-N2: 93.62(18), C26-Co1-C27: 86.2(2), C26-Co1-C28: 86.0(2), C26-Co1-C29: 176.1(2), C27-Co1-C28: 118.5(3), C28-Co1-C29: 96.7(2), N1-C1-N2: 118.3(4).

[Yb(MesForm)₂(μ -OH)]₂ (10)

Complex **10** (Fig. 4.12) crystallises in the monoclinic space group $C2/c$ (no. 15) with half of the molecule within the asymmetric unit. This dinuclear complex consists of two six coordinate Yb^{3+} metal centres that are bridged by two hydroxyl groups. Each Yb^{3+} metal centre is bound to two chelating MesForm ligands and two hydroxyl groups. The geometries about the Yb^{3+} centres are best described as the trigonal prismatic.

Chapter 4

The Yb-N bond lengths in **10** (2.315(4) - 2.382(4) Å) are slightly shorter than in the complex [$\text{Yb}(o\text{-TolForm})_2(\mu\text{-OH})(\text{thf})\}_2$] (2.378(6) to 2.420(6) Å).³⁴ The Yb-O_{hydroxyl} contacts in **10** (2.202(3) and 2.200(3) Å) are comparable to the complex [$\{\text{Yb}(o\text{-TolForm})_2(\mu\text{-OH})(\text{thf})\}_2$] (2.202(6) and 2.232(6) Å); however, are slightly shorter than the Yb-O_{hydroxyl} contacts found in [$\{\text{Yb}(\text{Cp}')_2(\mu\text{-OH})\}_2$] (Cp' = C₅H₄SiMe₃) (2.25(2) to 2.33(2) Å).⁵⁰

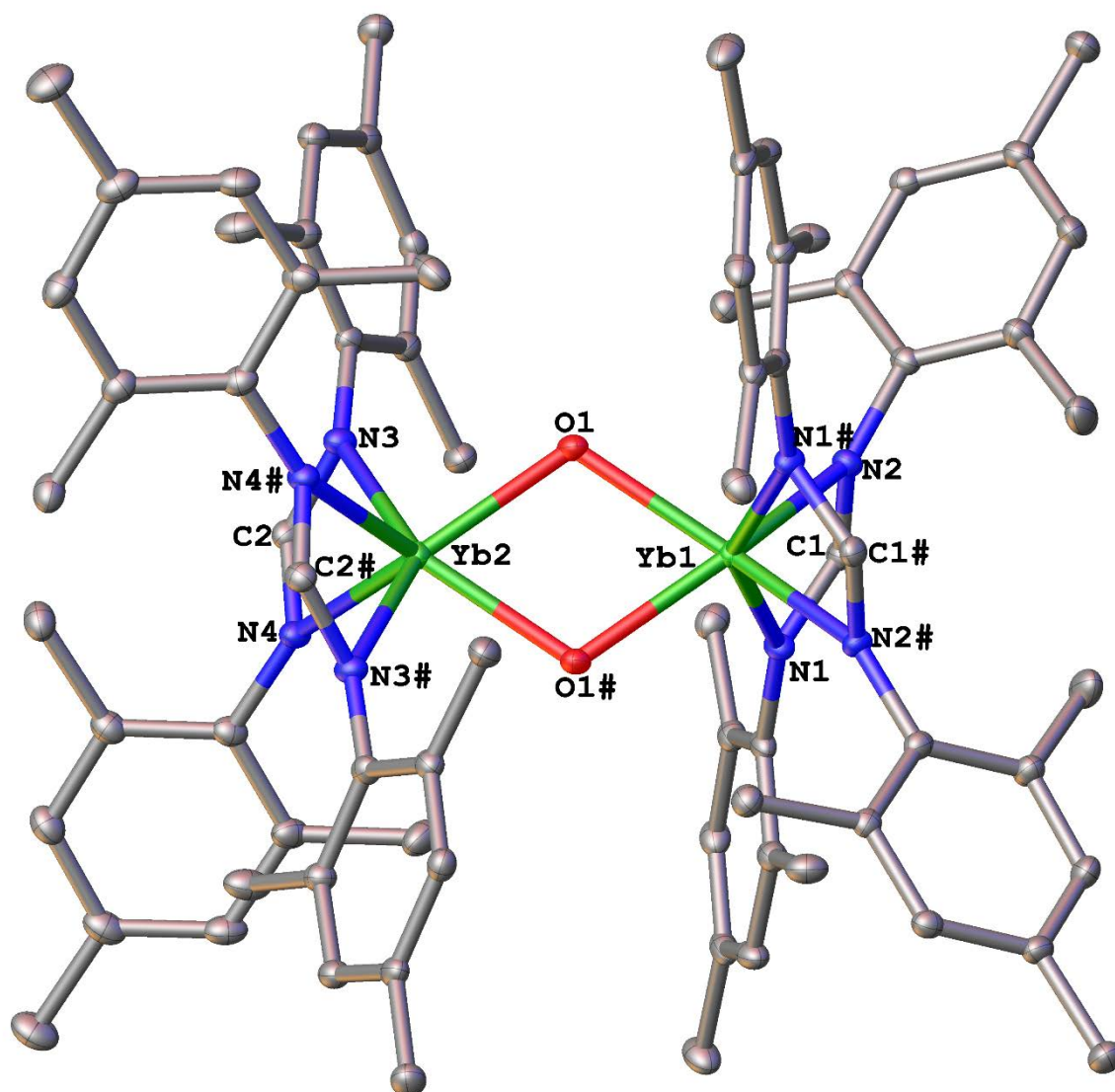


Fig. 4.12: Molecular structure of [$\text{Yb}(\text{MesForm})_2(\mu\text{-OH})\}_2$ (**10**). Ellipsoids have been shown at 50% probability; hydrogen atoms have been omitted for clarity. Selected bond lengths (Å) and angles (°) for **10**: Yb1-N1: 2.347(3), Yb1-N2: 2.360(3), Yb1-O1: 2.202(3), Yb2-N3: 2.382(4), Yb2-N4: 2.315(4), Yb2-O1: 2.200(3), N1-Yb1-N2: 57.74(12), N3-Yb2-N4: 58.01(13), O1-Yb1-O1#: 70.68(16), O1-Yb2-O1#: 70.75(17).

Chapter 4

[Eu(XylForm)₂(μ-OH)(thf)₂] (11)

X-ray shows the complex **11** crystallises in the triclinic space group *P*-1 (no. 2) with half the dimer in the asymmetric unit (Fig. 4.13) that is isostructural with [Eu(DFForm)₂OH(thf)₂]¹⁶. The Eu³⁺ centres have coordination number seven, coordinated by two terminal κ(N,N') XylForm ligands, a thf molecule and two of the bridging hydroxyl groups. The geometry of the Eu³⁺ centres is best described as a distorted N₃ facecapped triangular prism.

The Eu-N bond lengths in **11** fall in the range from 2.458(4) to 2.504(4) Å, and are slightly shorter than in the complex [Eu(DFForm)₂OH(thf)₂] (2.442(2) to 2.557(2) Å).¹⁶ The Eu-O_{hydroxyl} contacts in **11** (2.274(5) and 2.251(4) Å) are also somewhat shorter than Eu-O_{hydroxyl} contacts in the complex [Eu(DFForm)₂OH(thf)₂] (2.282(2) and 2.278(2) Å); however, the Eu-O_{thf} contacts in **11** and [Eu(DFForm)₂OH(thf)₂] are 2.474(3) and 2.463(2) Å, respectively, and are comparable to each other.¹⁶

[Eu(EtForm)₂(thf)₂] (12)

Complex **12** crystallises in the monoclinic space group *C*2/*c* (no. 15) with half of the monomer in the asymmetric unit (Fig. 4.14) and is isostructural with [Eu(DippForm)₂(thf)₂].¹³ The Eu²⁺ centre is coordinated by two chelating EtForm ligands and two *cis* thf donors, giving the Eu²⁺ centre a coordination number of six. The Eu-N bond lengths in **12** span the range from 2.458(4) to 2.504(4) Å and are somewhat shorter than the Eu-N contacts in [Eu(DippForm)₂(thf)₂]₂·2THF (2.593(7) to 2.597(6) Å). However, the Eu-O distance is slightly elongated in **12** (2.274(5) Å) compared to the Eu-O distance in [Eu(DippForm)₂(thf)₂]₂·2THF (2.556(6) Å).¹³

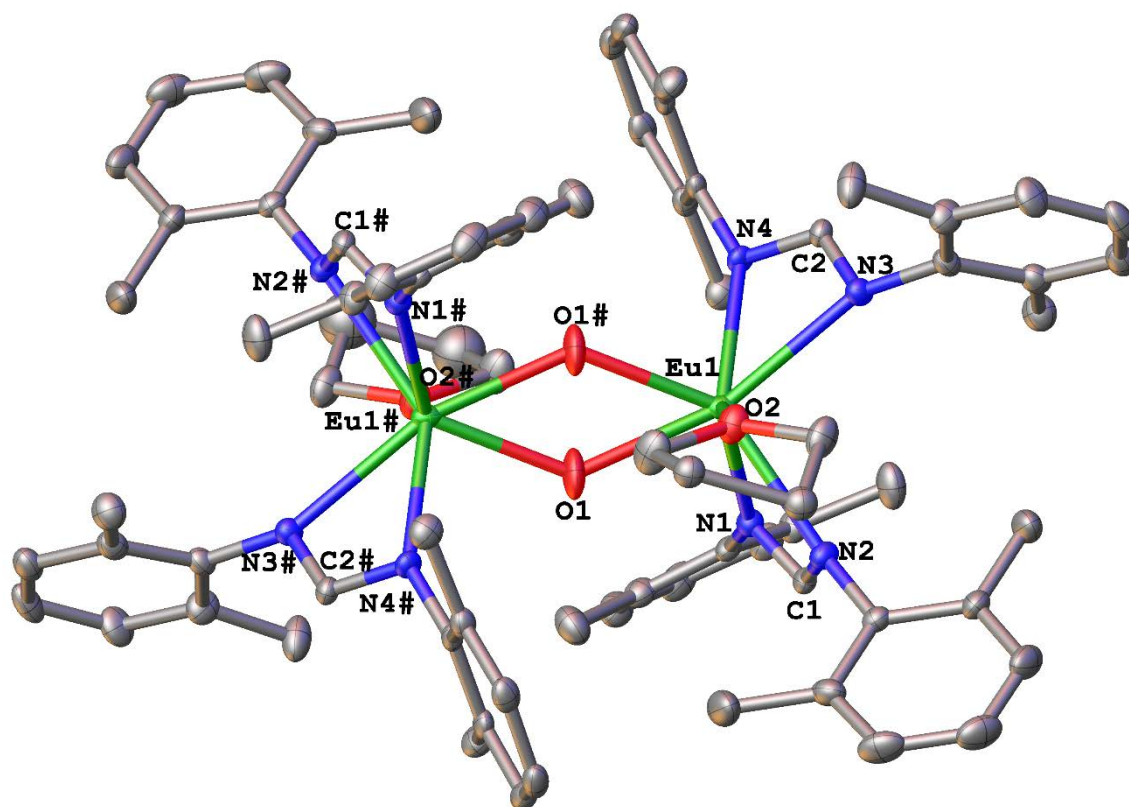


Fig. 4.13: Molecular structure of $[\text{Eu}(\text{XylForm})_2(\mu\text{-OH})(\text{thf})_2]$ (**11**). Ellipsoids have been shown at 50% probability and hydrogen atoms have been omitted for clarity. Selected bond lengths (\AA) and angles ($^\circ$) for **11**: Eu1-N1: 2.458(4), Eu1-N2: 2.504(4), Eu1-N3: 2.491(4), Eu1-N4: 2.472(4), Eu1-O1: 2.274(5), Eu1-O1 $\#$: 2.251(4), Eu1-O2: 2.474(3), N1-Eu1-N2: 54.66(12), N3-Eu1-N4: 54.96(13), O1-Eu1-O1 $\#$: 44.8(2), N1-C1-N2: 118.7(4), N3-C2-N4: 119.1(4).

[Yb(DippForm)(XylForm)₂].PhMe (13)

Complex **13** (Fig. 4.15) is the first ever deliberately synthesised mixed formamidinate species and crystallises in the triclinic space group $P\bar{1}$ (no. 2) with one molecule within the asymmetric unit. The Yb^{3+} centre embraces the coordination number of six, bound to two chelating XylForm and one DippForm ligands with a trigonal prismatic arrangement. The Yb-N contacts fall in the range from 2.317(2) to 2.344(2) \AA , slightly shorter than in complexes **3**, **4** and **5**. However, these are reasonably comparable with the Yb-N bond lengths reported in the isostructural complexes.³⁴

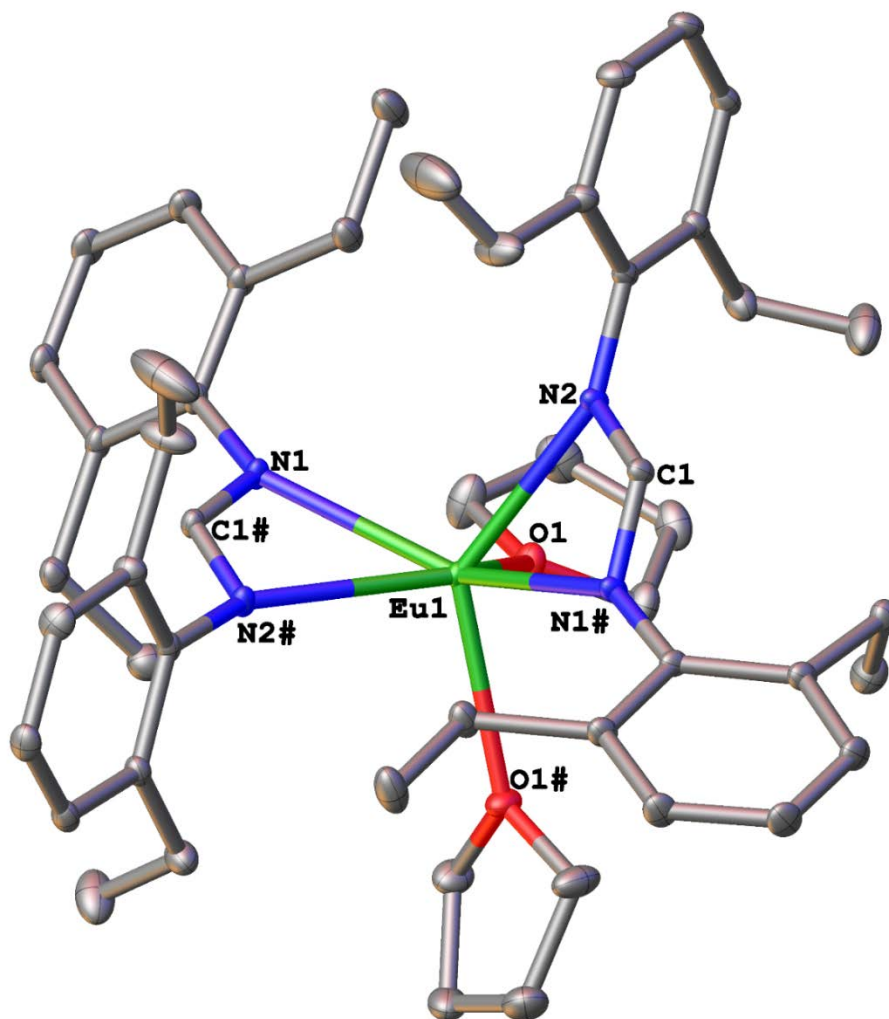


Fig. 4.14: Molecular structure of $[\text{Eu}(\text{EtForm})_2(\text{thf})_2]$ (**12**). Ellipsoids have been shown at 50% probability and hydrogen atoms have been omitted for clarity. Selected bond lengths (\AA) and angles ($^\circ$) for **11**: Eu1-N1: 2.458(4), Eu1-N2: 2.504(4), Eu1-O1: 2.274(5), N1-Eu1-N2#: 52.58(8), N1-Eu1-N2: 106.47(9), N1#-C1-N2: 121.0(3).

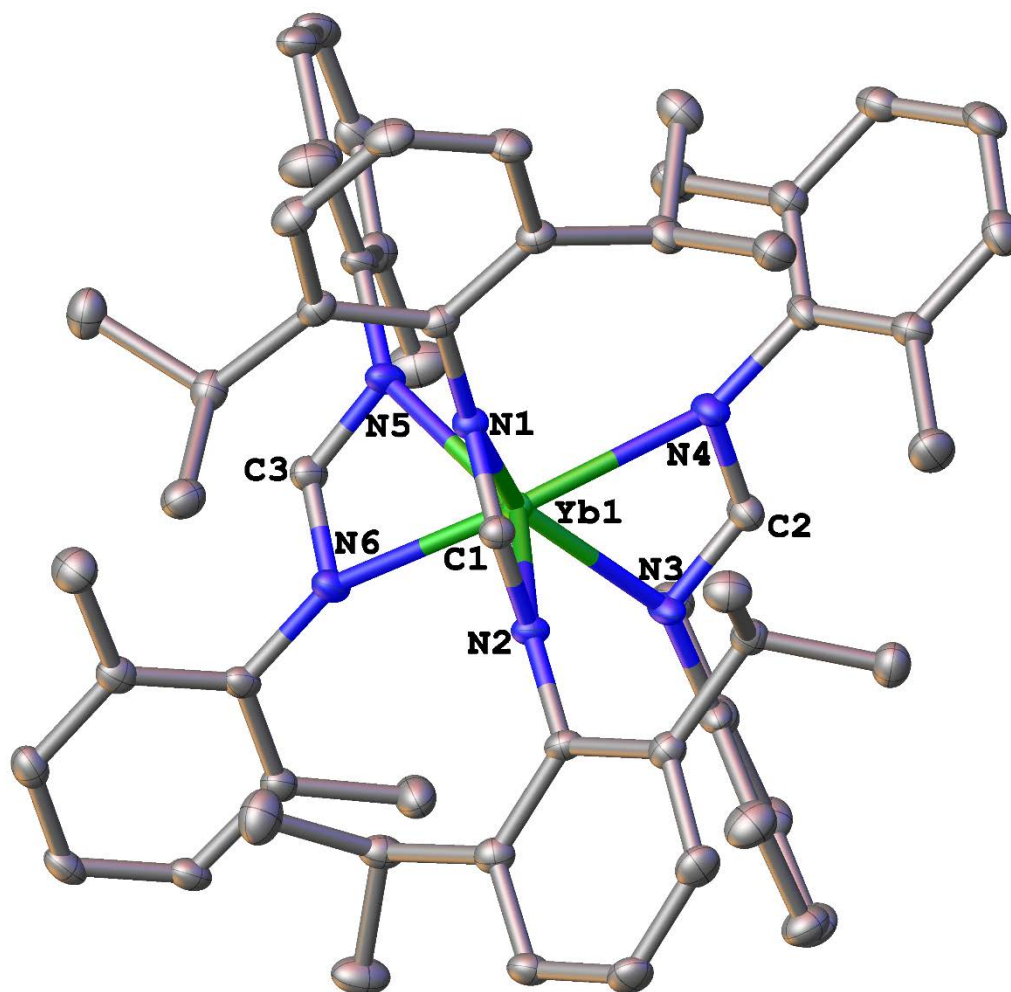


Fig. 4.15: Molecular structure of $[\text{Yb}(\text{DippForm})(\text{XylForm})_2]\cdot\text{PhMe}$ (**13**). Ellipsoids have been shown at 50% probability; hydrogen atoms and solvent of crystallisation have been omitted for clarity. Selected bond lengths (\AA) and angles ($^\circ$) for **13**: Yb1-N1: 2.333(2), Yb1-N2: 2.344(2), Yb1-N3: 2.337(2), Yb1-N4: 2.342(2), Yb1-N5: 2.317(2), Yb1-N6: 2.340(2), N1-Yb1-N2: 58.07(7), N3-Yb1-N4: 58.13(8), N5-Yb1-N6: 58.34(8), N1-C1-N2: 118.3(2), N3-C2-N4: 119.1(2), N5-C3-N6: 118.8(2).

4.3.3 Discussion

Reactivity of divalent formamidinate complexes $\text{Yb}(\text{Form})_2(\text{thf})_2$ (Form = $[\text{RNCHNR}]$; R = 2,6-Me₂ (XylForm); 2,4,6-Me₃ (MesForm); 2,6-Et₂ (EtForm); 2,6-ⁱPr₂ (DippForm)) has been studied by using different oxidants such as Cl_3CCl_3 , $\text{BrCH}_2\text{CH}_2\text{Br}$ and $\text{ICH}_2\text{CH}_2\text{I}$. Benzophenone has also been used to study the reactivity of less sterically demanding ytterbium formamidinate complexes.

Reactions of $[\text{Yb}(\text{DippForm})_2(\text{thf})_2] \cdot 2\text{THF}$ with $\text{BrCH}_2\text{CH}_2\text{Br}$ and $\text{ICH}_2\text{CH}_2\text{I}$ yielded the complexes $[\text{Yb}(\text{DippForm})_2\text{X}(\text{thf})]$ (X = Br, I). The Yb-N bond lengths in complexes range from 2.315(2) to 2.371(2) and 2.304(3) to 2.391(2) Å, respectively and are comparable to the complexes $[\text{Yb}(\text{DippForm})_2\text{Cl}(\text{thf})] \cdot \text{THF}$ and $[\text{Yb}(\text{DippForm})_2\text{Br}(\text{thf})] \cdot \text{Et}_2\text{O}$. The Yb-Br and Yb-I distances are longer than the Yb-Cl distance in $[\text{Yb}(\text{DippForm})_2\text{Cl}(\text{thf})] \cdot \text{THF}$. These differences in the Yb-Cl, Y-Br and Yb-I distances are expected due to the differences in the ionic radii of Cl, Br and I. However, all other divalent formamidinate complexes gave the homoleptic tris-formamidinate complexes $[\text{Yb}(\text{Form})_3]$ (Form = XylForm, MesForm and EtForm). Reactions with benzophenone reactions also resulted in the tris-formamidinate complexes. This is probably due to the redistribution of the less bulky formamidinates in the complexes. Complex $[\text{Yb}(\text{XylForm})_2(\text{thf})_3]$ was isolated from the treatment of $[\text{Yb}(\text{XylForm})_2(\text{thf})_2]$ with $\text{ICH}_2\text{CH}_2\text{I}$ followed by the addition of AlI_3 . The NMR spectra of these complexes could not be integrated due to their paramagnetic behaviour.

With the intention of the isolation of cationic complexes $[\text{L}_2\text{Ln}]^+[\text{AlX}_4/\text{BPh}_4/\text{SbCl}_6]^-$, a range of halide abstraction reactions has been performed using different halide abstracting reagents such as AlX_3 (X = Cl, Br, I), SbCl_5 and AgBPh_4 . Unexpectedly, all attempts to prepare cationic complexes from the halide abstraction reactions consistently gave ligand; however, on one occasion we isolated the reported complex $[\text{YbI}_2(\text{thf})_5]^+[\text{YbI}_4(\text{thf})_2]^-$.

A silver complex $[\text{Ag}(\text{DippForm})_2]$ was isolated from another attempted halide abstraction reaction involving $[\text{Yb}(\text{DippForm})_2\text{Cl}(\text{thf})]$ and AgBPh_4 instead of the expected cationic complex $[\text{Yb}(\text{DippForm})_2]^+[\text{BPh}_4]^-$. An isostructural complex $[\text{Ag}(\text{MesForm})_2]$ was isolated from the reaction of $[\text{Yb}(\text{MesForm})_2(\text{thf})_2]$ and AgBPh_4 at ambient temperature. The reaction between $[\text{Yb}(\text{DippForm})_2(\text{thf})_2]$ and cobalt carbonyl gave the cobalt complex

Chapter 4

$[\text{Co}(\text{DippFormCO})(\text{CO})_3]\cdot\text{THF}$ in place of the expected cationic complex $[\text{Yb}(\text{DippForm})_2]^+[\text{Co}(\text{CO})_4]^-$. In this complex, the cobalt was oxidised to Co^{1+} and a carbonyl group was inserted between the Co^{1+} centre and one of the nitrogens from the NCN backbone of the formamidinate.

A deliberate RTP reaction using two formamidines of dissimilar steric bulk such as DippFormH and XylFormH afforded the heteroleptic tris-formamidinate complex $[\text{Yb}(\text{DippForm})(\text{XylForm})_2]\cdot\text{PhMe}$ for the first time. In addition, $[\text{Eu}(\text{XylForm})_2(\mu\text{-OH})(\text{thf})_2]$ and $[\text{Eu}(\text{EtForm})_2(\text{thf})_2]$ have been synthesised by the RTP reactions using XylFormH and EtFormH, respectively. $[\text{Yb}(\text{MesForm})_2(\mu\text{-OH})_2]$ was also isolated by the similar procedure using ytterbium. The formation of $[\text{Yb}(\text{MesForm})_2(\mu\text{-OH})_2]$ and $[\text{Eu}(\text{XylForm})_2(\mu\text{-OH})(\text{thf})_2]$ probably involves a trace amount of water and the presence of the hydroxyl group was further confirmed from IR spectra.

4.4 Conclusions

Reactivity of divalent ytterbium formamidinate complexes has been studied and halide abstraction reactions have been performed for the synthesis of cationic lanthanoid complexes. Unfortunately, all attempts to prepare cationic complexes have been unsuccessful for this occasion. However, the reactivity studies yielded some novel complexes as well as some known complexes being synthesised from different reaction routes. For the first time, we deliberately synthesised a heteroleptic formamidinate complex from two different formamidinates of varying steric bulk.

4.5 Experimental

For general procedures, see Appendix 2.

Yb(DippForm)₂Br(thf) (1)

An orange solution of [Yb(DippForm)₂(thf)₂].2THF (0.59 g, 0.5 mmol) in toluene (15 mL) was added to a solution of BrCH₂CH₂Br (0.06 g, 0.3 mmol) in toluene (40 mL) with stirring. The solution was heated at 70 °C with stirring for 2 h. The volume of solution was reduced under vacuum, stored in fridge for 2 days and bright yellow crystals formed (0.41 g, 77%). Metal analysis (C₅₄H₇₈BrN₄OYb): cal. (%) Yb 16.45; found Yb 16.17. IR (Nujol, ν/cm⁻¹): 2725 (w), 1666 (m), 1528 (m), 1460 (s), 1377 (w), 1319 (w), 1273 (m), 1194 (w), 1098 (w), 1055 (w), 1012 (w), 946 (w), 934 (w), 859 (w), 801 (m), 775 (w), 757 (m), 722 (w).

Yb(DippForm)₂I(thf) (2)

An orange solution of [Yb(DippForm)₂(thf)₂].2THF (0.29 g, 0.25 mmol) in toluene (10 mL) was added to a solution of ICH₂CH₂I (0.04 g, 0.15 mmol) in toluene (30 mL) with stirring. The solution was heated at 70 °C with stirring for 2 h. The volume of solution was reduced under vacuum, stored in fridge for 2 days and bright yellow crystals formed (0.20 g, 73%). Metal analysis (C₅₄H₇₈IN₄OYb): cal. (%) Yb 15.74; found Yb 15.43. IR (Nujol, ν/cm⁻¹): 2560 (w), 1664 (m), 1587 (w), 1521 (m), 1460 (s), 1378 (m), 1318 (w), 1235 (m), 1189 (w), 1097 (w), 1055 (w), 1010 (w), 934 (w), 857 (w), 821 (w), 800 (m), 775 (m), 722 (w), 668 (w).

Chapter 4

Yb(XylForm)₃ (3)

A mixture of an excess of freshly filed Yb metal (0.20 g, 1.15 mmol), bis(pentafluorophenyl)mercury (0.49 g, 0.92 mmol) and XylFormH (0.46 g, 1.85 mmol) was taken in a Schlenk flask under purified nitrogen. Tetrahydrofuran (40 mL) was added to the mixture. The slurry was stirred at ambient temperature for 72 h and the red-coloured solution was filtered to separate excess Yb metal and elemental mercury deposited. Hexachloroethane (0.23 g, 0.95 mmol) was added to the red solution with stirring. The colour of the solution turned to yellow from red immediately. After 2h, the solution was filtered to remove any solid materials and reduced the volume under vacuum to 10 mL. Yellow crystals, suitable for X-ray were formed after 2 d (0.34 g, 59%). Metal analysis (C₅₁H₅₇N₆Yb): cal. (%) Yb 18.67; found Yb 18.21. IR (Nujol, ν/cm^{-1}): 2923 (s), 2349 (w), 2283 (w), 1651 (w), 1589 (w), 1532 (w), 1463 (s), 1377 (m), 1289 (w), 1202 (w), 1091 (w), 763 (w), 722 (w).

Yb(MesForm)₃ (4)

A mixture of an excess of freshly filed Yb metal (0.20 g, 1.15 mmol), bis(pentafluorophenyl)mercury (0.49 g, 0.92 mmol) and XylFormH (0.46 g, 1.85 mmol) was taken in a Schlenk flask under purified nitrogen. Tetrahydrofuran (40 mL) was added to the mixture. The slurry was stirred at ambient temperature for 72 h and the red-coloured solution was filtered to separate excess Yb metal and elemental mercury deposited. Hexachloroethane (0.23 g, 0.95 mmol) was added to the red solution with stirring. The colour of the solution turned to yellow from red immediately. After 2h, the solution was filtered to remove any solid materials and reduced the volume under vacuum to 10 mL. Yellow crystals, suitable for X-ray were formed after 2 d (0.36 g, 54%). Metal analysis (C₅₇H₆₉N₆Yb): cal. (%) Yb 17.11; found Yb 16.89. IR (Nujol, ν/cm^{-1}): 2722 (m), 1675 (m), 1622 (s), 1585 (m), 1460 (s), 1261 (m), 1194 (w), 1098 (m), 1017 (m), 870 (w), 802 (m), 722 (w).

Chapter 4

[Yb(EtForm)₃].2THF (5)

A mixture of an excess of freshly filed Yb metal (0.20 g, 1.15 mmol), bis(pentafluorophenyl)mercury (0.49 g, 0.92 mmol) and XylFormH (0.46 g, 1.85 mmol) was taken in a Schlenk flask under purified nitrogen. Tetrahydrofuran (40 mL) was added to the mixture. The slurry was stirred at ambient temperature for 72 h and the red-coloured solution was filtered to separate excess Yb metal and elemental mercury deposited. Hexachloroethane (0.23 g, 0.95 mmol) was added to the red solution with stirring. The colour of the solution turned to yellow from red immediately. After 2h, the solution was filtered to remove any solid materials and reduced the volume under vacuum to 10 mL. Yellow crystals, suitable for X-ray were formed after 2 d (0.42 g, 60%). Metal analysis (C₇₁H₉₂N₆O₂Yb): cal. (%) Yb 14.02; found Yb 13.91. IR (Nujol, ν/cm^{-1}): 2727 (w), 1637 (s), 1605 (w), 1510 (s), 1463 (s), 1377 (s), 1310 (w), 1262 (w), 1211 (w), 1172 (w), 1147 (w), 1120 (w), 1031 (m), 850 (m), 783 (w), 722 (7), 680 (w).

[{Ag(MesForm)}₂].PhMe (6)

[Yb(MesForm)₂(thf)₂] (0.21 g, 0.24 mmol) was dissolved in 40 mL of thf and AgBPh₄ (0.13 g, 0.29 mmol) was added to the orange solution with stirring. The solution was stirred for 2h at ambient temperature and filtered to remove any suspended materials. The solvent was then removed under vacuum and redissolved the solid in toluene (10mL). After storing in fridge, colourless crystals, suitable for crystallography were formed in two days (0.09 g, 43%).

[{Ag(DippForm)}₂].THF (7)

[Yb(DippForm)₂Cl(thf)].THF (0.55 g, 0.5 mmol) was dissolved in 40 mL of thf and AgBPh₄ (0.26 g, 0.6 mmol) was added to the yellow solution with stirring. The solution was stirred for 2h at ambient temperature and filtered to remove any suspended materials. The volume of the solution was then reduced to 10 mL under vacuum. Colourless crystals, suitable for crystallography were formed in two days (0.18 g, 35%). IR (Nujol, ν/cm^{-1}): 2854 (s), 1667 (w), 1596 (w), 1554 (m), 1460 (s), 1377 (s), 1339 (s), 1315 (w), 1239 (w), 1180 (w), 1099 (w), 802 (w), 755 (w), 722 (w).

Chapter 4

Yb(XylForm)₂(thf)₃ (**8**)

A mixture of [Yb(XylForm)₂(thf)₂] (0.76 g, 0.93 mol) and ICH₂CH₂I (0.16 g, 0.55 mmol) was taken in a Schlenk flask under purified nitrogen. Tetrahydrofuran (40 mL) was added to the mixture. The slurry was stirred at ambient temperature for 2 h and AlI₃ (0.38 g, 0.93 mmol) was added to the yellow solution with stirring. After heating the mixture for 2 h at 60 °C, the solution was filtered to remove any solid materials and reduced the volume under vacuum to 10 mL. Yellow crystals, suitable for X-ray were formed after 2 d (0.10 g, 60%). Metal analysis (C₂₉H₄₂I₂N₂O₃Yb): cal. (%) Yb 19.37; found Yb 19.03. IR (Nujol, ν/cm⁻¹): 2854 (s), 2360 (m), 2342 (w), 1672 (w), 1638 (w), 1525 (w), 1464 (s), 1377 (m), 1261 (w), 1188 (w), 1091 (w), 1038 (w), 1000 (w), 915 (w), 848 (w), 795 (w), 721 (w), 668 (w).

[Co(DippFormCO)(CO)₃].THF (**9**)

THF (30 mL) was added to a Schlenk charged with [Yb(DippForm)₂(thf)₂].2THF (0.46 g, 0.40 mmol) under purified nitrogen. Co₂(CO)₈ (0.16 g, 0.48 mmol) was added to the orange solution with stirring and stirred for 12 h at ambient temperature. The colour of the solution turned to dark brown from orange. The solution was filtered to remove any solid materials and reduced the volume under vacuum. The solution was then stored in fridge for 3 days during which time needle like crystals formed (0.35 g, 73%). IR (Nujol, ν/cm⁻¹): 2726 (m), 2071 (s), 2010 (s), 1985 (w), 1969 (s), 1667 (s), 1623 (m), 1588 (w), 1463 (s), 1377 (s), 1280 (m), 1199 (w), 1100 (w), 1009 (w), 897 (w), 801 (m), 758 (m), 722 (m), 659 (m).

[Yb(MesForm)₂(μ-OH)]₂ (**10**)

A mixture of an excess of freshly filed Yb metal (0.20 g, 1.15 mmol), bis(pentafluorophenyl)mercury (0.21 g, 0.40 mmol) and MesFormH (0.22 g, 0.81 mmol) was taken in a Schlenk flask under purified nitrogen. Tetrahydrofuran (40 mL) was added to the mixture. The slurry was stirred at ambient temperature for 72 h and the yellow-coloured solution was filtered to separate excess Yb metal and elemental mercury deposited. Then the volume of the solution was reduced under vacuum to 10 mL. Yellow crystals, suitable for X-ray were formed after 3 d (0.19 g, 63%). Metal analysis (C₃₈H₄₇N₄OYb): cal. (%) Yb 23.11; found Yb 22.96. IR (Nujol, ν/cm⁻¹): 3663 (s), 2720 (s), 2484 (w), 1878 (w),

Chapter 4

1718 (m), 1634 (s), 1600 (s), 1297 (s), 1263 (s), 1200 (s), 1145 (s), 1061 (s), 1010 (s), 956 (s), 909 (s), 720 (s), 669 (s).

[Eu(XylForm)₂(μ-OH)(thf)]₂ (**11**)

THF (40 mL) was added to a Schlenk flask charged with excess freshly filed Eu metal (0.10 g, 0.66 mmol), Hg(C₆F₅)₂ (0.37 g, 0.69 mmol) and XylFormH (0.35 g, 1.37 mmol), under purified nitrogen. The slurry was stirred at ambient temperature for 72 h and yielded a light brown solution after filtration. Concentration under reduced pressure and storage in fridge for several days gave light brown crystals (0.35 g, 69%). IR (Nujol, ν/cm⁻¹): 3265 (w), 2715 (w), 1633 (m), 1532 (w), 1463 (s), 1377 (s), 1302 (w), 1261 (w), 1201 (m), 1091 (w), 1032 (w), 802 (w), 759 (m), 722 (w).

[Eu(EtForm)₂(thf)]₂ (**12**)

THF (40 mL) was added to a Schlenk flask charged with excess freshly filed Eu metal (0.20 g, 1.32 mmol), Hg(C₆F₅)₂ (0.74 g, 1.38 mmol) and EtFormH (0.85 g, 2.74 mmol), under purified nitrogen. The slurry was stirred at ambient temperature for 72 h and yielded a light yellow solution after filtration. Concentration under reduced pressure and storage in fridge for several days gave light yellow crystals (0.82 g, 66%). Metal analysis (C₅₀H₇₀N₄O₂Eu): cal. (%) Eu 16.68; found Eu 16.31. IR (Nujol, ν/cm⁻¹): 1656 (w), 1633 (w), 1594 (w), 1525 (s), 1456 (s), 1192 (m), 1104 (m), 1074 (w), 1034 (w), 1007 (w), 968 (w), 889 (w), 868 (w), 805 (w), 767 (m), 757 (m), 722 (w).

[Yb(DippForm)(XylForm)₂].PhMe (**13**)

A mixture of an excess of freshly filed Yb metal (0.12 g, 0.69 mmol), bis(pentafluorophenyl)mercury (0.37 g, 0.69 mmol), DippFormH (0.25 g, 0.69 mmol) and XylFormH (0.20 g, 0.75 mmol) was taken in a Schlenk flask under purified nitrogen. Tetrahydrofuran (40 mL) was added to the mixture. The slurry was stirred at ambient temperature for 72 h and the red-coloured solution was filtered to separate excess Yb metal and elemental mercury deposited. Then the solvent was removed under vacuum and crystallised from toluene. Red crystals, suitable for X-ray were formed after several days

Chapter 4

(0.53 g, 68%). Metal analysis ($C_{66}H_{81}N_6Yb$): cal. (%) Yb 15.29; found Yb 15.26. IR (Nujol, ν/cm^{-1}): 2854 (s), 2360 (w), 1665 (w), 1529 (m), 1460 (m), 1377 (m), 1290 (w), 1202 (w), 1093 (w), 1037 (w), 934 (w), 880 (w), 800 (w), 764 (w), 727 (w).

4.6 X-ray crystal data

For general procedures, see Appendix 2.

Yb(DippForm)₂Br(thf) (1)

C₅₄H₇₈BrN₄OYb, $M_r = 1052.13$ g/mol, triclinic, space group $P-1$ (no. 2), $a = 11.415(2)$ Å, $b = 14.425(3)$ Å, $c = 16.253(3)$ Å, $\alpha = 83.99(3)^\circ$, $\beta = 77.74(3)^\circ$, $\gamma = 80.56(3)^\circ$, $V = 2573.0(10)$ Å³, $Z = 2$, $T = 173.15$ K, $\mu(\text{MoK}\alpha) = 2.633$ mm⁻¹, $D_{\text{calc}} = 1.355$ g/cm³, 21915 reflections measured ($2.57^\circ \leq 2\Theta \leq 55.782^\circ$), 11081 unique ($R_{\text{int}} = 0.0372$, $R_{\text{sigma}} = 0.0485$) which were used in all calculations. The final R_1 was 0.0302 ($I > 2\sigma(I)$) and wR_2 was 0.0802 (all data).

Yb(DippForm)₂I(thf) (2)

C₅₄H₇₈IN₄OYb ($M_r = 1099.19$ g/mol): triclinic, space group $P-1$ (no. 2), $a = 11.653(2)$ Å, $b = 14.425(3)$ Å, $c = 16.212(3)$ Å, $\alpha = 83.50(3)^\circ$, $\beta = 77.54(3)^\circ$, $\gamma = 79.94(3)^\circ$, $V = 2612(1)$ Å³, $Z = 2$, $T = 100.15$ K, $\mu(\text{Mo K}\alpha) = 2.420$ mm⁻¹, $D_{\text{calc}} = 1.3975$ g/cm³, 37350 reflections measured ($2.58^\circ \leq 2\Theta \leq 55.82^\circ$), 11392 unique ($R_{\text{int}} = 0.0588$, $R_{\text{sigma}} = 0.0548$) which were used in all calculations. The final R_1 was 0.0338 ($I \geq 2u(I)$) and wR_2 was 0.0989 (all data).

Yb(XylForm)₃ (3)

C₅₁H₅₇N₆Yb ($M_r = 927.06$ g/mol): orthorhombic, space group $P2_12_12_1$ (no. 19), $a = 10.695(2)$ Å, $b = 20.269(4)$ Å, $c = 21.005(4)$ Å, $V = 4553.4(16)$ Å³, $Z = 4$, $T = 296.15$ K, $\mu(\text{MoK}\alpha) = 2.094$ mm⁻¹, $D_{\text{calc}} = 1.352$ g/cm³, 56943 reflections measured ($2.792^\circ \leq 2\Theta \leq 54.998^\circ$), 10456 unique ($R_{\text{int}} = 0.1418$, $R_{\text{sigma}} = 0.1036$) which were used in all calculations. The final R_1 was 0.0470 ($I > 2\sigma(I)$) and wR_2 was 0.1393 (all data).

Yb(MesForm)₃ (4)

C₅₇H₆₉N₆Yb ($M_r = 1011.19$ g/mol): triclinic, space group $P-1$ (no. 2), $a = 10.9808(3)$ Å, $b = 12.2357(4)$ Å, $c = 21.5729(6)$ Å, $\alpha = 84.728(2)^\circ$, $\beta = 83.131(2)^\circ$, $\gamma = 84.594(2)^\circ$, $V =$

Chapter 4

2855.34(15) Å³, $Z = 2$, $T = 296.15$ K, $\mu(\text{MoK}\alpha) = 1.675$ mm⁻¹, $D_{\text{calc}} = 1.173$ g/cm³, 33823 reflections measured ($3.354^\circ \leq 2\Theta \leq 50^\circ$), 10026 unique ($R_{\text{int}} = 0.0514$, $R_{\text{sigma}} = 0.0512$) which were used in all calculations. The final R_1 was 0.0455 ($I > 2\sigma(I)$) and wR_2 was 0.1513 (all data).

[Yb(EtForm)₃].2THF (5)

C₇₁H₉₂N₆O₂Yb ($M_r = 1234.52$ g/mol): triclinic, space group $P-1$ (no. 2), $a = 13.182(3)$ Å, $b = 23.468(5)$ Å, $c = 24.268(5)$ Å, $\alpha = 62.31(3)^\circ$, $\beta = 89.13(3)^\circ$, $\gamma = 75.25(3)^\circ$, $V = 6382(3)$ Å³, $Z = 4$, $T = 293(2)$ K, $\mu(\text{MoK}\alpha) = 1.514$ mm⁻¹, $D_{\text{calc}} = 1.282$ g/cm³, 118755 reflections measured ($1.908^\circ \leq 2\Theta \leq 63.76^\circ$), 30947 unique ($R_{\text{int}} = 0.0604$, $R_{\text{sigma}} = 0.0525$) which were used in all calculations. The final R_1 was 0.0411 ($I > 2\sigma(I)$) and wR_2 was 0.1115 (all data).

[{Ag(MesForm)}₂].PhMe (6)

C₄₅H₅₄Ag₂N₄ ($M_r = 874.66$ g/mol): triclinic, space group $P-1$ (no. 2), $a = 11.8852(3)$ Å, $b = 12.0048(3)$ Å, $c = 15.7270(4)$ Å, $\alpha = 88.8710(10)^\circ$, $\beta = 72.3870(10)^\circ$, $\gamma = 84.2450(10)^\circ$, $V = 2127.82(9)$ Å³, $Z = 2$, $T = 296.15$ K, $\mu(\text{MoK}\alpha) = 0.956$ mm⁻¹, $D_{\text{calc}} = 1.365$ g/cm³, 23091 reflections measured ($2.718^\circ \leq 2\Theta \leq 49.998^\circ$), 7447 unique ($R_{\text{int}} = 0.0468$, $R_{\text{sigma}} = 0.0477$) which were used in all calculations. The final R_1 was 0.0379 ($I > 2\sigma(I)$) and wR_2 was 0.1090 (all data).

[{Ag(DippForm)}₂].THF (7)

C₅₄H₇₈Ag₂N₄O ($M_r = 1014.96$ g/mol): monoclinic, space group $P2_1/c$ (no. 14), $a = 23.500(5)$ Å, $b = 16.971(3)$ Å, $c = 16.962(3)$ Å, $\beta = 90.47(3)^\circ$, $V = 6765(2)$ Å³, $Z = 8$, $T = 173.15$ K, $\mu(\text{MoK}\alpha) = 0.614$ mm⁻¹, $D_{\text{calc}} = 1.067$ g/cm³, 84621 reflections measured ($1.732^\circ \leq 2\Theta \leq 55.848^\circ$), 16072 unique ($R_{\text{int}} = 0.0447$, $R_{\text{sigma}} = 0.0274$) which were used in all calculations. The final R_1 was 0.0934 ($I > 2\sigma(I)$) and wR_2 was 0.2885 (all data).

Chapter 4

Yb(XylForm)I₂(thf)₃ (**8**)

C₂₉H₄₂I₂N₂O₃Yb ($M_r = 893.48$ g/mol): triclinic, space group $P-1$ (no. 2), $a = 13.150(3)$ Å, $b = 13.748(3)$ Å, $c = 23.220(5)$ Å, $\alpha = 77.54(3)^\circ$, $\beta = 89.77(3)^\circ$, $\gamma = 61.96(3)^\circ$, $V = 3594.8(16)$ Å³, $Z = 4$, $T = 173.15$ K, $\mu(\text{MoK}\alpha) = 4.346$ mm⁻¹, $D_{\text{calc}} = 1.649$ g/cm³, 31672 reflections measured ($1.808^\circ \leq 2\Theta \leq 50^\circ$), 11609 unique ($R_{\text{int}} = 0.2129$, $R_{\text{sigma}} = 0.1826$) which were used in all calculations. The final R_1 was 0.1177 ($I > 2\sigma(I)$) and wR_2 was 0.3366 (all data).

[Co(DippFormCO)(CO)₃].THF (**9**)

C₃₃H₃₉CoN₂O₅ ($M_r = 602.59$ g/mol): monoclinic, space group $P2_1/n$ (no. 14), $a = 11.1122(10)$ Å, $b = 17.1592(17)$ Å, $c = 18.425(2)$ Å, $\beta = 100.195(4)^\circ$, $V = 3457.7(6)$ Å³, $Z = 4$, $T = 296.15$ K, $\mu(\text{MoK}\alpha) = 0.534$ mm⁻¹, $D_{\text{calc}} = 1.158$ g/cm³, 21302 reflections measured ($3.268^\circ \leq 2\Theta \leq 49.998^\circ$), 6021 unique ($R_{\text{int}} = 0.1003$, $R_{\text{sigma}} = 0.0940$) which were used in all calculations. The final R_1 was 0.0700 ($I > 2\sigma(I)$) and wR_2 was 0.2159 (all data).

[Yb(MesForm)₂(μ -OH)]₂ (**10**)

C₃₈H₄₇N₄OYb ($M_r = 748.86$ g/mol): monoclinic, space group $C2/c$ (no. 15), $a = 19.028$ Å, $b = 15.3$ Å, $c = 23.626$ Å, $\beta = 92.468^\circ$, $V = 6871.819549$ Å³, $Z = 8$, $T = 173.15$ K, $\mu(\text{Mo K}\alpha) = 2.756$ mm⁻¹, $D_{\text{calc}} = 1.4476$ g/cm³, 57256 reflections measured ($3.42^\circ \leq 2\Theta \leq 55^\circ$), 7884 unique ($R_{\text{int}} = 0.0595$, $R_{\text{sigma}} = 0.0300$) which were used in all calculations. The final R_1 was 0.0372 ($I \geq 2u(I)$) and wR_2 was 0.0950 (all data).

[Eu(XylForm)₂(μ -OH)(thf)]₂ (**11**)

C₃₈H₄₅EuN₄O₂ ($M_r = 741.71$ g/mol): triclinic, space group $P-1$ (no. 2), $a = 11.280(2)$ Å, $b = 12.030(2)$ Å, $c = 14.517(3)$ Å, $\alpha = 113.89(3)^\circ$, $\beta = 100.70(3)^\circ$, $\gamma = 99.90(3)^\circ$, $V = 1701.7(7)$ Å³, $Z = 2$, $T = 293(2)$ K, $\mu(\text{MoK}\alpha) = 1.881$ mm⁻¹, $D_{\text{calc}} = 1.442$ g/cm³, 18574 reflections measured ($5.452^\circ \leq 2\Theta \leq 63.446^\circ$), 8120 unique ($R_{\text{int}} = 0.0600$, $R_{\text{sigma}} = 0.0801$)

Chapter 4

which were used in all calculations. The final R_1 was 0.0495 ($I > 2\sigma(I)$) and wR_2 was 0.1212 (all data).

[Eu(EtForm)₂(thf)₂] (12)

C₂₅H₃₅Eu_{0.5}N₂O ($M_r = 455.51$ g/mol): monoclinic, space group $C2/c$ (no. 15), $a = 14.6956(5)$ Å, $b = 16.5752(6)$ Å, $c = 19.8387(7)$ Å, $\beta = 96.3170(10)^\circ$, $V = 4803.0(3)$ Å³, $Z = 8$, $T = 296.15$ K, $\mu(\text{MoK}\alpha) = 1.346$ mm⁻¹, $D_{\text{calc}} = 1.254$ g/cm³, 29143 reflections measured ($3.716^\circ \leq 2\Theta \leq 54.996^\circ$), 5521 unique ($R_{\text{int}} = 0.0507$, $R_{\text{sigma}} = 0.0369$) which were used in all calculations. The final R_1 was 0.0344 ($I > 2\sigma(I)$) and wR_2 was 0.0896 (all data).

[Yb(DippForm)(XylForm)₂].PhMe (13)

C₆₆H₈₁N₆Yb ($M_r = 1131.38$ g/mol): triclinic, space group $P-1$ (no. 2), $a = 11.766(2)$ Å, $b = 14.393(3)$ Å, $c = 17.710(4)$ Å, $\alpha = 84.48(3)^\circ$, $\beta = 71.75(3)^\circ$, $\gamma = 88.88(3)^\circ$, $V = 2835.0(11)$ Å³, $Z = 2$, $T = 293(2)$ K, $\mu(\text{MoK}\alpha) = 1.695$ mm⁻¹, $D_{\text{calc}} = 1.322$ g/cm³, 52041 reflections measured ($2.432^\circ \leq 2\Theta \leq 63.816^\circ$), 13807 unique ($R_{\text{int}} = 0.0502$, $R_{\text{sigma}} = 0.0416$) which were used in all calculations. The final R_1 was 0.0321 ($I > 2\sigma(I)$) and wR_2 was 0.0881 (all data).

4.7 References

1. R. Kempe, *Angew. Chem*, 2000, **112**, 478-504.
2. R. Anwender, in *Organolanthoid Chemistry: Synthesis, Structure, Catalysis*, Springer, Berlin, Heidelberg, 1996, pp. 33-112.
3. P. W. Roesky, *Chem. Soc. Rev.*, 2000, **29**, 335-345.
4. F. T. Edelmann, D. M. M. Freckmann and H. Schumann, *Chem. Rev.*, 2002, **102**, 1851-1896.
5. W. E. Piers and D. J. H. Emslie, *Coord. Chem. Rev.*, 2002, **233**, 131-155.
6. S. Cotton, in *Comprehensive Coordination Chemistry II*, eds. J. A. McCleverty and T. J. Meyer, Pergamon, Oxford, 2003, vol. 3, ch. 2, pp. 93-188.
7. F. T. Edelmann, in *Adv. Organomet. Chem.*, eds. F. A. Hill and M. J. Fink, Academic Press, Oxford, 2008, vol. 57, ch. 3, pp. 183-291.
8. F. T. Edelmann, *Chem. Soc. Rev.*, 2009, **38**, 2253-2268.
9. F. T. Edelmann, *Chem. Soc. Rev.*, 2012, **41**, 7657-7672.
10. F. T. Edelmann, in *Adv. Organomet. Chem.*, eds. F. A. Hill and M. J. Fink, Academic Press, 2013, vol. 61, ch. 2, pp. 55-289.
11. F. T. Edelmann, *Coord. Chem. Rev.*, 2016, **318**, 29-130.
12. F. T. Edelmann, *Coord. Chem. Rev.*, 2016, **306**, 346-419.
13. M. L. Cole, G. B. Deacon, C. M. Forsyth, P. C. Junk, K. Konstas, J. Wang, H. Bittig and D. Werner, *Chem. Eur. J.*, 2013, **19**, 1410-1420.
14. G. B. Deacon, P. C. Junk and D. Werner, *Polyhedron*, 2016, **103**, 178-186.
15. M. L. Cole and P. C. Junk, *Chem. Commun.*, 2005, 2695-2697.
16. G. B. Deacon, P. C. Junk and D. Werner, *Chem. Eur. J.*, 2016, **22**, 160-173.

Chapter 4

17. M. L. Cole, G. B. Deacon, C. M. Forsyth, P. C. Junk, K. Konstas and J. Wang, *Chem. Eur. J.*, 2007, **13**, 8092-8110.
18. G. B. Deacon, P. C. Junk, L. K. Macreadie and D. Werner, *Eur. J. Inorg. Chem.*, 2014, **2014**, 5240-5250.
19. G. B. Deacon, P. C. Junk and D. Werner, *Eur. J. Inorg. Chem.*, 2015, **2015**, 1484-1489.
20. D. Werner, G. B. Deacon, P. C. Junk and R. Anwander, *Chem. Eur. J.*, 2014, **20**, 4426-4438.
21. S. Hamidi, L. N. Jende, H. Martin Dietrich, C. c. Maichle-Mössmer, K. W. Törnroos, G. B. Deacon, P. C. Junk and R. Anwander, *Organometallics*, 2013, **32**, 1209-1223.
22. A. Zuyls, P. W. Roesky, G. B. Deacon, K. Konstas and P. C. Junk, *Eur. J. Org. Chem.*, 2008, **2008**, 693-697.
23. M. L. Cole, G. B. Deacon, C. M. Forsyth, P. C. Junk, D. Polo-Cerón and J. Wang, *Dalton Trans.*, 2010, **39**, 6732-6738.
24. M. L. Cole, G. B. Deacon, P. C. Junk and K. Konstas, *Chem. Commun.*, 2005, 1581-1583.
25. G. B. Deacon, C. M. Forsyth, P. C. Junk and J. Wang, *Inorg. Chem.*, 2007, **46**, 10022-10030.
26. M. L. Cole, G. B. Deacon, P. C. Junk and J. Wang, *Organometallics*, 2013, **32**, 1370-1378.
27. G. B. Deacon, P. C. Junk, J. Wang and D. Werner, *Inorg. Chem.*, 2014, **53**, 12553-12563.
28. D. Werner, X. Zhao, S. P. Best, L. Maron, P. C. Junk and G. B. Deacon, *Chem. Eur. J.*, 2017, **23**, 2084-2102.
29. G. B. Deacon, C. M. Forsyth, D. Freckmann, P. C. Junk, K. Konstas, J. Luu, G. Meyer and D. Werner, *Aust. J. Chem.*, 2014, **67**, 1860-1865.

Chapter 4

30. G. B. Deacon, M. E. Hossain, P. C. Junk and M. Salehisaki, *Coord. Chem. Rev.*, 2017, **340**, 247-265.
31. L. Guo, X. Zhu, S. Zhou, X. Mu, Y. Wei, S. Wang, Z. Feng, G. Zhang and B. Deng, *Dalton Trans.*, 2014, **43**, 6842-6847.
32. A. Edelmann, C. G. Hrib, L. Hilfert, S. Blaurock and F. T. Edelmann, *Acta Cryst.*, 2010, **E66**, m1675-m1676.
33. A. Edelmann, V. Lorenz, C. G. Hrib, L. Hilfert, S. Blaurock and F. T. Edelmann, *Organometallics*, 2012, **32**, 1435-1444.
34. M. L. Cole, G. B. Deacon, C. M. Forsyth, P. C. Junk, K. Konstas and J. Wang, *Chem. Euro. J.*, 2007, **13**, 8092-8110.
35. P. K. Bakshi, A. Linden, B. R. Vincent, S. P. Roe, D. Adhikesavalu, T. S. Cameron and O. Knop, *Can. J. Chem.*, 1994, **72**, 1273-1293.
36. M. Niemeyer, *Acta Cryst.*, 2001, **57E**, m363-m364.
37. W. J. Evans, I. Bloom, J. W. Grate, L. A. Hughes, W. E. Hunter and J. L. Atwood, *Inorg. Chem.*, 1985, **24**, 4620-4623.
38. A. W. Duff, P. B. Hitchcock, M. F. Lappert, R. G. Taylor and J. A. Segal, *J. Organomet. Chem.*, 1985, **293**, 271-283.
39. R. Shannon, *Acta Cryst.*, 1976, **A32**, 751-767.
40. A. C. Lane, M. V. Vollmer, C. H. Laber, D. Y. Melgarejo, G. M. Chiarella, J. P. Fackler, X. Yang, G. A. Baker and J. R. Walensky, *Inorg. Chem.*, 2014, **53**, 11357-11366.
41. J. P. Coyle, P. G. Gordon, A. P. Wells, D. J. Mandia, E. R. Sirianni, G. P. A. Yap and S. T. Barry, *Chem. Mater.*, 2013, **25**, 4566-4573.
42. F. A. Cotton, X. Feng, M. Matusz and R. Poli, *J. Am. Chem. Soc.*, 1988, **110**, 7077-7083.

Chapter 4

43. B. S. Lim, A. Rahtu, J.-S. Park and R. G. Gordon, *Inorg. Chem.*, 2003, **42**, 7951-7958.
44. S. J. Archibald, N. W. Alcock, D. H. Busch and D. R. Whitcomb, *Inorg. Chem.*, 1999, **38**, 5571-5578.
45. A. A. Mohamed, *Coord. Chem. Rev.*, 2010, **254**, 1918-1947.
46. A. Bondi, *J. Phys. Chem.*, 1964, **68**, 441-451.
47. D. Heitmann, C. Jones, D. P. Mills and A. Stasch, *Dalton Trans.*, 2010, **39**, 1877-1882.
48. D. Heitmann, C. Jones, P. C. Junk, K.-A. Lippert and A. Stasch, *Dalton Trans.*, 2007, 187-189.
49. J. A. Cabeza, P. García-Álvarez, E. Pérez-Carreño and D. Polo, *Chem. Eur. J.*, 2014, **20**, 8654-8663.
50. P. B. Hitchcock, M. F. Lappert and S. Prashar, *J. Organomet. Chem.*, 1991, **413**, 79-90.

CHAPTER 5

CONCLUDING REMARKS

Chapter 5

Investigation of the halogenoaluminate π -arene complexes of lanthanoids has yielded 17 new complexes, $[\text{Ln}(\text{arene})(\text{AlX}_4)_n]$ ($\text{Ln} = \text{La}, \text{Ce}, \text{Pr}, \text{Nd}, \text{Gd}, \text{Sm}, \text{Eu}, \text{Yb}$; arene = toluene, mesitylene; $\text{X} = \text{Br}, \text{I}$; $n = 2, 3$). Divalent compounds of Sm, Eu and Yb have lattice solvated toluene in their structures; however, the trivalent complexes are unsolvated. These complexes extend the structural diversity attainable within the halogenoaluminate lanthanoid arene series. $[\text{Eu}(\eta^6\text{-MeC}_6\text{H}_5)(\text{AlI}_4)_2]_n \cdot \text{PhMe}$, $[\text{Yb}(\eta^6\text{-MeC}_6\text{H}_5)(\text{AlI}_4)_2]_n \cdot 1/2\text{PhMe}$ and $[\text{Eu}(\eta^6\text{-MeC}_6\text{H}_5)(\text{AlBr}_4)_2]_n \cdot \text{PhMe}$ are the first examples of polymeric structures among these complexes. Moreover, $[\text{Yb}(\eta^6\text{-MeC}_6\text{H}_5)(\text{AlI}_4)_2]_n \cdot 1/2\text{PhMe}$ is the first example of an eight coordination in this series, evidence of the lanthanoid contraction.

The iodoaluminate and bromoaluminate complexes of lanthanoids were found to be isostructural and comparable with the reported chloroaluminate complexes.¹⁻¹⁹ Iodoaluminate complexes were first examples and bromoaluminate complexes significantly extend the known literature. The Ln-centroid and the average Ln-C bond distances in the trivalent compounds prepared in both toluene and mesitylene are similar, which suggest that the metal ligand interaction is independent of the substituents in the ligands. The Ln-X ($\text{X} = \text{Br}, \text{I}$), Ln-centroid and the average Ln-C bond distances in the divalent complexes are longer than that of the trivalent complexes as divalent ions are larger than trivalent ions. Moreover, the Ln-I distances in the iodoaluminate complexes are longer than the Ln-Br distances in the bromoaluminate complexes. These differences are associated with the larger ionic radii of Ln^{2+} and I^- ions than the Ln^{3+} and Br^- ions, respectively.²⁰

The geometry of all the complexes could be best described as distorted pentagonal bipyramidal, with the arene molecule at an axial position (the centroid-Ln-I/Br angles are close to the straight angle). The gradual decrease of the Ln-X, Ln-centroid and the average Ln-C bond distances in the trivalent complexes of lanthanoids (lanthanum to gadolinium) support the lanthanoid contraction effect. This trend is also accessible among the divalent complexes from samarium to ytterbium, and there is a dramatic change in ytterbium as it is the smallest metal among the complexes isolated here. The catalytic activity of $[\text{Nd}(\eta^6\text{-C}_6\text{H}_5\text{Me})(\text{AlI}_4)_3]$ in isoprene polymerisation was performed at ambient temperature, and was less effective than the literature results of analogous complexes.

Chapter 5

Study of the iodoaluminate π -arene complexes of alkaline earths has given five new complexes, $[\text{Ae}(\text{arene})_m(\text{AlI}_4)_2]$ (Ae = Ca, Sr, Ba; arene = toluene, mesitylene; $m = 1, 2$). The Ca-centroid and the average Ca-C distances in the mesitylene complex are somewhat reduced than that of the toluene complex. This fact suggests stronger Ca-arene interactions in the mesitylene complex than in the toluene analogue, presumably due to the electron donating effect of three methyl groups in mesitylene molecule (only one in toluene). Both complexes have a zigzag polymer structure. The strontium complex is isostructural with the samarium and europium complexes reported in chapter 2.

In the barium complex $[(\text{Ba}(\eta^4\text{-C}_6\text{H}_5\text{Me})_2(\text{AlI}_4)_2)]$, the barium centre is sandwiched between two toluene molecules both in an η^4 fashion giving barium centre an eight coordination. However, the other complexes have only one arene molecule bonded to the metal centre. The Ba-I, Ba-C contacts are comparable with other analogous complexes considering the ionic radii of metals and iodide. All the complexes were synthesised by the reaction of in situ prepared aluminium iodide and alkaline earth iodides in a one-pot reaction, leading to the isolation of various complexes by a convenient reaction scheme.

Reactivity of divalent formamidinate complexes $[\text{Yb}(\text{Form})_2(\text{thf})_2]$ (Form = $[\text{RNCHNR}]$; R = 2,6-Me₂ (XylForm); 2,4,6-Me₃ (MesForm); 2,6-Et₂ (EtForm); 2,6-ⁱPr₂ (DippForm)) has been studied by using different oxidants such as Cl_3CCCl_3 , $\text{BrCH}_2\text{CH}_2\text{Br}$ and $\text{ICH}_2\text{CH}_2\text{I}$. Benzophenone has also been used to study the reactivity of less sterically demanding ytterbium formamidinate complexes. The complex $[\text{Yb}(\text{DippForm})_2(\text{thf})_2] \cdot 2\text{THF}$ was oxidised to $[\text{Yb}(\text{DippForm})_2\text{X}(\text{thf})]$ (X = Br, I) by $\text{BrCH}_2\text{CH}_2\text{Br}$ and $\text{ICH}_2\text{CH}_2\text{I}$, respectively. However, the similar approach with other formamidinate complexes gave the homoleptic tris-formamidnates $[\text{Yb}(\text{Form})_3]$ (Form = XylForm, MesForm and EtForm). Reactions with benzophenone also resulted in the tris-formamidinate complexes. This is probably due to the redistribution of the less bulky formamidinates in the complexes. The nmr spectrum of these complexes could not be integrated due to the paramagnetic nature of trivalent ytterbium.

Chapter 5

For the isolation of cationic complexes $[L_2Ln]^+[AlX_4/BPh_4/SbCl_6]^-$, halide abstraction reactions have been performed using the halide abstracting reagents AlX_3 ($X = Cl, Br, I$), $SbCl_5$ and $AgBPh_4$. Surprisingly, ligand was isolated from all attempted halide abstraction reactions; however, on one occasion the reported complex $[YbI_2(thf)_5]^+[YbI_4(thf)_2]^-$ was isolated. A silver complex $[Ag(DippForm)]_2$ was obtained from another attempted halide abstraction reaction involving $[Yb(DippForm)_2Cl(thf)]$ and $AgBPh_4$ instead of the expected cationic complex $[Yb(DippForm)_2]^+[BPh_4]^-$. The reaction between $[Yb(DippForm)_2(thf)_2]$ and cobalt carbonyl gave the cobalt complex $[Co(DippFormCO)(CO)_3].THF$ in place of the expected cationic complex $[Yb(DippForm)_2]^+[Co(CO)_4]^-$.

A deliberate RTP reaction using two formamidines (DippForH and XylFormH) afforded the heteroleptic tris-formamidinate complex $[Yb(DippForm)(XylForm)_2].PhMe$ for the first time. In addition, $[Eu(XylForm)_2(\mu-OH)(thf)]_2$ and $[Eu(EtForm)_2(thf)_2]$ have been synthesised by the RTP reactions involving XylFormH and EtFormH, respectively. $[Yb(MesForm)_2(\mu-OH)]_2$ was also synthesised by the similar procedure using ytterbium metal. The formation of $[Yb(MesForm)_2(\mu-OH)]_2$ and $[Eu(XylForm)_2(\mu-OH)(thf)]_2$ probably involves a trace amount of water and the presence of hydroxyl group was further confirmed from IR spectrum.

Overall, this thesis represents a major contribution to the chemistry of halogenoaluminate π -arene complexes of rare earths and alkaline earths. The reactivity of some iodoaluminate complexes have also been studied and discussed in chapter 2 and in appendix 1. The reactivity of divalent lanthanoid formamidinate complexes have been studied as well.

References

1. S. Jin, J. Guan, H. Liang and Q. Shen, *J. Catal.*, 1993, **14**, 159-162.
2. F. A. Cotton and W. Schwotzer, *J. Am. Chem. Soc.*, 1986, **108**, 4657-4658.
3. F. A. Cotton and W. Schwotzer, *Organometallics*, 1987, **6**, 1275-1280.
4. B. Fan, Q. Shen and Y. Lin, *J. Organomet. Chem.*, 1989, **376**, 61-66.
5. B. Fan, Q. Shen and Y. Lin, *Chin. J. Org. Chem.*, 1989, **9**, 414-414.
6. B. Fan, S. Jin, Q. Shen and Y. Lin, *Chin. Sci. Bull.*, 1991, **36**, 84-85.
7. B. Fan, Q. Shen and Y. Lin, *Chin. J. Inorg. Chem.*, 1991, **7**, 143.
8. B. Fan, Y. Lin and Q. Shen, *Chin. J. Appl. Chem.*, 1990, **7**, 23.
9. H.-Z. Liang, J.-W. Guan, Y.-H. Lin and Q. Shen, *Chin. J. Org. Chem.*, 1994, **14**, 380-382.
10. B. Fan, Q. Shen and Y. Lin, *J. Organomet. Chem.*, 1989, **377**, 51-58.
11. H. Liang, Q. Shen, J. Guan and Y. Lin, *J. Organomet. Chem.*, 1994, **474**, 113-116.
12. Q. Liu, Y.-H. Lin and Q. Shen, *Acta Cryst.*, 1997, **C53**, 1579-1580.
13. B. Paolo, L. Gabriele and M. Roberto, *Gazz. Chim. Ital.*, 1994, **124**, 217-225.
14. Y.-M. Yao, Y. Zhang, Q. Shen, Q.-C. Liu, Q.-J. Meng and Y.-H. Lin, *Chin. J. Chem.*, 2001, **19**, 588-592.
15. Q. Liu, Q. Shen, Y. Lin and Y. Zhang, *Chin. J. Inorg. Chem.*, 1998, **14**, 194-198.
16. H. Liang, Q. Shen, S. Jin and Y. Lin, *J. Chin. Rare Earth Soc.*, 1994, **12**, 193-196.
17. H. Liang, Q. Shen, S. Jin and Y. Lin, *Chem. Commun.*, 1992, 480-481.
18. A. S. Filatov, A. Y. Rogachev and M. A. Petrukhina, *J. Mol. Struct.*, 2008, **890**, 116-122.
19. A. S. Filatov, S. N. Gifford, D. K. Kumar and M. A. Petrukhina, *Acta Cryst.*, 2009, **E65**, m286-m287.
20. R. Shannon, *Acta Cryst.*, 1976, **A32**, 751-767.

APPENDIX 1

**RELATED CHEMISTRY WITH
RELEVANCE TO THIS THESIS**

Appendix 1

The following complexes have been isolated throughout this work. Complexes **1** and **2** have been isolated during the study of reactivity of lanthanoid halogenoaluminate π -arene complexes (discussed in chapter two). Complex **3** has been synthesised deliberately from diethyl ether for the starting material of halide abstraction reactions. Other complexes (**4** to **7**) have been isolated unexpectedly during this research work.

[Al(DippForm)₂I] (**1**)

Synthesis: Iodoaluminate π -arene complex of lanthanum [La(η^6 -MeC₆H₅)(AlI₄)₃] was synthesised by the procedure described in chapter 2. Before storing [La(η^6 -MeC₆H₅)(AlI₄)₃] solution for crystallisation, KDippForm (0.67 g, 1.67 mmol) was added into it and heated for 12 h at 100 °C. The solution was filtered and stored at ambient temperature for crystallisation. Colourless crystals were obtained in 2 d.

Crystal data: C₅₀H₇₀AlIN₄ (*M_r* = 881.01 g/mol): monoclinic, space group *P*2₁/*c* (no. 14), *a* = 14.156(3) Å, *b* = 16.573(3) Å, *c* = 21.433(4) Å, β = 108.35(3)°, *V* = 4772.5(18) Å³, *Z* = 4, *T* = 100.15 K, μ (Mo K α) = 0.725 mm⁻¹, *D*_{calc} = 1.2233 g/cm³, 54486 reflections measured (3.04° ≤ 2 θ ≤ 63.9°), 13092 unique (*R*_{int} = 0.1347, *R*_{sigma} = 0.1371) which were used in all calculations. The final *R*₁ was 0.0703 (*I* ≥ 2 σ (*I*)) and *wR*₂ was 0.2129 (all data).

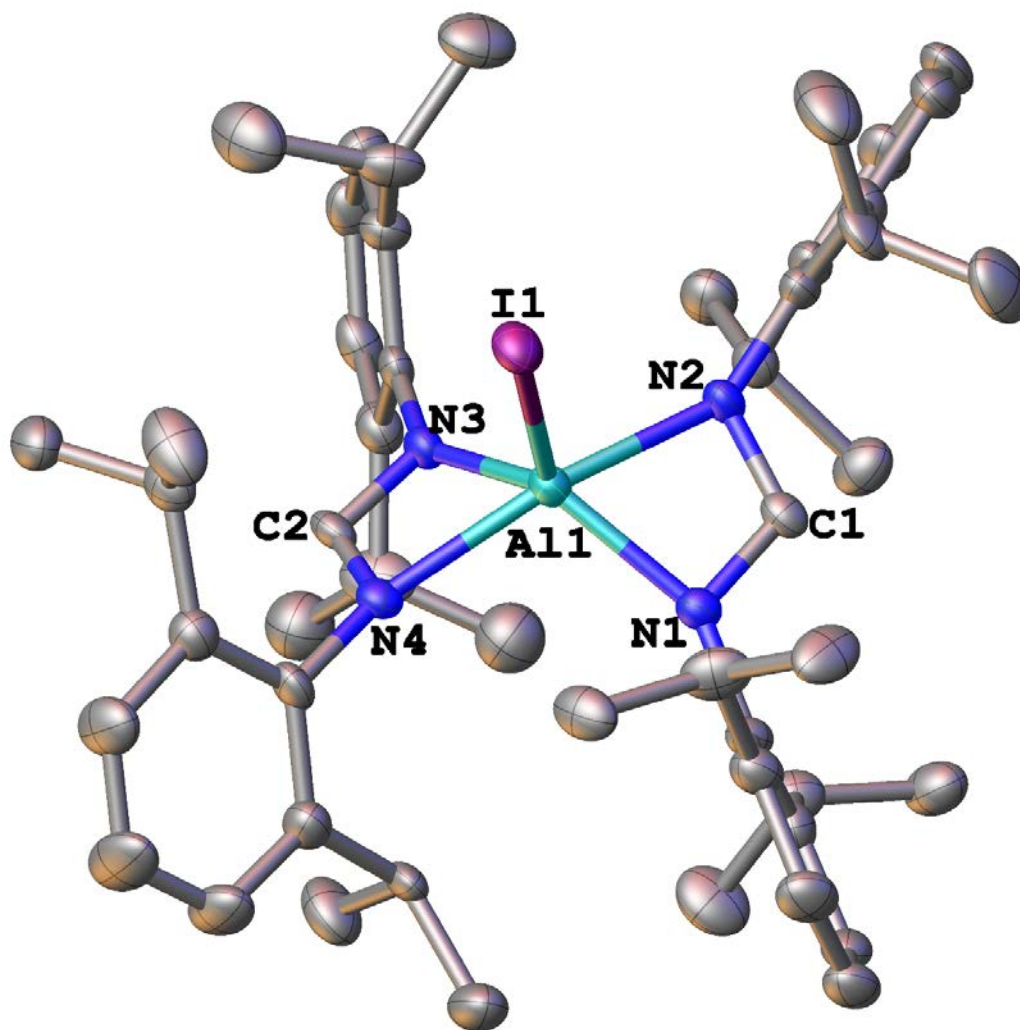


Fig. 1: X-ray structure of $[\text{Al}(\text{DippForm})_2\text{I}]$.



Synthesis: The divalent iodoaluminate π -arene complex of samarium $[\text{Sm}(\eta^6\text{-MeC}_6\text{H}_5)(\text{AlI}_4)_2]_n \cdot \text{PhMe}$ was synthesised by the procedure described in chapter 2. Before storing $[\text{Sm}(\eta^6\text{-MeC}_6\text{H}_5)(\text{AlI}_4)_2]_n \cdot \text{PhMe}$ solution for crystallisation, benzophenone (BP) (0.46 g, 2.50 mmol) was added into it and heated for 12 h at 100 °C. The solution was filtered and stored at ambient temperature for crystallisation. Colourless crystals were obtained in 2 d.

Appendix 1

Crystal data: $C_{72}H_{58}AlI_6O_5Sm$ ($M_r = 1941.91$ g/mol): monoclinic, space group Pc (no. 7), $a = 18.816(4)$ Å, $b = 22.221(4)$ Å, $c = 17.149(3)$ Å, $\beta = 100.47(3)^\circ$, $V = 7051(3)$ Å³, $Z = 4$, $T = 173.15$ K, $\mu(\text{MoK}\alpha) = 3.519$ mm⁻¹, $D_{\text{calc}} = 1.829$ g/cm³, 129408 reflections measured ($1.832^\circ \leq 2\theta \leq 63.952^\circ$), 36956 unique ($R_{\text{int}} = 0.0381$, $R_{\text{sigma}} = 0.0331$) which were used in all calculations. The final R_1 was 0.0316 ($I > 2\sigma(I)$) and wR_2 was 0.0873 (all data).

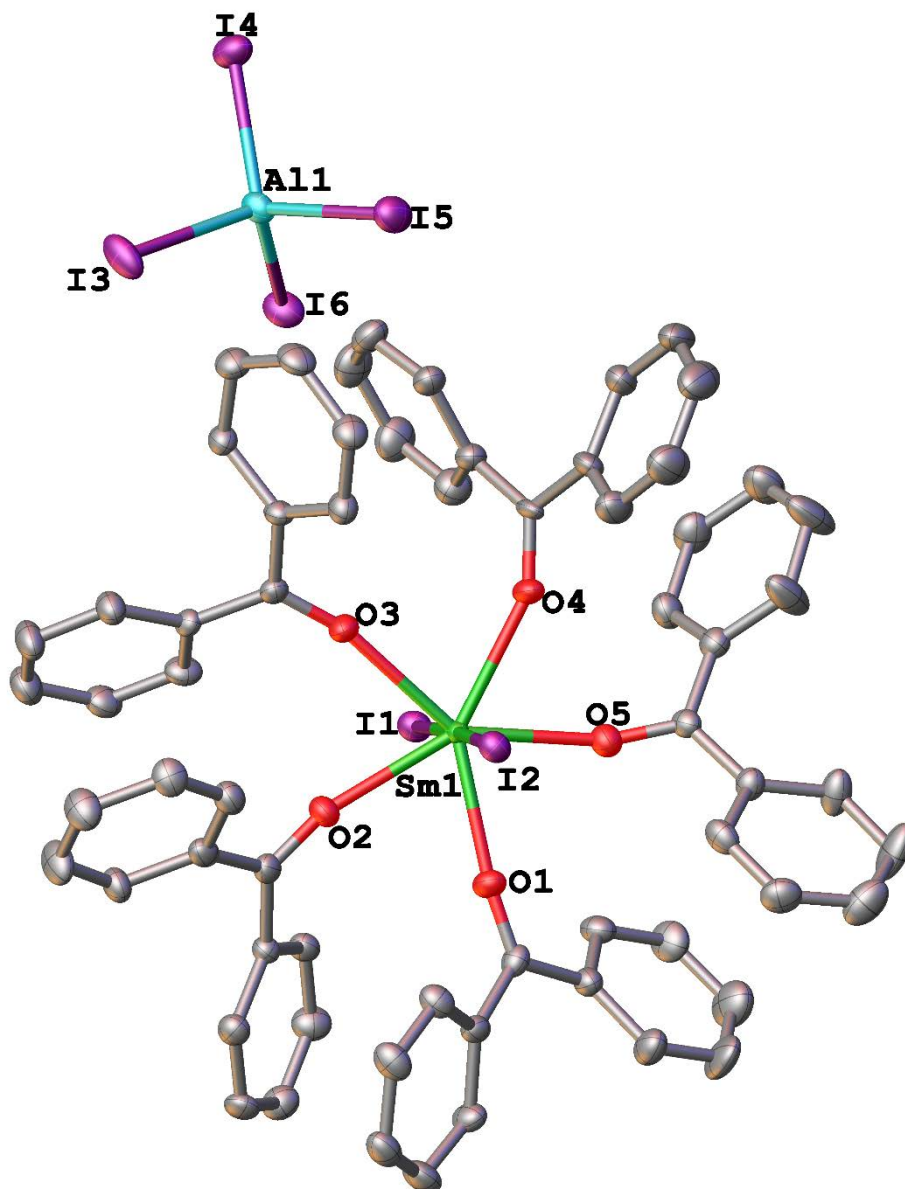


Fig. 2: X-ray structure of $[\text{SmI}_2(\text{BP})_5]^+[\text{AlI}_4]^- \cdot \text{PhMe}$.

Appendix 1

[La(DippForm)₂F(Et₂O)] (3)

Synthesis: Complex [La(DippForm)₂F(Et₂O)] was synthesised by the literature procedure using a different solvent (diethyl ether).¹ Lanthanum metal filings (0.12 g, 0.69 mmol), bis(pentafluorophenyl)mercury (0.37 g, 0.69 mmol) and DippFormH (0.50 g, 1.37 mmol) in diethyl ether (40 mL) were stirred at ambient temperature for 24 h, yielding an yellow solution after filtration. The volume of solution was reduced to 10 mL under vacuum and stored for several days in fridge gave yellow crystals.

Crystal data: C₅₄H₈₀FLa₁N₄O (*M_r* = 959.13 g/mol): monoclinic, space group *P*2₁/*c* (no. 14), *a* = 20.708(4) Å, *b* = 29.886(6) Å, *c* = 17.941(4) Å, β = 112.29(3)°, *V* = 10274(4) Å³, *Z* = 8, *T* = 100.15 K, μ(MoKα) = 0.875 mm⁻¹, *D_{calc}* = 1.240 g/cm³, 136675 reflections measured (2.126° ≤ 2θ ≤ 55°), 22758 unique (*R_{int}* = 0.1424, *R_{sigma}* = 0.0763) which were used in all calculations. The final *R*₁ was 0.0626 (*I* > 2σ(*I*)) and *wR*₂ was 0.1583 (all data).

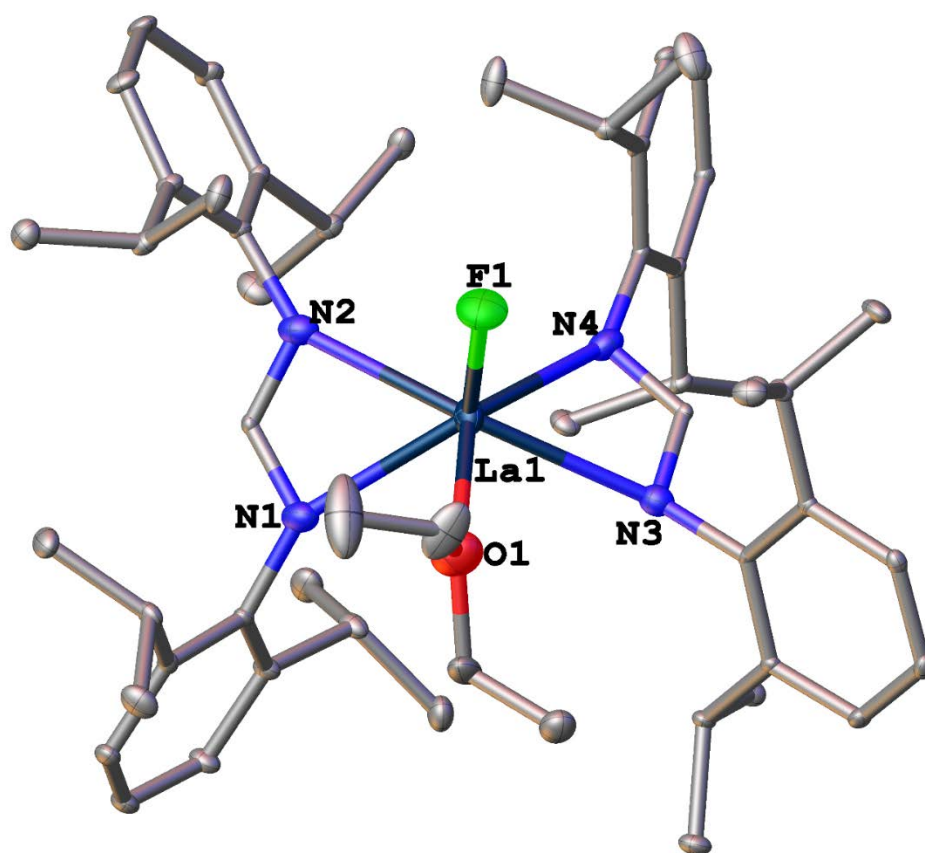


Fig. 3: X-ray structure of [La(DippForm)₂F(Et₂O)].

Appendix 1

[YbI₂(MeCN)₅] (4)

Synthesis: Complex [YbI₂(MeCN)₅] was synthesised by the literature procedure.² Ytterbium filings (0.12 g, 0.66 mmol), AlI₃ (0.82 g, 2.0 mmol) and diiodoethane (0.30 g, 1.06 mmol) were taken in a Schlenk flask. Acetonitrile (40 ml) was added and an exothermic reaction took place. The mixture was then sonicated for 12 h so that all traces of metal had been consumed. The solution was then filtered, and the solvent volume was reduced in vacuo until traces of material began to precipitate. After storing in fridge for overnight, orange crystals deposited, were collected and washed with cold acetonitrile.

Crystal data: C₁₀H₁₅I₂N₅Yb (M_r = 632.11 g/mol): orthorhombic, space group *Pbca* (no. 61), $a = 14.134(3)$ Å, $b = 14.466(3)$ Å, $c = 17.930(4)$ Å, $V = 3666.0(13)$ Å³, $Z = 8$, $T = 173.15$ K, $\mu(\text{Mo K}\alpha) = 8.463$ mm⁻¹, $D_{\text{calc}} = 2.2904$ g/cm³, 29107 reflections measured ($4.54^\circ \leq 2\theta \leq 55.82^\circ$), 4286 unique ($R_{\text{int}} = 0.0753$, $R_{\text{sigma}} = 0.0354$) which were used in all calculations. The final R_1 was 0.0347 ($I \geq 2u(I)$) and wR_2 was 0.0927 (all data).

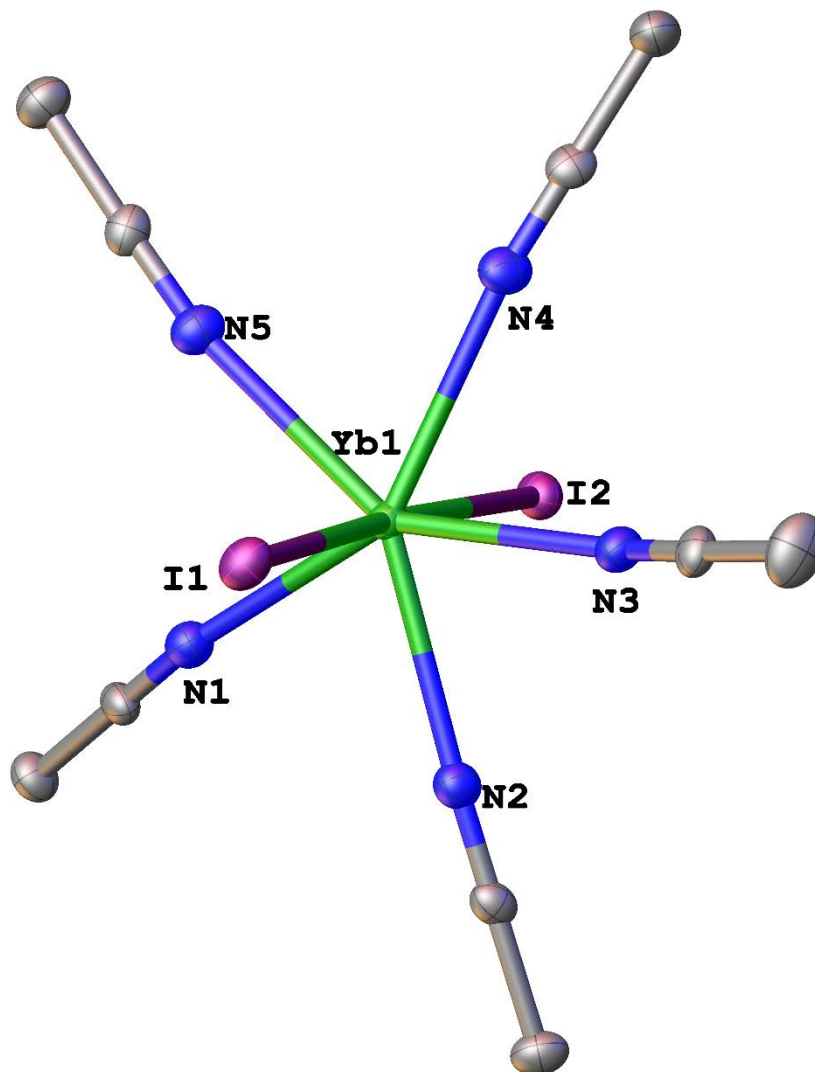


Fig. 4: X-ray structure of [YbI₂(MeCN)₅].

[LaCl₃(thf)₂]_n (**5**)

Synthesis: Complex [LaCl₃(thf)₂]_n was isolated from an attempted synthesis of cationic complex [La(DippForm)₂]⁺[AlCl₃F]⁻. This complex was reported before; however, the synthetic route was different.³ Moreover, the reported complex was crystallised with monoclinic space group *P*2₁/*c* whereas *C*2/*c* space group was observed here. [La(DippForm)₂F(thf)] was synthesised by the literature procedure⁴ in thf and treated with AlCl₃ (0.08 g, 0.60 mmol) at ambient temperature. After reducing the volume under vacuo and storing in the fridge for 2d, colourless crystals formed.

Appendix 1

Crystal data: C₂₄H₄₀Cl₉La₃O₆ (*M_r* = 1160.34 g/mol): monoclinic, space group *C2/c* (no. 15), *a* = 34.836(7) Å, *b* = 10.105(2) Å, *c* = 22.923(5) Å, *β* = 98.52(3)°, *V* = 7980(3) Å³, *Z* = 8, *T* = 100.15 K, *μ*(MoKα) = 3.789 mm⁻¹, *D_{calc}* = 1.932 g/cm³, 46380 reflections measured (2.364° ≤ 2Θ ≤ 53.04°), 8086 unique (*R_{int}* = 0.1968, *R_{sigma}* = 0.1221) which were used in all calculations. The final *R₁* was 0.1075 (*I* > 2σ(*I*)) and *wR₂* was 0.3089 (all data).

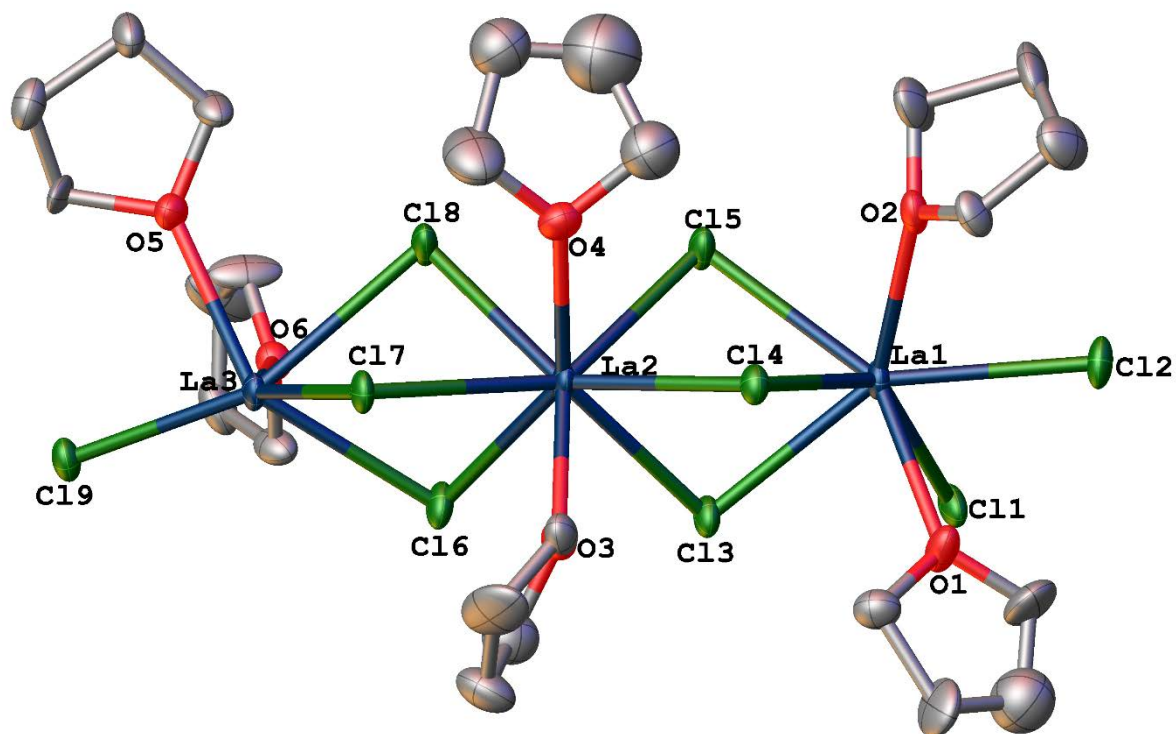


Fig. 5: X-ray structure of [La₃Cl₉(thf)₆]_n.

[SmCl₃(dme)₂] (**6**)

Synthesis: THF (40 mL) was taken to a Schlenk flask charged with freshly filed Sm metal (0.06 g, 0.40 mmol), HgC₆F₅)₂ (0.37 g, 0.69 mmol) and DippFormH (0.33 g, 0.91 mmol) under a purified nitrogen atmosphere. The resulting slurry was stirred at ambient temperature for 24 h to yield a pale yellow solution after filtration. Then AlCl₃ (0.07 g, 0.55 mmol) was added to the solution and stirred for 12 h at room temperature. After filtration and removal of volatiles gave a light yellow powder that was extracted into dme (10 mL) and stored in fridge for several days gave light yellow crystals.

Appendix 1

Crystal data: C₈H₂₀Cl₃O₄Sm (M_r = 436.94 g/mol): monoclinic, space group $P2_1/c$ (no. 14), $a = 11.451(2)$ Å, $b = 8.8370(18)$ Å, $c = 15.591(3)$ Å, $\beta = 104.77(3)^\circ$, $V = 1525.5(6)$ Å³, $Z = 4$, $T = 173.15$ K, $\mu(\text{MoK}\alpha) = 4.370$ mm⁻¹, $D_{\text{calc}} = 1.902$ g/cm³, 10424 reflections measured ($3.678^\circ \leq 2\theta \leq 55.782^\circ$), 3327 unique ($R_{\text{int}} = 0.0822$, $R_{\text{sigma}} = 0.0699$) which were used in all calculations. The final R_1 was 0.0385 ($I > 2\sigma(I)$) and wR_2 was 0.0976 (all data).

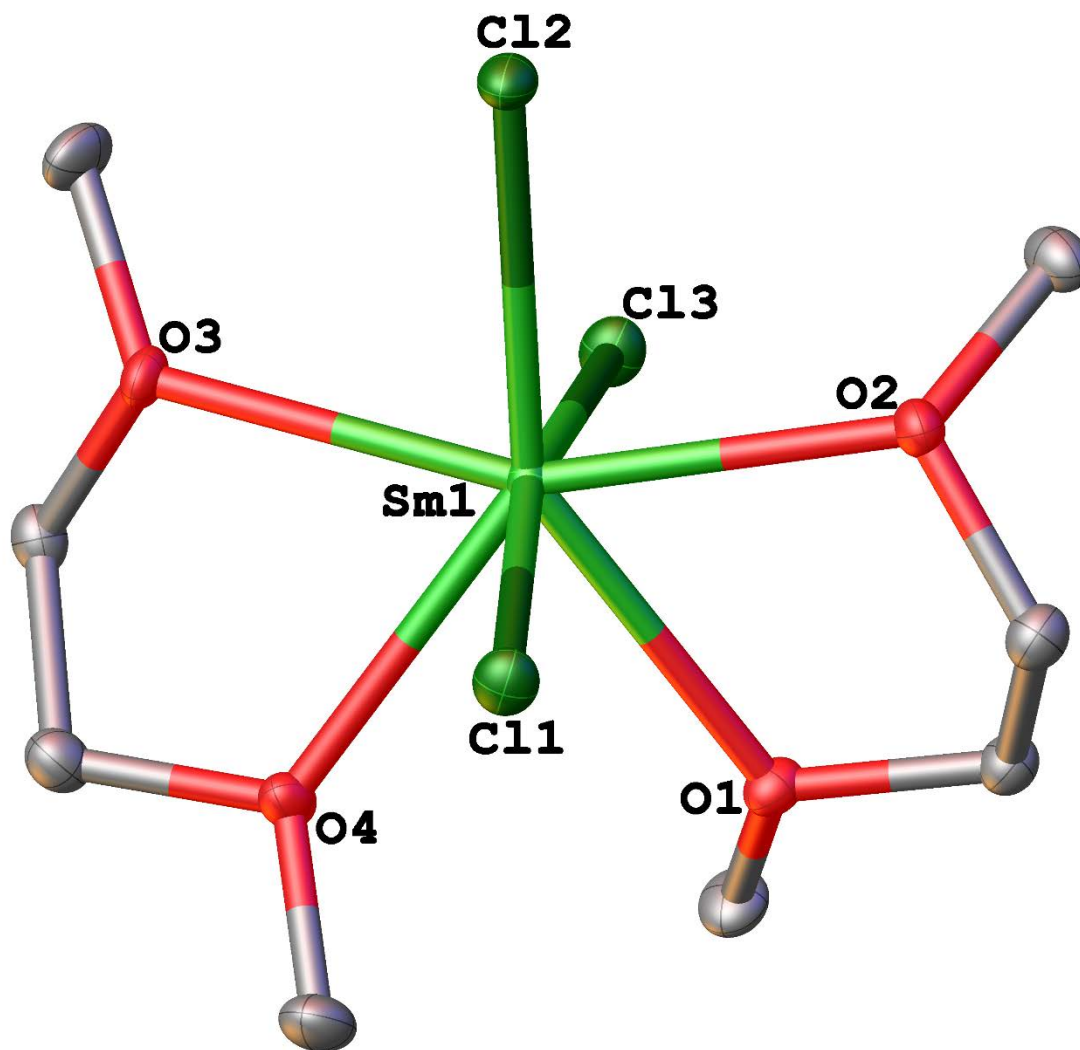


Fig. 6: X-ray structure of [SmCl₃(dme)₂].

References

1. M. L. Cole, G. B. Deacon, C. M. Forsyth, P. C. Junk, K. Konstas, J. Wang, H. Bittig and D. Werner, *Chem. Eur. J.*, 2013, **19**, 1410-1420.
2. G. B. Deacon, B. Gortler, P. C. Junk, E. Lork, R. Mews, J. Petersen and B. Zemva, *Dalton Trans.*, 1998, 3887-3892.
3. G. B. Deacon, T. Feng, P. C. Junk, B. W. Skelton, A. N. Sobolev and A. H. White, *Aust. J. Chem.*, 1998, **51**, 75-89.
4. M. L. Cole, G. B. Deacon, C. M. Forsyth, P. C. Junk, K. Konstas and J. Wang, *Chem. Euro. J.*, 2007, **13**, 8092-8110.

APPENDIX 2

EXPERIMENTAL PROCEDURES

Appendix 2

All reactions were carried out under dry nitrogen using glove box and standard Schlenk techniques, as lanthanoid metals and lanthanoid(II) and (III) products are highly air- and moisture-sensitive. All the reagents were supplied by Sigma Aldrich and Thermo Fisher Scientific and used without further purification unless stated otherwise. Toluene was dried over molecular sieves using LC Technology Solvent Purification Systems, collected in Schlenk flask, and stored over sodium. Acetonitrile was dried by distillation from calcium hydride. THF and hexane were dried and deoxygenated by refluxing over and distillation from sodium benzophenone ketyl under nitrogen. Formamidine ligands¹⁻³ and bis(pentafluorophenyl) mercury, $\text{Hg}(\text{C}_6\text{F}_5)_2$ ^{4,5} were prepared by literature methods.

Microanalysis were carried out at School of Human Sciences, London Metropolitan University, UK. Metal analyses were performed by complexometric titration using EDTA, and 5% sulphosalicylic acid to mask aluminum of the halogenoaluminate bimetallic complexes.⁶ Infrared spectra were collected on a Nicolet 6700 (Thermo Scientific) FTIR spectrophotometer, using NaCl plates with Nujol mull and the data were processed by using OMNIC software. Multinuclear NMR were obtained on a Bruker AscendTM 400 spectrometer using dry degassed deuterio-benzene (C_6D_6) as solvent, and resonances were referenced to the residual ^1H resonances of the deuterated solvent. Top Spin software were employed to process the data.

The X-ray data were collected using the MX1 beamline at the Australian Synchrotron, Clayton, Victoria as well as using the XRD at the advanced analytical centre of James Cook University. A crystal was mounted on a cryoloop and flash cooled to 100 K. Data were collected using a single wavelength ($\lambda = 0.712 \text{ \AA}$). The data were collected using the Blue Ice⁷ GUI and processed with the XDS⁸ software package. By using Olex2,⁹ the structures were solved by direct methods with ShelXS,¹⁰ structure solution program. The structures were refined with anisotropic thermal parameters for the non-hydrogen atoms with hydrogen atoms constrained in calculated positions with a riding model. Structure refinements were performed with version 2016/6 of ShelXL¹¹ using Least Squares minimisation. The graphical representations were generated using bitmap images GUI of Olex2.⁹

Appendix 2

Combustion analyses consistently gave variable results, and are therefore presented here. Metal analyses were generally more accurate and are presented in the respective chapters.

Table A1: Microanalysis results for chapter 2 complexes

	Calculated			Found		
	% C	% H	% N	% C	% H	% N
1	4.57	0.44	-	< 0.1	<0.1	-
2	4.58	0.44	-	4.55	0.47	-
3	4.57	0.44	-	4.02	2.03	-
4	4.54	0.44	-	4.57	0.50	-
5	11.98	1.15	-	3.91	1.17	-
6	11.96	1.15	-	3.28	2.98	-
7	9.14	0.88	-	4.09	1.74	-
8	5.80	0.65	-	-	-	-
9	5.80	0.65	-	9.41	1.82	-
10	5.8	0.65	-	7.48	6.27	-
11	5.79	0.65	-	5.10	1.86	-
12	5.77	0.65	-	3.91	1.71	-
13	5.75	0.64	-	4.57	0.50	-
14	-	-	-	-	-	-
15	-	-	-	-	-	-
16	-	-	-	-	-	-
17	-	-	-	-	-	-

Appendix 2

Table A2: Microanalysis results for chapter 3 complexes

	Calculated			Found		
	% C	% H	% N	% C	% H	% N
1	7.00	0.67	-	7.15	0.70	-
2	12.54	1.20	-	11.59	1.31	-
3	12.09	1.16	-	11.91	1.22	-
4	8.79	0.98	-	5.45	3.31	-
5	8.46	0.95	-	11.78	1.73	-

Table A3: Microanalysis results for chapter 4 complexes

	Calculated			Found		
	% C	% H	% N	% C	% H	% N
1	61.64	7.47	5.32	58.35	8.17	5.91
2	59.01	7.15	5.10	54.92	7.84	5.57
4	67.70	6.88	8.31	57.80	7.42	6.92
8	38.98	4.74	3.14	38.98	5.23	2.80
9	65.35	7.14	4.62	65.17	7.30	4.83
10	60.95	6.33	7.48	60.59	6.61	7.36
11	61.78	5.73	7.58	61.67	5.45	7.62

References

1. R. M. Roberts, *J. Org. Chem.*, 1949, **14**, 277-284.
2. R. M. Roberts, *J. Am. Chem. Soc.*, 1949, **71**, 3848-3849.
3. K. M. Kuhn and R. H. Grubbs, *Org. Lett.*, 2008, **10**, 2075-2077.
4. G. B. Deacon, J. E. Cosgriff, E. T. Lawrenz, C. M. Forsyth and D. L. Wilkinson, in *Synthetic Methods of Organometallic and Inorganic Chemistry*, eds. W. A. Herrmann and F. T. Edlmann, Georg Thieme Verlag, Stuttgart, 1997, vol. 6, p. 226.
5. S.-O. Hauber, J. W. Seo and M. Niemeyer, *Z. Anorg. Allg. Chem.*, 2010, **636**, 750-757.
6. G. Dchwarzenbach and H. A. Flaschka, *Complexometric Titrations*, Methuen Publishing Ltd, London, 1969.
7. T. M. McPhillips, S. E. McPhillips, H.-J. Chiu, A. E. Cohen, A. M. Deacon, P. J. Ellis, E. Garman, A. Gonzalez, N. K. Sauter, R. P. Phizackerley, S. M. Soltis and P. Kuhn, *J. Synchrotron Rad.*, 2002, **9**, 401-406.
8. W. Kabsch, *J. Appl. Crystallogr.*, 1993, **26**, 795-800.
9. O. V. Dolomanov, L. J. Bourhis, R. J. Gildea, J. A. K. Howard and H. Puschmann, *J. Appl. Crystallogr.*, 2009, **42**, 339-341.
10. G. M. Sheldrick, *Acta Cryst.*, 2008, **A64**, 112-122.
11. G. M. Sheldrick, *Acta Cryst.*, 2015, **C71**, 3-8.

APPENDIX 3

PUBLICATIONS



Review

Rare-earth N,N'-diarylformamidinate complexes

Glen B. Deacon^a, Md Elius Hossain^b, Peter C. Junk^{b,*}, Mehdi Salehisaki^b^aSchool of Chemistry, Monash University, Clayton, Victoria 3800, Australia^bCollege of Science & Engineering, James Cook University, Townsville, Queensland 4811, Australia

ARTICLE INFO

Article history:

Received 17 January 2017

Received in revised form 10 February 2017

Accepted 11 February 2017

Available online 15 February 2017

Keywords:

Lanthanoids

Lanthanoid(II)

Lanthanoid(III)

Lanthanoid(IV)

Formamidinates

ABSTRACT

This comprehensive review covers the progress of rare earth chemistry with formamidinate ligands to date. The ligands involved offer varying steric and electronic effects and focus on the N,N'-bis(aryl)formamidinates. Synthetic pathways to divalent, trivalent and tetravalent complexes, their structural aspects, reactivity and potential applications in catalysis are extensively discussed.

© 2017 Elsevier B.V. All rights reserved.

Contents

1. Introduction	247
2. Formamidinatanlanthanoid complexes	249
2.1. Synthesis	249
2.2. Divalent compounds	251
2.3. Trivalent compounds	252
2.4. Tetravalent compound(s) [34]	264
2.4.1. Synthesis of trivalent complexes that are potential precursor of tetravalent complexes	264
2.4.2. Protolysis of Ce(IV) amides to give Ce(IV) formamidinates	264
3. Catalysis	264
4. Conclusions and outlook	264
Acknowledgements	265
References	265

1. Introduction

Amidinate ligands ($[R^1NCR^2NR^3]^-$) (Fig. 1-1, $R^4 = H$, deprotonated) are anionic ligands which can be modified sterically and electronically to form stable and structurally interesting complexes with metals [1]. Fig. 1-1 shows the general structure of an amidine. Amidines are named based on the acid or amide obtained after hydrolysis [2]. Amidinate complexes have versatile applications in chemical and material sciences [3–6], including as precursors

for atomic layer deposition of rare-earth oxide films [3,4,7] and polymerisation of olefins [5,8]. In the case of $R^2 = H$, the compound is called a formamidine. N,N'-Diarylformamidinate ligands have advantages over amidinate and guanidinate ligands of greater simplicity. This impacts in ease of synthesis whereby formamidines, the proligands are readily prepared and can be easily modulated to vary steric and electronic effects. These can be as varied as anilines available as reactants. The corresponding formamidines open up a wide range of syntheses owing to the acidic N–H. By contrast amidinate and guanidinate ligands are harder to access, and although they have in the C–R and C–NR₂ moieties the opportunity for additional steric and electronic

* Corresponding author.

E-mail address: peter.junk@jcu.edu.au (P.C. Junk).

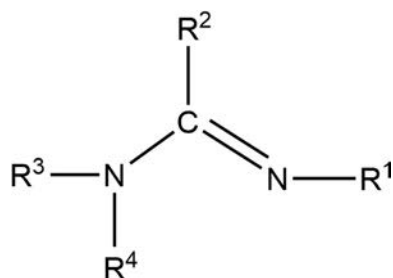
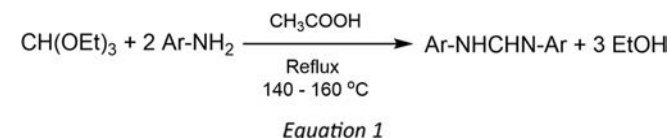


Fig. 1-1. The general structure of an amidine.

modulation, it also brings complexity in distinguishing these effects from those of the N-R groups. The N,N'-diarylformamidinates ((ArN)₂CH⁻, (ArForm⁻)), gives them a special place amongst the amidinate ligands with a wide variety of applications. For example, lanthanoid formamidinates are excellent reagents in catalysing the Tishchenko reaction [9].



There has been a lot of interest in developing N,N'-bis(aryl)formamidinates as ligands [13]. One important use is to kinetically

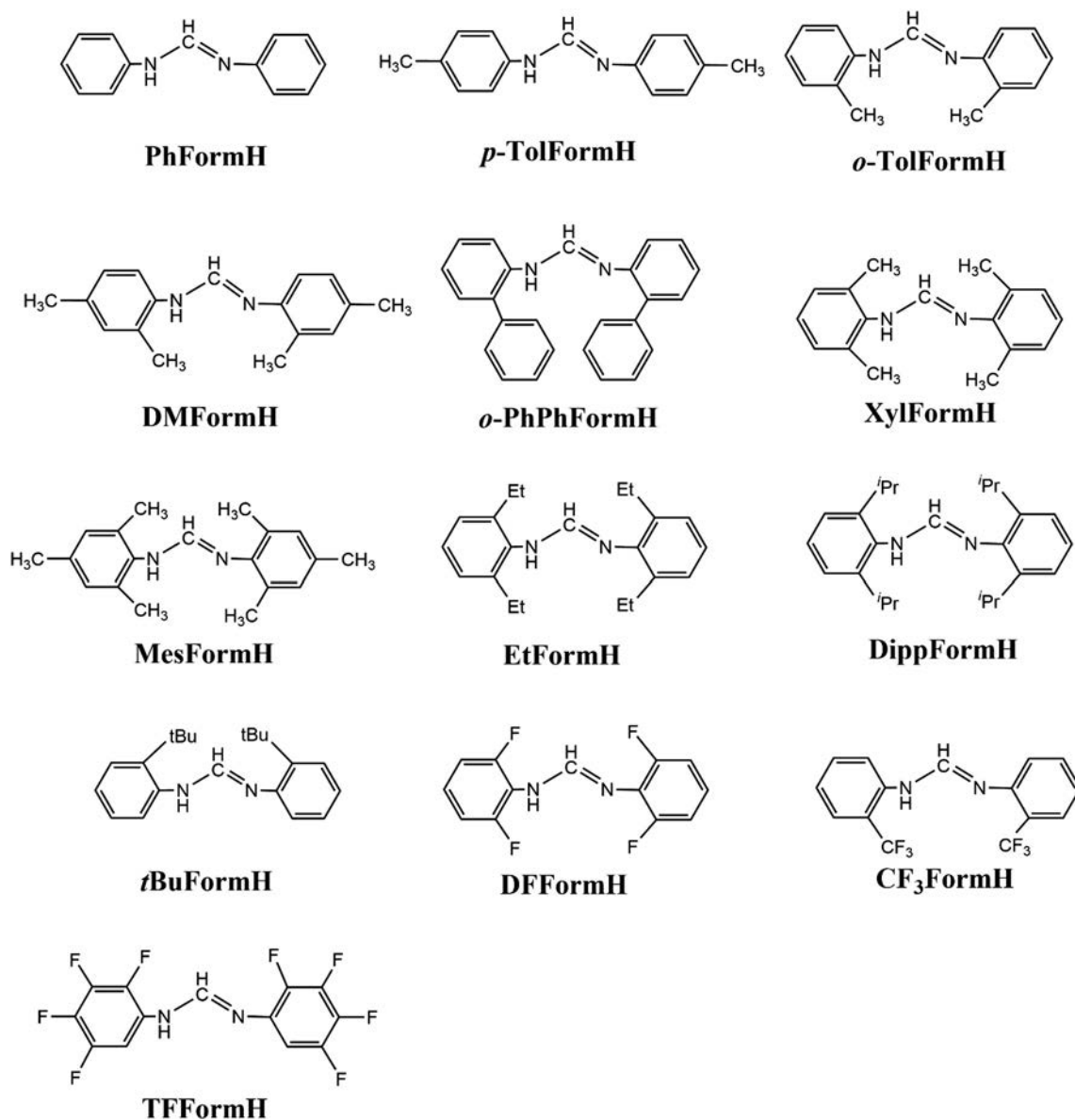


Fig. 1-2. Different Formamidine pro-Ligands.

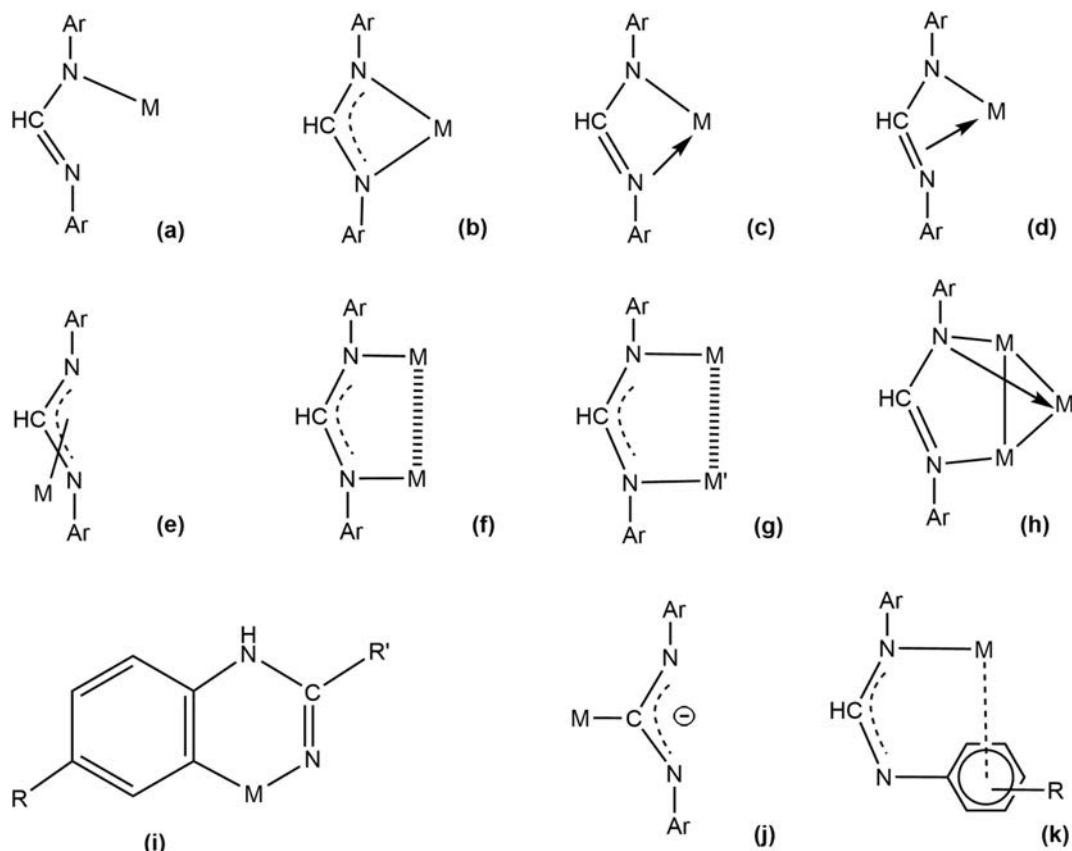


Fig. 1-3. Possible binding modes for N,N'-bis(aryl)formamidinate ligands.

stabilise group 13 hydride complexes by application of bulky ligands [13]. It has also been possible to sterically engineer carbon-fluorine bond activation [14]. Furthermore, they can act as anionic ligand supports for low valent compounds. These ligands bind rare earth metals well with the benefit of variations of the steric bulk and electronic functionality at the N donor atoms [15]. Moreover, rare-earth amidinate complexes have great versatility in material and chemical applications, for example, precursors that are used for atomic layer deposition of rare-earth oxide films [7] or polymerisation of olefins [3]. Fig. 1-2 shows some important types of formamidinate proligands. By using different derivatives of aniline as the precursor, various formamidinate ligands with different steric properties can be prepared. Therefore, different metal-organic compounds with different coordination number can be synthesized by using different formamidines. This can aid in inducing variations in reactivity.

Bis(aryl)formamidinate ligands can display various potential binding modes to metal centers (Fig. 1-3). Infrared and NMR spectroscopy can be used for studying the coordination of metal bis(aryl)formamidinate complexes. However, when more than one binding mode is present and/or the complex exhibits fluxional coordination in solution, the use of these methods is complicated significantly, meaning X-ray crystallography is important in determining the unambiguous structures of these complexes (in the solid state) [13]. Fig. 1-3 illustrates many of the possible bonding modes for the N,N'-bis(aryl)formamidinate ligands including monodentate (a), chelate (b-d), η^3 -allyl (e), bridging (f, g), capping (h), *ortho*-metallation (i), C-bonded (j), and η^6 bonding (k) [2]. Of these bonding modes, symmetric chelation (b) is the most commonly found in RE formamidinate chemistry.

2. Formamidinatolanthanoid complexes

This section presents examples of use of various formamidines to prepare formamidinatolanthanoid complexes.

2.1. Synthesis

Reactive rare earth complexes (organometallics, organoamides including formamidines and organo-oxides) can be synthesized by several reactions. Metathesis (salt elimination), protolysis, redox transmetallation and redox transmetallation/protolysis are the common synthetic routes to prepare rare earth metal-organic compounds.

Metathesis reactions, according to Eq. (2), involve the treatment of a rare earth halide with an alkali metal complex of the ligand [16–18].



M = alkali metal

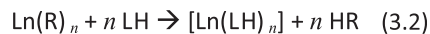
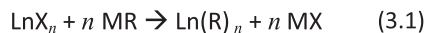
X = halide

Equation 2

In metathesis reactions the choice of lanthanoid halide and alkali metal salt as starting materials is important. For example, in many cases the use of lanthanide trichlorides and lithium salts results in either low yields or unwanted side-products where the

alkali metal is retained forming an 'ate' species, or the alkali metal halide is bound to the lanthanoid complex [18].

Protolysis reactions include treatment of a lanthanoid precursor (LnR_n) with an LH proligand (Eq. (3)).



R = usually $\text{N}(\text{SiMe}_3)_2$, $\text{N}(\text{SiHMe}_2)_2$ or C_6F_5
 $n = 2, 3$
 X = halide

Equation 3

Due to the high solubility of the reactants in common solvents, reaction 3.2 can be performed in the absence of coordinating/donor

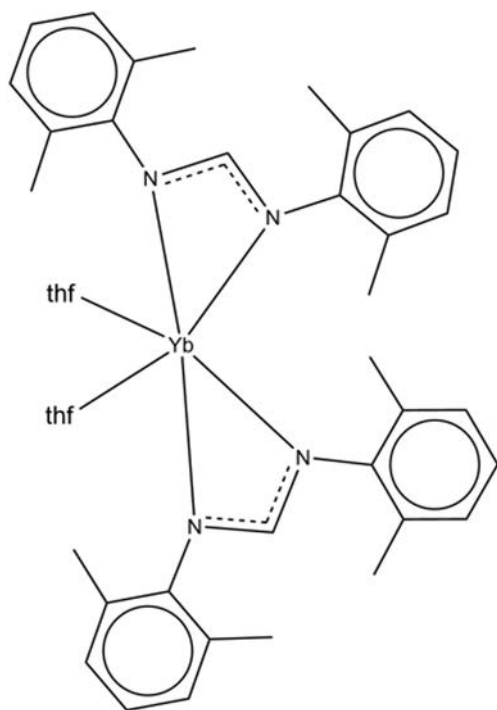


Fig. 2-1. Schematic of the X-ray structure of $[\text{Yb}(\text{XylForm})_2(\text{thf})_2]$ (1).

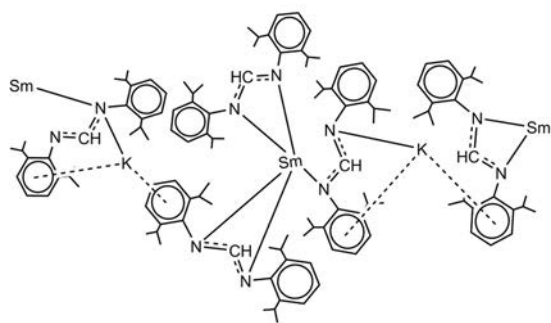


Fig. 2-2. Schematic and the X-ray structure of $[\text{KSm}(\text{DippForm})_3]$ (10).

solvents [16]. Thus, this route is a highly versatile approach for the synthesis of homoleptic lanthanoid complexes. Heteroleptic lanthanoid complexes can be synthesized using coordinating/donor solvents [6,19,20]. Protolysis reactions often involve two steps

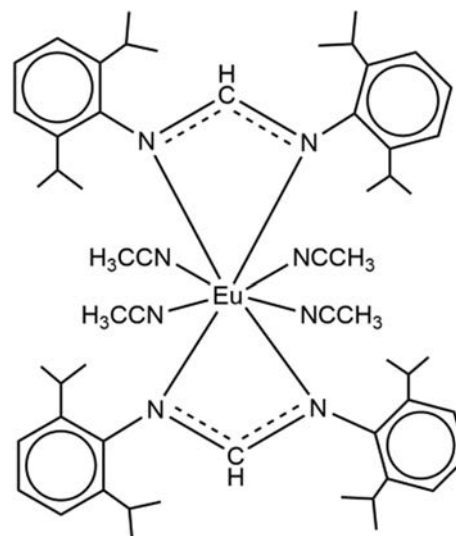


Fig. 2-3. Schematic of the X-ray structure of $[\text{Eu}(\text{DippForm})_2(\text{CH}_3\text{CN})_4]$ (14).

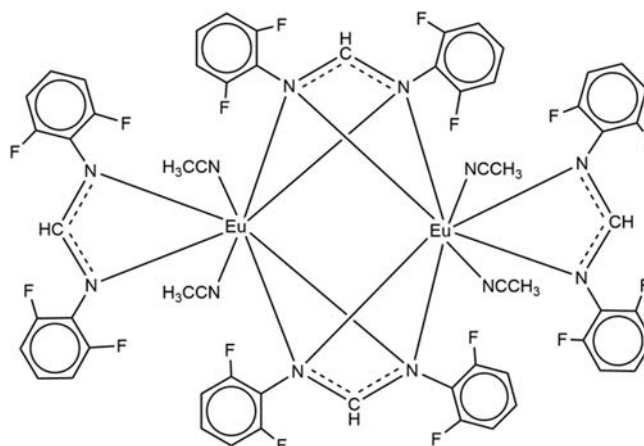
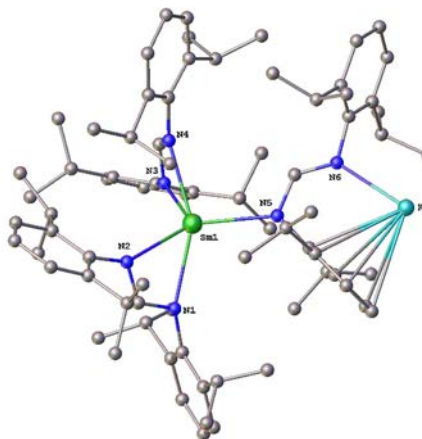


Fig. 2-4. Schematic of the X-ray structure of $[(\text{Eu}(\text{DFForm})_2(\text{CH}_3\text{CN})_2)_2]$ (15).



which is the main drawback of this method. Each step involves air and/or moisture sensitive compounds, and step 3.1 has the usual potential problems of metathesis reactions.

Redox transmetallation/protolysis (RTP) is another type of reaction for synthesizing rare earth metal-organic compounds. RTP involves the reaction of a rare earth metal with a diarylmercurial such as diphenylmercury [21] or bis(pentafluorophenyl)mercury [14,21–24] and a protic ligand (Eq. (4)).

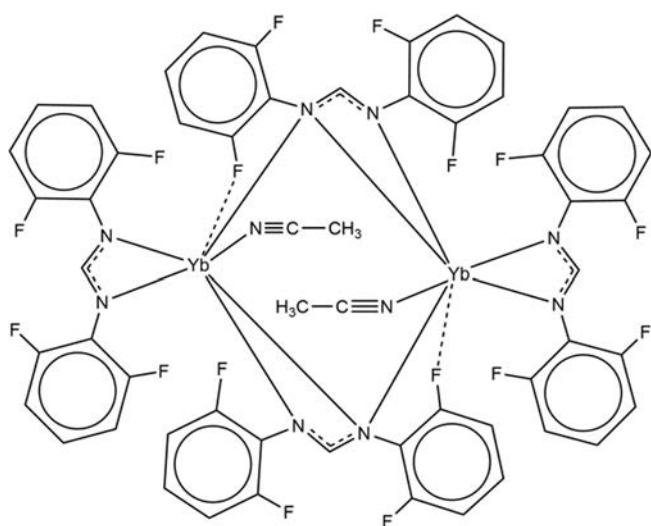
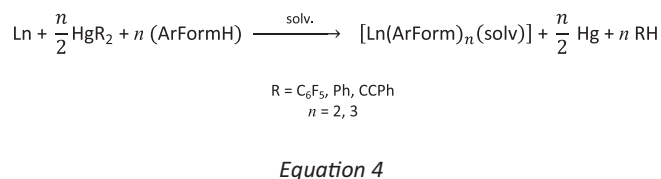


Fig. 2-5. Schematic of the X-ray structure of $[\text{Yb}(\text{DFForm})_2(\text{CH}_3\text{CN})]_2$ (**17**).

This method is a one-pot procedure. Therefore, compared with metathesis and protolysis synthetic routes, it is more straightforward, particularly since the only air-sensitive material is the lanthanoid metal. The isolation procedure is also straightforward involving a simple filtration to remove excess Ln metal and Hg produced in the reaction. Donor solvents tetrahydrofuran (THF) or 1,2-dimethoxyethane (DME) are normally used in RTP reactions. Reactions in non-donor solvents e.g. toluene normally require more forcing conditions such as heating [25]. Besides using mercury reagents, two or three drops of mercury can be added to the reaction mixture to activate the surface of rare earth metal by formation of an amalgam. Involvement of mercury reagents is the main drawback of this type of reaction since it raises environmental concerns and requires care in handling. Hg(C₆F₅)₂ and Hg(CPh)₂ are stronger oxidants compared with diphenylmercury. However, Hg(C₆F₅)₂ is more reactive than HgPh₂ and can yield rare Ln(Form)₂F complexes after C-F activation of the Ln(Form)₂C₆F₅ intermediate species [24]. Performing RTP reactions using diphenylmercury often requires activation of the metal (HgCl₂ or I₂) and heating [21].

2.2. Divalent compounds

Different lanthanoid formamidinate complexes namely [Yb(XylForm)₂(thf)₂] (**1**), [Yb(EtForm)₂(thf)₂] (**2**), [Yb(*o*-PhPhForm)₂(thf)₂] (**3**), [Yb(DippForm)₂(thf)₂] (**4**), [Yb(TFForm)₂(thf)₃] (**5**) (which is the result of crystallization of [Yb(TFForm)₂(thf)₂] (**6**) from THF), [Eu(DippForm)₂(thf)₂] (**7**), [Yb(MesForm)₂(thf)₂] (**8**) and [Yb(*o*-TolForm)₂(thf)₂] (**9**) have been prepared by RTP reactions between an excess of a lanthanoid metal, Hg(C₆F₅)₂ or HgPh₂ and the corresponding formamidinate ligand [26]. All the compounds are mononuclear. In the case of [Yb(TFForm)₂(thf)₃] (**5**) the ytterbium atom is seven coordinate whereas the metal centers of other complexes are six coordinate. The resulting compounds also have chelating N, N'-Form ligands and *cis*-thf donors (Fig. 2-1). The variation in the O-Yb-O angles is an interesting feature which cannot be related to the bulkiness of the Form ligands. The smallest O-Yb-O angles are found in the structures of [Yb(DippForm)₂(thf)₂] (**4**) and [Eu(DippForm)₂(thf)₂] (**7**) (75.49(10)°), and involve the bulkiest

Table 2.2.1
Divalent compounds.

Reaction	Compound/Product	Method	Refs.
Yb + XylFormH + Hg(C ₆ F ₅) ₂ in THF	[Yb(XylForm) ₂ (thf) ₂] (1)	RTP	[26]
Yb + EtFormH + Hg(C ₆ F ₅) ₂ in THF	[Yb(EtForm) ₂ (thf) ₂] (2)	RTP	[26]
Yb + Ph ₂ Hg + PhPhFormH in THF	[Yb(<i>o</i> -PhPhForm) ₂ (thf) ₂] (3)	RTP	[26]
Yb + DippFormH + Hg(C ₆ F ₅) ₂ in THF	[Yb(DippForm) ₂ (thf) ₂] (4)	RTP	[26]
Crystallisation of [Yb(TFForm) ₂ (thf) ₂] from THF	[Yb(TFForm) ₂ (thf) ₃] (5)	THF addition	[26]
Yb + TFFormH + Hg(C ₆ F ₅) ₂ in THF	[Yb(TFForm) ₂ (thf) ₂] (6)	RTP	[26]
Eu + DippFormH + Hg(C ₆ F ₅) ₂ in THF	[Eu(DippForm) ₂ (thf) ₂] (7)	RTP	[26]
Yb + MesFormH + Hg(C ₆ F ₅) ₂ in THF	[Yb(MesForm) ₂ (thf) ₂] (8)	RTP	[26]
Yb + <i>o</i> -TolFormH + Hg(C ₆ F ₅) ₂ in THF	[Yb(<i>o</i> -TolForm) ₂ (thf) ₂] (9)	RTP	[26]
[Sm(DippForm) ₃] + KC ₈ in toluene	[KSm(DippForm) ₃] (10)	Reduction	[27]
DippFormNa and [Sm] ₂ (THF) ₂ in THF or Sm + DippFormH + Hg(C ₆ F ₅) ₂ in THF	[Sm(DippForm) ₂ (thf) ₂] (11)	Metathesis/ Salt elimination or RTP	[28,29]
[[Yb(DFForm) ₂ (CH ₃ CN)] ₂] dissolved in PhMe and [Yb(DFForm) ₂ (thf) ₃] dissolved in PhMe, C ₆ D ₆ , ether	[Yb(DFForm) ₂] (13)	Ligand dissociation	[30]
Eu + DippFormH in CH ₃ CN	[Eu(DippForm) ₂ (CH ₃ CN) ₄] (14)	Direct metal synthesis	[30]
Eu + DFFormH in CH ₃ CN	[[Eu(DFForm) ₂ (CH ₃ CN) ₂] ₂] (15)	Direct metal synthesis	[30]
Yb + DFFormH + Hg in CH ₃ CN	[Yb(DFForm) ₂ (CH ₃ CN)] ₂ (17)	Direct metal synthesis	[30]
Yb + DFFormH + Hg in mixture of thf and CH ₃ CN	[Yb(DFForm) ₂ (thf) ₃] (18)	Direct metal synthesis and RTP	[30]
Yb + Hg(Ph) ₂ + DippFormH in thf	[Yb(DippForm) ₂ (thf)] (20)	RTP and crystallised from thf/hexane	[30]
Dissolution of [Yb(DippForm) ₂ (thf)] in CH ₃ CN	[Yb(DippForm) ₂ (CH ₃ CN) ₃] (21)	Solvent exchange	[30]
Crystallisation of [Yb(DippForm) ₂ (CH ₃ CN) ₃] from toluene or hexane	[Yb(DippForm) ₂ (CH ₃ CN) ₂] (22)	Dissociation of ligand	[30]
Yb + FFormH + Hg(C ₆ F ₅) ₂ in THF	[Yb(FForm) ₂ (thf) ₂] (23)	RTP	[31]
Compound (23) recrystallised from DME	[Yb(DFForm) ₂ (dme)] (24)	Recrystallised from dme	[31]

DippForm ligand. Using the least bulky ligand, XylForm, in $[\text{Yb}(\text{XylForm})_2(\text{thf})_2]$ (**1**) gives the next smallest O–Yb–O angle ($78.13(9)^\circ$) and the largest O–Yb–O angle ($87.4(2)^\circ$) is observed in $[\text{Yb}(\text{EtForm})_2(\text{thf})_2]$ (**2**), which has the second bulkiest Form ligand.

The preparation of a new heterobimetallic samarium(II) formamidinate complex and selected reactions of samarium(II) complexes and one samarium(III) formamidinate complex with benzophenone or CS_2 were reported in 2014 [27]. The heterobimetallic formamidinate samarium(II)/potassium complex $[\text{KSm}(\text{DippForm})_3]$ (**10**) was synthesized by the reaction of $[\text{Sm}(\text{DippForm})_3]$ with potassium graphite in toluene at elevated temperature (Fig. 2-2). $[\text{KSm}(\text{DippForm})_3]$ (**10**) and $[\text{Sm}(\text{DippForm})_2(\text{thf})_2]$ (**11**) are the only known divalent formamidinate-samarium species so far reported [28]. In $[\text{KSm}(\text{DippForm})_3]$ (**10**) samarium is five coordinated by two chelating $\kappa(\text{N},\text{N}')$ formamidinate ligands and a one 1κ formamidinate ligand which also binds to potassium by an η^6 -2,6-diisopropylphenyl group and the other N atom.

Reaction of sodium metallated DippForm with $[\text{Sm}(\text{I})_2(\text{thf})_2]$ has been reported as one method to synthesize $[\text{Sm}(\text{DippForm})_2(\text{thf})_2]$ (**11**) compound [29]. During this reaction, another complex, the trivalent samarate $[\text{Na}(\text{thf})_5][\text{Sm}(\text{I})_2(\text{DippForm})_2(\text{thf})]$ (**12**) (see Table 2.3.1) was isolated as a minor co-product.

It has been reported that reaction of Eu and Yb metal with N,N'-bis(2,6-diisopropylphenyl)formamidine or N,N'-bis(2,6-difluorophenyl)formamidine in CH_3CN can be an effective and efficient method of preparing divalent rare earth formamidinate complexes without the need of an organomercurial co-oxidant as in RTP syntheses [31]. Thus, $[\{\text{Yb}(\text{DFForm})_2(\text{CH}_3\text{CN})\}_2]$ (**17**) (Fig. 2-5) (and some $[\text{Yb}(\text{DFForm})_2]$ (**13**) and $[\text{Eu}(\text{DippForm})_2(\text{CH}_3\text{CN})_4]$ (**14**) were synthesized from DFFormH and DippFormH respectively and as a result, the highest coordination number for divalent rare earth ArForm complexes was observed in the latter compound (Fig. 2-3). Using DFFormH as the ligand yields $[\{\text{Eu}(\text{DFForm})_2(\text{CH}_3\text{CN})_2\}_2]$ (**15**) (Fig. 2-4) which has an unusual bridging coordination mode μ -1 $\kappa(\text{N}:\text{N}')$:2 $\kappa(\text{N}:\text{N}')$. This coordination mode is the first for divalent lanthanoid formamidinates and was only recently reported for trivalent formamidinates [15]. This paper reports that using thf in place of CH_3CN with the formamidine ligands yields the trivalent hydroxy-bridged dimer $[\{\text{Eu}(\text{DFForm})_2\text{OH}(\text{thf})\}_2]$ (**16**) establishing the importance of using CH_3CN . Success for these two ligands of disparate acidities and bulk suggests that the method should be widely applicable for most formamidines. The same method is viable for preparing $[\text{Yb}(\text{DFForm})_2(\text{thf})_3]$ (**18**) from CH_3CN and $\text{CH}_3\text{CN}/\text{THF}$ respectively, but activation of Yb by Hg metal is required. Tetrametallic oxide species $[\{\text{Yb}_2(\text{DFForm})_4(\text{O})\}_2]$ (**19**) was synthesized by exposing $[\text{Yb}(\text{DFForm})_2(\text{thf})_3]$ (**18**) to trace amounts of O_2 . This report compares this synthetic method to the RTP reaction which yields $[\text{Yb}(\text{DFForm})_2(\text{thf})_3]$ (**18**) and the lowest coordination number for divalent rare earth ArForm complexes, $[\text{Yb}(\text{DippForm})_2(\text{thf})]$ (**20**), in the case of using Yb as the metal. $[\text{Yb}(\text{DippForm})_2(\text{CH}_3\text{CN})_3]$ (**21**) was crystallised from $[\text{Yb}(\text{DippForm})_2(\text{thf})]$ (**20**) using CH_3CN as the solvent. Another Yb complex $[\text{Yb}(\text{DippForm})_2(\text{CH}_3\text{CN})_2]$ (**22**) can be obtained by evaporation of $[\text{Yb}(\text{DippForm})_2(\text{CH}_3\text{CN})_3]$ (**21**) in CH_3CN and recrystallization from PhMe. The center atoms in $[\{\text{Yb}(\text{DFForm})_2(\text{CH}_3\text{CN})\}_2]$ (**17**) are seven coordinate. They have one CH_3CN and one DFForm terminally bound and an unusual twisted DFForm bridging ligand, because of the close Yb–F bond ($2.626(2)\text{Å}$). Another divalent complex $[\text{Yb}(\text{FForm})_2(\text{thf})_2]$ (**23**) is the result of a RTP reaction between FFormH and an excess Yb metal [31]. Recrystallization of $[\text{Yb}(\text{FForm})_2(\text{thf})_2]$ (**23**) from dme yields another divalent complex $[\text{Yb}(\text{FForm})_2(\text{dme})_2]$ (**24**). All known divalent lanthanoid formamidinate compounds are listed in Table 2.2.1.

2.3. Trivalent compounds

A homoleptic monomer i.e. $[\text{La}(\text{CF}_3\text{Form})_3]$ (**25**) (Fig. 2-6) was obtained from a RTP reaction from CF_3FormH [32]. This compound easily undergoes C–F activation by heating in non-coordinating solvents such as C_6D_6 or PhMe to produce LaF_3 and $[(\text{CF}_3\text{Form})_2(\text{thq})]$ (thq = tetrahydroquinazoline) as the major and $[(\text{CF}_3\text{Form})_2\text{Benz}]$ (Benz = benzamidine) as the minor product. This process can be compared to the $[\text{Yb}(\text{CF}_3\text{Form})_3(\text{thf})]$ (**26**) complex (Fig. 2-7) which

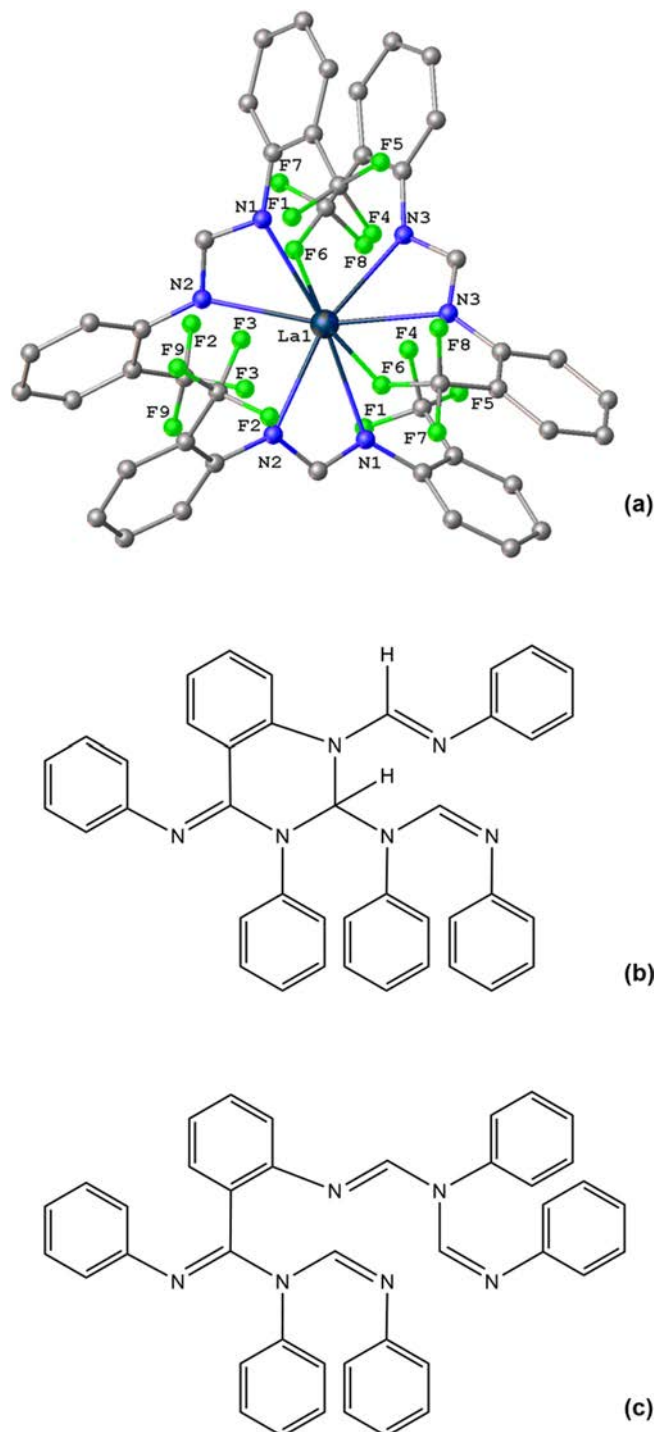


Fig. 2-6. X-ray structure of a) $[\text{La}(\text{CF}_3\text{Form})_3]$ (**25**) and simplified structures of b) $[(\text{CF}_3\text{Form})_2(\text{thq})]$ c) $[(\text{CF}_3\text{Form})_2\text{Benz}]$. All phenyl groups in b) and c) represent *ortho*-trifluoromethylphenyl groups, with the CF_3 groups removed for clarity.

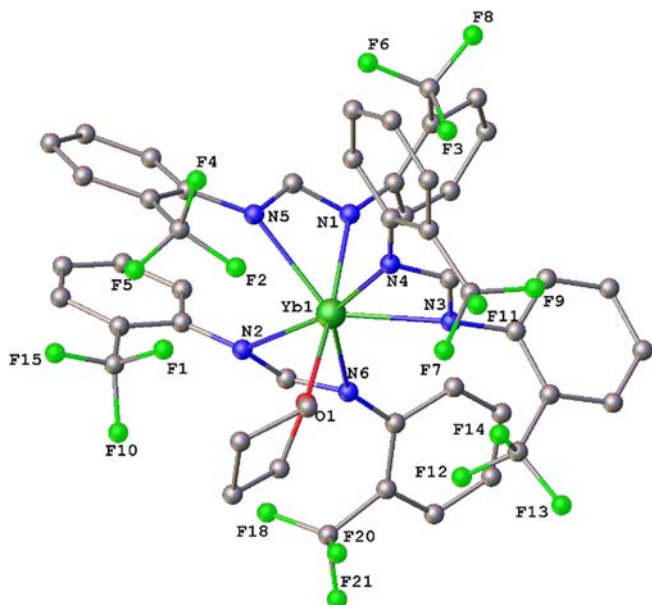


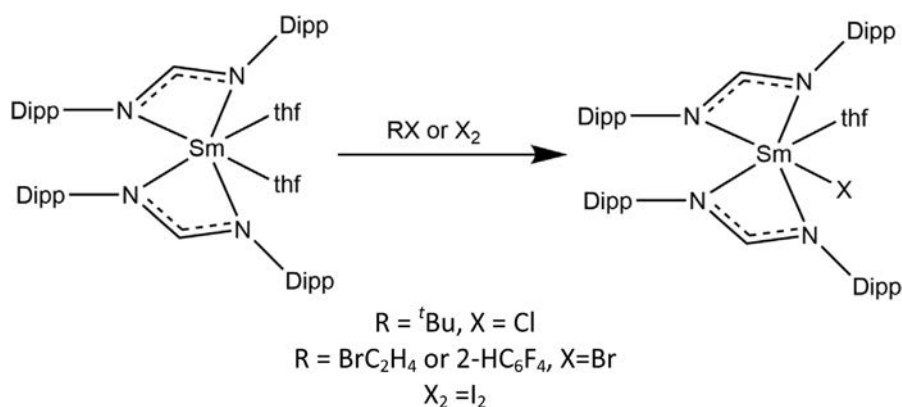
Fig. 2-7. X-ray structure of $[\text{Yb}(\text{CF}_3\text{Form})_3(\text{thf})]$ (**26**).

was synthesized in the same study. $[\text{Yb}(\text{CF}_3\text{Form})_3(\text{thf})]$ (**26**) can be C-F activated using the same method to yield the same compounds but with $[(\text{CF}_3\text{Form})_2\text{Benz}]$ as the major product. However, it has a

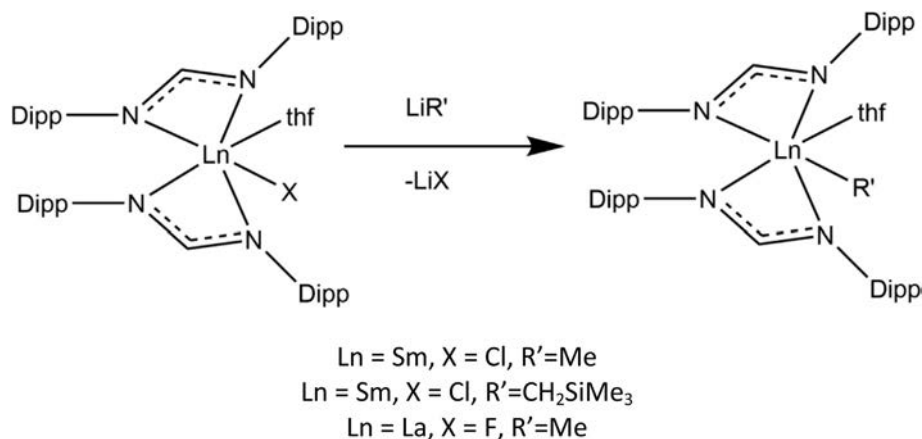
longer activation time perhaps due to the lack of significant Yb-F interactions ($\text{Yb-F} \geq 3.2427(17) \text{ \AA}$) compared with six La-F bonds in **2b**.

The oxidation of $[\text{Sm}(\text{DippForm})_2(\text{thf})_2]$ (**11**) by *tert*-butyl chloride, 1,2-dibromoethane and iodine at ambient temperature led to the formation of the samarium(III) halide complexes $[\text{Sm}(\text{DippForm})_2\text{Cl}(\text{thf})]$ (**27**), $[\text{Sm}(\text{DippForm})_2\text{Br}(\text{thf})]$ (**28**) and $[\text{Sm}(\text{DippForm})_2\text{I}(\text{thf})]$ (**29**) respectively in good yields (Scheme 2-1) [23]. The metathesis reaction of $[\text{Sm}(\text{DippForm})_2\text{Cl}(\text{thf})]$ (**27**) and $[\text{La}(\text{DippForm})_2\text{F}(\text{thf})]$ (**30**) with LiMe and $\text{LiCH}_2\text{SiMe}_3$ resulted in the formation of samarium alkyl complexes $[\text{Sm}(\text{DippForm})_2\text{Me}(\text{thf})]$ (**31**), $[\text{Sm}(\text{DippForm})_2\text{CH}_2\text{SiMe}_3(\text{thf})]$ (**32**) and $[\text{La}(\text{DippForm})_2\text{Me}(\text{thf})]$ (**33**). The complex $[\text{La}(\text{DippForm})_2\text{Me}(\text{thf})]$ (**33**) is the first reported La complex that contains a rare terminal methyl ligand (Scheme 2-2).

Bis(2-bromo-3,4,5,6-tetrafluorophenyl)mercury, DippFormH and Sm were used in a RTP reaction to yield $[\text{Sm}(\text{DippForm})\text{Br}_2(\text{thf})_3]$ (**34**) [23]. The divalent samarium compound, $[\text{Sm}(\text{DippForm})_2(\text{thf})_2]$ (**11**), was used in a redox reaction with diphenylmercury to yield $[\text{Sm}(\text{DippForm})_2(\text{OCH}=\text{CH}_2)(\text{thf})]$ (**35**). $[\text{Sm}(\text{DippForm})_2\text{Cl}(\text{thf})]$ (**27**), $[\text{Sm}(\text{DippForm})\text{Br}_2(\text{thf})_3]$ (**34**) (Fig. 2-8), $[\text{Sm}(\text{DippForm})_2\text{Me}(\text{thf})]$ (**31**), $[\text{Sm}(\text{DippForm})_2\text{CH}_2\text{SiMe}_3(\text{thf})]$ (**32**), $[\text{Sm}(\text{DippForm})_2(\text{OCH}=\text{CH}_2)(\text{thf})]$ (**35**) (Fig. 2-9) and $[\text{La}(\text{DippForm})_2\text{Me}(\text{thf})]$ (**33**) are mononuclear and the coordination number of the central metal is six in all compounds. Formamidinate ligands connect by chelation to the metal atom through two nitrogen donor atoms. Also, it has been reported benzophenone (bp) or halogenating agents like $\text{TiCl}_4(\text{thf})_2$, Ph_3CCl or C_2Cl_6 can be used as



Scheme 2-1. Schematic of the X-ray structure of $[\text{Sm}(\text{DippForm})_2\text{X}(\text{thf})]$. $\text{R} = \text{}^t\text{Bu}$, $\text{X} = \text{Cl}$, $\text{R} = \text{BrC}_2\text{H}_4$ or $2\text{-HC}_6\text{F}_4$, $\text{X} = \text{Br}$, $\text{X}_2 = \text{I}_2$.



Scheme 2-2. Schematic of the X-ray structure of $[\text{Ln}(\text{DippForm})_2\text{R}'(\text{thf})]$. $\text{Ln} = \text{Sm}$, $\text{X} = \text{Cl}$, $\text{R}' = \text{Me}$, $\text{Ln} = \text{Sm}$, $\text{X} = \text{Cl}$, $\text{R}' = \text{CH}_2\text{SiMe}_3$, $\text{Ln} = \text{La}$, $\text{X} = \text{F}$, $\text{R}' = \text{Me}$.

oxidants to synthesize $[\text{Yb}(\text{DFForm})_3(\text{bp})]$ (**36**) and $[\text{Yb}(\text{DFForm})_2\text{Cl}(\text{thf})_2]$ (**37**) from divalent $[\text{Yb}(\text{DFForm})_2(\text{thf})_3]$ (**18**) [30]. $[\text{Yb}(\text{DFForm})_3(\text{thf})]$ (**38**) was also obtained from an RTP reaction in this paper.

It has been reported divalent Yb complexes can induce C-X (X=F, Cl, Br) activation reactions with perfluorodecalin, hexachloroethane or 1,2-dichloroethane, and 1-bromo-2,3,4,5-tetrafluorobenzene, yielding $[\text{Yb}(\text{EtForm})_2\text{F}]_2$ (**39**), $[\text{Yb}(\text{o-PhPhForm})_2\text{F}]_2$ (**40**),

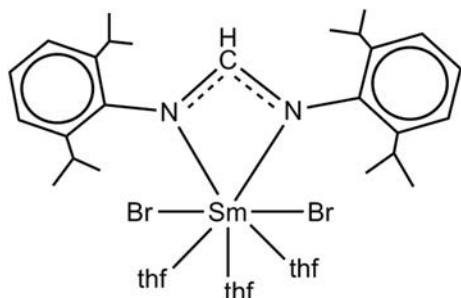


Fig. 2-8. Schematic of the X-ray structure of $[\text{Sm}(\text{DippForm})\text{Br}_2(\text{thf})_3]$ (**34**).

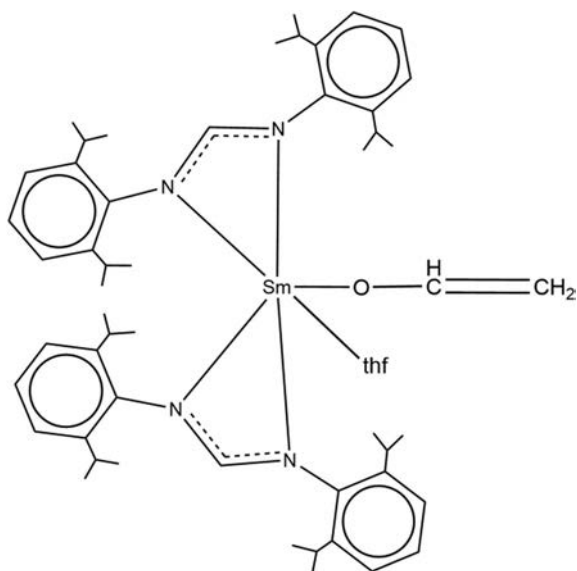


Fig. 2-9. Schematic of the X-ray structure of $[\text{Sm}(\text{DippForm})_2(\text{OCH}=\text{CH}_2)(\text{thf})]$ (**35**).

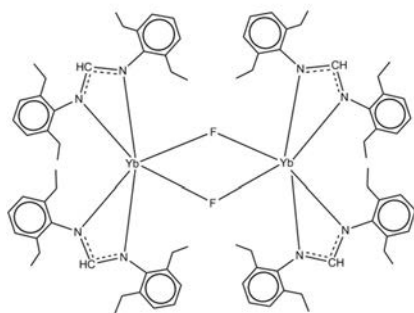
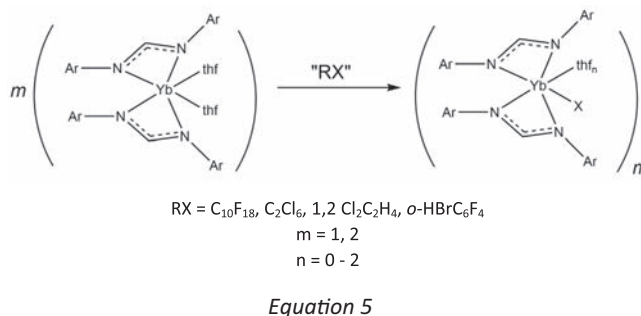


Fig. 2-10. Schematic and the X-ray structure of $[\text{Yb}(\text{EtForm})_2(\mu\text{-F})_2]$ (**39**).

$[\text{Yb}(\text{o-PhPhForm})_2\text{Cl}(\text{thf})_2]$ (**41**), $[\text{Yb}(\text{DippForm})_2\text{Cl}(\text{thf})]$ (**42**) and $[\text{Yb}(\text{DippForm})_2\text{Br}(\text{thf})]$ (**43**) (Eq. (5)) [26].



The coordination number for Yb in $[\text{Yb}(\text{EtForm})_2\text{F}]_2$ (**39**), $[\text{Yb}(\text{DippForm})_2\text{Cl}(\text{thf})]$ (**42**) and $[\text{Yb}(\text{DippForm})_2\text{Br}(\text{thf})]$ (**43**) is six. $[\text{Yb}(\text{EtForm})_2\text{F}]_2$ (**39**) has a dimeric structure containing fluoride-bridges (Fig. 2-10). However, $[\text{Yb}(\text{DippForm})_2\text{Cl}(\text{thf})]$ (**36**) and $[\text{Yb}(\text{DippForm})_2\text{Br}(\text{thf})]$ (**43**) are mononuclear. $[\text{Yb}(\text{o-PhPhForm})_2\text{Cl}]$

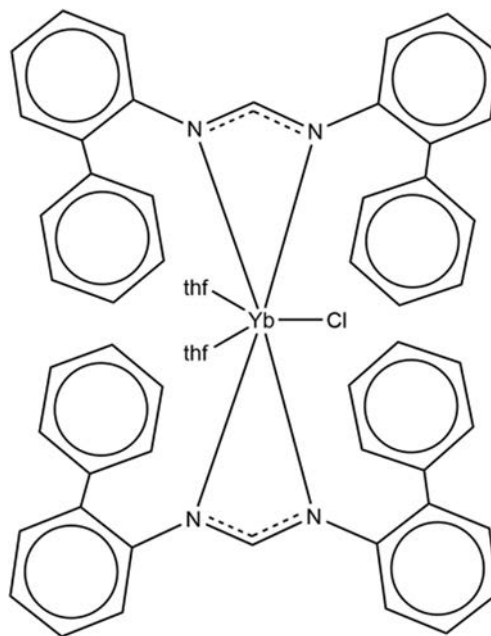
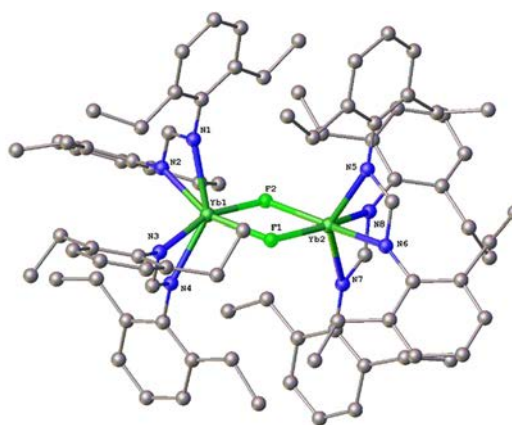
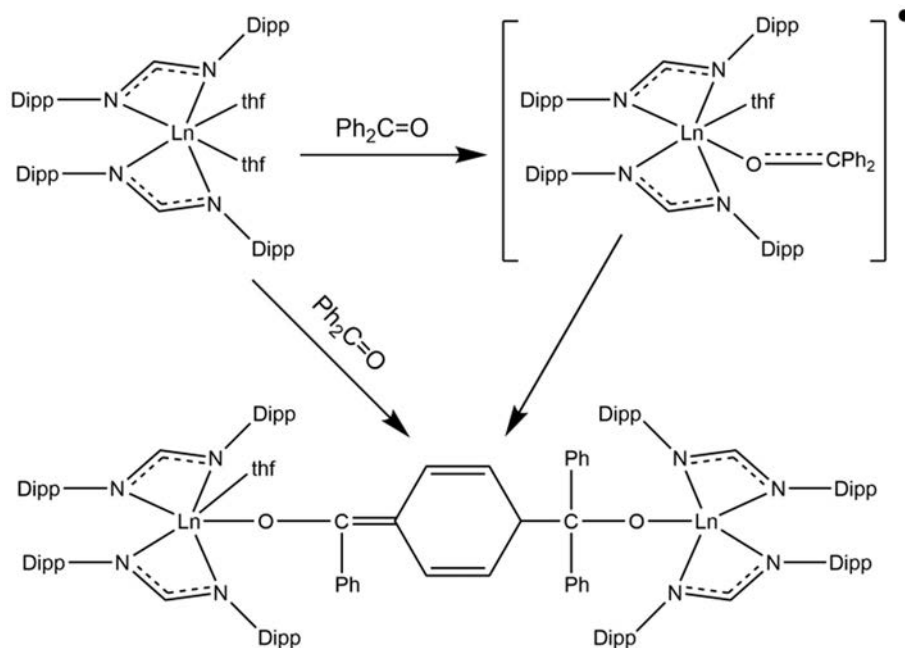
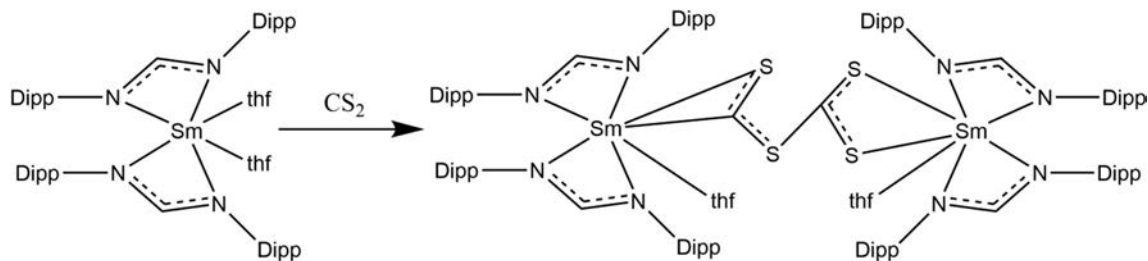


Fig. 2-11. Schematic of the X-ray structure of $[\text{Yb}(\text{o-PhPhForm})_2\text{Cl}(\text{thf})_2]$ (**41**).





Scheme 2-3. Schematic of the X-ray structure of $[\text{Ln}(\text{DippForm})_2(\text{thf})\{\mu\text{-OC}(\text{Ph}) = (\text{C}_6\text{H}_5)\text{-C}(\text{Ph})_2\text{O}\}\text{Ln}(\text{DippForm})_2]$ ($\text{Ln} = \text{Sm}$ (**47**), Yb (**48**)).



Scheme 2-4. Schematic and part of the X-ray structures of $[(\text{Sm}(\text{DippForm})_2(\text{thf})_2)\{\mu\text{-}\eta^2(\text{C},\text{S}):\kappa(\text{S},\text{S}'')\text{-SCSCS}_2\}]$ (**49**) highlighting the C_2S_4 fragment.

$(\text{thf})_2]$ (**41**) is a seven coordinated monomeric complex with two chelating formamidinate ligands, a terminal chloride and two THF donors (Fig. 2-11). In the case of using DippFormH and Hg $(2\text{-BrC}_6\text{F}_4)_2$ in RTP reactions, a series of complexes $[\text{Ln}(\text{DippForm})_2\text{-}$

$\text{Br}(\text{thf})]$ ($\text{Ln} = \text{La}$ (**44**), Nd (**45**)) was synthesized. For comparison purposes, a related complex $[\text{Tb}(\text{DippForm})_2\text{Cl}(\text{thf})_2]\cdot 2.5\text{THF}$ (**46**) was synthesized in this study using a metathesis reaction between TbCl_3 and $\text{Na}(\text{DippForm})$ [26].

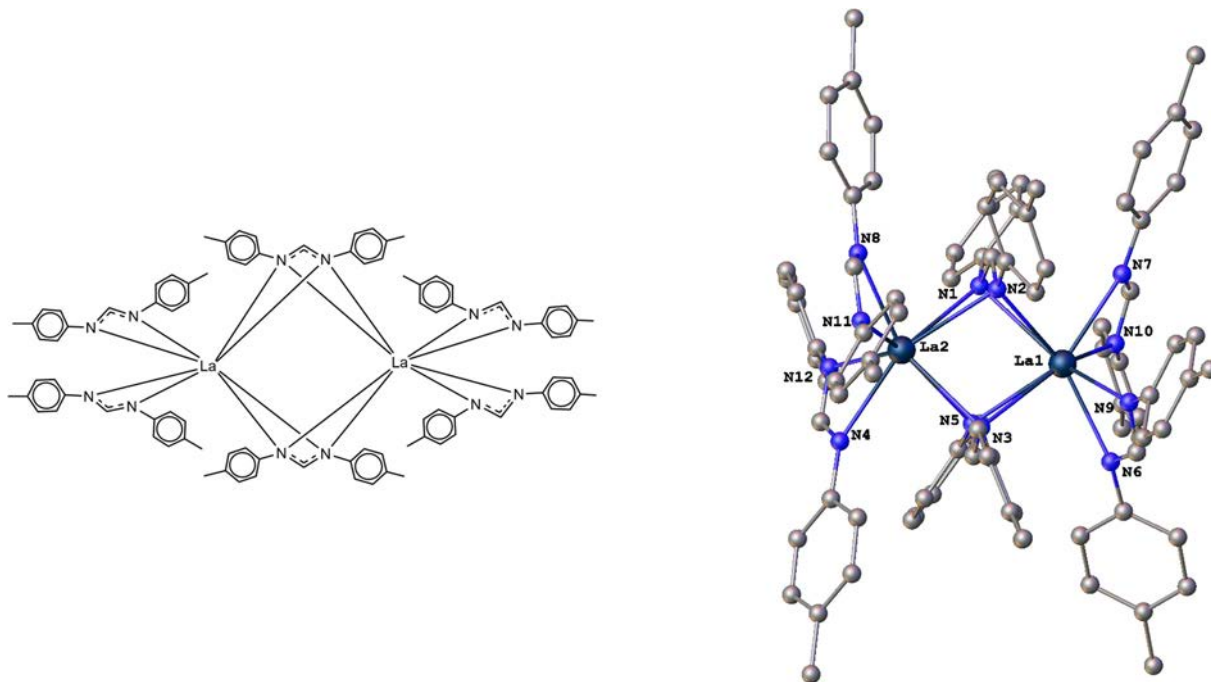


Fig. 2-12. Representative molecular structure of $[\text{La}(\text{p-TolForm})_3]_2$ (**50**).

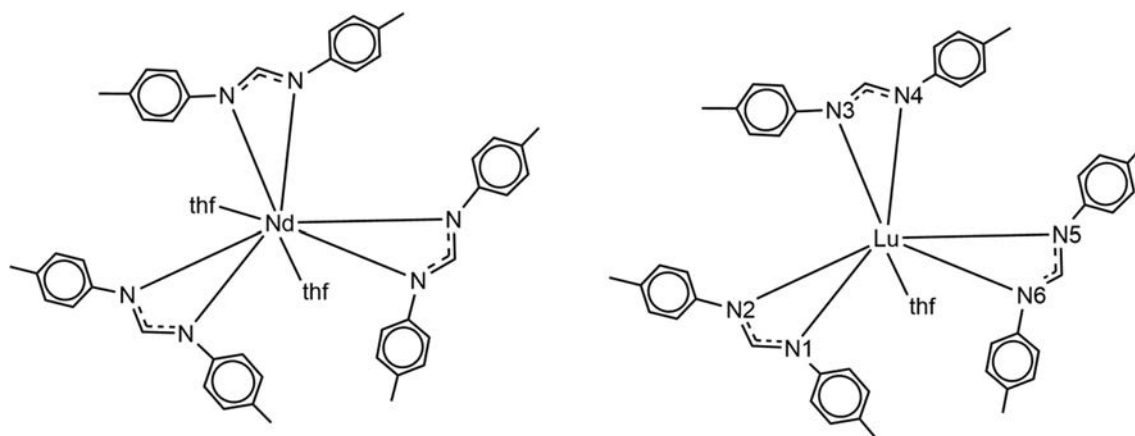


Fig. 2-13. Schematic molecular structures of $[\text{Nd}(\text{p-TolForm})_3(\text{thf})_2] \cdot \text{THF}$ (**56**) (left) and $[\text{Lu}(\text{p-TolForm})_3(\text{thf})] \cdot \text{THF}$ (**57**) (right) exemplifying the lowering of coordination number with lanthanoid size.

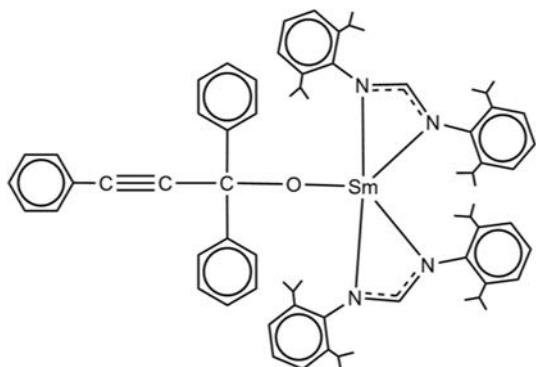


Fig. 2-14. Schematic of the X-ray structures of $[\text{Sm}(\text{DippForm})_2(\text{OC}-(\text{Ph})_2\text{C}_2\text{Ph})]$ (**60**).

The highly unusual $[\text{Sm}(\text{DippForm})_2(\text{thf})\{\mu\text{-OC}(\text{Ph})=(\text{C}_6\text{H}_5)\text{-C}(\text{Ph})_2\text{O}\}\text{Sm}(\text{DippForm})_2]$ (**47**) ($\text{C}_6\text{H}_5 = 1,4\text{-cyclohexadiene-3-yl-6-ylidene}$) compound was reported as the result of the reaction of $[\text{Sm}(\text{DippForm})_2(\text{thf})_2]$ (**11**) with benzophenone [27]. This compound contains rare C-C coupling between a carbonyl carbon and the carbon at the *para* position of a phenyl group of the OCPh_2 fragment. It was also found that the reaction of $[\text{Yb}(\text{DippForm})_2(\text{thf})_2]$ (**4**) with benzophenone gives a similar product (**48**) (Scheme 2-3), with a ketyl complex intermediate considered to be involved.

It was also reported that $[\text{Sm}(\text{DippForm})_2(\text{thf})_2]$ (**11**) reacts with carbon disulfide to form a dinuclear $[\{\text{Sm}(\text{DippForm})_2(\text{thf})_2\}_2(\mu\text{-}\eta^2(\text{C},\text{S}):\kappa(\text{S},\text{S}''\text{-SCSCS}_2)]$ (**49**) complex (Scheme 2-4). This complex has a rare thioformyl carbonotrithioate ($(\text{SCSCS}_2)^{2-}$) bridging ligand.

RTP reactions were carried out between $\text{Hg}(\text{C}_6\text{F}_5)_2$, *p*-TolForm and rare earth metals including La, Ce, Nd, Lu and Sm to yield trivalent lanthanoid formamidates. By using THF as the solvent, compounds were synthesized with the general form of

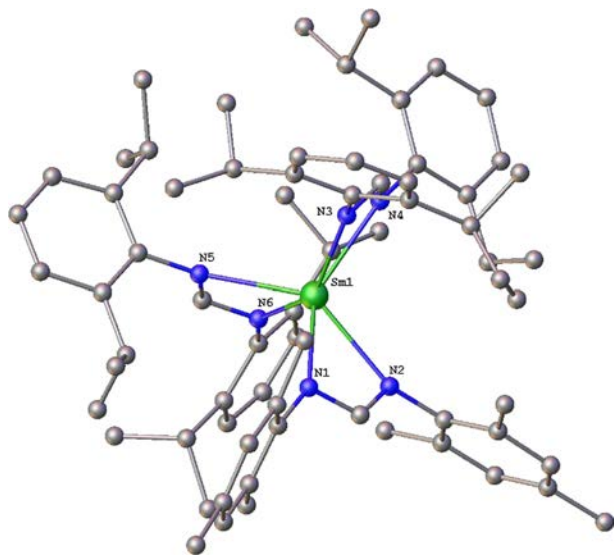


Fig. 2-15. X-ray structure of $[\text{Sm}(\text{DippForm})_2(\text{MesForm})]$ (**62**).

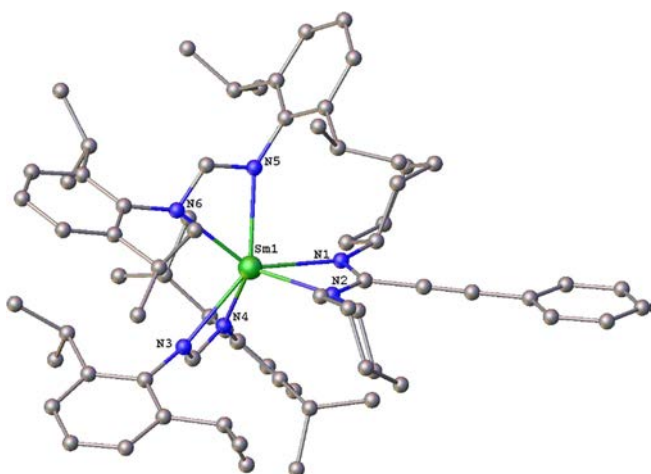


Fig. 2-16. X-ray structure of $[\text{Sm}(\text{DippForm})_2(\text{CyNC}(\text{CPh})\text{NCy})]$ (**65**).

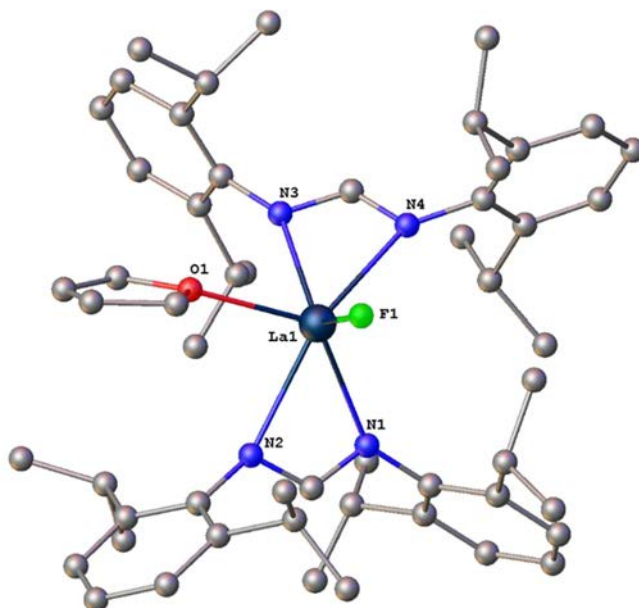
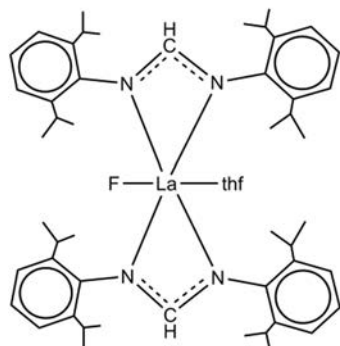


Fig. 2-17. Schematic and the X-ray structure of $[\text{LaF}(\text{DippForm})_2(\text{thf})]$ (**30**).

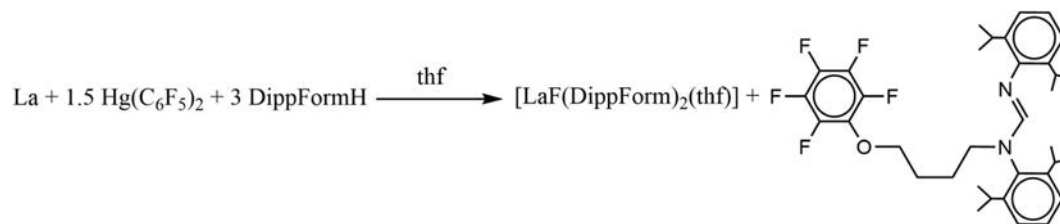
$[\text{Ln}(p\text{-TolForm})_3]$ or $[\text{Ln}(p\text{-TolForm})_3(\text{thf})_2]$ (Ln = rare earth metal). [15] It was the first time that the $\mu\text{-}1\kappa(\text{N},\text{N}')\text{:}2\kappa(\text{N},\text{N}')$ coordination mode had been achieved in trivalent rare earth formamidate chemistry and also discussed previously for the divalent Eu complex $[\{\text{Eu}(\text{DFForm})_2(\text{CH}_3\text{CN})_2\}_2]$ (**15**). Fig. 2-12 shows the X-ray structure of the $[\text{La}(p\text{-TolForm})_3]_2$ (**50**) which is same as the $[\text{Sm}(p\text{-TolForm})_3]_2$ (**51**). The cerium analogue has a similar structure but with an eclipsed rather than a staggered conformation [15]. Two $\mu\text{-}1\kappa(\text{N},\text{N}')\text{:}2\kappa(\text{N},\text{N}')$ bridging and four $\kappa(\text{N},\text{N}')$ terminal $p\text{-TolForm}$ ligands are present in the structure of each dimeric complex.

$[\text{Sm}(p\text{-TolForm})_3(\text{Ph}_3\text{PO})_2]$ (**52**) was synthesized by treating $[\text{Sm}(p\text{-TolForm})_3]$ (**51**) with triphenylphosphine oxide (Ph_3PO) and crystallizing from C_6D_6 . The reaction of DFFormH on $[\text{Sm}(p\text{-TolForm})_3]$ (**51**) was studied using PhMe. As a result of a protolysis reaction and crystallization from THF/hexane, three different complexes, $[\text{Sm}(\text{DFForm})_2(p\text{-TolForm})(\text{thf})_2]$ (**53**), $[\text{Sm}(p\text{-TolForm})_3]_2$ (**51**) and $[\text{Sm}(\text{DFForm})_3(\text{thf})_2]$ (**54**) were isolated. Another complex, $[\text{K}(18\text{-Crown-6})][\text{Sm}(p\text{-TolForm})_4]$ (**55**), was synthesized by reaction of $[\text{Sm}(p\text{-TolForm})_3]$ (**51**) in PhMe in the presence of 18-Crown-6 and a potassium mirror.

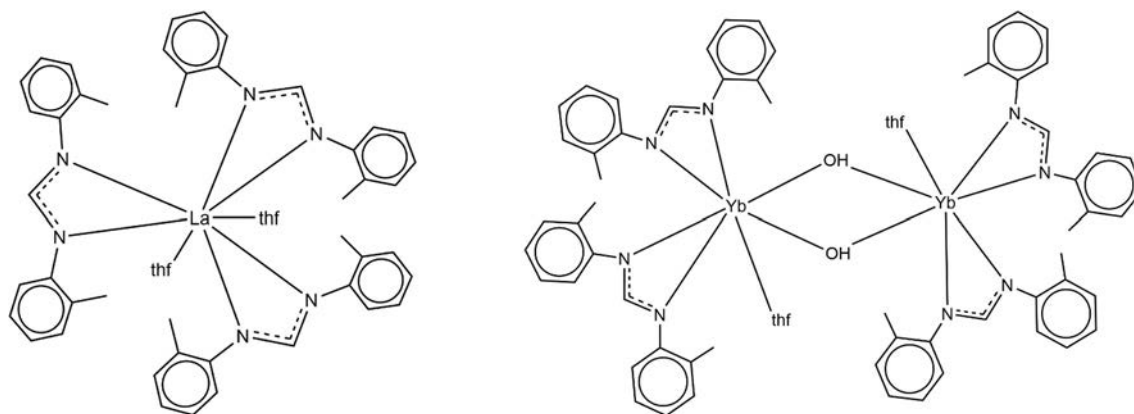
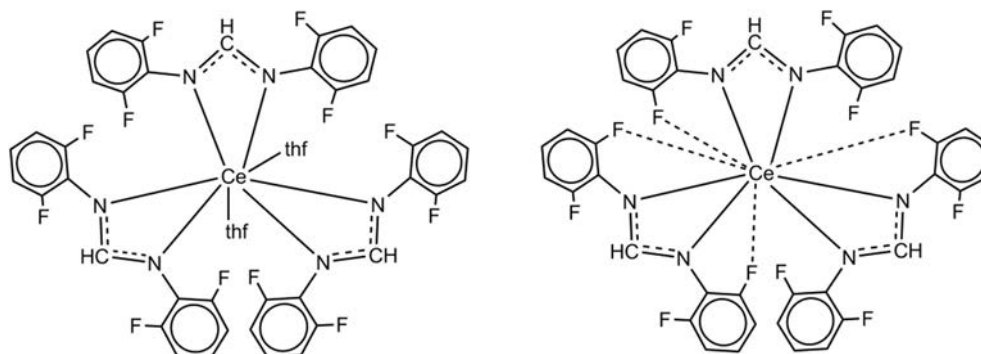
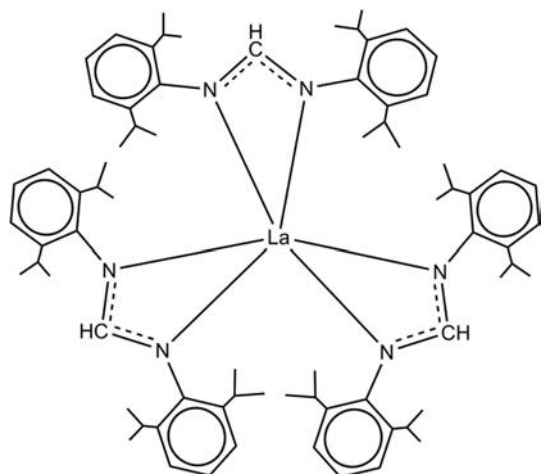
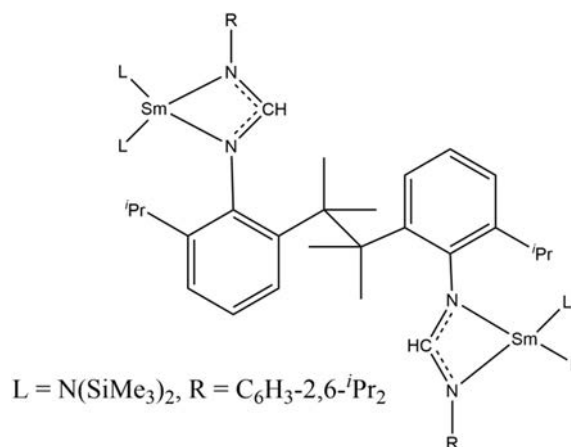
Fig. 2-13 shows the schematic structure for complexes in this study containing Nd (**56**) and Lu (**57**) [15]. The Nd atom is eight coordinated by three bidentate $p\text{-TolForm}$ ligands and two *transoid*-THF ligands ($\text{O}\text{--}\text{Nd}\text{--}\text{O}$: $153.61(6)^\circ$), in a distorted dodecahedral environment. The lutetium atom is seven coordinate with one symmetric ($\text{Lu}\text{--}\text{N}5$: 2.374(4), $\text{Lu}\text{--}\text{N}6$: 2.373(4)) and two asymmetric chelating $p\text{-TolForm}$ ligands ($\text{Lu}\text{--}\text{N}1$: 2.386(4), $\text{Lu}\text{--}\text{N}2$: 2.303(4), $\text{Lu}\text{--}\text{N}3$: 2.358(4), $\text{Lu}\text{--}\text{N}4$: 2.336(4)) and one THF ligand with the reduction in coordination number being a consequence of the lanthanoid contraction.

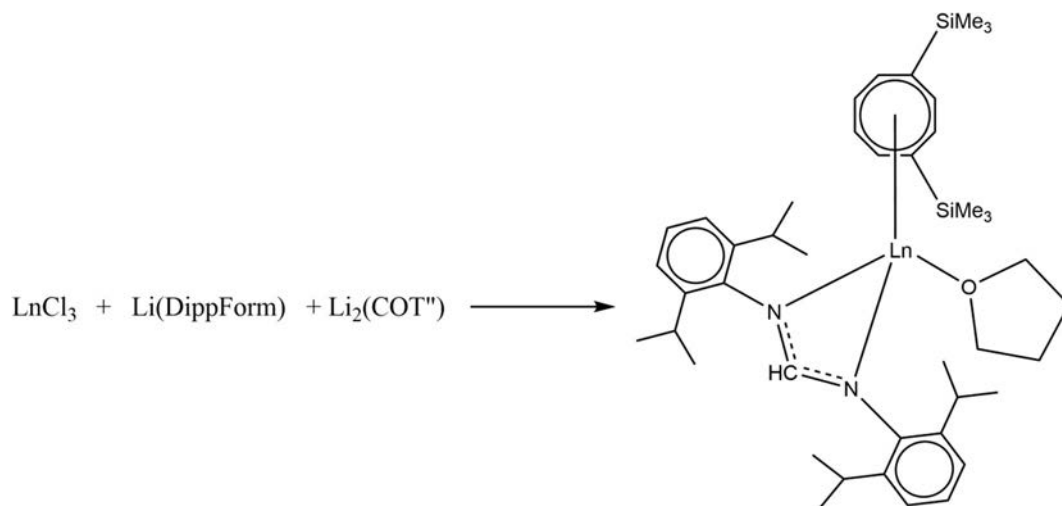
Trivalent $[\text{Sm}(\text{DippForm})_2(\text{CCPh})(\text{thf})]$ (**58**) can activate the $\text{C}=\text{O}$ bond of benzophenone and form $[\text{Sm}(\text{DippForm})_2\{\text{OC}(\text{Ph})_2\text{C}_2\text{Ph}\}(\text{thf})]$ (**59**) with unsolvated $[\text{Sm}(\text{DippForm})_2\{\text{OC}(\text{Ph})_2\text{C}_2\text{Ph}\}]$ (**60**) as a minor product. $\kappa(\text{N},\text{N}')$ -Bonding between a DippForm and samarium exists in all compounds (Fig. 2-14 [27]).

Oxidation of $[\text{Sm}(\text{DippForm})_2(\text{thf})_2]$ (**11**) with different oxidizing agents has been investigated in another study [28]. Oxidation of $[\text{Sm}(\text{DippForm})_2(\text{thf})_2]$ (**11**) with DippNCNDipp in PhMe can yield $[\text{Sm}(\text{DippForm})_3]$ (**61**). Using the less bulky carbodiimide, MesNCNMes, yields the heteroleptic $[\text{Sm}(\text{DippForm})_2(\text{MesForm})]$



Scheme 2-5.

Fig. 2-18. Schematic molecular structures of [La(o-TolForm)₃(thf)₂] (**67**) (left) and [Yb(o-TolForm)₂(μ-OH)(thf)₂] (**85**) (right).Fig. 2-19. Schematic of the X-ray molecular structures of [Ce(DFForm)₃(thf)₂] (**91**) (left) and [Ce(DFForm)₃] (**92**) (right).Fig. 2-20. Schematic of the X-ray structure of [La(DippForm)₃] (**97**).Fig. 2-21. Schematic of the X-ray structure of [((Me₃Si)₂N)₂Sm{μ-(RNC(H)N(Ar-Ar)NC(H)NR)}Sm{N(SiMe₃)₂}]₂ (**99**) complex.



Scheme 2-6. Schematic of the X-ray structure of $[\text{Ln}(\text{DippForm})(\text{COT}')(\text{thf})] \cdot \text{C}_7\text{H}_8$ complexes (Ln = Sm (**99**), Yb (**100**)).

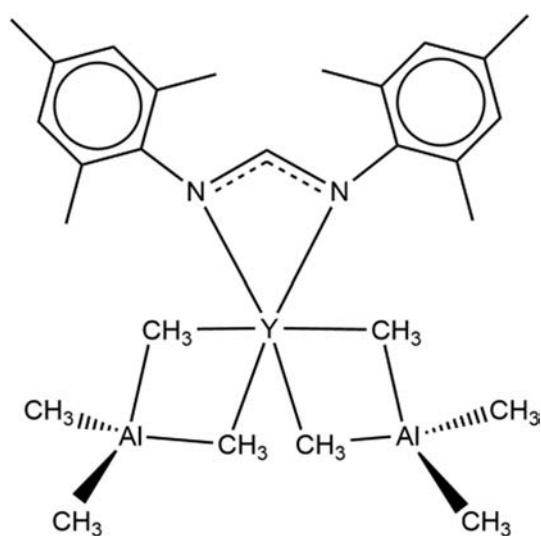


Fig. 2-22. Schematic of the X-ray structure of $[\text{Y}(\text{MesForm})(\text{AlMe}_4)_2]$ (**102**).

(**62**) (Fig. 2-15). It has been found that using *N,N'*-dicyclohexylcarbodiimide (CyNCNCy) as the oxidant in PhMe can yield two complexes, $[\text{Sm}(\text{DippForm})_2(\text{CyNC}(\text{CH}_2\text{Ph})\text{NCy})]$ (**63**) and $[\text{Sm}(\text{DippForm})_2(\text{CyNC}(\text{H})\text{NCy})]$ (**64**) in approximately equal yields, indicating activation of toluene has occurred. However, in the case of using thf as the solvent, only $[\text{Sm}(\text{DippForm})_2(\text{CyNC}(\text{H})\text{NCy})]$ (**64**) can be isolated. In this process an intermediate radical compound can receive a hydrogen atom from the solvent to give a formamidinate ligand. This paper also reports complexes $[\text{Sm}(\text{DippForm})_2(\text{CyNC}(\text{CPh})\text{NCy})]$ (**65**) (Fig. 2-16) and $[\text{Sm}(\text{DippForm})_2(\text{MesNC}(\text{CPh})\text{NMe}_2)]$ (**66**) as the result of the reaction of $[\text{Sm}(\text{DippForm})_2(\text{CPh})(\text{thf})]$ (**58**) with RNCNR (R = Cy, Mes) where the carbodiimide inserts into the Sm–CPh bond.

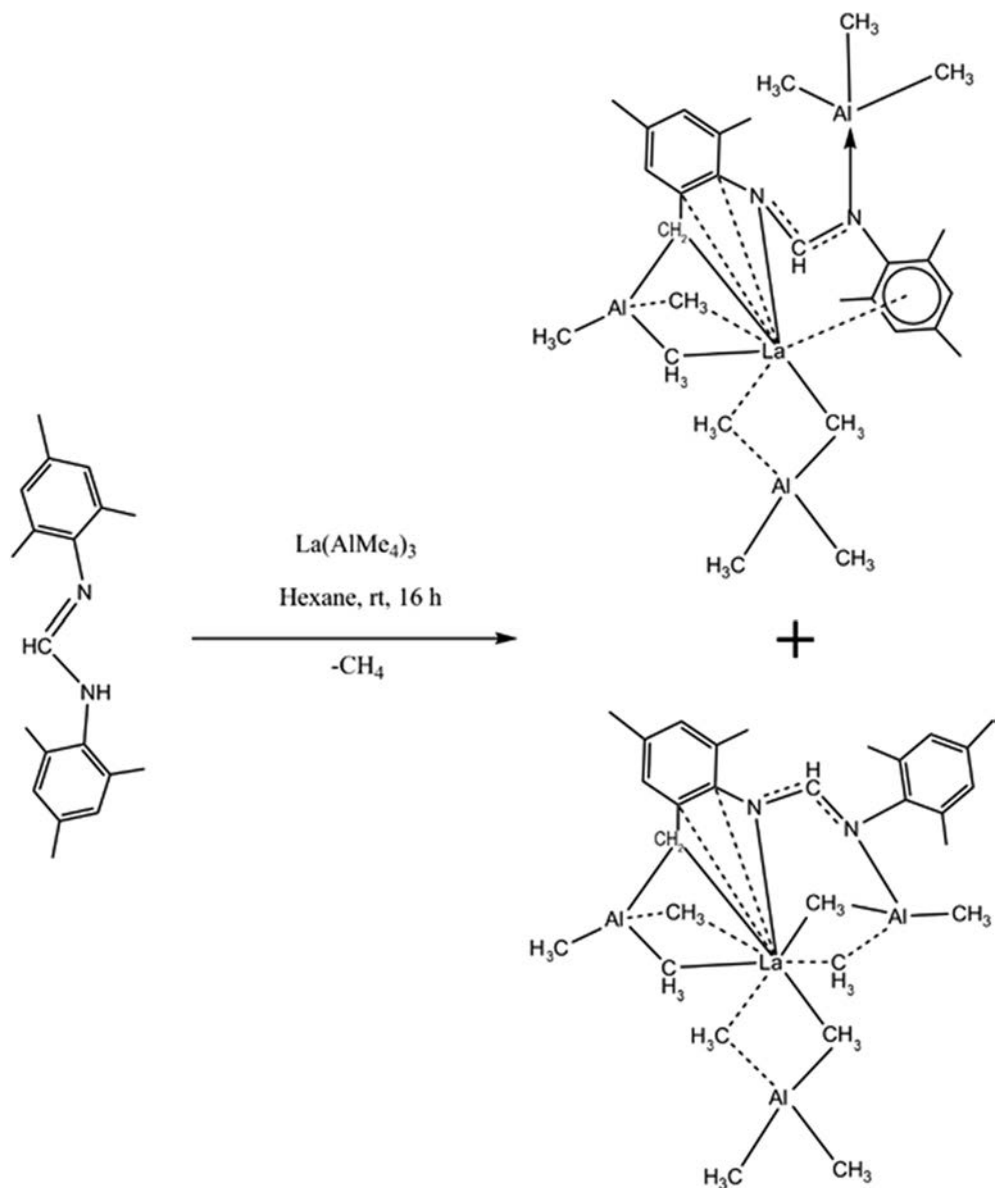
A functionalised formamidinate, $\text{DippForm}((\text{CH}_2)_4\text{OC}_6\text{F}_4\text{H}-o)$ and a rare terminal Ln–F bond were formed in an RTP study from DippFormH, lanthanum and $\text{Hg}(\text{C}_6\text{F}_5)_2$ (Scheme 3-5) [14]. The resulting compound, $[\text{LaF}(\text{DippForm})_2(\text{thf})]$ (**30**) (Fig. 2-17), shows that lanthanum is six coordinate and there are two chelating *cisoid* DippForm ligands. The main idea of this study was to use the RTP reaction with bis(pentafluorophenyl)mercury to synthesise a heteroleptic lanthanum fluoride $[\text{La}(\text{L})_2\text{F}]$ complex. This report

shows that the proposed $[\text{Ln}(\text{C}_6\text{F}_5)_2]$ intermediate undergoes C–F activation to yield $[\text{Ln}(\text{F})\text{L}_2]$ and a unique functionalised formamidinate, $\text{DippForm}((\text{CH}_2)_4\text{OC}_6\text{F}_4\text{H}-o)$ (Scheme 2-5) which arises from a substituted benzyne, a ring opened thf and DippFormH. In this study elemental lanthanum was used with bis(pentafluorophenyl)mercury and DippFormH in THF in a 1 : 1.5 : 3 stoichiometry.

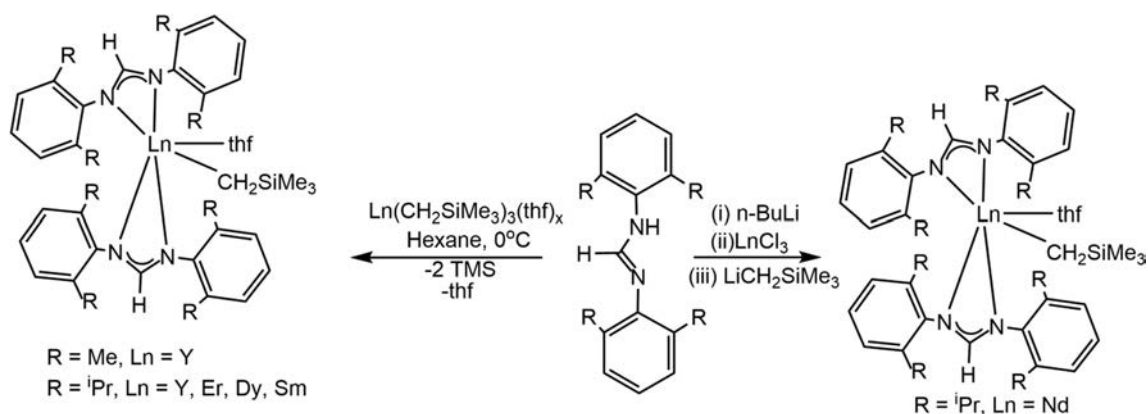
A series of tris(formamidinato)lanthanoid(III) complexes in the form of $[\text{Ln}(\text{Form})_3(\text{thf})_n]$ has been reported as the products of RTP reaction between different lanthanoids and *N,N'*-bis(aryl)formamidinate ligands [24]. The *o*-TolFormH ligand was used with La and Er to give $[\text{La}(\text{o-TolForm})_3(\text{thf})_2]$ (**67**) and $[\text{Er}(\text{o-TolForm})_3(\text{thf})]$ (**68**) respectively. $[\text{La}(\text{XylForm})_3(\text{thf})]$ (**69**) and $[\text{Sm}(\text{XylForm})_3]$ (**70**) were synthesized using XylFormH ligand and MesFormH as the proligand yielded $[\text{Ln}(\text{MesForm})_3]$ complexes (Ln = La (**71**), Nd (**72**), Sm (**73**) and Yb (**74**)). In the case of EtFormH, the $[\text{Ln}(\text{EtForm})_3]$ complexes were synthesized (Ln = La (**75**), Nd (**76**), Sm (**77**), Ho (**78**) and Yb (**79**)). The *o*-PhPhFormH ligand gave $[\text{Ln}(\text{o-PhPhFormH})_3]$ complexes (Ln = La (**80**), Nd (**81**), Sm (**82**) and Er (**83**)). In this study, $[\text{Yb}(\text{o-TolForm})_3(\text{thf})]$ (**84**) was isolated from a metathesis reaction route because the RTP reaction consistently gave $[\{\text{Yb}(\text{o-TolForm})_2(\mu\text{-OH})(\text{thf})_2\}]$ (**85**). The La metal center is eight-coordinate in **67** and the molecular unit exhibits two *transoid* THF donor molecules (O–La–O: 157.23 (17)°) (Fig. 2-18 left). In the Yb complex (**85**), each ytterbium center has two chelating *o*-TolForm ligands, one THF molecule and two bridging OH groups giving a seven-coordinate ytterbium atom (Fig. 2-18 right). The ionic radius of Yb^{3+} is smaller than La^{3+} due to the lanthanoid contraction giving the lanthanum complex a higher coordination number than the ytterbium complex [33].

Using DippFormH which is a bulkier ligand, C–F activation occurs to give $[\text{Ln}(\text{DippForm})_2\text{F}(\text{thf})]$ complexes (Ln = La (**30**), Ce (**86**), Nd (**87**), Sm (**88**) and Tm (**89**)) [26]. $[\text{Nd}(\text{DippForm})_2(\text{CPh})(\text{thf})]$ (**90**) was synthesized in this study by using bis(phenylethynyl)mercury ($\text{Hg}(\text{CPh})_2$) rather than $\text{Hg}(\text{C}_6\text{F}_5)_2$ in an RTP reaction and provides evidence for the formation of $[\text{Ln}(\text{Form})_2\text{R}]$ (R = C_6F_5 or CPh) intermediates. $\text{Hg}(\text{CPh})_2$ also was used to prepare $[\text{Sm}(\text{DippForm})_2(\text{CPh})(\text{thf})]$ (**58**) complex by oxidation of $[\text{Sm}(\text{DippForm})_2(\text{thf})_2]$ (**11**).

Three new cerium(III) formamidinate complexes comprising $[\text{Ce}(\text{DFForm})_3(\text{thf})_2]$ (**91**), $[\text{Ce}(\text{DFForm})_3]$ (**92**), and $[\text{Ce}(\text{EtForm})_3]$ (**93**) are the results of a protonolysis reactions between $[\text{Ce}(\text{N}(\text{SiMe}_3)_2)_3]$ and *N,N'*-bis(2,6-difluorophenyl)formamidinate (DFFormH) or EtFormH [34]. The unsolvated $[\text{Ce}(\text{DFForm})_3]$ (**92**)



Scheme 2-7. Synthetic pathway and the products for formation of $[\text{La}\{\eta^1(\text{N})\}\eta^6(\text{Ar})\text{-}2\text{-Me}_3\text{AlCH}_2\text{-}4,6\text{-Me}_2\text{C}_6\text{H}_2\text{NCHNMe}_2\}\{\text{AlMe}_3\}\{\text{AlMe}_4\}]$ (**107**) and $[\text{La}\{2\text{-Me}_3\text{AlCH}_2\text{-}4,6\text{-Me}_2\text{C}_6\text{H}_2\text{NCHNMe}_2\}\{\text{AlMe}_3\}\{\text{AlMe}_4\}]_2(\text{C}_6\text{H}_{14})_{1.5}$ (**108**) which cocrystallize 1:1.



Scheme 2-8. Structures of $\text{Ln}_2\text{RECH}_2\text{SiMe}_3\cdot\text{thf}$ [$\text{L} = \text{XylForm}, \text{RE} = \text{Y}$ (**113**) and $\text{L} = \text{DippForm}, \text{RE} = \text{Y}$ (**113**), **Er** (**114**), **Dy** (**115**), **Sm** (**116**), and **Nd** (**117**)].

Table 2.3.1
Trivalent compounds.

Reaction	Compound	Method	Refs.
[SmI ₂ (THF) ₂] + solution of [Sm(DippForm) ₂ (thf) ₂] in THF	[Na(thf) ₅][Sm(I) ₂ (DippForm) ₂ (thf)] (12)	Redox	[29]
Eu + DFFormH in THF	{[Eu(DFForm) ₂ OH(thf) ₂]} (16)	RTP	[30]
[Yb(DFForm) ₂ (thf) ₃] in PhMe exposed with trace O ₂	{[Yb ₂ (DFForm) ₄ (O)] ₂ } (19)	Oxidation	[30]
La + CF ₃ FormH + Hg(C ₆ F ₅) ₂ in THF	[La(CF ₃ Form) ₃] (25)	RT	[32]
Yb + CF ₃ FormH + Hg(C ₆ F ₅) ₂ in THF	[Yb(CF ₃ Form) ₃ (thf)] (26)	RT	[32]
[Sm(DippForm) ₂ (thf) ₂] + (CH ₃) ₃ CCl in PhMe	[Sm(DippForm) ₂ Cl(thf)] (27)	Oxidation	[23]
[Sm(DippForm) ₂ (thf) ₂] + BrCH ₂ CH ₂ Br in PhMe	[Sm(DippForm) ₂ Br(thf)] (28)	Oxidation	[23]
[Sm(DippForm) ₂ (thf) ₂] + I ₂ in PhMe	[Sm(DippForm) ₂ I(thf)] (29)	Oxidation	[23]
[Sm(DippForm) ₂ Cl(thf)] + MeLi in PhMe	[Sm(DippForm) ₂ Me(thf)] (31)	Metathesis	[23]
[Sm(DippForm) ₂ Cl(thf)] + SiMe ₃ CH ₂ Li	[Sm(DippForm) ₂ (CH ₂ SiMe ₃)(thf)] (32)	Metathesis	[23]
[La(DippForm) ₂ F(thf)] + MeLi in PhMe	[La(DippForm) ₂ Me(thf)] (33)	Metathesis	[23]
Sm + Hg(2-BrC ₆ F ₄) ₂ + DippFormH	[Sm(DippForm)Br ₂ (thf) ₃] (34)	RTP	[23]
[Sm(DippForm) ₂ (thf) ₂] and diphenylmercury in toluene	[Sm(DippForm) ₂ (OCH=CH ₂)(thf)] (35)	Oxidation + thf cleavage	[23]
[Yb(DFForm) ₂ (thf) ₃] + BP in DME (crystallised from PhMe)	[Yb(DFForm) ₃ (bp)] (36)	Oxidation and redistribution	[30]
[Yb(DFForm) ₂ (thf) ₃] + TiCl ₄ (thf) ₂ /Ph ₃ CCl in THF	[Yb(DFForm) ₂ Cl(thf) ₂] (37)	Oxidation	[30]
Yb + DFFormH + Hg(C ₆ F ₅) ₂ in THF	[Yb(DFForm) ₃ (thf)] (38)	RTP	[30]
Perfluorodecalin + [Yb(EtForm) ₂ (thf) ₂] in THF	{[Yb(EtForm) ₂ (μ ₂ -F)] ₂ } (39)	C–F activation	[26]
Perfluorodecalin + [Yb(<i>o</i> -PhPhForm) ₂ (thf) ₂] in THF	[Yb(<i>o</i> -PhPhForm) ₂ F] ₂ (40)	C–F activation	[26]
Hexachloroethane + [Yb(<i>o</i> -PhPhForm) ₂ (thf) ₂]-2THF in THF	[Yb(<i>o</i> -PhPhForm) ₂ Cl(thf) ₂] (41)	C–Cl activation	[26]
1,2-dichloroethane + [Yb(DippForm) ₂ (thf) ₂] in PhMe	[Yb(DippForm) ₂ Cl(thf)] (42)	C–Cl activation	[26]
Yb + Hg(2-BrC ₆ F ₄) ₂ + DippFormH in THF	[Yb(DippForm) ₂ Br(thf)] (43)	C–Br activation	[26]
Ln + Hg(2-BrC ₆ F ₄) ₂ + DippFormH in THF	[Ln(DippForm) ₂ Br(thf)] (Ln = La (44), Nd (45))	C–Br activation	[26]
[Na-(DippForm)(thf) ₃] + TlCl ₃ in THF	[Tl(DippForm) ₂ Cl(thf) ₂]-2.5THF (46)	Metathesis	[26]
[Sm(DippForm) ₂ (thf) ₂] + Benzophenone in toluene	[Sm(DippForm) ₂ (thf) {μ-OC(Ph)=(C ₆ H ₅)C-(Ph) ₂ O}Sm(DippForm) ₂] (47)	Ketyl rearrangement	[27]
[Yb(DippForm) ₂ (thf) ₂] + Benzophenone in toluene	[Yb(DippForm) ₂ (thf) {μ-OC(Ph)=(C ₆ H ₅)C(Ph) ₂ O}Yb(DippForm) ₂] (48)	Ketyl rearrangement	[27]
[Sm(DippForm) ₂ (thf) ₂] + CS ₂ in C ₆ D ₆	{[Sm(DippForm) ₂ (thf) ₂] ₂ (μ ² -η ² (C,S):κ(S',S'') SCSCS ₂)] (49)	Oxidation	[27]
Ln + <i>p</i> -TolFormH + Hg(C ₆ F ₅) ₂ in THF	[Ln(<i>p</i> -TolForm) ₃] ₂ (Ln = La (50), Ce (96), Sm (51), Nd (127))	RTP	[15]
[Sm(<i>p</i> -TolForm) ₃] ₂ .1/2 thf + Ph ₃ PO in PhMe	[Sm(<i>p</i> -TolForm) ₃ (Ph ₃ PO) ₂] (52)	Bridge splitting	[15]
[Sm(<i>p</i> -TolForm) ₃] ₂ .1/2 thf + DFFormH in PhMe (crystallised from THF/Hexane mixture)	[Sm(<i>p</i> -TolForm)(DFForm) ₂ (thf) ₂] (53)	Bridge splitting	[15]
[Sm(<i>p</i> -TolForm) ₃] ₂ .1/2 thf + DFFormH in PhMe (crystallised from THF/Hexane mixture)	[Sm(DFForm) ₃ (thf) ₂] (54)	Bridge splitting	[15]
KC ₈ + 18-Crown-6 + [Sm(<i>p</i> -TolForm) ₃] ₂ in PhMe	[K(18-Crown-6)][Sm(<i>p</i> -TolForm) ₄] (55)	Attempted reduction	[15]
[Nd(<i>p</i> -TolForm) ₃] ₂ .PhMe dissolved in THF and layered with hexane	[Nd(<i>p</i> -TolForm) ₃ (thf) ₂] (56)	Bridge splitting	[15]
Lu + <i>p</i> -TolFormH + Hg(C ₆ F ₅) ₂ in THF	[Lu(<i>p</i> -TolForm) ₃ (thf)] (57)	RTP	[15]
[Sm(DippForm) ₂ (thf) ₂] + Hg(CPh) ₂ in Toluene	[Sm(DippForm) ₂ (C≡CPh)(thf)] (58)	Oxidation	[24]
[Sm(DippForm) ₂ (CCPh)(thf)] + Benzophenone in toluene	[Sm(DippForm) ₂ (OC(Ph) ₂ C ₂ Ph)(thf)] (59) (major) [Sm(DippForm) ₂ (OC(Ph) ₂ C ₂ Ph)] (60) (minor)	Insertion	[27]
Dissolution of [Na(THF) ₅][SmI ₂ (DippForm) ₂ (THF)] in hexane	[Sm(DippForm) ₃] (61)	Rearrangement	[29]
[Sm(DippForm) ₂ (thf) ₂] + DippNCNDipp in toluene	[Sm(DippForm) ₃] (61)	Oxidation	[28]
MesNCNMes + [Sm(DippForm) ₂ (thf) ₂] in PhMe (crystallised from hexane)	[Sm(DippForm) ₂ (MesForm)] (62)	Oxidation	[28]
N,N'-dicyclohexylcarbodiimide (CyNCNCy) + [Sm(DippForm) ₂ (thf) ₂] in PhMe	[Sm(DippForm) ₂ (CyNC(CH ₂ Ph)NCy)] (63) and [Sm(DippForm) ₂ (CyNC(H)NCy)] (64)	Oxidation	[28]
[Sm(DippForm) ₂ (C≡CPh)(thf)] + N,N'-dicyclohexylcarbodiimide (CyNCNCy) in PhMe	[Sm(DippForm) ₂ (CyNC(C≡CPh)NCy)] (65)	Insertion	[28]
[Sm(DippForm) ₂ (C≡CPh)(thf)] + MesNCNMes in PhMe	[Sm(DippForm) ₂ (MesNC(C≡CPh)NMes)] (66)	Insertion	[28]
La + <i>o</i> -TolFormH + Hg(C ₆ F ₅) ₂ in THF	[La(<i>o</i> -TolForm) ₃ (thf) ₂] (67)	RTP	[24]
Er + <i>o</i> -TolFormH + Hg(C ₆ F ₅) ₂ in THF	[Er(<i>o</i> -TolForm) ₃ (thf)] (68)	RTP	[24]
La + XylFormH + Hg(C ₆ F ₅) ₂ in THF	[La(XylForm) ₃ (thf)] (69)	RTP	[24]
Sm + XylFormH + Hg(C ₆ F ₅) ₂ in THF	[Sm(XylForm) ₃] (70)	RTP	[24]
Ln + MesFormH + Hg(C ₆ F ₅) ₂ in THF	[Ln(MesForm) ₃] (Ln = La (71), Nd (72), Sm (73) and Yb (74))	RTP	[24]
Ln + EtFormH + Hg(C ₆ F ₅) ₂ in THF	[Ln(EtForm) ₃] (Ln = La (75), Nd (76), Sm (77), Ho (78) and Yb (79))	RTP	[24]
Ln + <i>o</i> -PhPhFormH + Hg(C ₆ F ₅) ₂ in THF	[Ln(<i>o</i> -PhPhForm) ₃] (Ln = La (80), Nd (81), Sm (82) and Er (83))	RTP	[24]
YbCl ₃ + <i>o</i> -TolFormLi in THF	[Yb(<i>o</i> -TolForm) ₃ (thf)] (84)	Metathesis	[24]
Yb + <i>o</i> -TolFormH + Hg(C ₆ F ₅) ₂ in THF	{[Yb(<i>o</i> -TolForm) ₂ (μ-OH)(thf) ₂]} (85)	RTP	[24]
Ln + DippFormH + Hg(C ₆ F ₅) ₂ in THF	[Ln(DippForm) ₂ F(thf)] (Ln = La (30), Ce (86), Nd (87), Sm (88) and Tm (89))	RTP + C–F activation	[24]
Nd + DippFormH + Hg(CPh) ₂ in THF	[Nd(DippForm) ₂ (C≡CPh)(thf)] (90)	RTP	[24]
[Ce(N(SiMe ₃) ₂) ₃] + DFFormH in THF	[Ce(DFForm) ₃ (thf) ₂] (91)	Protolysis	[34]
[Ce(N(SiMe ₃) ₂) ₃] + DFFormH in PhMe	[Ce(DFForm) ₃] (92)	Protolysis	[34]
[Ce(N(SiMe ₃) ₂) ₃] + EtFormH in THF	[Ce(EtForm) ₃] (93)	Protolysis	[34]
Oxidation of [Ce(DFForm) ₃ (thf) ₂] with Ph ₃ CCl	[Ce ₃ Cl ₅ (DFForm) ₄ (thf) ₄] (94)	Attempted oxidation	[34]
[Ce(EtForm) ₃] + Ph ₃ CCl in THF	[Ce(EtForm)Cl ₂ (thf) ₃] (95)	Redox	[34]
[La(DippForm) ₂ Me(thf)] + H ₂ C ₃ Ph ₄ in C ₆ D ₆	[La(DippForm) ₃] (97)	–	[23]

(continued on next page)

Table 2.3.1 (continued)

Reaction	Compound	Method	Refs.
[Sm{N(SiMe ₃) ₂ }(THF) ₂] and N,N'-bis(2,6-diisopropylphenyl)carbodiimide in hexane	{[(Me ₃ Si) ₂ N] ₂ Sm{μ-(RNC(H)N(Ar-Ar) (R = C ₆ H ₃ -2,6- ⁱ Pr ₂ ; Ar-Ar = C ₆ H ₃ -2- ⁱ Pr-6-C(CH ₃) ₂ C(CH ₃) ₂ -6'-C ₆ H ₃ -2- ⁱ Pr)NC(H)-NR)}Sm{N(SiMe ₃) ₂ }}] (98)	Oxidation + Radical coupling	[35]
SmCl ₃ + DippFormLi + Li ₂ COT'' in THF	Sm(DippForm)(COT'')(THF) (COT'' = 1,4-bis-(trimethylsilyl)cyclooctatetraenyl dianion) (99)	Metathesis	[36]
YbCl ₃ + DippFormLi + Li ₂ COT'' in THF	Yb(DippForm)(COT'')(THF) (COT'' = 1,4-bis-(trimethylsilyl)cyclooctatetraenyl dianion) (100)	Metathesis	[37]
Y(AlMe ₄) ₃ + EtFormH in hexane	Y(EtForm)(AlMe ₄) ₂ (101)	Protolysis	[20]
Y(AlMe ₄) ₃ + MesFormH in hexane	Y(MesFormAlMe ₃)(AlMe ₄) ₂ (102)	Protolysis	[20]
Ln(AlMe ₄) ₃ + DippFormH in hexane	Ln(DippForm)(AlMe ₄) ₂ (Ln = Y (103), La (105))	Protolysis	[20]
Ln(AlMe ₄) ₃ + tBuFormH in hexane	Ln(tBuForm)(AlMe ₄) ₂ (Ln = Y (104), La (106))	Protolysis	[20]
La(AlMe ₄) ₃ + MesFormH in hexane	[La{η ¹ (N):η ⁶ (Ar)-2-Me ₃ AlCH ₂ -4,6-Me ₂ C ₆ H ₂ NCHNMe ₃ }(AlMe ₃)(AlMe ₄)] (107) and [La(2-Me ₃ AlCH ₂ -4,6-Me ₂ C ₆ H ₂ NCHNMe ₃)(AlMe ₃)(AlMe ₄)](C ₆ H ₁₄) _{1.5} (108)	Protolysis	[20]
La(AlMe ₄) ₃ + EtFormH in toluene	[La{η ¹ (N):η ⁶ (Ar)-EtFormAlMe ₃ }(AlMe ₄) ₂](C ₇ H ₈) _{1.5} (109)	Protolysis	[20]
Y[N(SiHMe ₂) ₂] ₃ (thf) ₂ + EtFormH in hexane	Y(EtForm)[N(SiHMe ₂) ₂] ₂ (thf) (110)	Protolysis	[20]
Y[N(SiHMe ₂) ₂] ₃ (thf) ₂ + DippFormH in hexane	Y(DippForm)[N(SiHMe ₂) ₂] ₂ (thf) (111)	Protolysis	[20]
Y(CH ₂ SiMe ₃) ₃ (THF) ₂ + XylFormH in Hexane	Y(XylForm) ₂ (CH ₂ SiMe ₃)(thf) (112)	Protolysis	[38]
Ln(CH ₂ SiMe ₃) ₃ (THF) ₂ + DippFormH in Hexane	Ln[DippForm] ₂ (CH ₂ SiMe ₃)(thf) (Ln = Y (113), Er (114), Dy (115), Sm (116))	Protolysis	[38]
n-BuLi + DippFormH + NdCl ₃ + LiCH ₂ SiMe ₃	Nd[DippForm] ₂ (CH ₂ SiMe ₃)(thf) (117)	Metathesis	[38]
Yb + FFormH + Hg(C ₆ F ₅) ₂ in THF	[Yb(FForm) ₃ (thf)] (118)	RTP	[31]
La + FFormH + Hg(C ₆ F ₅) ₂ in THF	[La(FForm) ₃ (thf) ₂].thf (119)	RTP	[31]
Nd + FFormH + Hg(C ₆ F ₅) ₂ in THF	[Nd(FForm) ₃ (thf) _x] (x = 1 (120), x = 2 (121))	RTP	[31]
[La(FForm) ₃ (thf) ₂].thf dissolved in DME	[La(FForm) ₃ (dme)] (122)	Ligand exchange	[31]
Nd + FFormH + Hg(C ₆ F ₅) ₂ in THF (crystallised from diglyme)	[Nd(FForm) ₃ (diglyme)].diglyme (123)	RTP	[31]
Nd + TFFormH + Hg(C ₆ F ₅) ₂ in THF (crystallised from a mixture of DME and toluene)	[Nd(TFForm) ₃ (dme)] (124)	RTP	[31]
[Yb(TFForm) ₂ (thf) ₂] was dissolved in toluene and crystallised from mixture of toluene and hexane	[Yb(TFForm) ₃ (thf) ₂] (125)	-	[31]
[Yb(TFForm) ₂ (thf) ₂] was dissolved in diglyme and crystallised from mixture of toluene and hexane	[Yb(TFForm)(diglyme) ₂][Yb(TFForm) ₄] (126)	-	[31]
[Ce{N(SiHMe ₂) ₂] ₃ (thf) ₂] + [Li{N(SiHMe ₂) ₂ }] + DFFormH in PhMe	[LiCe(DFForm) ₄] (128)	Protolysis	[34]

complex was prepared and isolated from toluene. The THF solvated species [Ce(DFForm)₃(thf)₂] (**93**) (Fig. 2-19), can be formed by adding THF to [Ce(DFForm)₃] (**92**) but this process is irreversible. The absence of THF in the [Ce(DFForm)₃] (**92**) complex may be the main reason for having shorter Ce-N bonds in this complex compared to the Ce-N bonds in [Ce(DFForm)₃(thf)₂] (**93**). The shorter Ce-N bonds in [Ce(DFForm)₃] (**92**) allow fluorine coordination. Because of the coordinating fluorine the C_{ipso}-N-CH angle (126.4(2)–128.3(2)°) is higher compared to the [Ce(DFForm)₃(thf)₂] (**93**) complex (116.1(4)–121.4(4)°). It has been reported another Ce(III) complex [Ce₃Cl₅(DFForm)₄(thf)₄] (**94**) was synthesized by attempted oxidation of [Ce(DFForm)₃(thf)₂] with Ph₃CCl (**93**) while [Ce(EtForm)Cl₂(thf)₃] (**95**) was isolated from a similar reaction of [Ce(EtForm)₃] (**92**).

Moreover, the cerium(III) formamidinate {[Ce(*p*-TolForm)₃]₂} (**96**) was prepared in good yield (96%) using a protolysis reaction between [Ce{N(SiMe₃)₂]₃] and *p*-TolFormH ligand [34]. The structure was determined following an alternative RTP synthesis [15].

Unexpectedly, the homoleptic tris-(formamidinato)lanthanum complex [La(DippForm)₃] (**97**) (Fig. 2-20) was isolated in a very low yield from the ligand exchange reaction of [La(DippForm)₂-Me(thf)] (**33**) with 1,2,3,4-tetraphenylcyclopentadiene [23]. An earlier attempt to prepare this complex by metathesis was unsuccessful [29].

The {(Me₃Si)₂N}₂Sm{μ-(RNC(H)N(Ar-Ar)NC(H)NR)}Sm{N(SiMe₃)₂}] (**98**) complex with a coupled, bis(formamidinate) ligand (Fig. 2-21) was synthesized by reaction of solutions of N,N'-bis(2,6-diisopropylphenyl)carbodiimide and [Sm{N(SiMe₃)₂}(thf)₂] in hexane [35].

It has been reported that [N,N'-bis(2,6-diisopropylphenyl)formamidinato][η⁸-1,4-bis(trimethylsilyl)cyclooctatetraenyl](tetrahydrofuran)samarium(III) toluene monosolvate (**99**) can be synthesized by the treatment of Li(DippForm) with anhydrous samarium

trichloride and Li₂(COT'') [COT'' = 1,4-bis(trimethylsilyl)cyclooctatetraenyl] in thf [36]. The same procedure was also used to synthesize [(COT'')Yb-(DippForm)(thf)] (**100**) (Scheme 2-6) [37].

A series of Y(Form)(AlMe₄)₂ (Form = EtForm (**101**), MesForm (**102**), DippForm (**103**), tBuForm (**104**)) complexes have been synthesized by protolysis of Y(AlMe₄)₃ species (Fig. 2-22). Using the same route and La metal, La(Form)(AlMe₄)₂ (Form = DippForm (**105**), tBuForm (**106**)) complexes can be prepared [20]. Adding La(AlMe₄)₃ to one equivalent of MesFormH in hexane yields a yellow solution, from which the complexes [La{η¹(N):η⁶(Ar)-2-Me₃AlCH₂-4,6-Me₂C₆H₂NCHNMe₃}(AlMe₃)(AlMe₄)] (**107**) and [La(2-Me₃AlCH₂-4,6-Me₂C₆H₂NCHNMe₃)(AlMe₃)(AlMe₄)](C₆H₁₄)_{1.5} (**108**) have been co-crystallised in a 1:1 ratio and result from C–H activation of a C–Me group of the mesityl moiety. The presence of a methylene ligand is the most interesting structural characteristic of this compound. The methylene ligand increases the coordination saturation of the lanthanum center and helps the η² binding of two aromatic carbon atoms (Scheme 2-7). The same method was used to synthesize [La{η¹(N):η⁶(Ar)-EtFormAlMe₃}(AlMe₄)₂](C₇H₈)_{1.5} (**109**). In this study Y[N(SiHMe₂)₂]₃(thf)₂ was treated with EtFormH and DippFormH in protolysis reactions to yield Y(EtForm)[N(SiHMe₂)₂]₂(thf) (**110**) and Y(DippForm)[N(SiHMe₂)₂]₂(thf) (**111**) respectively.

The coordination number in [La{η¹(N):η⁶(Ar)-2-Me₃AlCH₂-4,6-Me₂C₆H₂NCHNMe₃}(AlMe₃)(AlMe₄)] (**107**) is 10 and this complex contains the η¹(N):η⁶(Ar) binding mode of the metallated Form ligand. The coordination number for the La center in [La(2-Me₃AlCH₂-4,6-Me₂C₆H₂NCHNMe₃)(AlMe₃)(AlMe₄)] (**108**) is nine and AlMe₃ bridges a nitrogen donor atom and the lanthanum atom via two methyl groups. The upper product (Scheme 2-7) can be isolated pure from the filtrate after isolation of the 1:1 mixture.

A series of rare-earth metal monoalkyl complexes of formamidinates, LnL₂CH₂SiMe₃-thf [L₂ = (XylForm)₂, Ln = Y (**112**), L₂ =

(DippForm)₂, Ln = Y (**113**), Er (**114**), Dy (**115**), Sm (**116**), and Nd (**117**) (Scheme 2-8) were synthesized by alkyl elimination or salt metathesis reactions in good yields (64–73%) [38]. These compounds are similar to the reported complexes in another study (see above Scheme 2-2) [23].

Using the FFormH ligand in RTP reactions yielded [Yb(FForm)₃(-thf)] (**118**), [La(FForm)₃(thf)₂].thf (**119**) and [Nd(FForm)₃(thf)_x] (x = 1–2) (**120**, **121**) complexes [31]. These compounds were crys-

talized either from DME or diglyme/hexane to give [La(FForm)₃(dme)] (**122**) and [Nd(FForm)₃(diglyme)]₂.diglyme (**123**) complexes to allow X-ray crystal structural determinations. In an RTP reaction with Nd and after recrystallization from dme, [Nd(TFForm)₃(dme)] (**124**) was isolated. Two other complexes [Yb(TFForm)₃(thf)₂] (**125**) and [Yb(TFForm)(diglyme)₂][Yb(TFForm)₄] (**126**) were synthesized by heating [Yb(TFForm)₂(thf)₃] (**5**) in PhMe and diglyme respectively.

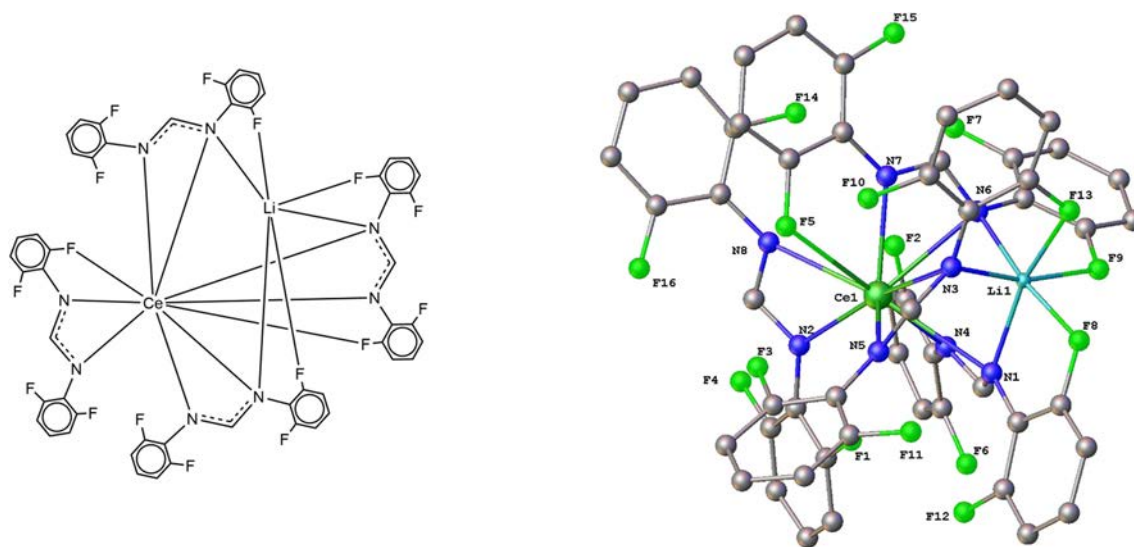
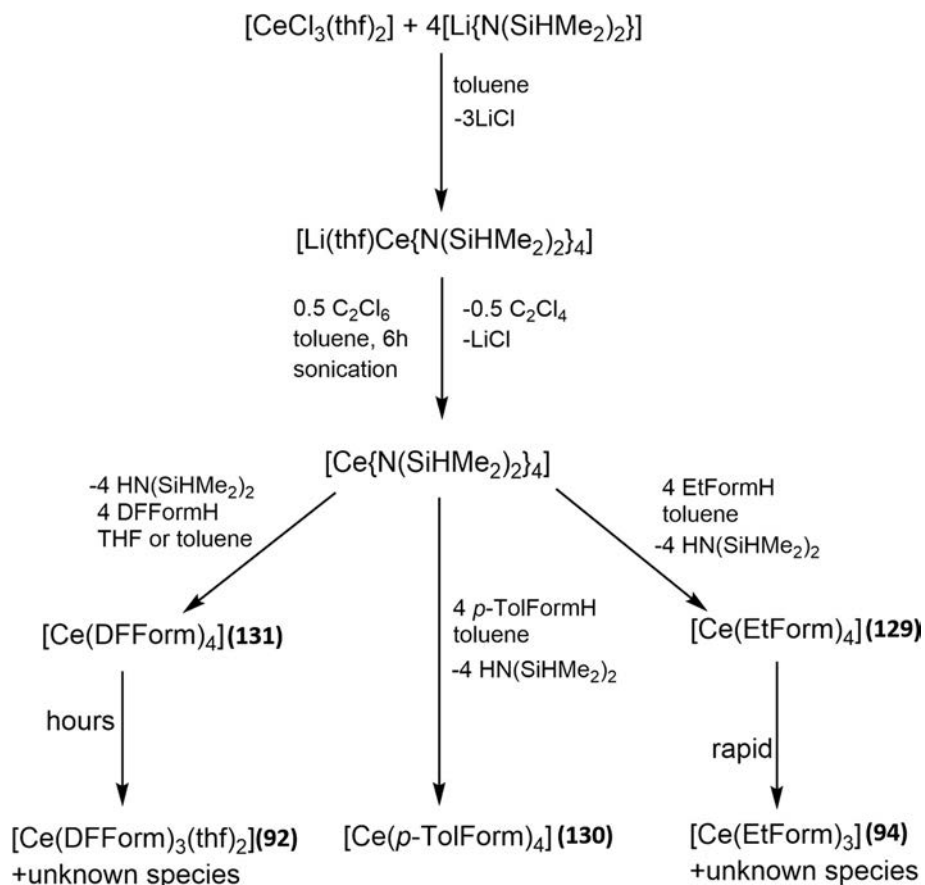


Fig. 2-23. Schematic and the X-ray structure of [LiCe(DFForm)₄] (**128**).



Scheme 2-9. The procedure of making [Ce{N(SiHMe₂)₂}₄] complex and formamidine-promoted protonolysis reactions.

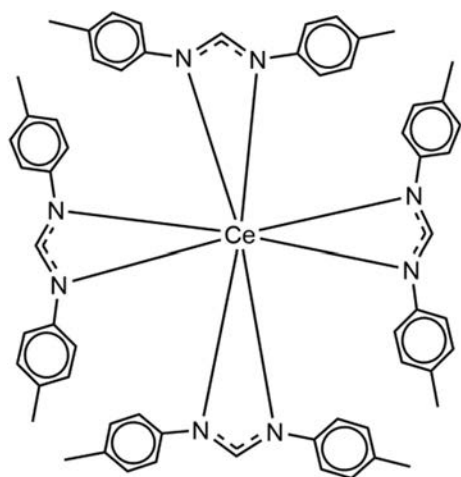


Fig. 2-24. Schematic of the X-ray structure of $[\text{Ce}(\text{p-TolForm})_4]$ (**130**).

All trivalent lanthanoid formamidinato compounds are listed in Table 2.3.1.

2.4. Tetravalent compound(s) [34]

2.4.1. Synthesis of trivalent complexes that are potential precursor of tetravalent complexes

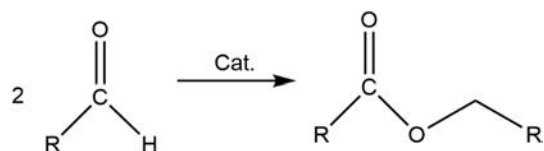
Treating a mixture of $[\text{Ce}\{\text{N}(\text{SiHMe}_2)_2\}_3(\text{thf})_2]$ and $[\text{Li}\{\text{N}(\text{SiHMe}_2)_2\}_2]$ with four equivalents of DFFormH in toluene resulted in the bimetallic cerium lithium complex $[\text{LiCe}(\text{DFForm})_4]$ (**128**). The cerium–lithium bimetallic complex $[\text{LiCe}(\text{DFForm})_4]$ (**128**) was the first reported trivalent rare-earth complex with four coordinating formamidinate ligands. The cerium atom is ten-coordinated, with eight nitrogen and two fluorine donor atoms (Fig. 2-23). The lithium atom is six-coordinate and it has closer fluorine interactions than the bridging lithium–nitrogen bond lengths. Bridging of the ligands to the larger, higher charged cerium atom maybe the main reason for inability of the lithium metal to bind closer to nitrogen. It can be seen that this complex has one terminal formamidinate ligand bound N, N', F to cerium and three formamidinate ligands bridging between cerium and lithium. The bridging formamidinate ligands have one nitrogen bridging Ce and Li, and are bond just to Ce, i.e. the ligands are chelating to Ce and unidentate to Li.

2.4.2. Protolysis of Ce(IV) amides to give Ce(IV) formamidinates

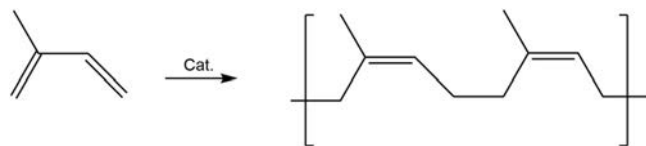
It has been reported [34] that the product of the reaction of $[\text{Ce}\{\text{N}(\text{SiHMe}_2)_2\}_4]$ with DFFormH and EtFormH are cerium(IV) complexes, e.g. $[\text{Ce}(\text{EtForm})_4]$ (**129**), which decompose before possible isolation (Scheme 2-9). Using a protolysis reaction between $[\text{Ce}\{\text{N}(\text{SiHMe}_2)_2\}_4]$ and four equivalents of *p*-TolFormH, the first structurally characterized homoleptic cerium(IV) formamidinate complex $[\text{Ce}(\text{p-TolForm})_4]$ (**130**) was obtained [35]. The coordination number of cerium in this compound is eight (Fig. 2-24). Scheme 2-9 shows the procedure of synthesising $[\text{Ce}\{\text{N}(\text{SiHMe}_2)_2\}_4]$ and the subsequent formamidine-promoted protolysis reactions. However, reaction of $[\text{Ce}\{\text{N}(\text{SiHMe}_2)_2\}_4]$ with bulkier formamidines leads to reduction giving Ce^{III} complexes (Scheme 2-9).

3. Catalysis

A series of tris(formamidinato)lanthanum(III) complexes $[\text{La}(\text{o-TolForm})_3(\text{thf})_2]$ (**57**), $[\text{La}(\text{XylForm})_3(\text{thf})]$ (**59**) and $[\text{La}(\text{EtForm})_3]$ (**65**) (synthesis by RTP reactions [26]–Table 2.3.1) have been



Scheme 3-1. Tishchenko reaction.



Scheme 3-2. Isoprene polymerisation showing only the *cis*-1,4 isomer.

reported to be precatalysts for the Tishchenko reaction. The Tishchenko reaction is the dimerization of an aldehyde to form the corresponding carboxylic ester (Scheme 3-1) and is an industrially important reaction [9]. Generally, aluminum alkoxides have been used as homogeneous catalysts for the Tishchenko reaction. [39–41] However, other catalysts such as boric acid [42] and a few transition-metal complexes have been used in the recent past [43]. Recently, some Mg compounds have been tested as catalysts for the Tishchenko reaction [44]. But these alternative catalysts are often either very expensive (e.g. $[\text{H}_2\text{Ru}(\text{PPh}_3)_2]$) [41] or give low yields (e.g. $\text{K}_2[\text{Fe}(\text{CO})_4]$) [42,44], or they are only reactive under extreme reaction conditions (e.g. boric acid) or slow (e.g. $[(\text{C}_5\text{H}_5)_2\text{-ZrH}_2]$) [43]. The lanthanoid formamidinate compounds are the most active catalyst system ever reported. Catalytic activity increases with reduced steric effect of the formamidinate ligands, with $[\text{La}(\text{o-TolForm})_3(\text{thf})_2]$ (**57**) the most effective, La is the most effective metal.

The catalytic activity of the compounds $[\text{Ln}(\text{Form})(\text{AlMe}_4)_2]$ ($\text{Ln} = \text{Y, La}$; Form = EtForm (**89, 93**), DippForm (**91, 95**)) in isoprene polymerization was investigated by activating them with $[\text{Ph}_3\text{C}][\text{B}(\text{C}_6\text{F}_5)_4]$ or $[\text{PhNMe}_2\text{H}][\text{B}(\text{C}_6\text{F}_5)_4]$. At ambient temperature, polyisoprene of narrow molecular weight distribution ($\text{PDI} < 1.2$) was produced. The stereochemical outcome of the polymerization was dependent on the catalyst; trityl tetrakis(pentafluorophenyl)borate gave *trans*-1,4-selectivity (maximum 87%), while the anilinium borate favours *cis*-1,4-selectivity (maximum 82%) [20]. The general isoprene polymerisation reaction is illustrated in Scheme 3-2 (only the *cis*-1,4 isomer is shown, *trans*-1,4, 1,2 and 3,4 polymers are also possible).

Moreover, a series of rare-earth metal monoalkyl complexes of formamidinates $\text{LnL}_2\text{CH}_2\text{SiMe}_3\cdot\text{thf}$ [$\text{L} = \text{XylForm}$, $\text{Ln} = \text{Y}$, $\text{L} = \text{DippForm}$, $\text{Ln} = \text{Y, Er, Dy, Sm, and Nd}$] were combined with $[\text{Ph}_3\text{C}][\text{B}(\text{C}_6\text{F}_5)_4]$ and alkylaluminium species to test the catalytic activity for isoprene polymerisation. The catalytic activity towards isoprene polymerization provided polyisoprenes with high molecular weight ($M_n > 10^4$) and narrow molecular weight distributions ($\text{PDI} < 2.0$) were obtained. If the catalysts were added in the order $[\text{RE}]/[\text{alkylaluminium}]/[\text{B}(\text{C}_6\text{F}_5)_4]$, 1,4-regioselectivity was reported as high as 98%. However, there was no appreciable selectivity between *cis*-1,4- and *trans*-1,4- isomers in the polymers [38].

4. Conclusions and outlook

The formamidinate complexes of rare earth metals have been reviewed. By varying the metals or the steric and electronic effects of the ligands, the structures and reactivity of the resulting complexes can be widely varied. By using formamidinates with fluorinated substituents on the arene rings, C-F activation can be

promoted. The current review offers many openings to future research involving these easy to prepare ligands, and many other related ligands can be used to provide new reactivity and structures. Unusual oxidation state chemistry for the rare earth metals remains a challenge, e.g. divalent complexes other than Eu(II), Sm(II) and Yb(II) and tetravalent complexes other than Ce(IV). The chemical and catalytic activity of some of these compounds presented has been explored but there still remains much more to be studied.

Acknowledgements

We are grateful to the Australian Research Council (DP160101640) for funding of this project.

References

- [1] F.T. Edelmann, *Adv. Organomet. Chem.*, in: A.F. Hill, M.J. Fink (Eds.), 61, Elsevier Science, 2013, pp. 55–374.
- [2] J. Barker, M. Kilner, *Coord. Chem. Rev.* 133 (1994) 219–300.
- [3] F.T. Edelmann, *Chem. Soc. Rev.* 38 (2009) 2253–2268.
- [4] F.T. Edelmann, *Chem. Soc. Rev.* 41 (2012) 7657–7672.
- [5] F.T. Edelmann, *Adv. Organomet. Chem.*, in: A.F. Hill, M.J. Fink (Eds.), 57, Elsevier Science, 2008, p. 183.
- [6] F.T. Edelmann, D.M. Freckmann, H. Schumann, *Chem. Rev.* 102 (2002) 1851–1896.
- [7] B.S. Lim, A. Rahtu, R.G. Gordon, *Nat. Mater.* 2 (2003) 749–754.
- [8] S. Bambirra, M.W. Bouwkamp, A. Meetsma, B. Hessen, *J. Am. Chem. Soc.* 126 (2004) 9182–9183.
- [9] A. Zuyls, P.W. Roesky, G.B. Deacon, K. Konstas, P.C. Junk, *Eur. J. Org. Chem.* (2008) 693–697.
- [10] M.L. Cole, P.C. Junk, *New. J. Chem.* 29 (2005) 135–140.
- [11] M.L. Cole, G.B. Deacon, C.M. Forsyth, K. Konstas, P.C. Junk, *Dalton Trans.* (2006) 3360–3367.
- [12] R.M. Roberts, *J. Org. Chem.* 14 (1949) 277–284.
- [13] P.C. Junk, M.L. Cole, *Chem. Commun.* (2007) 1579–1590.
- [14] M.L. Cole, G.B. Deacon, P.C. Junk, K. Konstas, *Chem. Commun.* (2005) 1581–1583.
- [15] G.B. Deacon, P.C. Junk, L.K. Macreadie, D. Werner, *Eur. J. Inorg. Chem.* (2014) 5240–5250.
- [16] T.J. Boyle, L.A.M. Ottley, *Chem. Rev.* 108 (2008) 1896–1917.
- [17] N. Bochkarev, L.N. Zakharov, G.S. Kalinina, *Organoderivatives of Rare Earth Elements*, Kluwer Academic Publishers 3 (1995).
- [18] K. Izod, S.T. Liddle, W. Clegg, *Inorg. Chem.* 43 (2004) 214–218.
- [19] D.M. Barnhart, D.L. Clark, J.C. Gordon, J.C. Huffman, R.L. Vincent, J.G. Watkin, B. D. Zwick, *Inorg. Chem.* 33 (1994) 3487–3497.
- [20] S. Hamidi, L.N. Jende, H. Martin Dietrich, C.C. Maichle-Mössmer, K.W. Törnroos, G.B. Deacon, P.C. Junk, R. Anwender, *Organometallics* 32 (2013) 1209–1223.
- [21] G.B. Deacon, C.M. Forsyth, S. Nickel, *J. Organomet. Chem.* 647 (2002) 50–60.
- [22] G.B. Deacon, P.C. Junk, A. Urbatsch, *Aust. J. Chem.* 65 (2012) 802–810.
- [23] M.L. Cole, G.B. Deacon, P.C. Junk, J. Wang, *Organometallics* 32 (2013) 1370–1378.
- [24] M.L. Cole, G.B. Deacon, C.M. Forsyth, P.C. Junk, K. Konstas, J. Wang, *Chem. Eur. J.* 13 (2007) 8092–8110.
- [25] G.B. Deacon, T. Feng, C.M. Forsyth, A. Gitlits, D.C. Hockless, Q. Shen, B.W. Skelton, A.H. White, *J. Chem. Soc. Dalton Trans.* (2000) 961–966.
- [26] M.L. Cole, G.B. Deacon, C.M. Forsyth, P.C. Junk, K. Konstas, J. Wang, H. Bittig, D. Werner, *Chem. Eur. J.* 19 (2013) 1410–1420.
- [27] G.B. Deacon, P.C. Junk, J. Wang, D. Werner, *Inorg. Chem.* 53 (2014) 12553–12563.
- [28] M.L. Cole, G.B. Deacon, C.M. Forsyth, P.C. Junk, D. Polo-Cerón, J. Wang, *Dalton Trans.* 39 (2010) 6732–6738.
- [29] M.L. Cole, P.C. Junk, *Chem. Commun.* (2005) 2695–2697.
- [30] G.B. Deacon, P.C. Junk, D. Werner, *Chem. Eur. J.* 22 (2016) 160–173.
- [31] G.B. Deacon, P.C. Junk, D. Werner, *Polyhedron* 103 (2016) 178–186.
- [32] G.B. Deacon, P.C. Junk, D. Werner, *Eur. J. Inorg. Chem.* (2015) 1484–1489.
- [33] R.D. Shannon, *Acta. Crystallogr. A* 32 (1976) 751–767.
- [34] D. Werner, G.B. Deacon, P.C. Junk, R. Anwender, *Chem. Eur. J.* 20 (2014) 4426–4438.
- [35] G.B. Deacon, C.M. Forsyth, P.C. Junk, J. Wang, *Inorg. Chem.* 46 (2007) 10022–10030.
- [36] A. Edelmann, C.G. Hrib, L. Hilfert, S. Blaurock, F.T. Edelmann, *Acta. Crystallogr. E* 66 (2010) m1675–m1676.
- [37] A. Edelmann, V. Lorenz, C.G. Hrib, L. Hilfert, S. Blaurock, F.T. Edelmann, *Organometallics* 32 (2012) 1435–1444.
- [38] L. Guo, X. Zhu, S. Zhou, X. Mu, Y. Wei, S. Wang, Z. Feng, G. Zhang, B. Deng, *Dalton Trans.* 43 (2014) 6842–6847.
- [39] E. Hawkins, D. Long, F. Major, *J. Chem. Soc.* (1955) 1462–1468.
- [40] F.J. Villani, F. Nord, *J. Am. Chem. Soc.* 69 (1947) 2605–2607.
- [41] I. Lin, A.R. Day, *J. Am. Chem. Soc.* 74 (1952) 5133–5135.
- [42] P.R. Stapp, *J. Org. Chem.* 38 (1973) 1433–1434.
- [43] K. Morita, Y. Nishiyama, Y. Ishii, *Organometallics* 12 (1993) 3748–3752.
- [44] B.M. Day, W. Knowelden, M.P. Coles, *Dalton Trans.* 41 (2012) 10930–10933.